

AN ABSTRACT OF THE THESIS OF

Robert Thurlow Milhous for the Doctor of Philosophy  
(Name) (Degree)

in Civil Engineering presented on 3 May 1973  
(Major) (Date)

Title: SEDIMENT TRANSPORT IN A GRAVEL-BOTTOMED  
STREAM

Abstract approved:

Peter C. Klingeman

Sediment transport in a gravel-bottomed stream located in the Oregon Coast Range was studied to determine the effects of a single layer of large particles (the armour layer) located at the surface of the bed material. The bed load transport system was studied jointly with suspended sediment transport to understand the total transport system. The bed load was sampled using a vortex trough in the stream bed which transported the bed load material into a sampling pit adjacent to the stream.

It was found that the armour layer controls the bed load transport system by preventing sand and finer material from the bed from being entrained in the flow unless the armouring particles are first moved. The bed load of an armoured stream can be calculated using the simplified Einstein bed load function with a representative diameter for the stability parameter equal to the particle size of armouring

material at which 35% of the material is finer ( $D_{35}$  size) and a representative size for the transport parameter equal to the median size of bed material below the armour layer. The critical discharge for disturbing the armour layer is related to a size equal to 69% of the  $D_{65}$  size. The critical shear stress of the armouring material is at a minimum for a particle equal to the  $0.69 D_{65}$  size. Smaller particles are hidden in the armour layer and larger particles are heavier than the critical particle.

From observation of the maximum size of particles transported for various stream discharges, the Shields parameter was found to be 0.025 for a rough bed and for a transport rate of very nearly zero.

The suspended sediment transport system was found to be partially related to the past history of the stream because the past history of flows and sediment load controls the ability of the armour layer to remove sand and finer material from the water in the stream or to supply these smaller particles to the water.

Both the bed load and suspended load of Oak Creek are quite variable when the discharge is below the critical discharge of the armour layer.

**Sediment Transport in a Gravel-Bottomed Stream**

by

**Robert Thurlow Milhous**

**A THESIS**

submitted to

**Oregon State University**

in partial fulfillment of  
the requirements for the  
degree of

**Doctor of Philosophy**

**Completed May 3, 1973**

**Commencement June 1973**

APPROVED:

---

Associate Professor of Civil Engineering  
in charge of major

---

Head of Department of Civil Engineering

---

Dean of Graduate School

Date thesis is presented

3 May 1973

Typed by Cheryl E. Curb for

Robert Thurlow Milhous

## ACKNOWLEDGEMENTS

My appreciation goes to Dr. Peter C. Klingeman for his inception of the research topic, his guidance throughout the field and laboratory studies and his help in the final phase of writing this thesis. I am grateful to Mr. Erik A. Helland-Hansen for his assistance during the experiments and particularly for our discussions about gravel stability and transport. Many of the ideas in this thesis were developed as a result of our discussions. I am also indebted to Dr. George Brown of the Forest Sciences Laboratory, OSU, for his assistance throughout the study. The field work and laboratory analysis were accomplished with the assistance of a number of civil engineering students, particularly Jeff Davis, Bob Luke, Bob Mann, and Dave Harbaugh.

Financial support of this study was provided during 1968-1970 by the Federal Water Quality Administration, U.S. Department of the Interior, under Grant WP-423, and during 1970-1972 by the Engineering Experiment Station, School of Engineering, at Oregon State University and the Water Resources Research Institute of Oregon State University (the latter through funds received under the Water Resources Research Act of 1964 and administered by the Office of Water Resources Research, U. S. Department of the Interior).

## TABLE OF CONTENTS

<u>Chapter</u>		<u>Page</u>
I	INTRODUCTION	1
	The Problem	1
	The Research Program	3
II	STUDY AREA	5
	The Watershed	5
	The Stream Channel	6
	The Bed Material	16
	Variation of Manning's "n" with Discharge	31
III	OAK CREEK VORTEX BED LOAD SAMPLER	36
	Introduction	36
	Design of Sampler	37
	Performance of Sampler	44
	Sampler Efficiency	54
IV	THE INCIPIENT MOVEMENT OF THE ARMOUR LAYER	60
	Introduction	60
	Incipient Motion of Individual Particles	62
	Literature Review	62
	Critical Shear Stress	62
	Interpretation of Critical Shear Stress	66
	Application of Concepts to Oak Creek	70
	Incipient Motion of the Armour Layer	76
	Critical Discharge and Critical Shear Stress	76
	Fine Material in the Armour Layer	82
	Minimum Critical Shear Stress for "Breakup" of Heterogeneous Armour	86
	Probability of Armour Layer Movement	89
	Relationship Between Probability of Movement and Bed Load Transport	97
	Stationarity of the Probability Function	101
	Sediment Transport at Low Shear Stress	103
	Paintal's Experiments	103
	Interpretation of Helland-Hanson's Experiments	103
	Comparison of Concepts with Paintal Data	114

## TABLE OF CONTENTS (Cont. )

<u>Chapter</u>		<u>Page</u>
V	THE MOVEMENT OF SEDIMENT IN A GRAVEL BOTTOMED STREAM	120
	Bed Load Transport	121
	Transport Rate	121
	Grain Size of Bed Load Material	129
	Bed Load Transport and Stability Functions	150
	Bed Load Transport Model for Oak Creek	157
	Proposed Model	157
	Information Supporting the Model	161
	Divisions Between Bed Material and Suspended Load	172
	Suspended Sediment Load	176
	Interaction Between Bed Load and Suspended Load	179
	Conceptual Framework	179
	Supporting Data	185
VI	SUMMARY AND CONCLUSIONS	205
VII	BIBLIOGRAPHY	209
	APPENDIX I: BED LOAD DATA	212
	APPENDIX II: SUSPENDED LOAD DATA	227

## LIST OF TABLES

<u>Table</u>		<u>Page</u>
1	Durations of high flows in Oak Creek.	12
2	Representative particle sizes for armour material in Oak Creek near the sediment trap.	16
3	Summary of sizes for armour and bed material samples obtained in July 1971.	19
4	Size data for two bed material samples from upstream end of study reach.	24
5	Size data for two bed load samples obtained during the winter of 1971.	25
6	Comparison of water slopes upstream of weir/trap for trap closed and trap open.	52
7	Values of the Shields parameter suggested by various investigators.	65
8	Critical particle sizes for peak flows during 1971 sampling period.	81
9	Shields parameter for the Oak Creek armour layer.	89
10	Helland-Hansen data on long-term bed material movement at low flows.	105
11	Einstein and Shields parameters for the Helland-Hansen data.	112
12	Bed load sampling periods during Oak Creek study.	121
13	Bed load data for the November 13-14 1971 runoff event.	145
14	Suspended load data for the November 13 and 14 1971 runoff event.	147



## LIST OF TABLES (Cont.)

<u>Table</u>		<u>Page</u>
15	Increment weights of transported material for two sets of data used to compare falling limb to rising limb bed load transport.	163
16	Variation of bed load transport efficiency.	169
17	Suspended load data for the October 16-22 1971 period.	198
18	Bed load data for the October 16-22 1971 period.	198

## LIST OF APPENDIX TABLES

I-1	Bed load data for samples obtained during the winter of 1969-70.	216
I-2	Gradation data for bed load samples obtained in the winter of 1969-70.	217
I-3	Bed load data for samples obtained during the winter of 1971.	218
I-4	Gradation data for bed load samples obtained in the winter of 1971.	221
I-5	Bed load data for samples obtained during the fall of 1971.	222
I-6	Gradation data for the bed load samples obtained in fall of 1971.	224
I-7	Corrected bed load discharge for the fall 1971 samples.	225
II-1	Oak Creek suspended sediment concentrations, winter 1969-70.	228
II-2	Oak Creek suspended sediment data for the winter and spring of 1971.	229
II-3	Oak Creek suspended sediment data for the fall of 1971.	231

## LIST OF FIGURES

<u>Figure</u>		<u>Page</u>
1	Channel topography in late February 1970.	8
2	Locations of cross-sectioning stations and staff gages.	10
3	Sequential changes in cross-sectional shape at section 8, October 1969 to March 1971.	11
4	Change in cross-sectional shape at section 8 resulting from high flows during two winters.	13
5	Variation of $D_{35}$ size of armour layer along Oak Creek study reach.	18
6	Variation of median particle size of bed and armour material along Oak Creek.	21
7	Gradiation curves for Oak Creek bed material and bed load material.	23
8	Variation of maximum particle size along Oak Creek in the fall of 1970.	28
9	Relationship between Manning's "n" and river discharge for Oak Creek, 1971.	34
10	Schematic view of Oak Creek weir-and-sediment trap facility.	39
11	The bed load sampler.	40
12	Broad-crested weir and vortex-type sediment sampling system (weir/trap structure).	42
13	The pit cleaning tool.	46
14	Discharge capacity of the vortex bed load sampler.	48
15	Relationship between Froude number at upstream edge of weir/trap and stream discharge.	49

## LIST OF FIGURES (Cont. )

<u>Figure</u>		<u>Page</u>
16	Variation of Froude number with discharge during operation of the vortex bed load sampler.	50
17	Relationship between mean velocity at upstream edge of weir/trap and stream discharge.	53
18	Efficiency of sampling box; grouped samples.	57
19	Variation of sampling box efficiency with grain size for two bed load samples.	58
20	Weight of largest particle in a bed load sample compared to maximum discharge for the sample.	72
21	Maximum transported particle size as a function of shear stress.	73
22	Laboratory and field data on critical shear stress required to initiate movement of particles.	75
23	Bed load discharge as a function of stream discharge above a critical rate; 1971 data.	79
24	Discharge of bed material greater than $D_{35}$ of the armour layer versus river discharge greater than a critical discharge.	80
25	Critical shear stress for various sizes in a non-uniform armour layer.	87
26	Gessler's probability of grains to stay as part of armour coat, $q$ versus $\tau_c / \tau$ .	92
27	Gessler's data compared with theoretical relationship from Benedict and Christensen.	95
28	Probability of particles remaining in a bed, given the Shields parameter.	96
29	Kalinske's bed load equation.	100

LIST OF FIGURES (Cont. )

<u>Figure</u>		<u>Page</u>
30	Conceptual relationship between bed load transport rate and time for a constant stream discharge.	102
31	Gravel transport rate as function of mean stream flow rate during period.	106
32	Grain size distribution curves for gravel bed and transported material.	109
33	Shields parameter versus Einstein bed load transport parameter for the Helland-Hansen data.	111
34	Shields parameter versus Einstein bed load transport parameter for Paintal series "A".	116
35	Shield's parameter versus Einstein bed load transport parameter for Paintal series "B" and "C".	117
36	Bed load in Oak Creek as a function of water discharge, winter 1969-70.	123
37	Bed load in Oak Creek as a function of water discharge, winter 1971.	124
38	Bed load in Oak Creek as a function of water discharge, fall 1971.	125
39	Bed load discharge versus stream power, winter 1971 samples from Oak Creek.	127
40	Median size of bed load material versus stream discharge, winter 1969-70.	130
41	Median size of bed load material versus stream discharge, winter 1971.	131
42	Variation of mean size of bed load samples with discharge, 1971 samples 1-9.	134

## LIST OF FIGURES (Cont.)

<u>Figure</u>		<u>Page</u>
43	Variation of mean size of bed load samples with discharge, 1971 samples 10-32.	135
44	Variation of mean size of bed load samples with discharge, 1971 samples 32-43.	136
45	Variation of mean size of bed load samples with discharge, 1971 samples 42-48.	137
46	Variation of mean size of bed load samples with discharge, 1971 samples 48-58.	138
47	Variation of mean size of bed load samples with discharge, 1971 samples 59-66.	139
48	Variation of mean size of bed load samples with discharge, fall 1971 samples.	142
49	Variation of mean size of bed load samples with discharge, all 1971 samples.	144
50	Hydrograph of the November 13-14, 1971 runoff event, showing bed load and suspended load sampling schedule.	146
51	Gradation curves for bed load samples 110 and 111, fall 1971.	149
52	Comparison of winter 1971 Oak Creek data to Einstein bed load function for Assumption 1.	152
53	Comparison of winter 1971 Oak Creek data to Einstein bed load function for Assumption 2.	154
54	Comparison of winter 1971 Oak Creek data to Einstein bed load function for Assumption 3.	155
55	Comparison of winter 1969-70 Oak Creek data to Einstein bed load function using Assumption 3.	158

## LIST OF FIGURES (Cont.)

<u>Figure</u>		<u>Page</u>
56	Comparison of all winter Oak Creek bed load data to the Einstein bed load function using Assumption 3.	159
57	Comparison of bed load transport of rising and falling limbs of hydrographs.	162
58	Comparison of bed load transport on a falling limb and after a period of steady low flow.	167
59	Specific information for early 1971 bed load data (to March 10, 1971).	168
60	Specific information for bed load data for March 10-11, 1971.	171
61	Particle diameter forming the division between bed material load and suspended load.	174
62	Suspended load discharge in Oak Creek (winter 1971).	177
63	Variation of bed load to suspended load ratio with discharge (winter 1971 data).	178
64	Conceptual variation of suspended load with a step increase and decrease in stream discharge.	184
65	Suspended sediment data in groups by period of sampling.	187
66	Suspended sediment load curves superimposed from Figure 65.	189
67	Suspended sediment load for the "empty reservoir" case.	190
68	Suspended sediment load in the fall of 1971.	192

## LIST OF FIGURES (Cont.)

<u>Figure</u>		<u>Page</u>
69	Bed load discharge versus stream discharge - winter 1971 (prior to 10 March ).	193
70	Bed load discharge versus stream discharge, fall 1971.	195
71	Hydrograph for October 16-22, 1971, showing bed load and suspended load sampling schedule.	197
72	Path of the suspended load versus discharge relationship during two runoff events, fall 1971.	200
73	Suspended sediment concentration versus discharge, November 7-16, 1971,	201

# SEDIMENT TRANSPORT IN A GRAVEL-BOTTOMED STREAM

## I. INTRODUCTION

Over the last century, tremendous progress has been made in understanding the nature of sediment transport. Studies have been made both in the field and in the laboratory. These studies have resulted in an understanding of many facets of the movement of sediment by water. Nevertheless, many aspects of sediment transport are not understood and need to be investigated further. One such poorly understood facet is investigated in this dissertation.

### The Problem

Numerous watershed studies have been made with the objective of developing an understanding of the effect of land use on the yield of sediment from the watershed. In most watershed studies, only the suspended load had been measured. The measured suspended load was then related to land use. If the stream is in an alluvial bed, the measured suspended load is from two principle sources - the fine material "washed" in from the watershed, and the material in suspension from the bed. The first source reflects the nature of the watershed and the availability of fine material and the second source is related to the nature of the bed material and the nature of the flow in the channel.



In most watershed studies the bed load of the stream is not measured. However, a number of theories have been developed to calculate the bed material load of a stream. Much of the work has been in the laboratory under stringently controlled conditions. Some work has also been done in the field, most of it on streams with sand beds. The basic problem with any type of field study of bed material transport is that the measurement of bed load had proved to be very difficult. Thus, no general satisfactory method for all types of streams has been developed. As a result, theoretical and empirical methods have been developed in order to estimate the bed load.

Examples are the Einstein method of calculating the bed material load of a stream on the basis of the ratios of the bed shear stress to a particle control shear stress, the Colby 'method' of relating the total bed material load to the amount and size distribution of suspended material transported, and the method used by Yalin based on excess shear stress. In each case a basic but implicit assumption is that the bed material is homogeneous with depth. But not all stream beds are homogeneous with depth; consequently, the existing methods of estimating bed material transport are not always applicable.

Many of the watershed studies were made in regions where the bed material of the stream is gravel and is non-homogeneous with depth. Also, many streams in the Northwest have bed materials that are very non-homogeneous with depth. Three example streams

examined by the writer are Oak Creek and Deer Creek in the Oregon Coast Range, and the Warm Springs River in Central Oregon. In each case the upper-most layer is considerably coarser than the material directly below it. This upper layer is generally referred to as an armour layer,

The problem at hand is to develop some concepts which describe in a qualitative and semi-quantitative manner the nature of the sediment transport in the case where an armour layer is present. The ultimate goal is to be able to calculate the bed material load of a stream having an armour layer,

The importance of understanding the sediment transport system in an armoured stream is related to two factors: (1) the difficulty in evaluating the considerable variation in suspended load in an armoured stream; and (2) the fact that many of the spawning areas for anadromous fish are in streams with an armoured bed.

The field research reported on here was carried out on Oak Creek, a small stream located in the east central part of the Oregon Coast Range near Corvallis, Oregon.

### The Research Program

The research program was based on the concept that a reach of a stream be studied in considerable detail with an objective of understanding the basic mechanisms involved in the movement of the bed

material. The bed material load was measured using a "vortex sampler" (described later) which sampled the total bed load during the period of sampling. The suspended sediment was measured using standard techniques. The bed material in the stream was studied extensively and the hydraulic properties of the study reach were determined.

The initial part of the research program involved the development and construction of the vortex bed load sampler. The sampler was constructed during the summer of 1969. During the winter of 1969-70, the bed load was sampled. The bed material, hydraulic properties of the reach and of the sampler, and related aspects were also studied during 1969-70. As a result of the knowledge gained from these studies, a more intensive research program was developed for the winter of 1970-71 and fall of 1971. As information was acquired about the sediment transport system in a gravel bottomed with an armour layer, the research program was modified and improved.

## II. THE STUDY AREA

To develop an understanding of sediment transport in a gravel-bottomed stream, a bed load sampler was constructed on a stream located just outside of Corvallis, Oregon. Information on the stream, including its watershed, channel, and bed material, are presented in this chapter.

### The Watershed

Oak Creek is a small creek located in McDonald State Forest near Corvallis, Oregon. The watershed is located on the eastern edge of the Coast Range. The drainage area tributary to the reach studied is approximately 2.6 square miles. The terrain ranges in elevation from 480 feet (MSL) to 2178 feet for a basin relief of 1700 feet. The channel length is 2.2 miles and the ratio of basin relief to channel length is 0.15 foot/foot. The channel slope in the study area is 0.014 foot/foot. The mean annual precipitation is approximately 50 inches.

The mean annual runoff is estimated to be 18 inches, which is an average mean annual discharge of 3.5 cubic feet per second (cfs). The instantaneous peak discharges in the water years 1970 through 1972 were:

1970	215 cfs
1971	300 cfs
1972	225 cfs

for an average instantaneous peak discharge of 247 cfs. The lengths of time that flows were greater than 40 cfs during the same period were:

1970	329 hours
1971	292 hours
1972	236 hours

for an average of 252 hours per year which is about 3 percent of the total time per year. The writer's subjective estimate is that at least 98 percent of the sediment transported by Oak Creek is transported when the flows are greater than 40 cfs.

The watershed is a Douglas Fir forest with meadows and with some clearcut patches. The geologic formation in the watershed is the Siletz River Volcanics of Eocene age, with the earth materials in the watershed being dense basalts and their weathering products (Snively et al., 1968).

#### The Channel

The bed material of the stream is predominantly gravel. An armour layer exists for the bed, such that the top layer of particles is of nearly uniform distribution. The material below the armour layer is small and is usually well graded.

A plan view of the study reach upstream of the bed load sampling station is given on Figure 1. The topography of the stream bed in February, 1970, is also shown. The general form of the bed has remained essentially the same during the study period (Fall 1969 to Spring 1972) although there has been considerable local change in the bed during this time.

Just downstream of the weir/trap structure, there is a deep pool which is 10 to 12 feet deep during low flow (14 to 16 feet deep during high flows). Below the pool, the stream makes a series of meanders for about 300 feet and then is relatively straight for about 800 feet. Any particle leaving the study reach must pass through the deep pool. Studies of the bed material along the stream indicate that the pool traps particles greater in size than about 3 inches (median diameter) and permits the smaller particles to pass on downstream. Debris jams occur at distances of about 20 feet and 60 feet downstream of the weir/trap. The jam at 60 feet downstream is quite large. In the fall of 1970, Maccaferri gabions were installed at 39 feet and 87 feet below the bed load sampler. The spaces behind the gabions filled during the first major storm following their placement, but another hole developed upstream of the first gabion between it and the sampler. This hole was then stabilized in location with another gabion and remained stable during the study period.

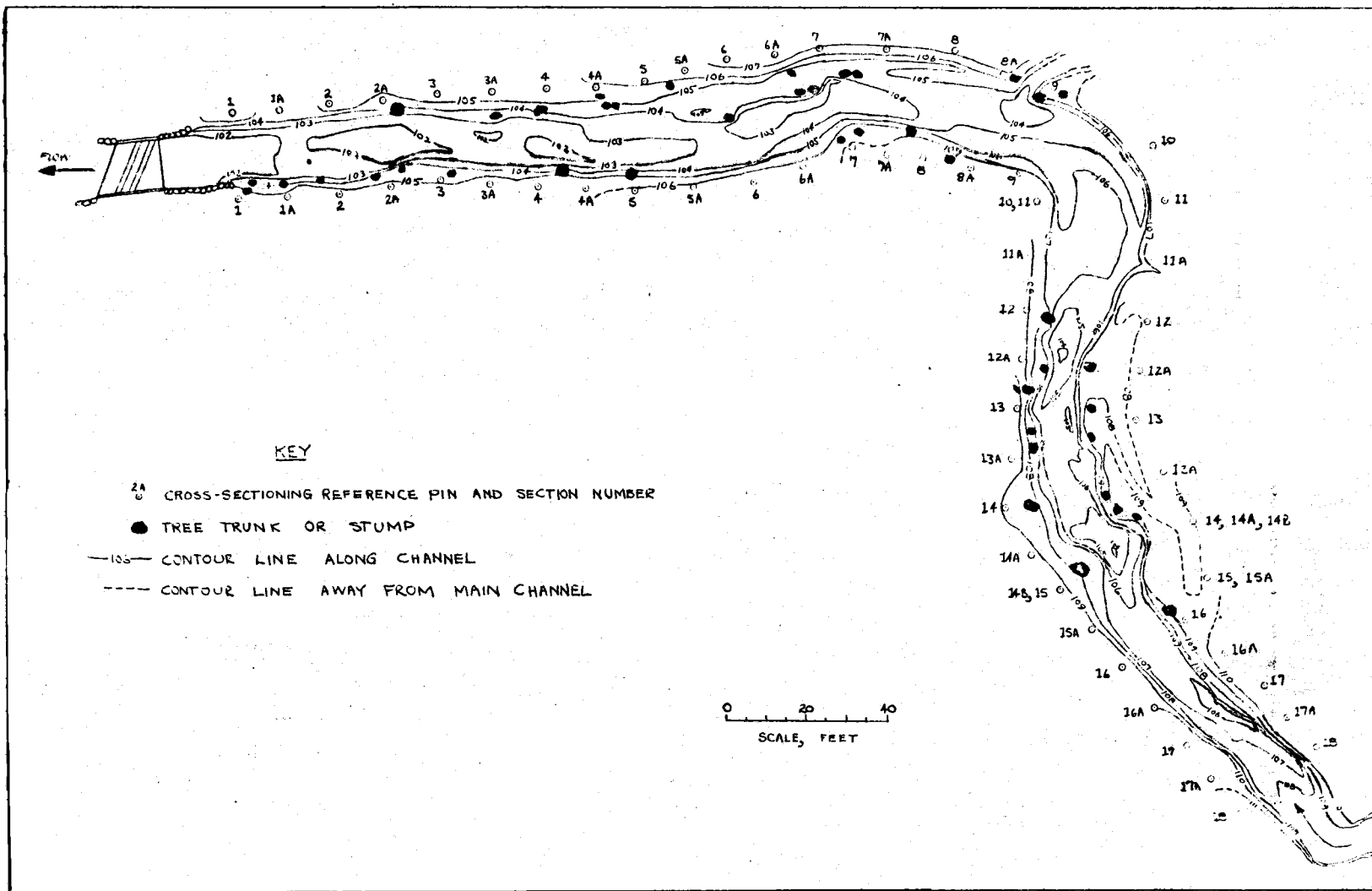


Figure 1. Channel topography in late February 1970.

In order to determine the hydraulic properties of the study reach, staff gages were located along the reach and permanent cross section stations were established. The locations of these are shown in Figure 2.

The main study reach is the reach between staff gage 3 (cross section 6A) and the bed load sampler. The hydraulic radius for the reach was estimated with data from the measured cross sections, using a procedure similar to that given by Einstein (Einstein, 1950). The reference section is staff gage 2. The equation for the hydraulic radius is  $R = 0.63(E - 102.3)$ , where  $R$  is the hydraulic radius, and  $E$  is the elevation of the water surface at staff gage 2 relative to the study datum. The equation gives a hydraulic radius that is representative of the study reach rather than being an exact hydraulic radius for some given point.

The bottom width of the channel averages about 12 feet and most of the bed material movement occurs in this region. When a transport rate per unit width of channel is given in this thesis, it is based on a width of 12 feet.

Measurements of cross-sectioned shape were repeated several times during the study period. This permitted investigation of the variation of the shape of the cross section over time. Figure 3 shows the changes in one cross section in the study reach resulting from intervening stream discharges which were adequate to move the armour



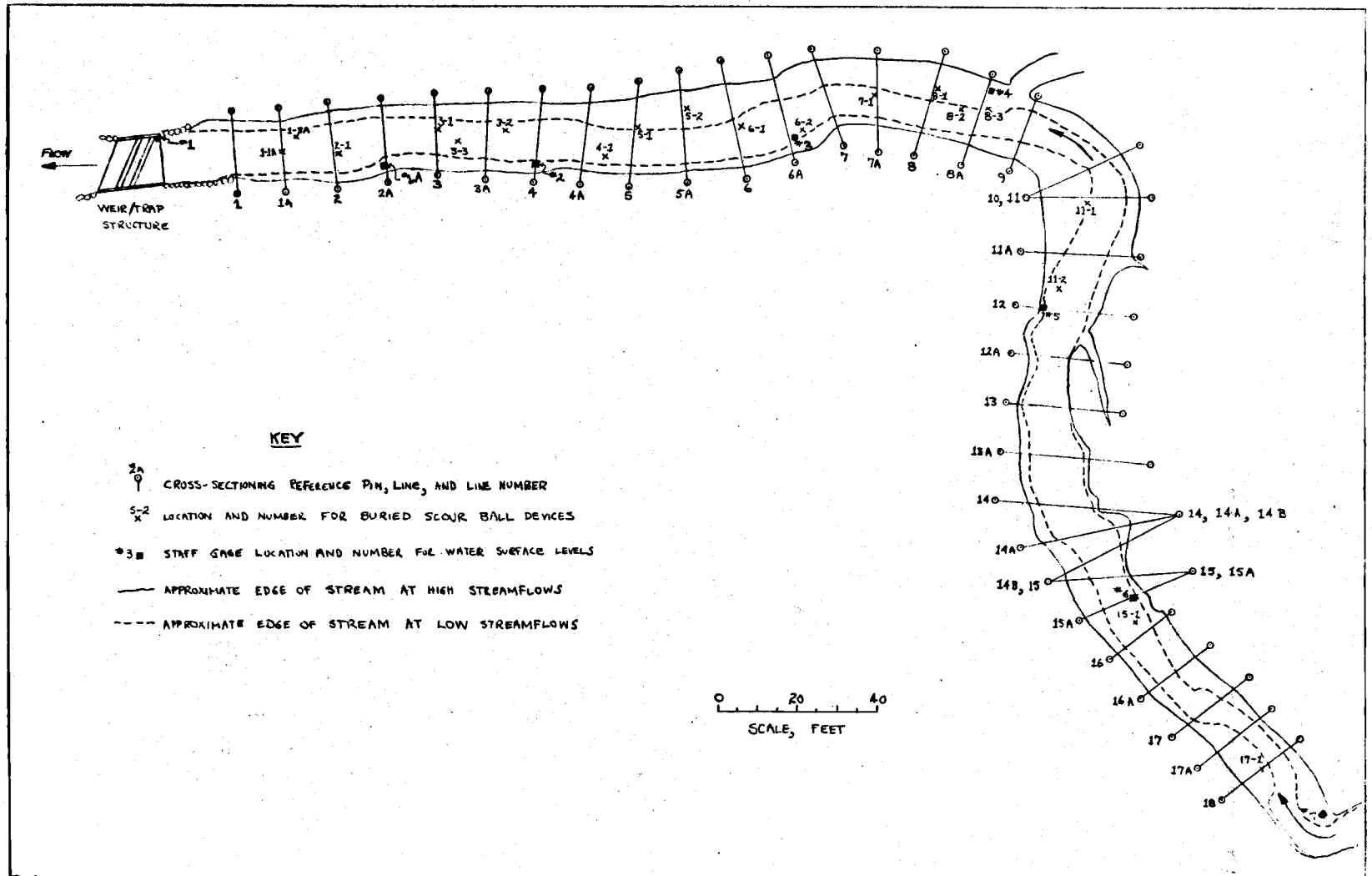


Figure 2. Locations of cross-sectioning stations and staff gages.

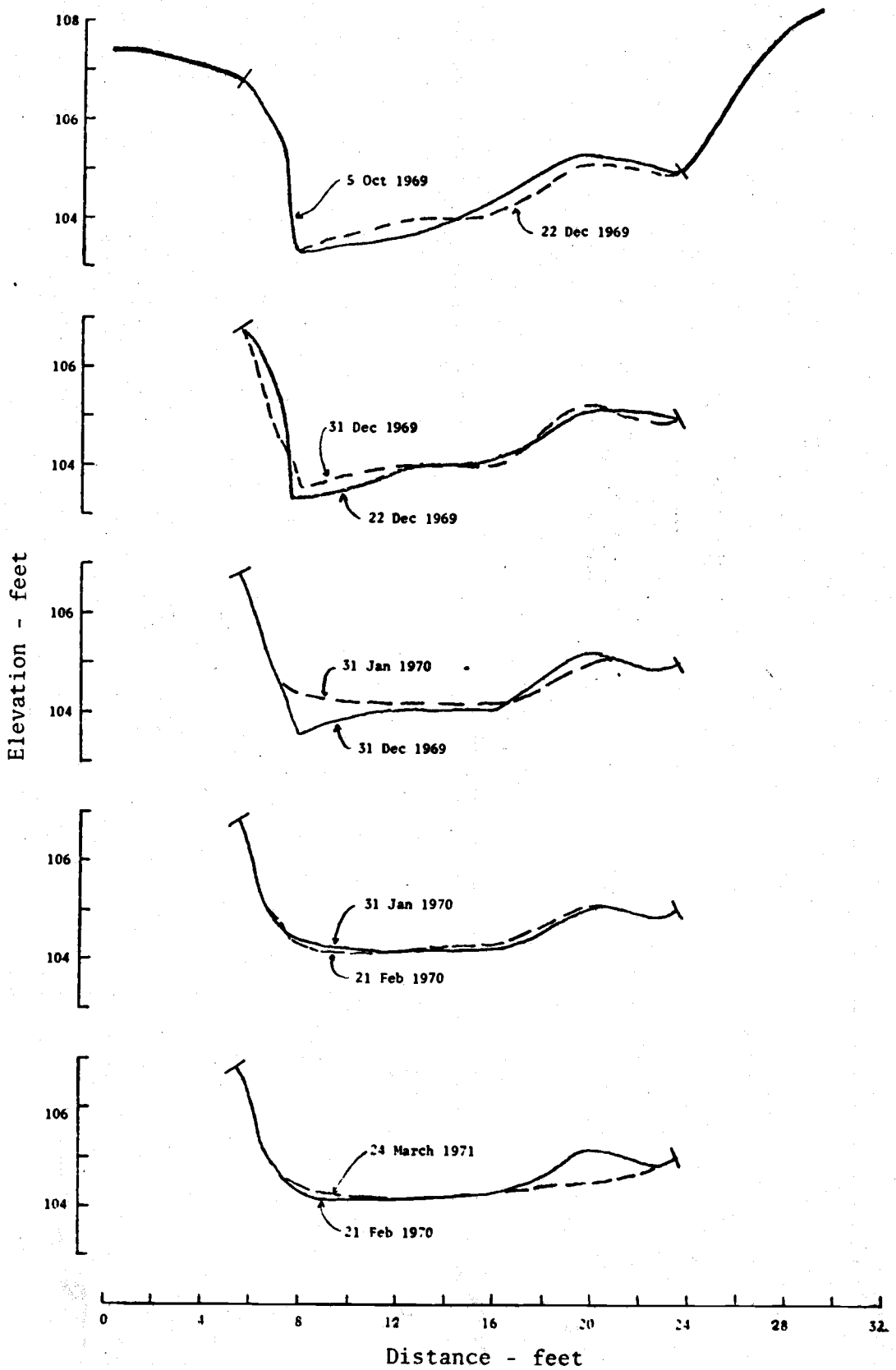


Figure 3. Sequential changes in cross-sectional shape at section 8, October 1969 to March 1971.

layer. The first four overlay drawings for measurements of the cross section show changes resulting essentially from individual storms or storm groups. The fifth overlay of measurements shows the net change during the following winter (1970-71). Information on the duration of flows which could move the armour layer is given in Table 1. However, it is not possible to relate the change in the cross section to the duration of any given level of flow.

Table 1. Durations of high flows in Oak Creek.

Period	Time, in hours, that streamflow exceeded:			Instantaneous peak flow, cfs
	40 cfs	70 cfs	100 cfs	
5 Oct 1969-22 Dec 1969	24	13	2	115
22 Dec 1969-31 Dec 1969	8	2	0	76
31 Dec 1969-31 Jan 1970	273	81	23	215
31 Jan 1970-21 Feb 1970	24	14	3	144
21 Feb 1970-24 Mar 1971	280	134	69	300

cfs = cubic feet per second

The net change in cross-sectional shape at one cross section over two wet winters is given in Figure 4. As is shown, the change is quite pronounced. In October, 1969, a group of styrofoam balls were placed under rocks of the armour layer at this cross section at the edge of the low water channel, 8 feet out from the reference station on the bank. In January 1972, after a period of high streamflow, three of the balls were found underneath armour particles at this location. Apparently these armour particles had been buried by the

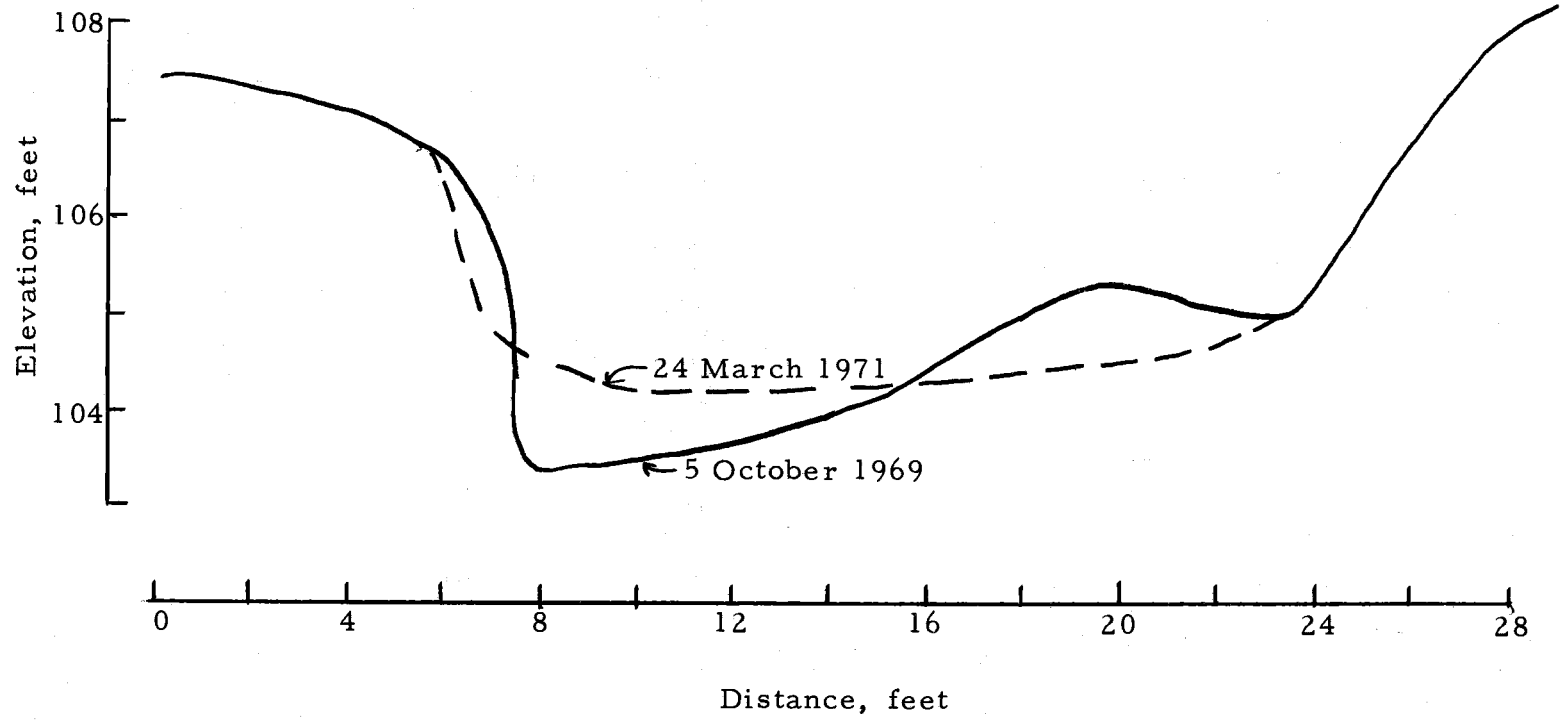


Figure 4. Change in cross sectional shape at section 8 resulting from flood flows during two winters.

first storm runoff in the fall of 1969. The depth of burial was about 1.2 feet by March 1971 (see Figure 4). This 1.2 feet of deposit was then removed between March 1971 and January 1972.

The amount of scour during an individual storm runoff event has been estimated using perforated buried ping pong balls. In general, the maximum scour during bed load movement exceeded the net scour over the runoff period by 0.2 to 0.3 feet if the bed had been disturbed during the high flow. There were areas with only deposition during the storm runoff, areas where there was not refill after scour, areas with no scour or fill, and areas with both scour and fill. In terms of sediment transport, there were areas acting as sinks where material was lost, areas acting as sources, areas where the only transport feature was that the transported material was moved over the area with no movement of the material in place, and other areas where the bed was actively involved in the transport process.

The channel consists of a sequence of pools and riffles, although the principal study reach is mostly riffles or transitional with a few pools. In order to obtain some idea on the movement of individual particles in the channel, a set of experiments was conducted during the study which traced the movement of individual particles. In order to do this, particles of the stream bed material were collected, painted yellow, and placed in one group in the stream bed. After the next period of storm runoff and bed load transport, their

new locations were determined. Following the first period of high flow after the particles were placed, the recovery rates were often low due to burial of some particles during transport. But each successive storm usually exposed or brought additional yellow particles to the surface. The highest recovery rates have been for particles of the same size as the armour material and lowest recovery for the smaller particle sizes not often found in the armour layer. The inference from these studies is that individual particles will be transported as bed load and then redeposited in the bed--sometimes at the surface and sometimes at some depth. The distances of travel have been quite variable and the individual particles became dispersed over a considerable length of the stream.

One of the "painted rock" studies provided information on the development of the bed structure. In this experiment a group of yellow particles, all of gravel size, were placed in the stream bed at the downstream end of a riffle near cross section 17. After a period of high flow the stream was searched for yellow particles but few particles from this group were found. At the site where the particles had been placed initially, a yellow rock was observed that was nearly buried. In the process of removing this rock a large number of yellow particles were found buried from 2 to 6 inches below the surface. Apparently the riffle was moving downstream and had covered the yellow particles, although there was evidence that they had been moved

enough to cause the larger particles to be near the top of the bed and the smaller ones a short distance below the bed surface.

### The Bed Material

The bed material of the study reach has been studied in considerable detail. Samples of the armour layer were obtained at intervals during the study period and samples of the material below the armour layer were obtained in 1971. The particle shapes are blocky.

There is considerable variability of median particle size with time and with location along the stream. This can be seen from Table 2 where, for the 175-foot reach immediately upstream of the sediment trap, the median size and the range of the median value for the armour layer (based on samples taken at many points within the reach) at different times are shown. Most of the bed load samples discussed later in this paper were obtained when the median size of the armour layer was 6.3 centimeters (cm).

Table 2. Representative particle sizes for armour material in Oak Creek near the sediment trap.

Date	Median Size for Grouped Samples, cm	Range of Median, Size of Samples, cm	D <sub>65</sub> cm	D <sub>35</sub> cm	D <sub>65</sub> /D <sub>35</sub>
26 October 1969	4.8	4.3 - 5.0	5.8	4.1	1.42
26 October 1970	5.2	4.6 - 6.3	5.9	4.3	1.37
29 January 1971	6.3	4.3 - 8.4	7.3	5.2	1.43
27 July 1971	6.3	4.5 - 7.6	7.4	5.2	1.42

The particle size such that 35 percent of the material is finer ( $D_{35}$ ) is often taken as the representative grain diameter for bed load transport. The variation with time of  $D_{35}$  for the stream bed armour layer is shown in Table 2 and its variation with location along the channel is shown on Figure 5. As may be seen in Table 2, the mean  $D_{35}$  for the January 29 and July 27 samples was 5.2 cm.

The mean  $D_{35}$  size for 1969-70 sampling period was 4.2 cm. Almost all of the bed load samples obtained during 1971 were obtained when the mean  $D_{35}$  size of the armour layer was 5.2 cm. The samples obtained at the start of 1971 when the mean  $D_{35}$  size of the armour layer was 4.3 cm were for flows of less than 16 cubic feet per second (cfs). In Figure 5, station 0 is about 20 feet upstream of the trap. The seven samples between stations 0 and 175 feet were used in determining an average value for  $D_{35}$  (and the  $D_{50}$  presented previously). Only four samples were obtained in this section on October 26, 1970; consequently, the sample base is not the same for the October 26th samples, as for the other two sets of samples.

During the earlier part of the study period the bed material below the armour layer was not sampled extensively. For three samples obtained in the upstream part of study area (from 350 to 426 feet upstream of the trap) and for one sample taken about 400 feet downstream of the trap, the median size obtained was 2.4 cm (the sample medians ranged from 1.3 cm to 4.5 cm), less than half that of the



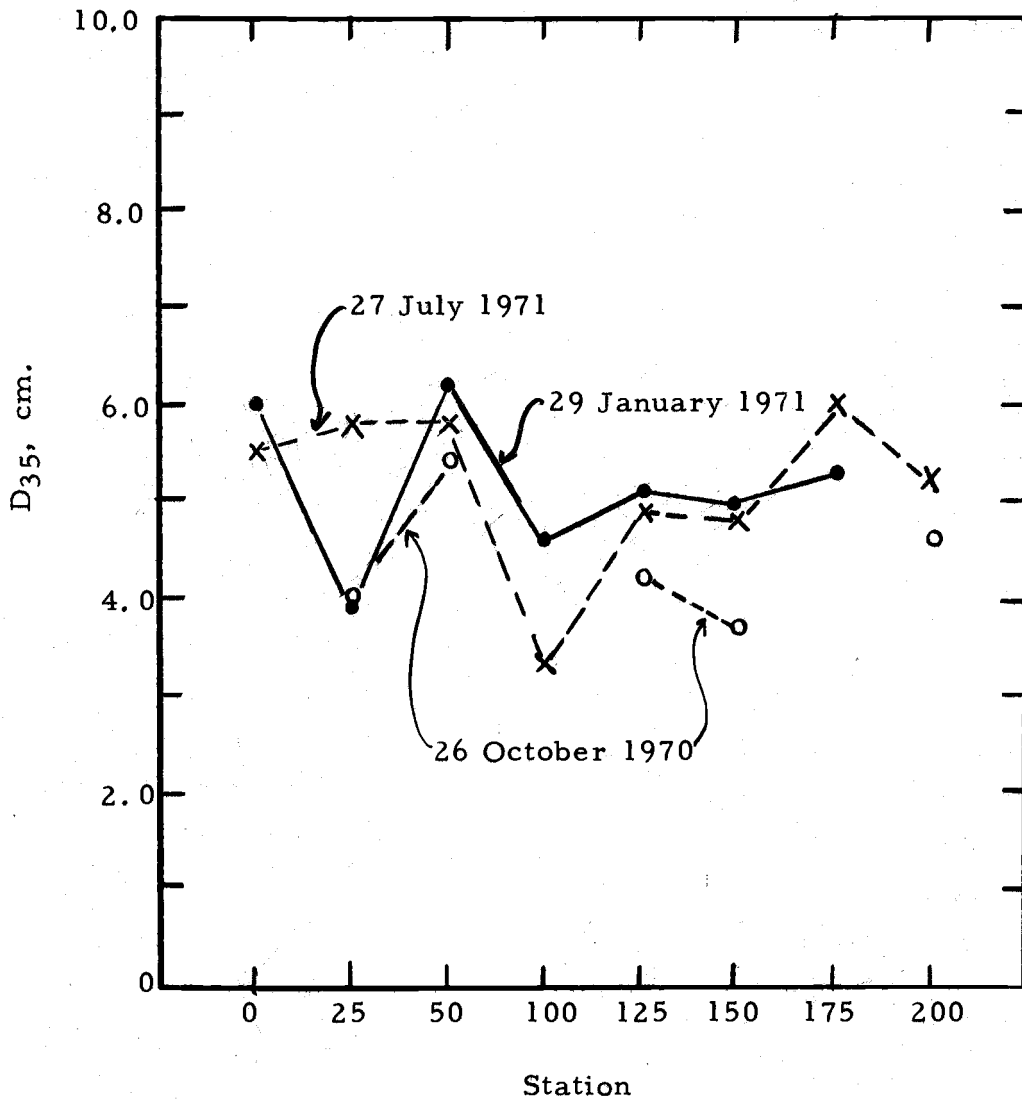


Figure 5. Variation of the  $D_{35}$  size of the armour layer along the Oak Creek study reach.

armour layer. The  $D_{35}$  size was 1.8 cm (ranging from 0.7 to 3.5 cm).

In July 1971, samples of the armour layer and the material below the armour layer were again obtained. Both the armour layer and the material below the armour layer are the bed material of the stream, but for convenience the terminology being used here is "armour layer" or "armour material" for the armour layer and "bed material" for the material below the armour layer. The armour layer samples were obtained using a different technique than in the earlier work and the bed material samples were obtained using a sampler described by McNeil and Ahnell (1964). A summary of these data is given in Table 3. The data for the bed material indicate the bed material below the cross layer in the study reach has a median size of 2 centimeters compared to a median size of 6 centimeters for the armour layer compared to 6.3 cm from Table 2. As stated previously the data in Table 3 was obtained using a slightly different technique than for the data in Table 2.

Table 3. Summary of sizes for armour and bed material samples obtained in July 1971.

Size	Average*		Limits			
	Armour	Bed	Armour		Bed	
	cm	cm	Maximum cm	Minimum cm	Maximum cm	Minimum cm
D10	3.2	0.16	4.0	2.8	0.17	0.16
D35	5.2	0.86	5.6	4.6	0.94	0.98
D50	6.0	2.0	6.4	5.3	2.3	1.4
D65	6.8	3.3	7.2	6.1	4.0	2.9
D90	8.6	6.5	9.8	8.0	8.0	5.1
D65/D35	1.31	3.84	---	---	---	---

\* Calculated using the data for samples from cross sections 1, 3, 5 and 7.

Note: Measurement error is estimated to be  $\pm 10$  percent.

An investigation was made in the fall of 1970 to determine if the particle size of the bed material decreases in the downstream direction. In making this study samples of the bed were obtained at several locations over a total distance of about 3000 feet. The bed material is structured such that the particles at the very surface are larger than the particles found just below the top layer.

At each sampling point the armour layer was first sampled, followed by the material below the armour layer. It was observed that the material below the armour layer also was structured in that the first few inches encountered contained more larger particles than the next four to six inches. The median sizes of both the armour layer and the bed material have been determined and plotted versus location along the stream; these are given in Figure 6.

The ratio of the size for which 65 percent of the material is finer ( $D_{65}$ ) to the size for which 35 percent of the material is finer has been determined and shown next to each sample point in Figure 6. One interesting observation is that the two bed material samples which have median sizes much larger than the majority also have much smaller  $D_{65}/D_{35}$  ratios. In fact, the median size and the  $D_{65}/D_{35}$  ratio for the samples with  $D_{65}/D_{35}$  ratios of 1.3 and 1.6 are more nearly those of the armour layer than of the bed material.

The graphed results indicate the median size of the armour layer tends to decrease in the downstream direction, except for the

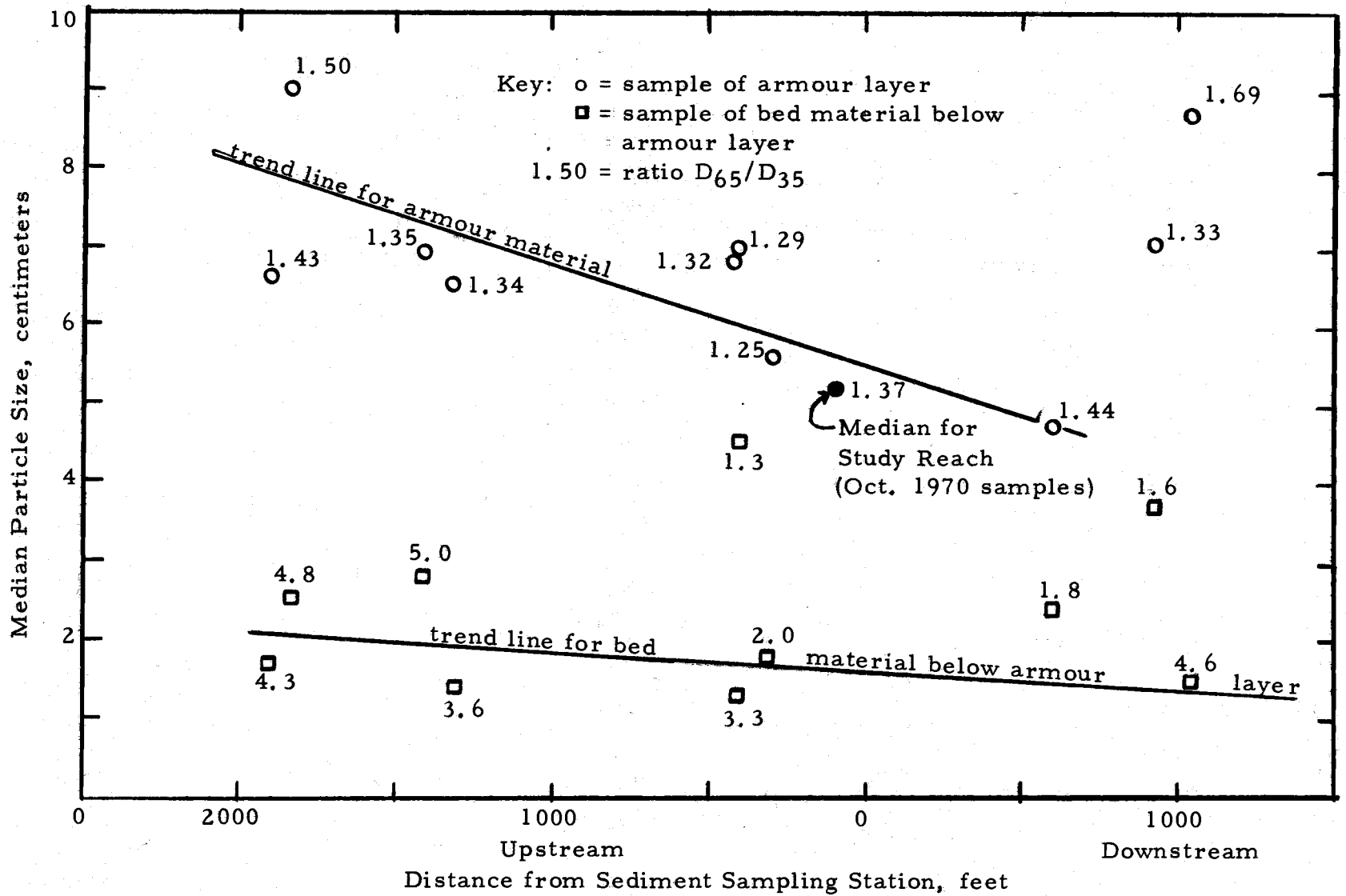


Figure 6. Variation of median particle size of bed and armour material along Oak Creek.

fact that at about 1000 feet below the sediment sampling station the median size increases, as will be discussed later. Excluding the two downstream samples, a line of best fit may be drawn to show this trend.

The median size of the bed material samples are much more scattered than for the armour samples. If a line is drawn that best fits the data for bed material points with  $D_{65}/D_{35}$  of 2 or greater (as was done in Figure 6) it is seen that there is a trend line showing a general decrease in median bed material size. But the rate of decrease in median size with distance is less than for the armour material. Also, there is no increase in the median size at a distance of about 1000 feet below the sediment sampling structure. Evidently, the increase in size there was confined to the armour material.

The cause of the increase in median size with a decrease in  $D_{65}/D_{35}$  ratio can be studied by looking at the two samples obtained from locations 409 and 416 feet upstream of the sediment sampling station. These two samples were thus obtained within about seven feet of each other. One of the samples had a  $D_{65}/D_{35}$  ratio of 1.3 and the other a ratio of 3.3. The armour layers of the two samples were essentially the same, differing only slightly and within the limits of measurement error. The grain size distribution curves of these two samples are presented in Figure 7 and the various characterizing sizes used in sediment transport calculations are given in Table 4.

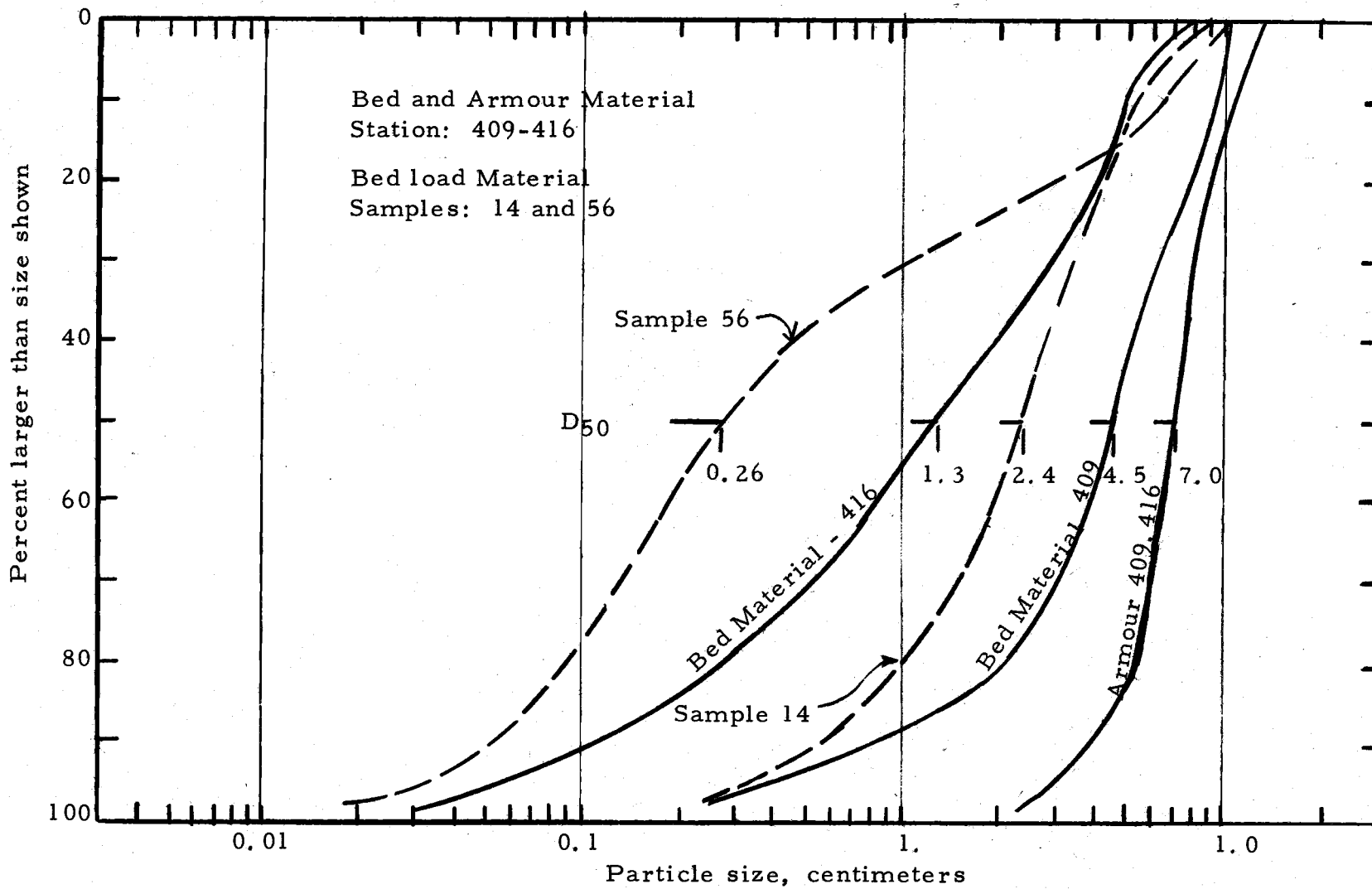


Figure 7. Gradation curves for Oak Creek bed material and bed load material.

The bed material samples were taken in an area where a bar was in the process of forming and where the turbulence of the stream could be very strong during periods of high flow with the result that fine particles would not be deposited. Another way of looking at this is to say that the material was deposited when the bed load discharge rate was high and much of the sand material in suspension; consequently, only the coarser fraction of the bed material load was deposited.

Table 4. Data for two bed material samples from upstream end of study reach.

Size	Armour cm	Bed Material	
		409* cm	416* cm
D <sub>90</sub>	10.0	9.0	4.9
D <sub>65</sub>	7.8	5.6	2.3
D <sub>50</sub>	6.9	4.5	1.3
D <sub>35</sub>	6.0	3.5	0.7
D <sub>10</sub>	4.2	0.8	0.13
D <sub>65</sub> /D <sub>35</sub>	1.30	1.60	3.29

\* Distance upstream of the sediment sampling station

To further pursue this idea, we can look at size distribution curves for bed load samples obtained at the sediment sampling station about 410 feet downstream. Data on two of the samples are given on Figure 7 with size information in Table 5. One of these is for bed load sample 56, obtained during a period of moderate discharge (62 cfs) and bed load transport rates (43 kilograms per hour [kg/hour]). The material is much finer than either of the bed material samples. The

particle size distribution curve for bed load sample 14 when material was transported at a higher discharge (120 cfs) and a much higher bed load rate (1175 kg/hour) is also shown on Figure 7. As shown, the curve occurs between the two bed material samples and represents a coarser bed load than at the lower stream discharge.

Table 5. Size data for two bed load samples obtained during the winter of 1971.

Size	Sample 14 cm	Sample 56 cm
D <sub>90</sub>	5.6	6.2
D <sub>65</sub>	3.1	0.61
D <sub>50</sub>	2.4	0.26
D <sub>35</sub>	1.9	0.16
D <sub>10</sub>	0.6	0.056
D <sub>65</sub> /D <sub>35</sub>	1.63	3.81
Stream Discharge, cfs	120	62
Bed Load Discharge, kg/hour	1175	43

If the local bed shear stress was sufficient to disturb the armour layer and material below the armour layer but not sufficient to move the large particles out of the general area, but instead forms a bar, than the fines would be transported and effectively removing them from the bed material at the bar. Both samples contain coarse particle sizes that could be left behind to form a bar with the fines being removed by turbulence in the stream. The rate of bar formation would vary depending on the bed load transport rate, but either rate could build a bar which is void of the finer fraction of particles if the



flow conditions were right. Consequently, it is not possible to say at what rate of bed load transport a bar would form. Cary (1951) described openwork gravels (gravels deposited with large voids) found in alluvial deposits and in present day rivers in the northwest. The writer has observed openwork gravel in alluvial deposits in Southern California. It appears probable that the uniform bar deposits and Cary's openwork gravel have similar origins. Cary's view is that "A vortex, forming at the downstream face of a bar, would lower the hydraulic pressure at the bar face, and would cause a movement of water outward from within the interstices of the gravel bar." The outward flow force would prevent sand and fine gravel from being deposited in the downstream face of the bar. In a paper on intragravel flow, Vaux (1968) concludes, on the basis of analytical studies, that the flow of water is outward on the downstream face of a riffle or bar. This supports Cary's idea on the origin of openwork gravels.

The sample at 600 feet below the sediment sampling structure was obtained from a bar deposit formed behind a debris dam in the creek. The turbulence would likely be of lesser intensity in such a location than on the downstream face of a bar. The median size would be expected to be smaller and the  $D_{65}/D_{35}$  ratio larger than for a bar face. This is the case observed. Unfortunately, no supplemental information was obtained on the hydraulic environment at the site where a  $D_{65}/D_{35}$  ratio of 1.6 was found at a location 920 feet

downstream of the sediment sampler.

The main idea to be derived from the foregoing discussion is that a bar could be formed with larger and more uniform material than the usual bed material and that the bed material is not uniform within a reach but is variable depending on the hydraulic environment.

Now, we can return to the problem of the increase in median size of the armour material about 1000 feet below the sediment sampling station. After it was determined that there was an increase in the median size of armour layer over a short distance within the study reach, a study was made to determine the variation in the largest particle found over a 4100 foot section of Oak Creek spanning the study reach. The procedure used was to determine the weight of the largest particle found at intervals of 100 feet along the reach, with a few particles also being measured at intermediate points. The results of the study are presented in Figure 8.

Two features are immediately noticed from the information on Figure 8. First, there is a general tendency for the maximum particle size to decrease with distance downstream. Second, there is (with the exception of a single particle at station 2620 feet) a decrease in maximum particle size for a distance of about 2000 feet between station 1500 and 3500; then seven points within a distance of 400 feet that are considerably above the trend line. The particle at station 2620 feet was almost buried while all of the others were on the surface;

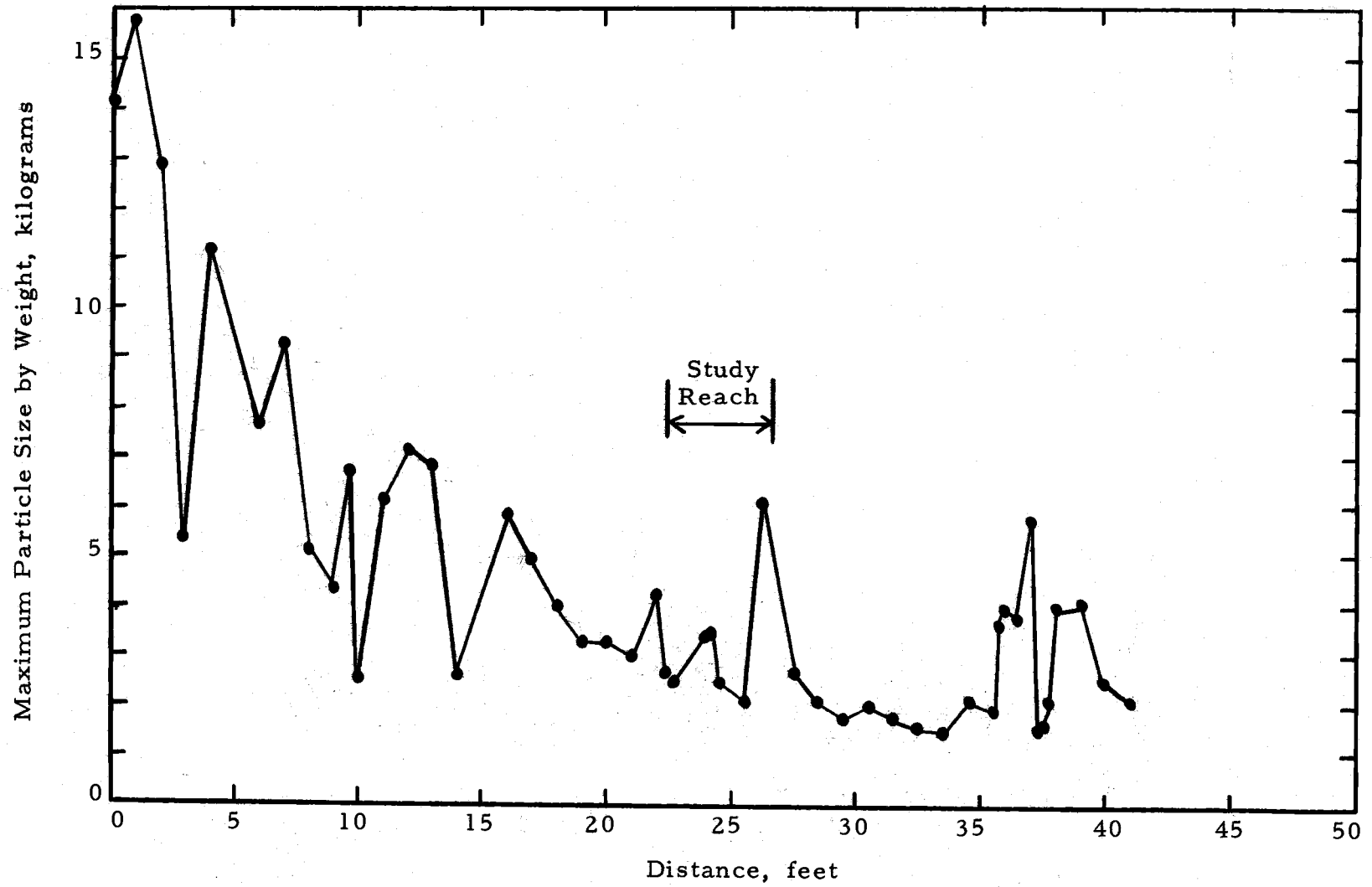


Figure 8. Variation of maximum particle size along Oak Creek in the fall of 1970.

hence, the particle is not typical of the armour particles in the immediate surrounding area (in fact, that particle is not entirely a part of the armour layer) while all of the other particles sampled are only slightly bigger than others in the area from which they were obtained and were definitely part of the armour layer.

The cause of the increase in mean size of the armour layer near the lower end of the reach examined is not known but there are two likely possibilities. One is that there is a source area of bed material nearby. The problem with this explanation is that the banks do not appear to be eroding, which suggests that this explanation is probably not applicable. The second possible cause is that the sediment transport system is not constant over time and at times transports larger particles as waves through the system or includes temporary "sinks" for large particles in the system. The first idea just mentioned is based on a possibility that larger particles tend to be left behind if the flow is not strong enough to move them. For instance, the particle at station 2620 feet has been estimated to have a critical discharge of 140 cfs (using Shield's criteria [1936] and the hydraulic properties of the reach where the particle was located). A discharge of 140 cfs in this part of Oak Creek has a return period of five years, on the average; so this particle might be moved with a five-year return period while the armour layer as a whole will probably be moved at least once each year. Consequently, the larger particles are likely

to remain in place and work their way into the material below the armour layer by removal of material from around the large particles. Evidence of the reverse of this type of action is available; a long period (61 hours) of flow greater than 100 cfs caused the median and  $D_{90}$  particle sizes in the study reach to increase, which suggests that the large particles may have been returned from the bed material to the armour material. If the model described above is correct, then a period of less severe storm runoff should result in the larger particles returning to the bed material. Consequently, the fact that larger particles are found below the sediment sampling structure could also be related to the past history of storm runoff which may have caused enough larger particles to reach the area that some of the larger particles have remained in the armour layer.

Another possible explanation is that a large and deep pool of recent formation just below the sampling structure could act as a sink for particles above some weight or size and that the pool did not exist at the time when the larger particles found downstream were transported past the site of the present pool. There is no way to confirm this idea for the study area.

The information given in the previous paragraphs illustrates that sediment movement and the dynamics of the stream bed are very complex and very multidimensional. The bed materials in a reach are related to the past history of high flows as well as to the material

available. The bed of the stream is not in a steady state during a high flow period. In some places, material will be deposited on the downstream face of a bar during high flows with the result that the bed material will be coarser and more uniform than for other areas of the bed. The movement of individual particles is intermittent, with periods of rest even during times of appreciable bed material movement and with individual particles being deposited and scoured in a non-uniform and unsteady manner.

#### Variation of Manning's "n" with Discharge

Of interest in understanding the sediment transport system in a gravel bottomed stream is the variation of Manning's "n" with discharge. There is a relatively large energy loss in a stream such as Oak Creek because of the riffle and pool sequence with numerous contractions and expansions. During low flows the contractions and expansions are relatively important; but during high flow, the pool and riffle sequence has less effect on the energy loss than does the general roughness of the stream bed.

The variation of relative roughness can be investigated by studying the variation of Manning's "n" with discharge. The reach used to study the variation in "n" is the main study reach from the stilling well gage, just upstream of the samples, to staff gage number three, 153 feet upstream. Manning's equation is:

$$Q = \frac{1.49}{n} A R^{2/3} S^{1/2} \quad (1)$$

where:

Q = the stream discharge

A = the cross-sectional area

R = the hydraulic radius

S = the energy slope

n = Manning's "n"

Defining the conveyance Z as

$$Z = AR^{2/3} \quad (2)$$

we write

$$Q = \frac{1.49}{n} Z S^{1/2} \quad (3)$$

For a long reach such as that selected in Oak Creek, the conveyance will vary with location along the stream. The geometric mean of the conveyance term for two adjacent sections is an estimate of the conveyance for the reach between the sections. For two adjacent sections  $i$  and  $j$ , the conveyance for the reach between is:

$$\bar{Z} = \sqrt{(Z_i)(Z_j)} \quad (4)$$

For a reach with a number of cross-sections, the average conveyance,  $\bar{Z}$ , can be estimated using:

$$\bar{Z} = \frac{1}{L} \sum_{i=1}^n (L_i, i+1) \sqrt{(Z_i)(Z_{i+1})} \quad (5)$$

where L is the total length of the reach,  $L_{i, i+1}$  is the distance between

adjacent cross-section  $i$  and  $i+1$ . Using the average conveyance for a reach we have:

$$Q = \frac{1.49}{n} \bar{Z} S^{1/2} \quad (6)$$

and we can estimate "n".

$$n = \frac{1.49}{Q} \bar{Z} S^{1/2} \quad (7)$$

The Manning's "n" was estimated for Oak Creek using the equations given above. The results for the 1971 measurements are given in Figure 9.

The Manning's "n" for grain roughness can be estimated using Stricklers equation (Chow, 1959).

$$n' = 0.0342 k^{1/6} \quad (8)$$

where  $k$  is the median size of the bed material (in feet). The median size during most of 1971 was 6.3 centimeters (0.207 feet) and

$$n' = 0.026 \quad (8a)$$

The calculated Manning's "n" is approximately 0.05 for discharges in excess of the critical discharge for the armour layer (see Chapter IV).

The Manning's "n" was estimated to be between 0.04 and 0.05 for flows in excess of the critical discharge. In an earlier report (Klingeman and Milhous, 1970), the Manning's "n" was estimated for a relatively uniform cross-section just upstream of the sampler. The Manning's "n" was found to be approximately 0.035.



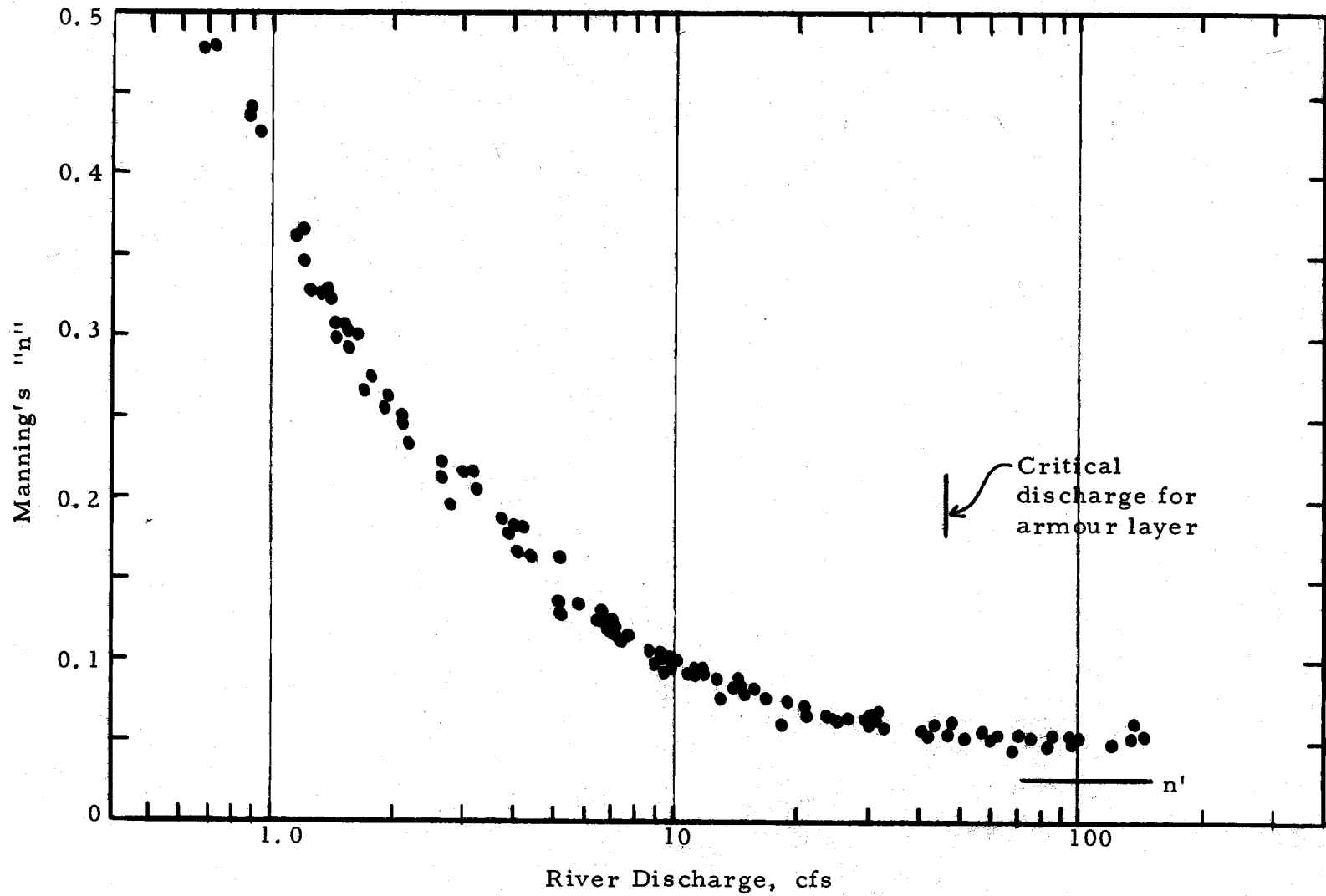


Figure 9. Relationship between Manning's "n" and river discharge for Oak Creek (1971).

The conclusions of the analysis of the roughness are (1) the Manning's "n" is relatively constant for discharges in excess of the critical discharge; (2) the Manning's "n" for discharges in excess of the critical discharge is 0.05 and includes the combined roughnesses due to grain roughness, bank roughness (probably minor), and channel form roughness; and (3) the Manning's "n" increases rapidly as the discharge decreases below the critical discharge; probably because channel form roughness becomes more important.

### III. OAK CREEK VORTEX BED SAMPLER LOAD

#### Introduction

The ability to accurately measure sediment transport rates in streams has long been of concern to hydrologists. A variety of instruments have been developed over the years to sample streamflow and its sediment load above and at the streambed. Because the various types of samplers tend to somewhat alter the flow pattern of the nearby water, questions arise as to the reliability of samples in estimating the sediment load of the water.

Sampling to estimate the suspended sediment loads of streams is presently done with far greater confidence than is true for bed measurements. Differences in particle sizes between the suspended load and bed load are partly responsible, as the bed load sampler must provide a larger orifice for the entry of bigger sediment. This means that larger equipment is needed and that greater local disturbance of the flow may result. Hence, sampling efficiencies must be determined for bed load samplers by means of calibration tests under controlled conditions, such as are offered in laboratory channels. Unfortunately, sampling efficiencies of such apparatus appear to be sensitive to the size of the transported sediment and to the hydraulic conditions of the flow.

The important practical problems of determining total sediment yields from watersheds and total sediment transport into impoundments depend for their solution upon reliable sampling of the two modes of sediment transport in streams--as suspended load or as bed load. Indirect methods are frequently used to estimate the rate of bed-load transport, such as measuring the rate of accumulation of sediment behind weirs or in reservoirs. Alternatively, bed load transport equations, most of them derived for steady-state laboratory and field conditions, are also used to calculate this portion of the total load. Unfortunately, the application of such relationships becomes questionable for mountain streams with coarse gravel beds, shallow flow depths, and frequent riffles and pools.

The study reach of Oak Creek is instrumented so that the total sediment yield can be determined by separate measurement of the suspended and bed loads. To accomplish this, a bed load sampling system was developed which operates on a vortex principle to remove the bed load from the stream to a sampling area. Continuous or discrete sampling of the bed load passing through this reach of Oak Creek is possible.

#### Design of Sampler

During a literature review on sediment sampling, prior to the design of the Oak Creek research facilities, it was thought that a

bed load trap for in-stream sediment collection might be devised with features similar to those used in some of the large flumes in various hydraulic laboratories. However, a vortex tube sand trap described by Robinson (1962) for excluding unwanted sediment from irrigation and other canals appeared to have possibilities for adaptation as a bed load sampler. Little hydraulic and sediment information was available for Oak Creek upon which to base a careful design; therefore, only a rough correspondence to Robinson's design criteria could be achieved. Subsequent operation of the bed load sampler indicated no major difficulties although several changes might be made in any future sampler.

The bed load sampler was incorporated in a broad-crested weir for convenience. The weir acts as a control for water level at a nearby stilling well to provide a stable stage-discharge relation. The streamflow data are essential for determining the discharges at which different rates of bed load transport occur.

A schematic diagram of the weir-and-sediment-trap structure at Oak Creek is given in Figure 10 and a photograph of the structure is shown in Figure 11. A flume placed diagonally across the weir floor generates a vortex-type flow to remove bed load from the stream, along with a fraction of the total streamflow. The flume leads to an off-channel trap where the sample is collected and from which the vortex water is returned to the stream. Plan and

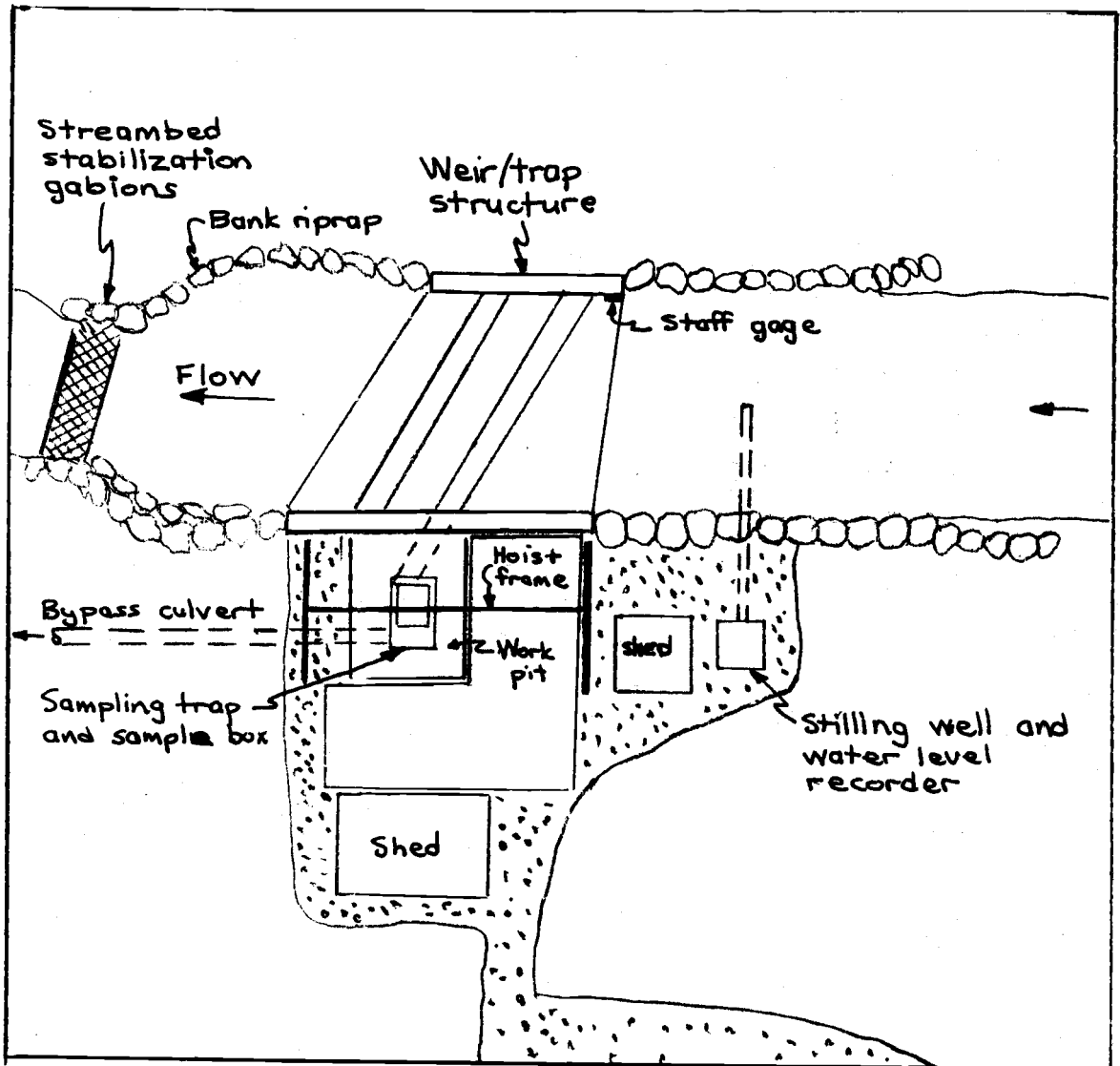


Figure 10. Schematic view of Oak Creek weir-and-sediment-trap facility.



Figure 11. The bed load sampler.

cross-sectional views of the sampling structure are given in Figure 12.

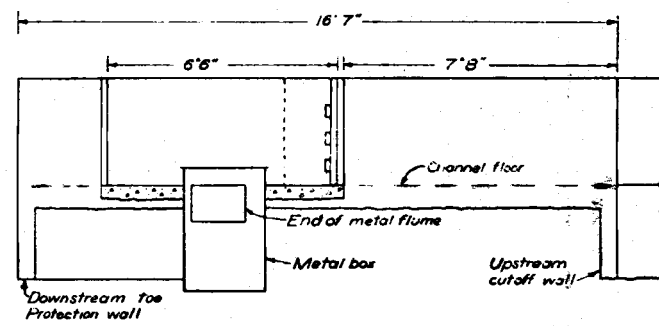
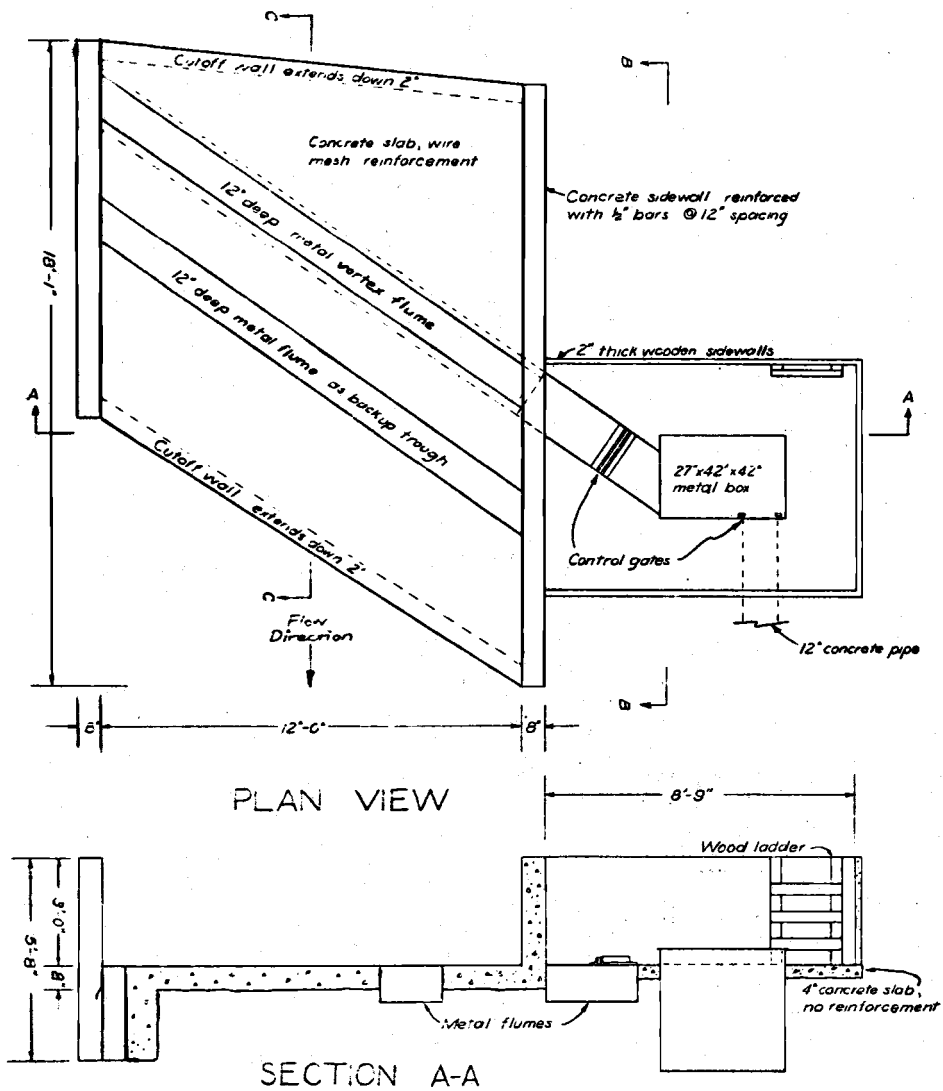
In designing the vortex bed load sampler, doubts existed as to the capability of the vortex flume for handling coarse gravel and cobbles up to six inches in diameter (major axis). Therefore a second trough was placed two feet downstream of and parallel to the vortex flume in order to act as a backup trough.

The vortex flume and backup trough have an angle of orientation of almost 60 degrees to the direction of flow. The orientation was determined as much by tree roots in the streambanks as by the criterion of 45 degrees recommended by Robinson.

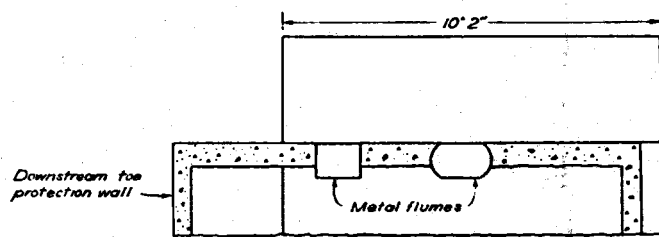
The vortex flume is placed horizontally and has its upstream and downstream edges at the same level. In cross-sectional shape the bottom is flat and 12 inches wide whereas the sidewalls are curved and have a maximum width of 18 inches. The top opening is 12 inches wide. Total depth of the flume is 12 inches. The shape was selected for easy fabrication. The total flow length of the vortex flume is 19.5 feet and the length of opening in the concrete channel floor is 14.5 feet (stream width is 12 feet at the weir). A vortex develops readily at all stream stages when the control gates are opened.

The backup trough is horizontal with upstream and downstream edges at the same level. It has a square 12-inch by 12-inch cross-sectional shape.





SECTION B-B



SECTION C-C

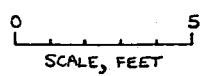


Figure 12. Broad-crested weir and vortex-type sediment sampling system (weir/trap structure).

The concrete channel floor, in addition to holding in place the two sampling troughs, acts as a broad-crested weir to stabilize the stage-discharge relation. However, operation of the vortex flume causes a backwater curve that changes the stages for a short distance upstream extending to the stilling well. Since the bed-load sampler is not always in use, either a correction curve or a dual rating curve is required to convert the water-level data to the corresponding discharges both when the vortex bed load sampler is open for use and when it is closed. (Placement of the stilling well a greater distance upstream could avoid or minimize this problem.)

The vortex flume leads from the stream to a work pit having a concrete floor at the same level as the channel floor. This pit greatly increases the ease of collecting samples. Flat metal plates with handles serve as control gates in the work pit to regulate the vortex flow. The vortex flume opens into a deep metal box, or sampling trap, in the floor of the work pit. A smaller sample box can be placed in position at the vortex exit within the sampling trap to catch the bed load as it decelerates upon leaving the vortex flume.

Sample boxes are raised from and lowered into the sampling trap by means of a chain hoist attached to a pulley and supported by a hoist frame. The hoist frame also permits shifting of the sample box to higher ground outside of the work pit where the sample can be stored or transferred to containers for subsequent laboratory analyses.

After the bed load has been deposited in the sampling box, the water drawn into the sampling area is returned to the stream by means of a return pipe. Because of local topographic features, a 100-foot line of 12-inch diameter culvert pipe was used. (Under different circumstances a shorter "bypass" or return line would be equally effective.) The difference in energy head across the bypass culvert depends upon river stage and has a mean value of approximately three feet.

#### Performance of Sampler

The bed load sampler has been used to sample bed load discharge rates below 1500 kg/hr quite successfully, although rates below 5 grams per hour are probably subject to considerable error.

The procedure used in obtaining a bed load sample was to open the flow control gates described previously, permitting flow through the vortex plume and the sampler. When the sampler is first opened, the material deposited in the vortex flume after the previous closing of the flow control gates will be transported by the vortex flow into the sampling pit. Hence, the time interval associated with a bed load sample is the period between successive closures of the flow control gates.

After the flow through the sampling pit is stopped, the sample box is removed using the chain hoist. Because of part of the material

entering the work pit from the vortex flume misses the sample box and falls into the open pit area behind the box, the pit is cleaned after the box is removed. This is done by using a broom to sweep the material in the pit to one corner and then remove the material from the pit using the special tool shown in Figure 13.

After the pit is cleaned an empty sample box is placed in the pit and the flow control gates are opened.

During periods of high bed load transport, sediment falls into the vortex flume at such a rate that the flume could be filled with sediment unless the flow control gate is closed, the sample box removed, the pit cleaned, a clean box is placed in the pit, and the gate is opened in a very short time. The time required to perform a sample box change was from 10 to 12 minutes.

Field experience with the sampler demonstrated that the vortex action was not strong enough to remove all the sediment deposited in the vortex flume at the end across the stream from the sampling trap. Hence, the flume was "walked" at the end of each sampling period and the material pushed by foot or by using a broom until the material was transported by the vortex action into the sampling pit. When the bed load transport rates were high, the vortex flume was kept clear by walking it at frequent intervals during the sampling periods. The task of walking the flume is not an easy one when the flows are rapid (an individual with sufficient mass not to be washed downstream is



Figure 13. The pit cleaning tool.

required for the job).

The amount of flow through the vortex flume is a function of the river discharge. The function is shown in Figure 14. The system appears to be regulated principally by "inlet control" at the entry to the culvert from the sampling pit. At streamflows of less than 2.35 cfs the vortex diverted the entire creek flow as is shown in Figure 14. The strength of the vortex increased considerably with increasing streamflow and water stage. At intermediate stream depths a distinct breaker of white water occurred directly over the downstream edge of the vortex flume. At highest stages the stream surface was generally wavy and the breaker was no longer visible, although a strong vortex could be felt if one stood in the flume in wading boots. From Figure 14 it may be seen that the vortex handled an increasing quantity but a decreasing proportion of the total flow as the river discharge increased. For example, at a river discharge of 40.9 cfs, 8.1 cfs or 20 percent of the streamflow was diverted through the vortex. During discharges exceeding 150 cfs it was estimated that the vortex flow did not exceed 15 cfs (i. e., 10 percent or less of the total river flow). For comparison, Robinson (1962) indicates a flow removal of from 5 to 15 percent of the total flow as a criterion for successful operation with sand.

In Figures 15 and 16 are the variability of Froude number (the mean flow velocity divided by the square root of the product of

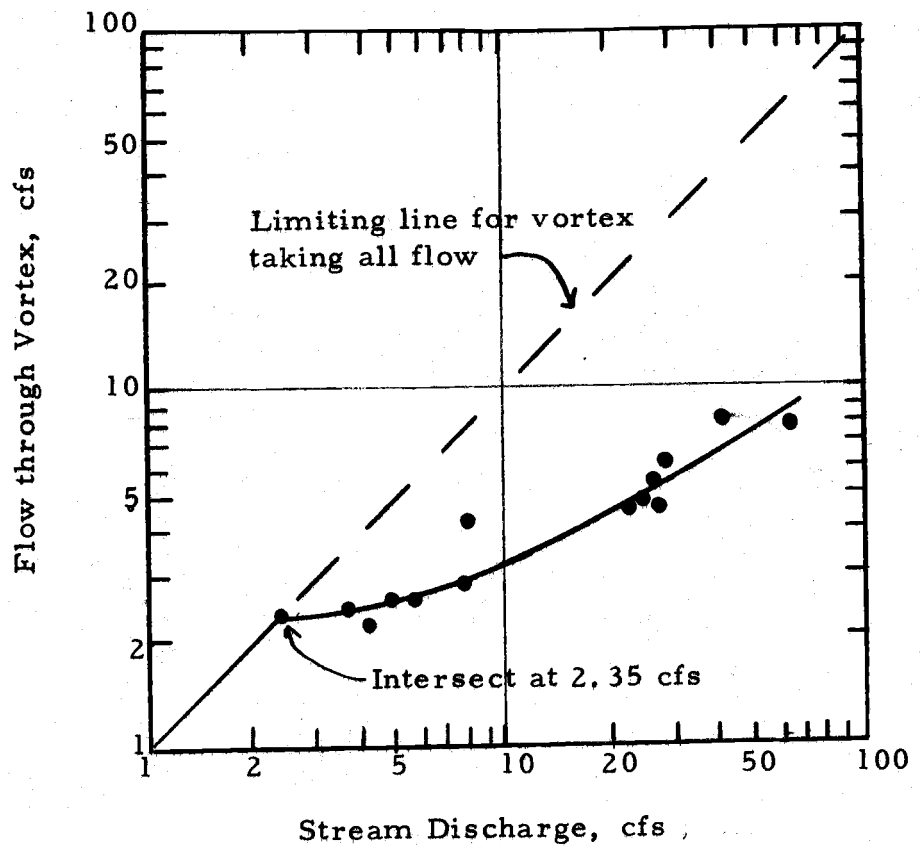


Figure 14. Discharge capacity of the Oak Creek vortex bed load sampler.

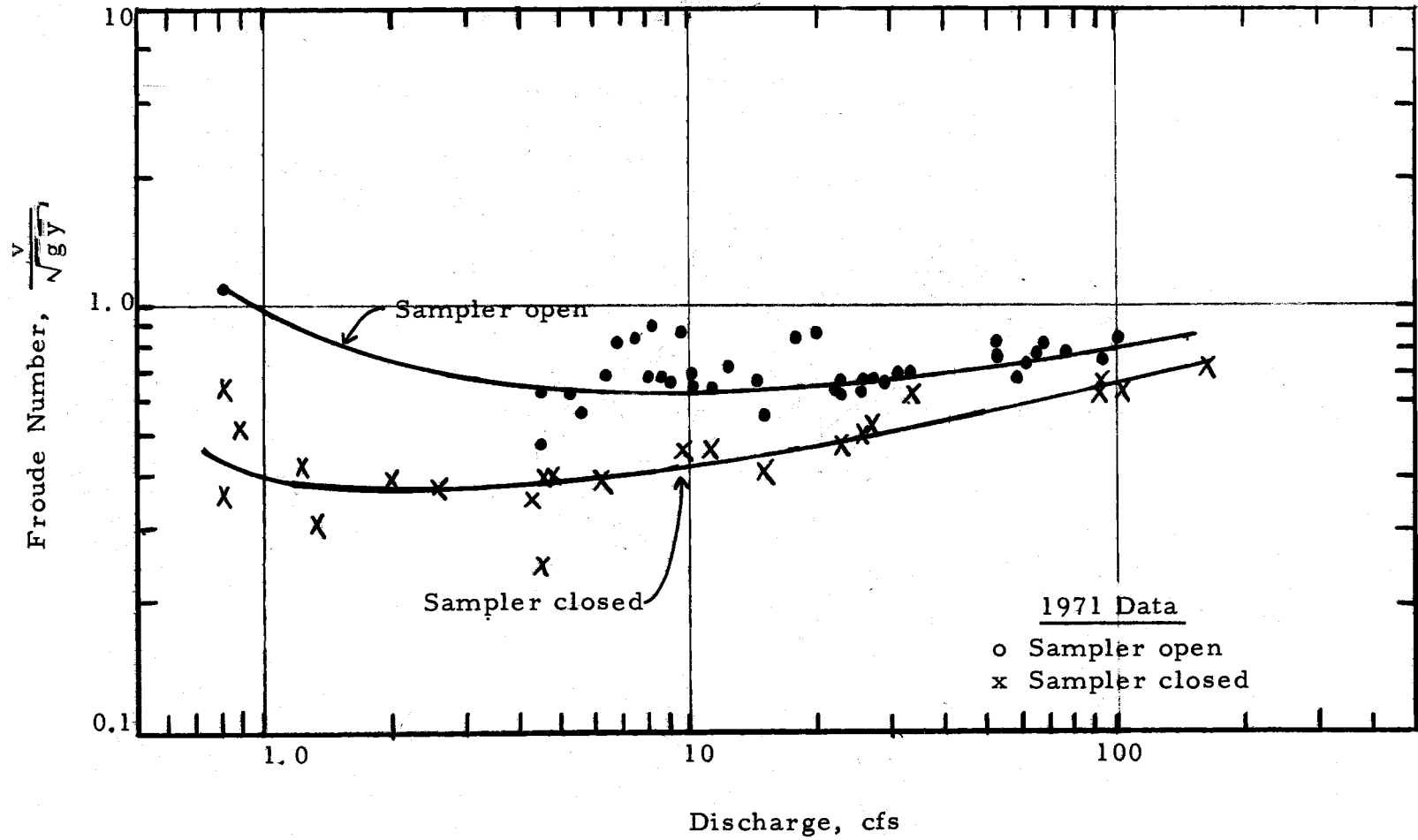


Figure 15. The relationship between Froude number at the upstream edge of weir/trap and stream discharge.



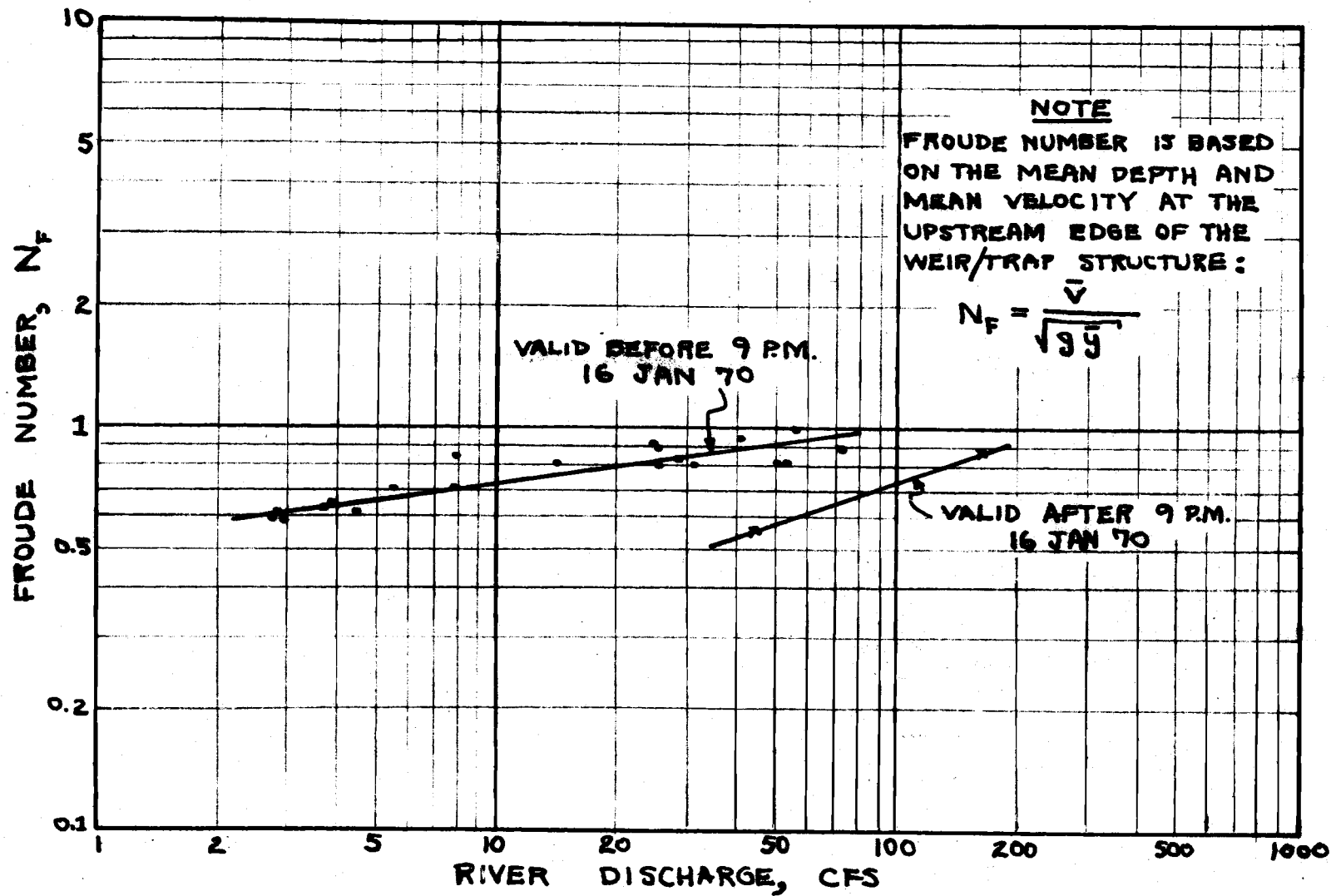


Figure 16. Variation of Froude number with discharge during operation of the vortex bed load sampler.

gravitational acceleration ( $g$ ) and mean depth of flow) with streamflow is shown. The Froude number is calculated for the weir cross-section just upstream of the vortex flume.

Data collected during the winter of 1969-70 are shown on Figure 16. A shift in the location of the control point for the stage-discharge relationship occurred during the night of January 16th due to deposition behind a protective structure just downstream of the weir/trap structure and accounts for the different line in Figure 16.

The data collected during 1971 are shown on Figure 15 and include data for both the case with flow in the vortex and the case without vortex flow. An interesting observation is that there is considerably more scatter of points with vortex flow than without. The cause of this is possibly a result of more local fluctuation of the stage at the point of measurement when there is vortex flow in comparison to the case of non-vortex flow. As Figure 15 indicates, the Froude number with vortex flow is greater than without vortex flow.

The change in the Froude number versus discharge relationship between the spring of 1970 and 1971 is a result of the flow downstream of the trap being constricted by changes made in the stream immediately downstream of the weir/trap but above the control section.

During periods of bed load transport measurement the Froude number ranged from 0.5 to less than 1.0, indicating sub-critical flow approaching the vortex trough during all the sampling periods.

The variation of velocity as a function of river discharge is shown on Figure 17 using the 1971 data. As is shown, for a given discharge the velocity is greater with vortex flow than without. The hydraulic slope between the upstream edge of the trap and the stilling well seven feet upstream has been measured in a few cases. The data are given in Table 6. The data for the case where there is vortex flow are considerably more scattered than the without vortex flow case. Nevertheless, it can be concluded that the slope is greater with vortex flow than without although there are data where the opposite is true and the stream power immediately upstream of the weir is greater with vortex flow than without for a given discharge.

Table 6. Comparison of water slopes upstream of weir/trap for trap closed and trap open.

River Discharge cfs	Water Slope, ft/ft	
	Trap Closed	Trap Open
4.2	0.012	0.020
4.5	0.008	0.006
9.6	0.011	0.048
12.0	0.011	0.023
15.0	0.008	0.014
23.0	0.007	0.016
25.0	0.006	0.002
27.0	0.007	0.023
92.0	0.004	0.010
100.0	0.011	0.008

If the sampler has not been operated for some time and the vortex is opened, the increase in stream power immediately upstream of the sampler probably results in the measured bed load being greater than

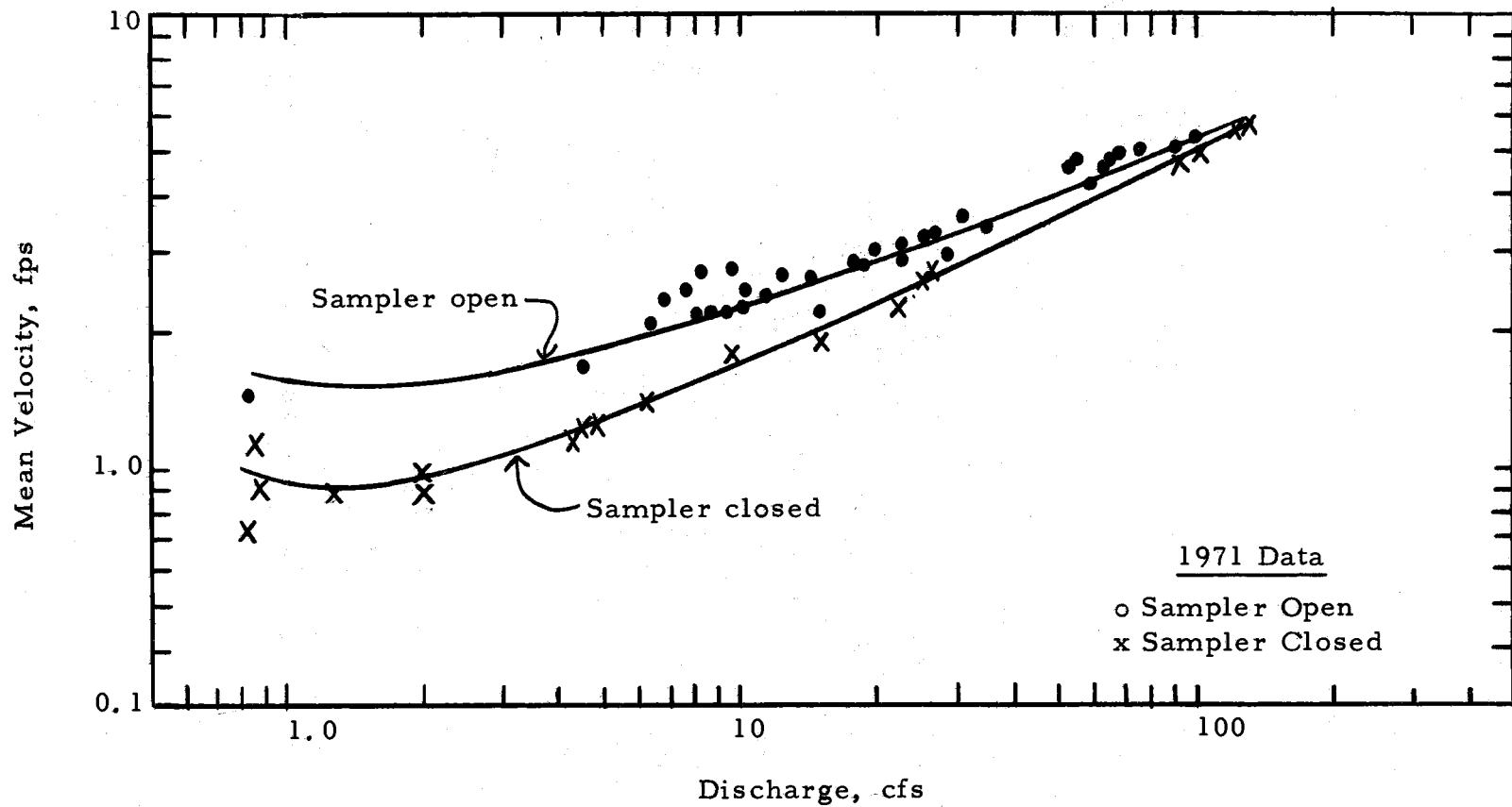


Figure 17. Relationship between mean velocity at upstream edge of weir/trap and stream discharge.

the bed load without sample operation because the section just upstream of the sampler will have to adjust to the increase in stream power.

### Sampler Efficiency

The efficiency of the sampler has been evaluated on the basis of indirect evidence. There are two elements of the system which determine the efficiency of the system: the efficiency of the vortex flume in removing bed load from the flow and the efficiency of the sampling trap in containing the sediment transported to the pit by the vortex action. The efficiency equation is of the form

$$e = e_v \cdot e_p \quad (9)$$

where  $e$  is the total efficiency,  $e_v$  the efficiency of the vortex tube and  $e_p$  the efficiency of the sampling pit.

When the sampler was designed it was thought that any large material escaping from the vortex flume would fall into the downstream trough where it could be collected. By use of the two troughs it was thus hoped to have a 100 percent efficient bed load trap. Hindsight indicates that the second trough was unnecessary insofar as the coarse bed load material was concerned, because little material was trapped in the downstream trough and that material trapped there was sand. Hence it was concluded that all particles larger than No. 4 sieve size (U. S. Standard Series) in diameter (4.76 mm) were trapped and held

by the vortex for all streamflows, with none reaching the backup trough when the vortex trap was operated.

A 1970 paper by Porph, Sagiv, and Seginer (1970), on the bed load sampling efficiency of slots, was used to estimate the efficiency of the Oak Creek sampler when the vortex is closed because the information paper did not have a flow into the trough. It was estimated that the trap efficiency of the sampler would be near unity for all sizes of bed material being transported by Oak Creek as bed load. Based on the Porph paper and observations of the downstream trough it is assumed that  $e_p \approx 1$  for the bed load material in Oak Creek.

Operational experience has shown that most of the bed load drops into the sample box. However, sufficient turbulence occurs in the sampling trap so that some of the finer sand deposits in the bottom of the pit instead of collecting in the sample box. Except for very low bed load transport rates subsequent collection of this sand poses no special problems other than some inconvenience and loss of time.

One problem caused because some of the bed load sample misses the sample box and falls into the pit is that the pit cannot be cleaned to the same state each time and tends to either act as a reservoir or sink for material in the individual samples. This is especially true of samples for bed load transport rates less than about 10 grams per hour because the pit samples tend to be nearly the same size as the box sample.

Data on the fraction of the total sample deposited in the sample box have been obtained and the results are given in Figure 18. The apparent bed load discharge is calculated using the material deposited in the sampling box and total sample is the sum of the weights of material removed from the sample box and from the pit.

Some idea of what happens to the fine particles can be obtained by investigating the sample box efficiencies for the various grain sizes of two samples. The efficiencies of collecting the individual grain sizes of two samples are given on Figure 19. As is shown, the apparent efficiency decreases over the range from 10 to 0.6 mm and tends to increase for decreasing sizes of less than 0.6 mm.

Because flow turbulence transports material over the sample box into the pit, it seems reasonable to assume that the turbulence also causes some of the fine material to be removed from the trap altogether. Hence, the apparent rise in efficiency with decreasing size below 0.6 mm is caused by an increase in the fraction of the total material in the size range being removed from the sampler. In general, as particle size became smaller in the sand range, the trap efficiency decreased and became dependent upon vortex action, according to inferences made from the data given above. Particles finer than 0.074 millimeter were trapped in such relatively small amounts that it is believed that the trap efficiency for silt-sized and smaller particles was quite small. As stated above, the trap

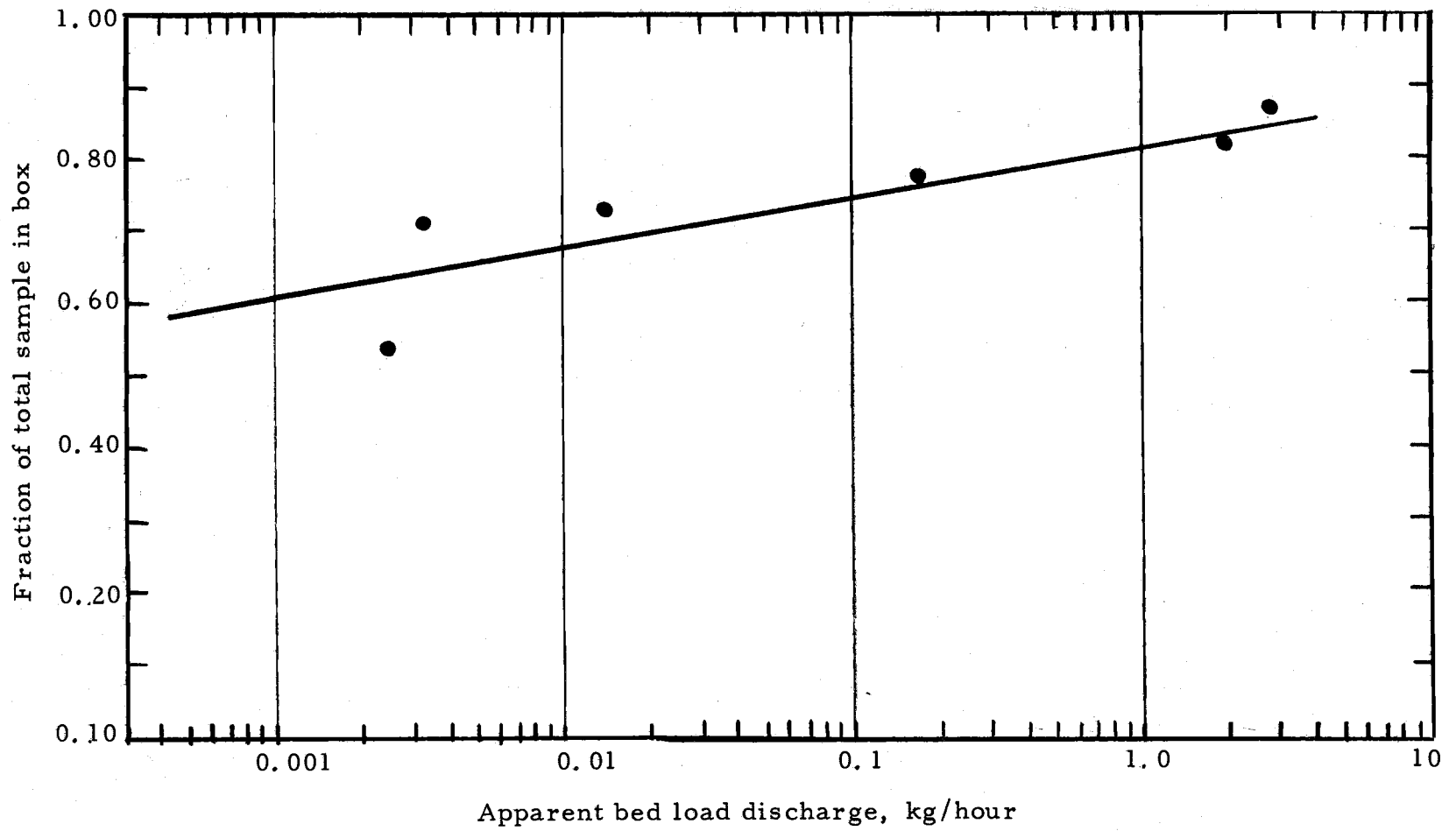


Figure 18. Efficiency of sampling box; grouped samples.



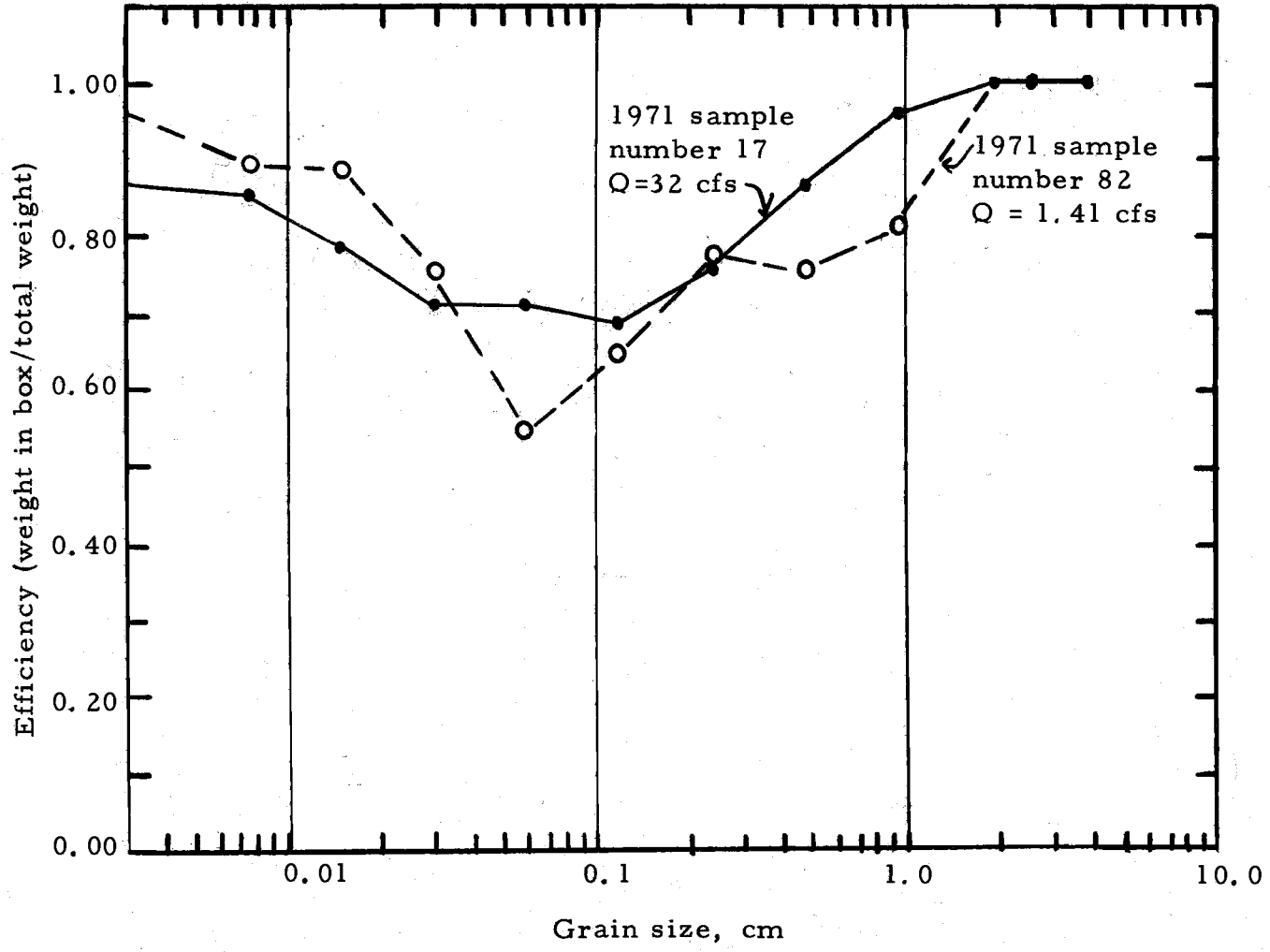


Figure 19. Variation of sampling box efficiency with grain size for two bed load samples.

efficiencies of less than 100 percent for the finer fraction of bed load are believed to be explained by the turbulence of flow in the vortex, such that the finer particles were temporarily placed in suspension and carried past the trap and into the bypass culvert.

The overall efficiency of the trap is a function of the river discharge (i. e., the vortex turbulence) and the size of material being transported. The nature of this relationship is not known but a subjective estimate of the overall efficiency of the trap is that it is at least 0.95 at a bed load rate of 10 kg per hour, falling to perhaps 0.85 at 0.01 kg/hour.

An improvement in the sampling station would be the use of a larger sampling trap in order to use larger sampling boxes and to achieve a greater reduction in water velocity and turbulence.

#### IV. THE INCIPIENT MOVEMENT OF THE ARMOUR LAYER

##### Introduction

The bed material in a gravel bottomed stream with an armour layer is essentially stable during all but the highest flows. This is because the armour layer prevents movement of the material below it except when the armour layer itself is being moved. Bed load samples were obtained when the stream flow was below that discharge required to move the armouring material. These samples were predominantly sand and silt with, in some of the samples, a large particle. These samples indicate that a small amount of fines do move around and among the armour particles when the armour particles are not moving. Early in the bed load sampling program, it appeared that there was a "critical" discharge for the armour layer. Below the "critical" discharge the armour material was stable; above the "critical" discharge a considerable amount of armour size material was found in the bed load samples.

During the bed load sampling, it appeared that the "critical" discharge in the Oak Creek study reach is approximately 40 cfs. Another subjective observation was that when the discharge was above about 70 cfs the whole bed seemed to be in motion. In general, the subjective field observations indicated that:

$Q < 40$  cfs - little armour material movement

$40 < Q < 70$  cfs - transition for armour material movement

$Q > 70$  - considerable armour material movement

It appeared that for the study reach the individual armouring particles are essentially at rest when the flow is below 40 cfs and, if in the armour layer, moving when the flow is greater than 70 cfs. Consequently, we can (as a first approximation) say:

$Q < 40$  cfs - particle is at rest.

$40 < Q < 70$  cfs - particle alternates from being at rest and moving with the fraction of time at rest decreasing as the discharge increases.

$Q > 70$  cfs - particle moving if it is located in the armour layer.

The "break up" of the armour layer is related to the movement of individual particles of the armouring material. The work in the winter of 1969-70 suggested the individual armouring particles could be transported at comparatively low discharges. As a result of this observation, the weight of the largest particle in each bed load sample was determined.

The purpose of this chapter is to examine incipient movement criterion for individual particles, and to develop an incipient motion criterion for the armour layer as a whole.

## Incipient Motion of Individual Particles

### Literature Review

Critical Shear Stress. The beginning of particle motion in a uniform (or nearly uniform) bed has been studied by several investigators. The initial work that is most frequently referred to is that done by Shields (Shields, 1936). A very adequate review of incipient motion concepts is given in Graf (1971). The incipient motion of a particle is related to a "critical" shear stress applied to the particle by the flowing fluid.

The basic concept of a critical shear stress is that when the forces on the particle due to the flowing water overcome the weight of the particle, then the particle will move. The force (F) applied to a particle is related to the area of the particle (A) and the bed shear stress ( $\tau_o$ ). We can write that

$$F = C_f \tau_o A \quad (10)$$

where  $C_f$  is a constant dependent on the flow and bed configuration.

The resisting force is related to the buoyant weight of the particle and can be written as

$$F_R = C_s (\gamma_s - \gamma) (D)(A) \quad (11)$$

where  $F_R$  is the resisting force with a direction opposite to the hydraulic force applied to the particle,  $C_s$  is a coefficient related to the bed configuration,  $\gamma_s$  the unit weight of the particle,  $\gamma$  the unit

weight of the fluid, and  $D$  the nominal particle diameter. At the state of critical shear stress ( $\tau_c$ ), these two forces will be equal (hence  $\tau_c = \tau_o$ ). Thus we have:

$$C_f(\tau_c)A = C_s(\gamma_s - \gamma)(D)(A) \quad (12)$$

This may be rearranged to give

$$\frac{\tau_c}{(\gamma_s - \gamma)d} = \frac{C_s}{C_f} = f_s \quad (13)$$

which is called herein the Shields parameter. It seems reasonable to suspect that  $C_f$  is not a constant but is instead a function of the boundary layer which can be related to the Reynolds number of the particles. The latter can be written as

$$R_e^* = \left( \frac{\sqrt{\tau / (\gamma/g)} D}{\nu} \right) \quad (14)$$

where  $R_e^*$  is the particle Reynolds number,  $g$  is the gravitation acceleration, and  $\nu$  is the fluid kinematic viscosity. The experiments of Shields indicated that  $f_s$  is constant for  $R_e^*$  greater than 1000. In other words,  $f_s$  is constant for a hydraulically rough flow.

Einstein used hydraulic stability parameter ( $\psi$ ) in his work.

The hydraulic stability parameter may be written as

$$\psi = \frac{(\gamma_s - \gamma) D}{\gamma RS} \quad (15)$$

For open channel flow the bed shear stress is given by

$$\tau_o = RS \quad (16a)$$

At the critical shear stress, with  $\tau_o$  equal to  $\tau_c$ , we have

$$\tau_c = \gamma R S \quad (16b)$$

Substitution of this latter equation into the expression for yields

$$\psi = \frac{\gamma_s - \gamma D}{\tau_c} \quad (17)$$

and from equation (13) we see that

$$\psi = \frac{1}{f_s} \quad (18)$$

or that  $\psi$  equals the reciprocal of  $f_s$  at critical shear stress conditions.

The general equation for the critical shear stress when the flow is rough is given by rearrangement of equation (13):

$$\tau_c = f_s (\gamma_s - \gamma) D \quad (19)$$

Values of the Shields parameter given in the literature indicate that  $f_s$  ranges from 0.017 to 0.076. The work of Shields indicated a value of 0.06. Chien (1954) tabulated the values of  $f_s$  proposed by various investigators. These values are given in Table 7, as are other values of the Shield parameter given in Graf (1971). The Einstein bed load function is not usually considered to have a "critical" value for the hydraulic stability parameter  $\psi$ . But a plot of the function at high values of  $\psi$  indicates the function tends to become asymptotic to a value of  $\psi$  equal to 40, which gives a value of 0.025 for the Shields parameter.

Table 7. Values of the Shields parameter suggested by various investigators.

Author	$\psi_{cr}$	$f_s$
<u>As reported by Chien (1954)</u>		
P. E. I.	13.2	0.076
Krey, Shields	16.7	0.060
Meyer-Peter (1)	21.4	0.047
White	22.2	0.045
Kalinske	25.7	0.038
O'Brien and Rindland	29.5	0.034
Meyer-Peter (2)	33.3	0.030
Chang	45.2	0.022
Kramer	60.2	0.017
<u>As reported by Graf (1971)</u>		
Zeller	21.4	0.047
Schoklitsch	13.2	0.076
Leliavsky (3)	10.0	0.10

(1) Meyer-Peter, Müller 1948 function

(2) Meyer-Peter 1934 function

(3) Assuming particles with a specific gravity of 2.65



Interpretation of Critical Shear Stress. The wide range in the value of the Shields parameter ( $f_s$ ) indicates that the various investigators are not looking at "critical" shear stress in the same way. The range in values may be due to at least two possible explanations. These are: (1) the way in which the critical shear stress is defined, and (2) the way in which the critical shear stress is measured.

The first explanation for variability of critical shear stress is illustrated by a report of the U.S. Waterways Experiment Station (1935), which defines the critical tractive force as the tractive force which brings about general motion of the bed. In contrast, Shields (1936) extrapolated the curve relating bed material discharge with fluid shear stress to the point of zero bed material discharge and called this intercept the critical shear stress. The method of estimating the critical shear stress used by Shields implied that there is no movement of a uniform bed material at the critical shear stress. Another definition is that used at the St. Anthony Falls Hydraulic Laboratory (Paintal, 1969), which identifies the critical shear stress as that at which 3% of the surface particles are moved during every hour.

The flow in a river or stream is turbulent with the result that the force applied to the bed by the water is not constant but varies with time. Usually, the time average value of shear stress is calculated and compared to the particle stability. In actual fact, the shear

stress varies and a probability distribution of the actual shear stress exists with a median value equal to the time average shear stress. If the critical shear stress is equal to the time average shear stress, then, for a uniform bed material, the probability of a particle being moved equals the probability of the particle remaining at rest.

Gessler (1970) developed a function which relates the probability of remaining stationary to the ratio of the critical shear stress ( $\tau_c$ ) and the mean shear stress ( $\tau_o$ ). The Shields parameter used by Gessler had a value of 0.047 which was taken to correspond to a 50% chance of the particle remaining stable. Hence, we can write that the probability of movement is related to

$$\frac{\tau_c}{\tau_o} = \frac{0.047 (\gamma_s - \gamma) D}{\tau_o} \quad (20)$$

Furthermore, using equation (16a) in the above equation and comparing the results with equation (15), the probability of movement is related to

$$0.047 \left( \frac{\gamma_s - \gamma}{\gamma} \right) \left( \frac{D}{R S} \right) = 0.047 \psi \quad (21)$$

Based on the probability concepts given above, Gessler defined the critical shear stress for a particle to be the time average shear stress at which the "probability of being eroded equals the probability of remaining at rest."

Neill (1968) considered Gessler's definition to be incomplete because the definition does not include a period of time over which the probability of remaining stationary equals the probability of moving. At a time period of zero, all particles would remain in place but as the time period lengthens the probability of particles moving would be likely to increase. An alternative interpretation is that at a given point the shear stress exceeds the critical shear stress for the particles half of the time when the mean bed shear stress of the flowing fluid equals the critical shear stress of the particles.

The importance of the definition of critical shear stress is illustrated by attempting to estimate the value of the Shields parameter associated with the St. Anthony Falls definition of critical shear stress given, Gessler's definition of critical shear stress and his probability function. Using Gessler's probability function, the ratio  $\tau_c / \tau_0$  has a value of 2.1 when the probability of remaining in place is 3%. Using 0.047 for the  $f_s$  at 50% probability of movement the estimated value of  $f_s$  for the St. Anthony Falls criteria of 3% movement is  $0.047/2.1 = 0.022$ . This is a value well within the range of values proposed by various investigators. Unfortunately, Gessler's probability function does not allow the evaluation of the probability of movement per unit time.

The St. Anthony Falls definition implies that time rate of particle movement is an important factor in the determination of the

critical shear stress. Alternative definitions of the critical shear stress used by Paintal are related to the rate of movement, with the critical stress being defined as the average shear stress when the time rate of bed load is, alternatively, 1, 5, and 10 pounds/foot of channel width per hour. In contrast, both Shields and Meyer-Peter, Müller (1948) extrapolate a function of bed material load to zero load in order to determine  $f_s$ .

The points raised above regarding the ways in which critical shear stress is defined, then, lead to the second possible cause of the wide range in the value of  $f_s$ . This cause is the variation in the method of measuring the critical shear stress. If the critical shear stress is assumed to occur when there is zero bed load transport, then we can measure the critical shear stress by extrapolating the transport rate function to zero transport, as was done by Shields. An alternative method of measuring critical shear stress is to increase the flow over a bed until particles are observed to move, as done by McNeil. If the time interval between step changes in the discharge function is "short", it would seem that the value of  $f_s$  should be larger than for the case where the critical shear stress is determined using "long" intervals between steps in the discharge function. The cause of this is that if the probability of a particle being moved is low, the probability that a particle will be observed to move will be smaller when the step intervals are "short" than when they are "long".

Consequently, the expected discharge at which a particle will be observed to move will be larger for the "short" step intervals than for the "long" step intervals.

### Application of Concepts to Oak Creek

The flow in Oak Creek is fully turbulent. The value of  $\tau_o/\gamma$  during the 1971 sampling period was from 0.002 feet to 0.019 feet and the  $D_{65}$  size was 7.4 cm (0.24 ft).

The water temperature during periods of significant sediment transport was in the order of 40°F. Hence, the kinematic viscosity was  $1.7 \times 10^{-5}$  ft/sec. Consequently, substitution into equation (14) gives

$$Re^*)_{\text{minimum}} = \frac{\sqrt{0.002g} \cdot 0.24}{1.7 \times 10^{-5}} = 3600 \quad (22)$$

Thus, the Shields parameter is a constant and not a function of the flow conditions.

As part of the study of bed load transport, the weights of the largest particles transported in each sampling period were determined. It was then assumed that the largest particle was transported by the maximum discharge associated with each bed load discharge sample. The particle size was furthermore assumed to be the same as the diameter of a sphere with a specific gravity of 2.85 (the average specific gravity of Oak Creek gravel), and the same weight as the particle.

The weight of the largest particle in a bed load sample compared to the maximum discharge associated with the sample is shown on Figure 20 for all of the 1971 samples. The samples collected during the fall of 1971 contained particles that were comparatively larger than for the winter 1971 samples. This results from the large amount of leaves and other woody debris found in the stream in the fall. The leaves tend to catch on the exposed particles, increasing the area exposed to drag forces without increasing the resisting forces. Hence, larger particles were able to move at lower discharges. Consequently, the winter data are better to use in studying incipient motion of individual particles than the fall data, which should not be used because of the leaf-caused increase in drag forces.

The winter, 1971, data are on Figure 21 in terms of the average bed shear stress divided by the unit weight of water ( $\tau_o/\gamma$ ) versus calculated particle diameter, where  $R$  is the hydraulic radius and  $S$  is the energy slope in the study reach. Also shown on the Figure 21 are lines for various values of  $f_s$ . A value of  $f_s=0.017$  is the absolute lower bound for the data on the figure and for the values of various investigators given in Table 7. The line with  $f_s=0.025$  is an effective lower bound on the data and is also the value of  $f_s$  estimated from the Einstein bed load function. The lower effective bound represents the "critical shear stress" for the conditions that exist in Oak Creek and for the method used to define the particle size. Leopold, Wolman, and

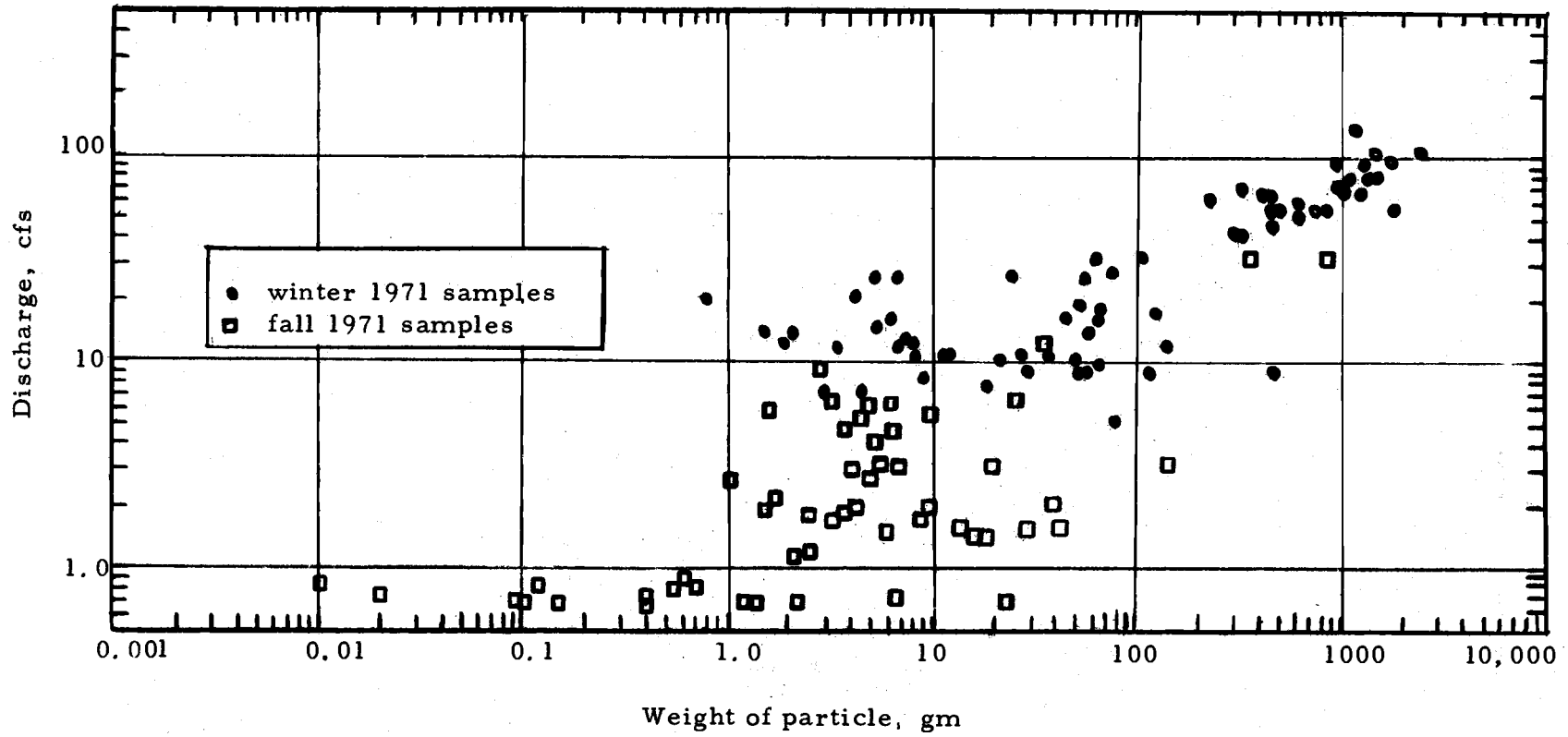


Figure 20. Weight of largest particle in a bed load compared to maximum discharge for the sample.

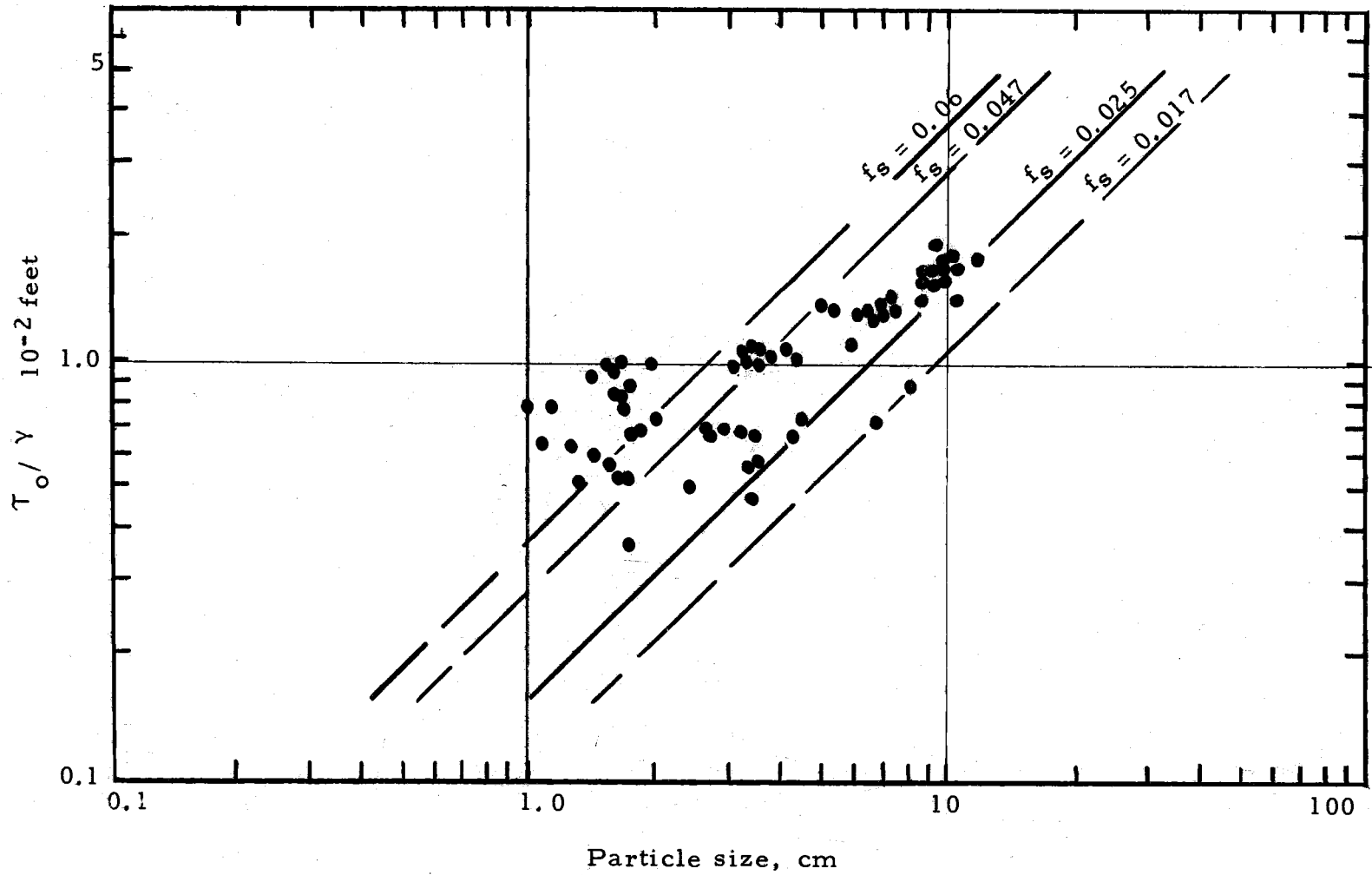


Figure 21. Maximum transported particle size as a function of shear stress.



Miller (1964) have developed a diagram showing field and laboratory data for the critical shear stress required to initiate movement of various sizes and particles. The effective lower bound from Figure 21 has been plotted on the diagram from Leopold, Wolman, and Miller (1964) and the results are given as Figure 22.

There is good agreement between the critical shear stress from Oak Creek and the other data on Figure 22.

The Shields parameter,  $f_s$ , has a value of 0.017 for the absolute lower bound shown in Figure 21. The lower bound of  $f_s$  for all the data on Figure 22 is 0.012. However, the White River data (Fahnestock, 1963) were taken by a man standing in a stream holding a screen, which may have caused the actual shear stress to be higher than the measured values. Nothing is known by the writer about the Chitty Ho data.

The writer's conclusion is that the minimum value of  $f_s$  is 0.017 and that the probability of a particle moving is quite low with an  $f_s$  of 0.025. The value of the Shields parameter to use in most estimates of the critical shear stress for a given size particle is 0.025, unless the estimate is based on probability of particles moving.

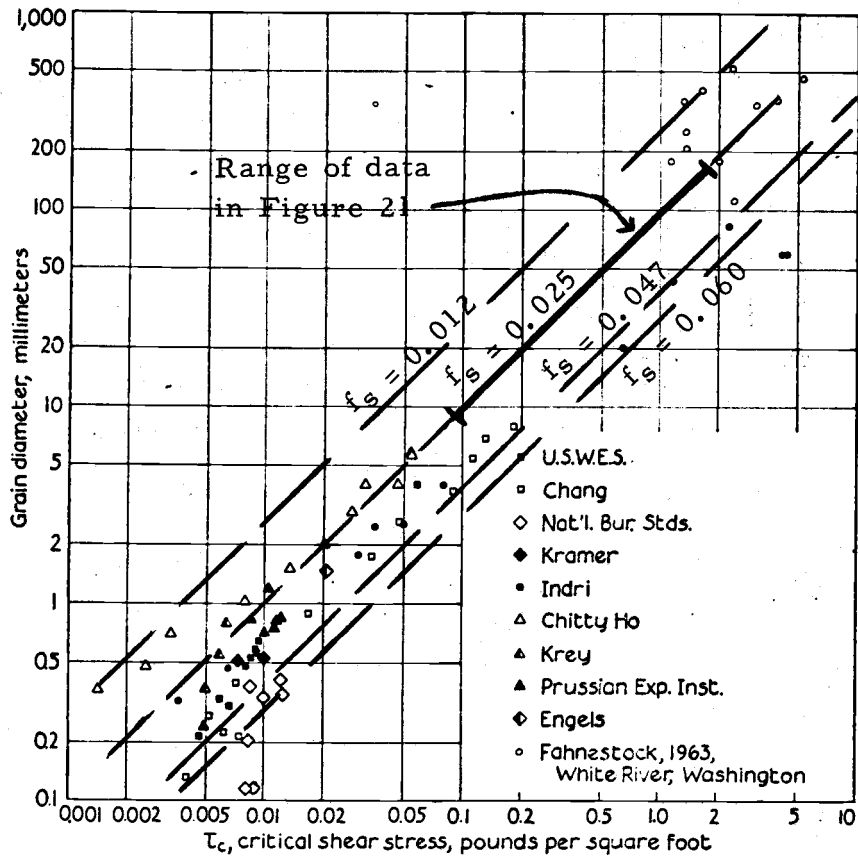


Figure 22. Laboratory and field data on critical shear stress required to initiate movement of particles (after Leopold, Wolman and Miller, 1964, Figure 6-11, p. 170).

## Incipient Motion of the Armour Layer

### Critical Discharge and Critical Shear Stress

Subjective observations in the field suggested that the armour layer "broke up" at discharge in the order of 40 cfs. In other words, the armour layer ceased to protect the underlying bed material at a discharge of 40 cfs. The  $D_{35}$  size of the armour layer in Oak Creek, considered by Einstein to be representative of bed material transport, was 5.2 cm during much of the study period. The range in the critical shear stress in Oak Creek for a particle of 5.2 cm, diameter, and specific gravity of 2.85 (hence with  $(\gamma_s - \gamma)D = 19.6$ ) is from 0.29 to 1.49 pounds per square feet (psf). For Oak Creek this is equivalent to discharges ranging from 7 to 250 cfs on the basis of the relationship between the average shear stress for the study reach and the stream discharge developed from the 1971 data.

At 40 cfs, the shear stress is 0.5 to 0.57 psf. For these conditions, the value of the Shields parameter ( $f_s$ ) from equation (16) is from 0.026 to 0.030 and the transport rate in the order of 2.2 kg/hour (see Figure 37). It has been proposed by the U.S. Waterways Experiment Station (Paintal, 1969) that the critical tractive force exists when the bed load rate is 1 lb/ft/hour which is about 6 kg/hour in Oak Creek and occurs at a discharge of 45 cfs. The shear stress in Oak Creek is in the range of 0.53 to 0.62 psf at a discharge of 45 cfs. Hence,

the corresponding Shields parameter is in the order of 0.030 for the Oak Creek armour.

The calculations above are based on a subjective observation of a critical discharge for the armour layer. Another procedure to determine the critical discharge is to use the bed load measurement obtained for Oak Creek. Information on the bed load study is given in the following chapter except for the data on critical discharge which follow.

By using a critical shear stress or a critical discharge for an armour layer the calculated Shields parameter represents a condition for the armour as a whole and a general state of movement rather than the isolated movement of individual particles. During the bed load sampling period, it generally appeared that the bed load transport rate was low and the transported material consisted mainly of sand until some critical stream discharge was reached, whereafter the whole bed moved and the bed load material was fairly coarse. The bed load data were plotted on arithmetic paper in order to make an initial estimate of this critical discharge ( $Q_{cr}$ ). Using the initial estimate of the critical discharge a plot of the bed load discharge versus  $(Q - Q_{cr})$  was made and the estimate of the critical discharge adjusted. This adjusted estimate of the critical discharge for the 1971 data, prior to a peak flow on March 10th, was 47 cfs but dropped to 29 cfs after that peak flow. Using these estimates and the bed load data, a plot of

$(Q-Q_{cr})$  versus bed load discharge for the 1971 data was made. This is shown in Figure 23. The bed load equation estimated from the data is

$$Q_{BL} = 0.27(Q-Q_{cr})^2 \quad (22)$$

All of the data are well grouped around the line.

The data in Figure 23 are for the total bed material load measured. In looking at the critical discharge of the armour layer it is logical to ask about the discharge of armour size particles. These data are given in Figure 24. Both the 1969-70 and the 1971 data are included. The critical discharge for the 1969-70 data was estimated using the procedure described previously and was determined to be 29 cfs. The  $D_{35}$  size of the armour layer was used as the division between armour size and bed size particles. The  $D_{35}$  size was 4.2 cm during the winter of 1969-70 and 5.2 cm during part of the winter of 1971. Most of the bed load sampling during the winter of 1971 was done when the  $D_{35}$  size of the armour layer was 5.2 cm.

Few of the bed load samples obtained during the winter (1971) when the mean discharge was less than the critical value contained particles greater than the  $D_{35}$  of the armour layer. When a particle larger than the  $D_{35}$  size was found in a low flow sample, either the actual discharge during the sampling period was greater than the critical discharge for a period of time (in six cases) or the sample contained a single particle greater than the  $D_{35}$  size (two cases).

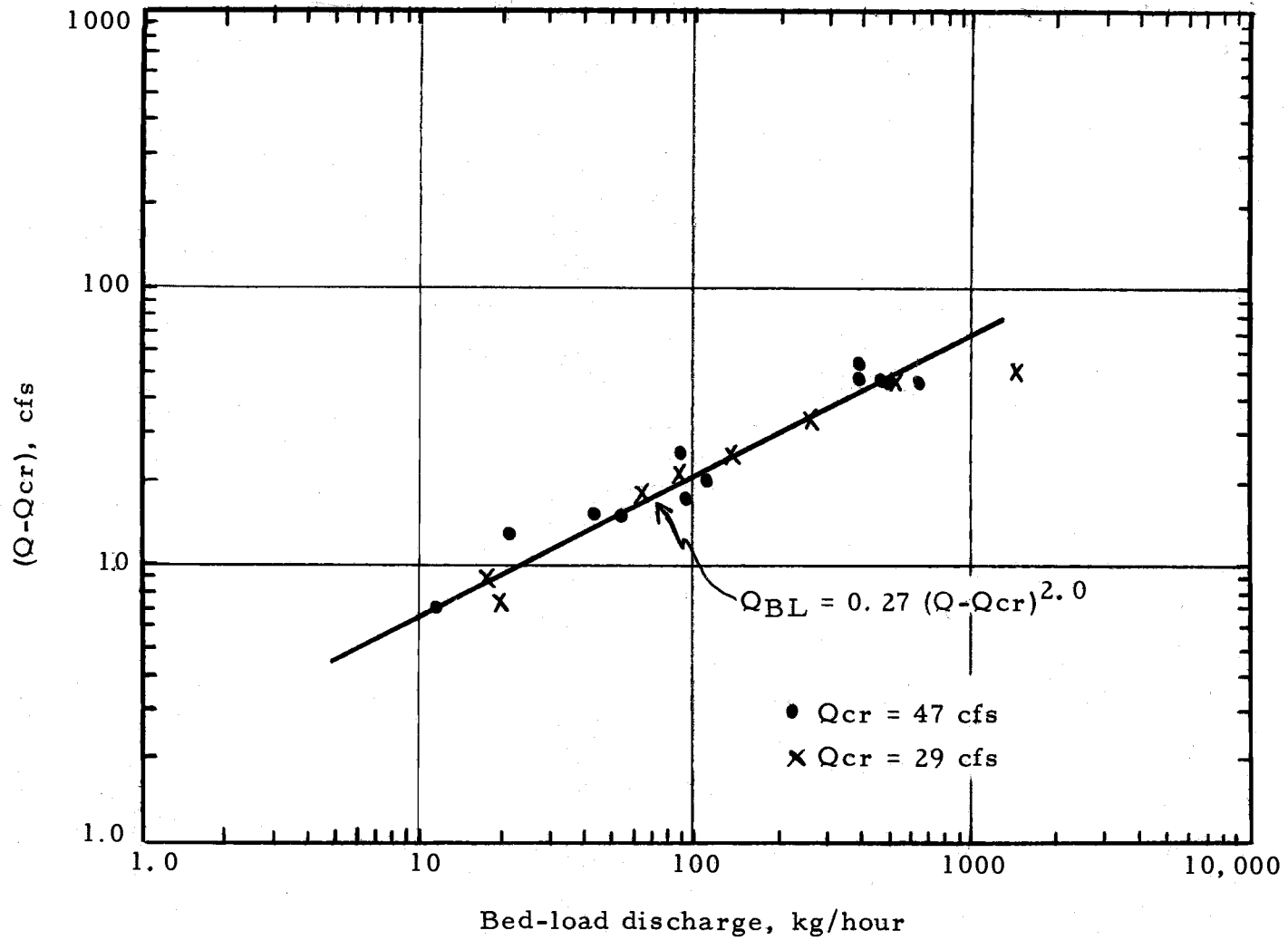


Figure 23. Bed load discharge as a function of stream discharge above a critical rate, 1971 data.

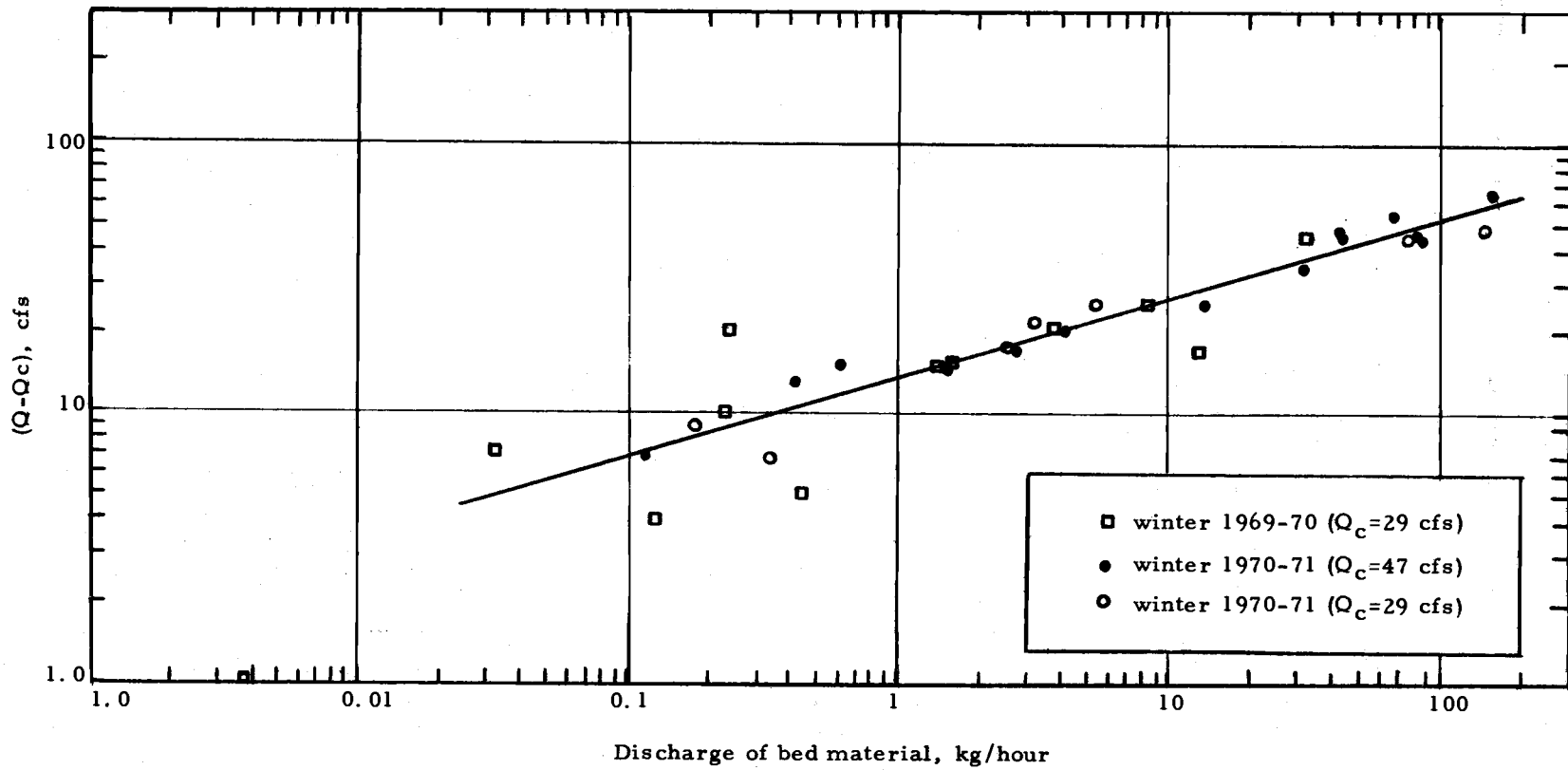


Figure 24. Discharge of bed material greater than  $D_{35}$  of the armour layer versus river discharge greater than a critical discharge.

Only two of these eight cases were for 1971 data.

The scatter of the 1969-70 samples is much greater for the 1971 samples because the quality of the sampling program was improved during the study period.

The critical shear stress for some of the 1971 samples is the same as for the 1969-70 samples. These samples were obtained on March 10 and 11, 1971, on the falling limb of a runoff event that had a peak flow of 115 cfs and on the rising limb of the runoff event that followed. The data suggest that a shift in the transport rate was due to a change in critical discharge for the armour material due to the March 10 event. The armour material was sampled on January 29, 1971, and July 27, 1971. The mean size was the same on each occasion but the  $D_{90}$  size had decreased from 8.8 cm in January to 7.7 cm in July. These data indicate the armour material was similar in July 1971. The change in critical discharge may have resulted from a temporary change in the armour material. After the bed load samples were collected on March 11th, the stream flow continued to increase and reach a new peak of 170 cfs. The critical particle size associated with the peak flows are given in Table 8.

Table 8. Critical particle sizes for peak flows during 1971 sampling period.

Date	Peak Flow, cfs	Critical Grain Size, cm ( $f_s = 0.025$ )	Probability of Particle Movement at Peak Discharge for Indicated Size	
			5.2 cm	4.2 cm
16 January 1971	280	16	0.83	0.89
10 March 1971	115	11	0.58	0.75
11 March 1971	170	13	0.70	0.82

\* Probability of a particle of size  $d$  being moved by the peak discharge (see text).



The size of particles in the armour layer is probably related to the peak discharge as well as the duration of the peak. Consequently, the storm on March 10th may have reduced the coarseness of the bed armour more than is indicated by samples of the armour obtained after the second storm peak on March 11th (the July samples), with the result that the critical discharge of 29 cfs may be associated with an armour layer of a mean size less than 6.3 cm. The fact that the critical discharge for the winter of 1969-70 was also 29 cfs suggests that the median size may have been in the order of 5.2 cm. The process may have been that larger particles were not transported effectively by the peak flow on March 10th (which had associated with it a critical grain size of 11 cm) and instead worked their way down into the bed as other particles were moved from around them, with the result that the particles on the bed surface at the time of sampling were finer than prior to the peak. On March 11th, the duration and the peak were large and may have returned some of the larger particles to the armour layer.

#### Fine Material in the Armour Layer

The conclusion from the above analysis of critical shear stress analysis is that there is a critical shear associated with the armour layer. But in actual fact, particles of a wide range of sizes are found in the armour and many of the particles are small enough that they

could be transported by flows of less than the critical discharge if they were not protected by the larger particles. In other words, the smaller particles are hidden from the hydraulic forces of the stream by larger stable particles.

The ability of a particle to hide is related to the uniformity of the bed material. If the mean size is large and the standard deviation of the material is also large, some of the smaller particles may be "hidden" by larger particles. Hence, the critical shear for these hidden particles will be larger than for particles of the same size in a uniform bed.

Einstein has used a "hiding factor" in his method for calculating rate of bed material movement. Using equation 17-II-23 from Einstein (1964) we have:

$$\psi_* = \mathfrak{f} Y \left[ \frac{\log 10.6}{\log 10.6 \frac{X}{D_{65}}} \right]^2 \frac{\rho_s - \rho_f}{\rho_f} \frac{D}{R S} \quad (23)$$

where:

$\psi_*$  = flow intensity parameter or stability parameter;

$\mathfrak{f}$  = a correction of effective flow for various grains (hiding factor);

$Y$  = a correction of lift force in transition between hydraulically rough and smooth beds, in terms of  $D_{65}/\delta$ , where  $\delta$  is the thickness of the laminar sublayer;

$X$  = a reference grain size for a particular bed;

$\chi$  = a correction factor in terms of  $D_{65}/\delta$  for surface drag;

$\rho_s, \rho_f$  = densities of the sediment and fluid, respectively.

For a rough bed,  $\beta$  is 1.0,  $X$  equals  $0.77 D_{65}/\chi$  and  $Y$  equals 0.52.

Using equations (15) and (18), we can write for rough bed that:

$$\psi_* = \beta Y \left[ \frac{\log 10.6}{\log 10.6 \frac{0.77 D_{65} \chi}{D_{65} \chi}} \right]^2 \frac{1}{f_s} = 0.66(\beta) \left( \frac{1}{f_s} \right) \quad (24)$$

for a uniform rough bed  $\beta = 1$  and we have

$$\psi_* = 0.66 \frac{1}{f_s} \quad (25)$$

Einstein (1950) states that for a uniform rough bed:

$$\beta = 1$$

$$Y = 1$$

$$\left[ \frac{\log 10.6}{\log 10.6 \frac{X \chi}{D_{65}}} \right]^2 = 1$$

Hence,  $\psi_*$  equals  $1/f_s$ . Apparently, there is a discontinuity in Einstein's procedure.

An armour layer is sufficiently uniform that the pressure correction ( $Y$ ) would be equal to unity and the velocity correction (term in brackets above) would also equal unity; but there are numerous hiding places in the armour layer. Therefore, the Einstein hiding

factor appears to be an appropriate way of handling smaller particles in an armour layer. (Further research into the hiding factor for an armour layer would be valuable.)

Using the concepts above, the stability parameter is essentially

$$\psi_* = \left(\mathfrak{F}\right)\left(\frac{1}{f_s}\right) \quad (26)$$

The hiding factor is a function of the  $D/D_{65}$  ratio.

The function relating  $\mathfrak{F}$  to  $D/D_{65}$  can be linearized by two functions by a linearized approximation to the function above  $X/D$  greater than 0.5 which was then projected back to the  $X/D$  equal to 0.69 (see Figure 7.11 of Graf). The resulting functions are:

$$\mathfrak{F} = 1 \quad \text{at } D \geq 0.69 D_{65} \quad (27a)$$

$$\mathfrak{F} = 0.77 \frac{x}{D}^{2.39} = 0.42 (D_{65}/D)^{2.39} \quad \text{at } D \leq 0.69 D_{65} \quad (27b)$$

If we take the reciprocal of the stability factor  $\psi$ , we have the parameter  $f_s$ . Using the reciprocal of  $\psi_*$  as  $f'_s$ , we can write:

$$f'_s = f_s = 1/\psi_* \quad \text{at } D \geq 0.69 D_{65} \quad (28a)$$

$$f'_s = 0.42 (D_{65}/D)^{2.39} f_s \quad \text{at } D \leq 0.69 D_{65} \quad (28b)$$

Hence, the stability of a particle increases as its size in a heterogeneous bed decreases below  $0.69 D_{65}$ .

During most of the 1971 sampling program, the  $D_{65}$  size for the armour layer was 7.4 cm; hence, particles with a diameter smaller

than 4.8 cm were "hidden" by the flow. This size corresponds to the  $D_{30}$  size of the armour layer. In other words, about 30% of the bed surface is "hidden" from the fluid shear effects. During the 1969-70 sampling period the  $D_{65}$  size of the armour layer was 5.8 cm. Hence, the  $0.69 D_{65}$  size is 4.0 cm which is also about the  $D_{30}$  size of the armour material. To illustrate the hiding effect, support that we are interested in  $f_s'$  for particles of 0.2 cm in size during 1971. We then have:

$$f_s' = 0.42 \frac{7.4}{0.2}^{2.39} f_s = 2320 f_s$$

which indicates the critical shear stress for sand size particles is very high. The  $f_s'$  calculated using the equation above is probably much too large, since sand was obtained in the low flow bed load samples. Nevertheless, even a value an order of magnitude smaller (230) indicates the sand particles would be difficult to entrain in the flow.

#### Minimum Critical Shear Stress for "Break-Up" of Heterogeneous Armour

Using the  $D_{65}$  size of 7.4 cm, a Shields parameter of 0.032, and the equations developed above, the critical shear stress for each size of material in the armour layer was calculated. The resulting plot of the critical shear stress versus grain size is given in Figure 25.

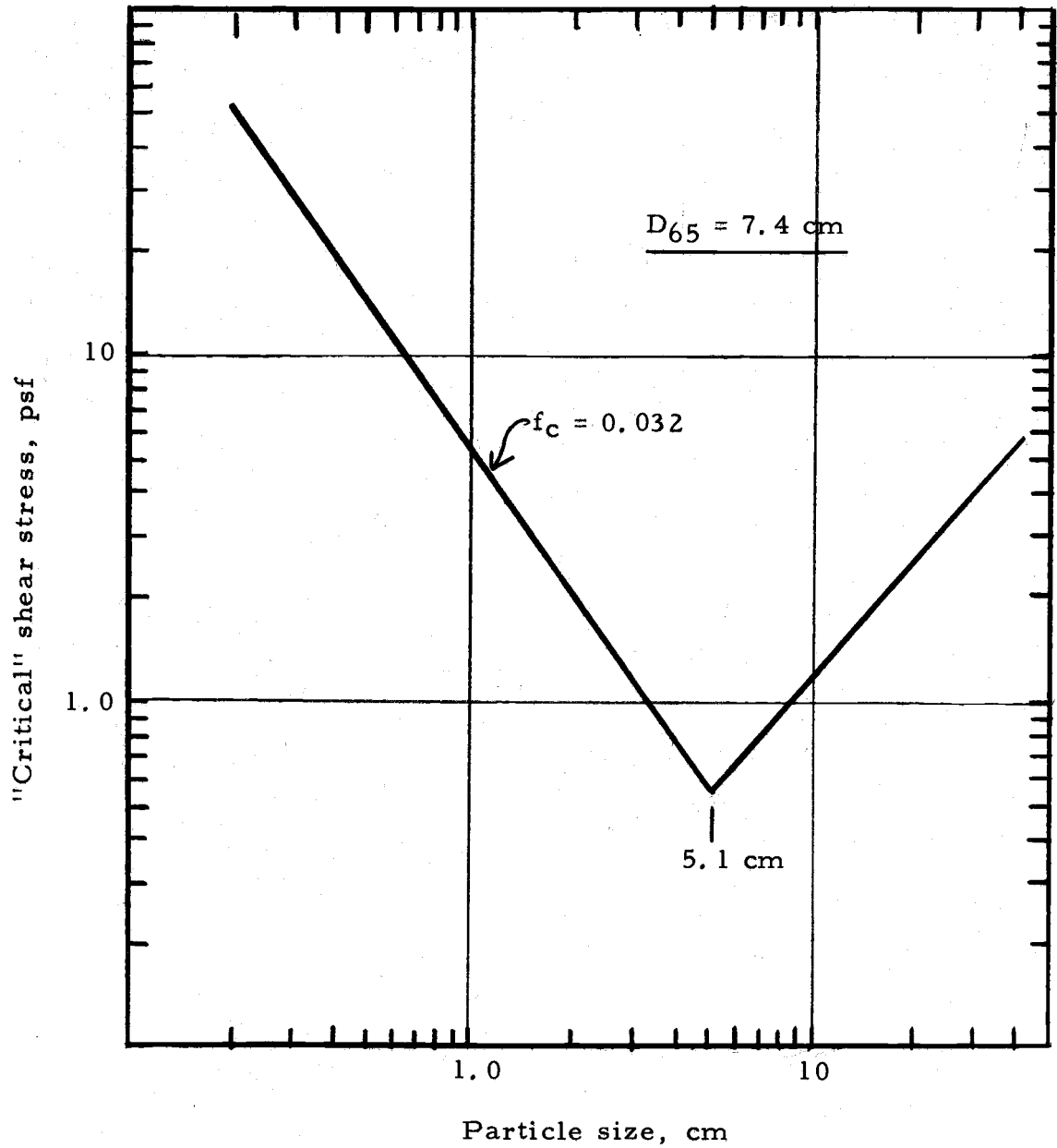


Figure 25. Critical shear stress for various sizes in a non-uniform armour layer.

The minimum critical shear stress occurs for the 0.69 D<sub>65</sub> size.

The diagram also indicates the sand size particles (D < 0.2 cm) should be very stable.

The 0.69 D<sub>65</sub> size may be considered as the size of a particle in an armour layer having the minimum stability. This is because the particles of larger size are more stable because they are bigger, and smaller sizes are more stable because they are hidden. Consequently, it is expected that when the critical shear stress associated with the 0.69 D<sub>65</sub> size is exceeded by the time average shear stress the armour layer will begin to "break up" and the bed load will become significant. Hence, the Shields parameter associated with the critical discharge and the 0.69 D<sub>65</sub> size represents a stability term for incipient motion of the armour layer. The Shields parameter has been calculated for the 1969-70 and the 1971 data. Results are presented in Table 9. The average value of the Shields parameter using the 0.69 D<sub>65</sub> size is 0.032 and for the D<sub>65</sub> size is 0.047. Hence, we can say

$$(\tau_o)_{\text{critical}} = 0.047 (\gamma_s - \gamma) D_{65} \quad (29)$$

The equation is similar to the equation developed by Meyer-Peter, Müller (1948) except that the D size in the Meyer-Peter, Müller equation is the mean size, which Meyer-Peter, and Müller consider to be between the D<sub>50</sub> and D<sub>60</sub> sizes.

Table 9. Shields parameter for the Oak Creek armour layer.

Critical Discharge, cfs	Bounds for Shear Stress, psf	D <sub>65</sub> cm	Range in Shields Parameter 0.69 D <sub>65</sub> size	Mean Shields Parameter for shown diameter	
				0.69 D <sub>65</sub>	D <sub>65</sub>
29	0.44-0.56	5.8	0.029-0.035	0.033	0.048
47	0.52-0.62	7.4	0.030-0.034	0.032	0.046

The equations and information above suggests that the D<sub>65</sub> controls the movement of the armour because the size with the minimum critical shear stress is related to the D<sub>65</sub> size. We could just as well conclude that the "critical" shear stress for the armoured stream bed in Oak Creek is the shear stress corresponding to the minimum critical stress calculated using the hiding factor given above. This critical shear stress will correspond to the critical shear stress of the particle with size D equal to 0.69 D<sub>65</sub>. No information is available to the writer on the applicability of the concept given above for streams other than Oak Creek.

#### Probability of Armour Layer Movement

The next point to be examined is the nature of the critical shear term. If we consider a system where the velocity at a point is random variable with the form

$$U = \bar{U} + U' \quad (30)$$

where U is the instantaneous velocity,  $\bar{U}$  is the time average velocity



and  $U'$  is a random variable with a mean value of zero. The variation in velocity causes a variation in the "entrainment" forces being applied to particles on the stream.

First, we shall start with the friction force. The logarithmic velocity function can be arranged as:

$$\frac{v}{\tau_o/e} = 8.5 + 2.5 \ln \left( \frac{y}{k} \right) = 2.5 \ln \left( \frac{30y}{k} \right) \quad (31)$$

where  $v$  is the velocity at some point of height  $y$  above the bed,  $\tau_o$  is the bed shear stress,  $\rho$  is the fluid density, and  $k$  is the size of roughness.

For a given height above the bed we can say:

$$\tau_y = C_y \cdot \gamma \frac{v^2}{2g} \quad (32)$$

Consequently, as the velocity varies the shear stress on the stream bed will vary as well, but as a function of the velocity squared. If we consider the drag force to be a function of  $\tau$ , and the lift force to be related to the drag force, we can write

$$F_D \sim C_D \gamma \frac{v^2}{2g} \quad (33a)$$

$$F_L \sim C_L \gamma \frac{v^2}{2g} \quad (33b)$$

Hence, both the drag force and lift force are a function of the velocity squared.

Gessler (1970, 1971) conducted a series of experiments on the nature of the armouring process. He started with a bed of well mixed heterogeneous material and allowed the water flowing over the bed to remove the finer material with the end result that the bed became armoured and the removal of material by flow ceased. As a result of his experiments, he developed data on the relationship between the ratio of the critical shear stress and the mean shear stress ( $\tau_c/\tau_o$ ) versus the probability of a particle remaining in the armour layer. This diagram is given in Figure 26. On Figure 26,  $\tau_c$  is critical shear stress for a given size particle, and  $\tau_o$  is the time average shear stress on the stream bed. Gessler postulated a normal distribution for the probability function but this would not satisfy the boundary conditions. The principal boundary condition not satisfied is that as  $\tau_c/\tau_o$  approaches zero then the probability of a particle remaining in the bed should also approach zero, which did not happen for Gessler's distribution.

Benedict and Christensen (1971), in a discussion of the Gessler paper, suggested the use of an analytical probability function. Their deviation of the function starts with

$$\tau = C \gamma \frac{U^2}{2g} \quad (34)$$

Assuming that the mean shear stress is given by

$$\tau_o = C \gamma \frac{\bar{U}^2}{2g} \quad (35)$$

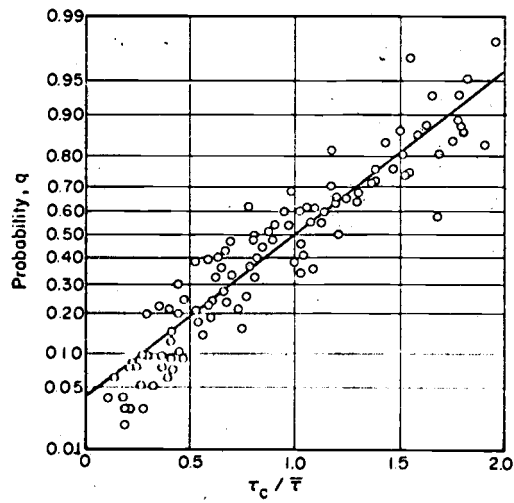


Figure 26. Gessler's probability of grains remaining in the y layer,  $q$  versus  $\tau_c / \tau_o$  ( $= \circ$ ) (from Gessler, 1970).

and taking the ratio

$$\frac{\tau}{\tau_0} = \left( \frac{U}{\bar{U}} \right)^2 \quad (36)$$

and using the equation for U, we have:

$$\frac{\tau}{\tau_0} = \left( \frac{\bar{U} + U'}{\bar{U}} \right)^2 = 1 + \left( \frac{U'}{\bar{U}} \right)^2 \quad (37)$$

remembering that U' is a random variable, we can write'

$$\frac{\tau}{\tau_0} = (1 + ns)^2 \quad (38)$$

where s is the coefficient of variation ( $\sigma_\mu/\bar{U}$ ), n is the normalized velocity fluctuation  $U'/\sigma_\mu$ , and  $\sigma_\mu$  is the standard deviation of velocity fluctuations. Typically, it is assumed the velocity fluctuations are normally distributed. Information in the Benedict and Christensen discussion and in the closure by Gessler indicate a coefficient of variation of 0.28 at a distance equal to one roughness height from a rough wall. Consequently, we have

$$\frac{\tau}{\tau_0} = (1 + 0.28 n)^2 \quad (39)$$

If the mean shear stress and the critical shear stress are known, then the probability of a particle remaining in the bed can be calculated. If we assume a particle moves when  $\tau_c/\tau_0$  is less than one, then the probability of a particle remaining in a bed will be the same as the probability of being n standard deviations from the mean. We can calculate n using the equation

$$n = \frac{1}{s} \left( \sqrt{\frac{\tau_c}{\tau_o}} - 1 \right)$$

As an example, let us assume that the ratio  $\tau_c / \tau_o$  is 1.5, and  $s$  is 0.28. Hence,  $n$  is 0.805 and the probability of the particle remaining in the bed is 0.79 for normally distributed velocity fluctuations.

Benedict and Christensen presented Gessler's diagram with the probability functions for  $s = 0.18$  and  $0.28$  shown on the figure. This diagram is given as Figure 27. When  $\tau_c / \tau_o$  is zero, then  $n$  is -3.58, and the probability of a particle remaining in the bed is 0.0002 for the model postulated above. For various probabilities ( $P_r$ ) of a particle remaining in the bed we have:

$P_r$	$n$	$\tau_c / \tau_o$	$f_{s'} / f_s$	$f_{s'}$
0.999	3.1	3.50	0.29	0.014
0.99	2.3	2.70	0.37	0.017
0.98	2.1	2.53	0.40	0.019

where  $f_{s'}$  is the value of  $\tau_c / (\gamma_s / \gamma) D$  when the probability of remaining in the bed is as stated above, and  $f_s$  is defined as the value of  $f_s$  when the probability of a particle being moved is 0.50. Information in Gessler's paper indicates that  $f_s$  is 0.047. Using the value of 0.047 for  $f_s$ , the value of  $f_{s'}$  for various probabilities of a particle remaining in the bed are given in Figure 28. The probability of particles

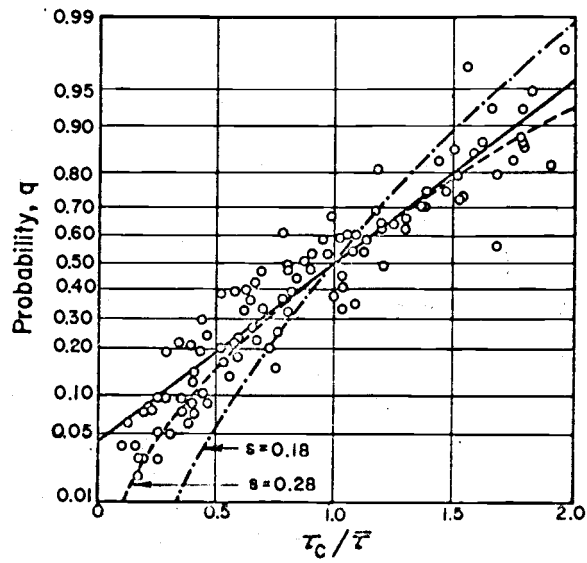


Figure 27. Gessler's data compared with theoretical relationship (from Benedict and Christensen, 1971).

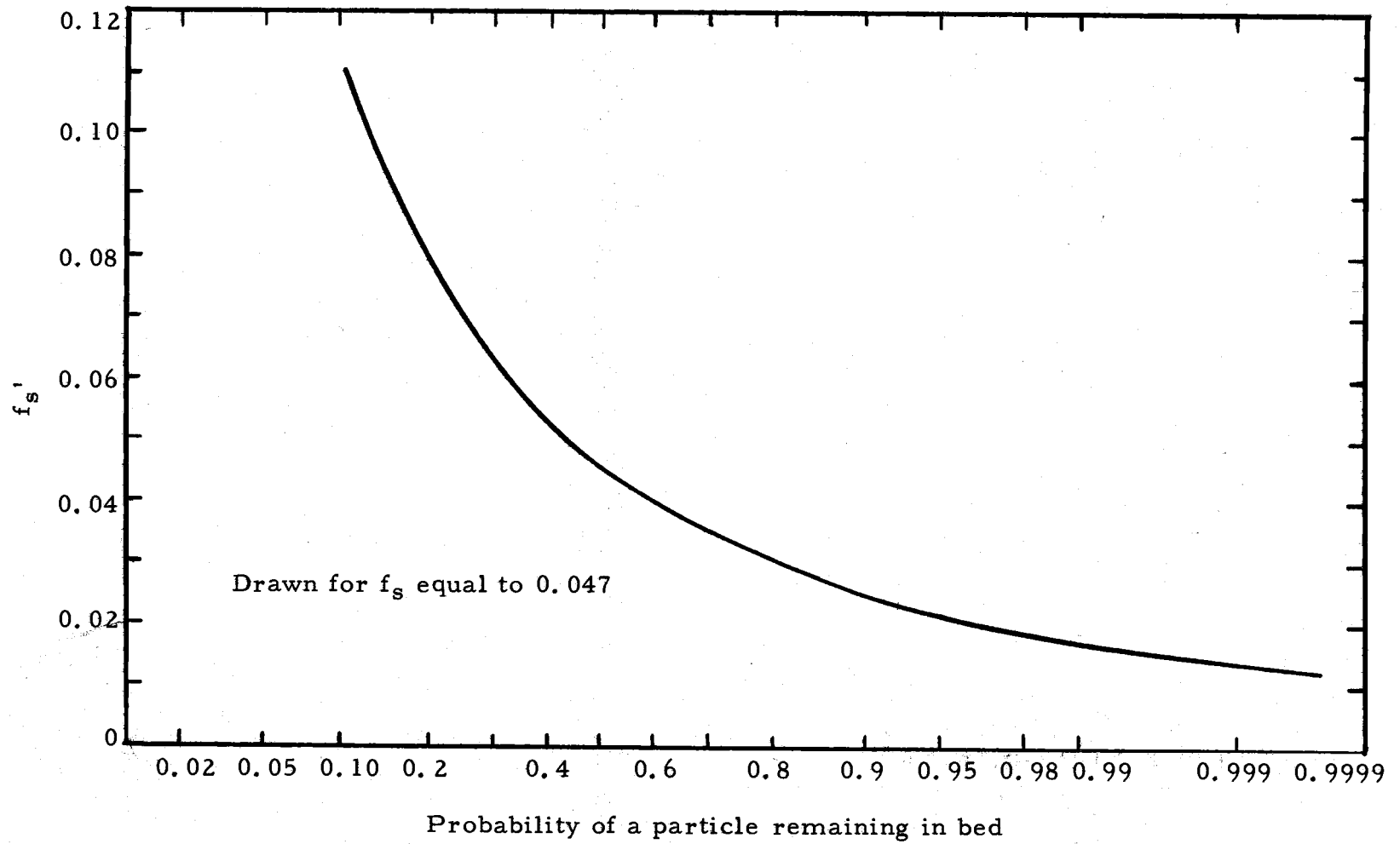


Figure 28. Probability of particles remaining in a bed, given the Shields parameter.

remaining in the bed when  $f_s'$  equals 0.032 is 0.78. For calculating the critical shear stress and discharge in Oak Creek, 0.032 is the estimated value for  $f_s$ . The values of  $\tau_c/(\gamma_s - \gamma)D$  are from 0.017 to 0.076 which corresponds to a probability ranging from 0.33 to 0.82. The value of  $f_s'$  at a probability of 0.9999 is 0.012, which can be taken as a lower bound on  $f_s'$  and is the same as the lower bound on Figure 22.

The value of  $f_s$  at 0.99 probability of a particle remaining in the bed is 0.017, which is the lower bound on the published values as well as for the Oak Creek data. This corresponds to a minimum shear stress (at  $D_{65} = 7.4$  cm) of 0.33 psf, which occurs at a flow of 3 cfs. A value of 3 cfs is a low flow in Oak Creek, although the summer flows are lower (approximately 60% of the time flows are greater than 3 cfs). We can interpret the above as saying that during much of the year the flow is capable of dislodging particles from the armour even though the probability of actually doing so is quite low.

#### Relationship Between Probability of Movement and Bed Load Transport

The conclusions reached above all seem reasonable but there should be some way of calculating the rate of transport, given the probability of particles being moved. This can be investigated by developing a conceptual relationship between the ratio of the mean shear stress to critical shear stress and the transport rate. This is



given in the following paragraphs.

The number of particles removed in any time interval can be calculated using the model that the number (N) of particles in motion at any one time will be

$$N = \int_{D_{\min.}}^{D_{\max.}} F_D P_D A dD \quad (41)$$

where  $P_D$  = the probability of a particle of size D will be in motion

$A$  = the area of stream bed

$F_C$  = the friction of a unit surface area with particles of size D

If we assume a uniform bed material and that, for a particle in motion, the velocity ( $V_D$ ) of a given size particle (D) is constant for that size and has a weight (W), then the number ( $N_T$ ) of particles crossing a line of unit width in a time interval  $\Delta t$ , is:

$$N_T = \left( \Delta t \frac{q_s}{W} \right) = \left[ (V_D \Delta t) P_D \right] \quad (42)$$

from which we can write:

$$q_s = (V_D P_D) (W) \quad (43)$$

if the particle velocity is a direct function of the shear velocity

$\sqrt{\tau_0 / e}$  we can write:

$$V_D = f(\sqrt{\tau_0 / e}) = K_d \sqrt{\tau_0 / e} \quad (44)$$

where  $K_d$  is a constant. From this we can write:

$$q_s = K_d \sqrt{\frac{\tau_o}{e}} P_D W \quad (45)$$

but,

$$P_D = f(\tau_o / \tau_c) \quad (46)$$

hence,

$$q_s = \left[ K_D \sqrt{\frac{\tau_o}{\tau}} W \right] \left[ f(\tau_o / \tau_c) \right] \quad (47)$$

This is different than the Meyer-Peter, Müller equation, which can be written in the form,

$$q_s = K(\tau_o - \tau_c)^{3/2} \quad (48)$$

The difference between the two relationships is that transport is possible (but with low rates) in the first relation but not in the second relation at shear stresses below the critical shear stress, as actually occurs.

The Kalinske bed load equation, like equation (47), is of the form:

$$q_s = f\left(\frac{\tau_o}{\tau_c}\right) \quad (49)$$

The Kalinske function is given in Figure 29, along with the probabilities of a particle remaining in the bed, as developed by Gessler. The Shields parameter used by Gessler was 0.047 and that used by Kalinske was 0.038. The Kalinske diagram clearly illustrates that

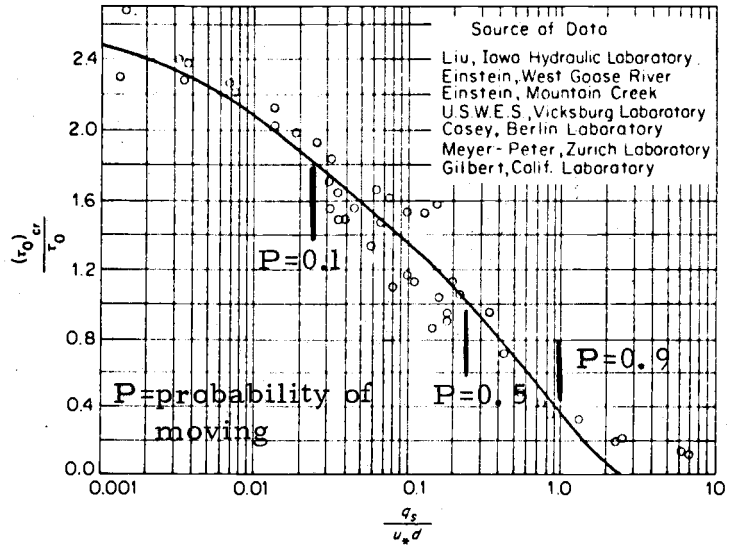


Figure 29. Kalinske's bed load equation (after Kalinske, 1947, presented in Graf, 1971).

the transport rate associated with low probabilities of movement is quite low.

### Stationarity of the Probability Function

Subjective field observation suggested that the armouring particles increase in stability with time following a high flow, provided that the critical discharge is not exceeded. If this observation is correct, it probably results from the fact that after disturbance (and/or general movement) some particles are exposed to the drag and lift forces of the stream more than others. These particles will be moved first (actually, they have a higher probability of being moved). After such a particle is moved, there is some probability that the particle will come to rest in a more stable position than it had when it started. The net result over a period of time is that the "stability" of the bed will increase. A possible relationship of the transport rate over time for a discharge less than the critical discharge, following a discharge greater than critical, is shown on Figure 30.

The brief discussion above indicates that the probability of particle movement is not a constant but is likely to be a variable which depends on the past history of flows. From the viewpoint of probability concepts, this means that the probability function is non-stationary with time. In other words, the probability of a given size

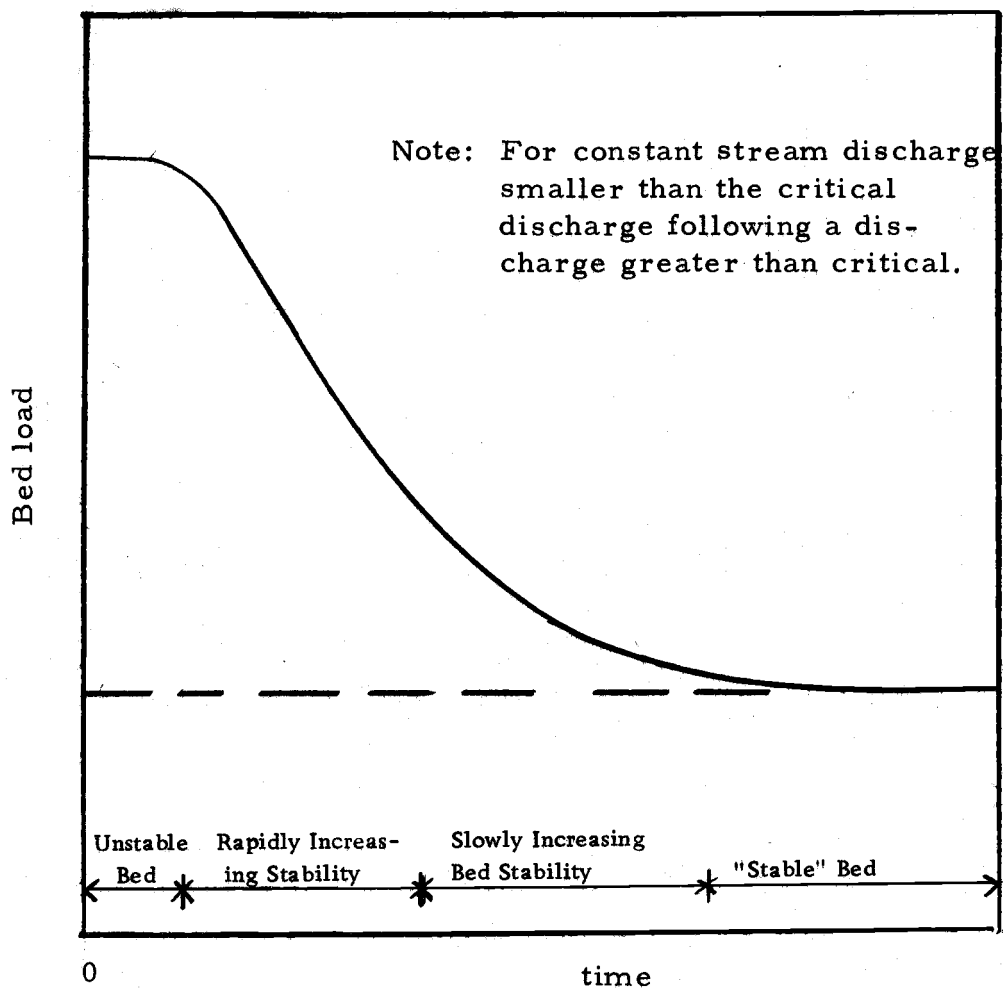


Figure 30. Conceptual relationship between bed load transport rate and time for a constant stream discharge.

particle moving is not the same at time  $t$  as it is at time  $t + \Delta t$ .

### Sediment Transport at Low Shear Stresses

#### Paintal's Experiment

Some methods of estimating the bed material movement in a stream assume that the sediment transport rate is zero below some critical shear stress. Based on the probability function described previously, it is obvious that there is some probability of sediment transport at all levels of bed shear stress and, in the words of Paintal (1969), "this probability is never zero except in still water."

Considerable work by Paintal (1969) on the movement of sediment demonstrates that bed material will be transported at very low shear stresses. Paintal's experiments were carried out with the Shields parameter ( $f_s$ ) in the range  $0.007 < f_s < 0.08$ . He concluded that the sediment transport rate at low shear stress for a given sediment size is proportional to the 16th power of the Shields parameter.

#### Interpretation of Helland-Hansen's Experiments

Experiments at low shear stress have also been carried out at Oregon State University by Helland-Hansen (1971, 1972) using a long concrete flume located across a meander loop of Oak Creek. The flume discharge was dependent upon the creek discharge. However,

flow reduction could be achieved by manipulation of a set of entry stoplogs. A gravel bed was placed in the flume such as to have a deep pool at the downstream end of the gravel bed. The gravel was discoid (rounded and flattened) in shape with a gravity of 2.65. The median size of the gravel was 2.5 cm, the maximum size was 3.8 cm,  $D_{35}$  was 2.0 cm, and  $D_{65}$  was 2.8 cm and the maximum size was 3.8 cm. All of the gravel transported out of the bed was trapped in the pool behind a downstream stoplog structure and was collected as desired. Experiments were conducted continuously during the spring of 1971, under gradually decreasing flume discharges. Gravel in the downstream pool trap was removed periodically.

The results of Helland-Hansen's experiments are given in Table 10. A plot of discharge versus rate of bed material transport is given in Figure 31.

Samples 1 through 6 pertain to an undisturbed, hydraulically formed gravel bed. The gravel was typically rounded with a flat-to-spherical shape and with a gradation similar to that in Shields experiments. The surface particle had formed an imbricated surface pattern.

A series of short-time experiments on incipient motion with temporarily higher discharges, surging and some disturbance of the gravel surface were carried between samples 7 and 8. After this date, however, the bed was again left undisturbed. The flume was left

Table 10. Helland-Hansen data on long-term bed material movement at low flows.

Sample Number	Average Discharge per unit width, cfs/ft	Depth of flow, ft	Mean Velocity, fps	Bed Material Load, gm/hour	Maximum Size Fraction in Sample, inches
1	2.2	0.62	3.55	17.0	1
2	1.45	0.51	2.84	7.6	3/4
3	1.20	0.46	2.61	6.55	1
4	0.85	0.40	2.12	2.06	3/4
5	0.85	0.40	2.12	2.30	3/4
6	0.72	0.36	2.00	1.14	3/4
7	0.62	0.33	1.88	12.5	1
8	0.52	0.30	1.73	1.87	1
9	0.46	0.27	1.70	2.19	1
10	0.42	0.25	1.68	0.78	3/8
11	0.34	0.22	1.63	0.15	3/8

Data source, Helland-Hansen (1971)



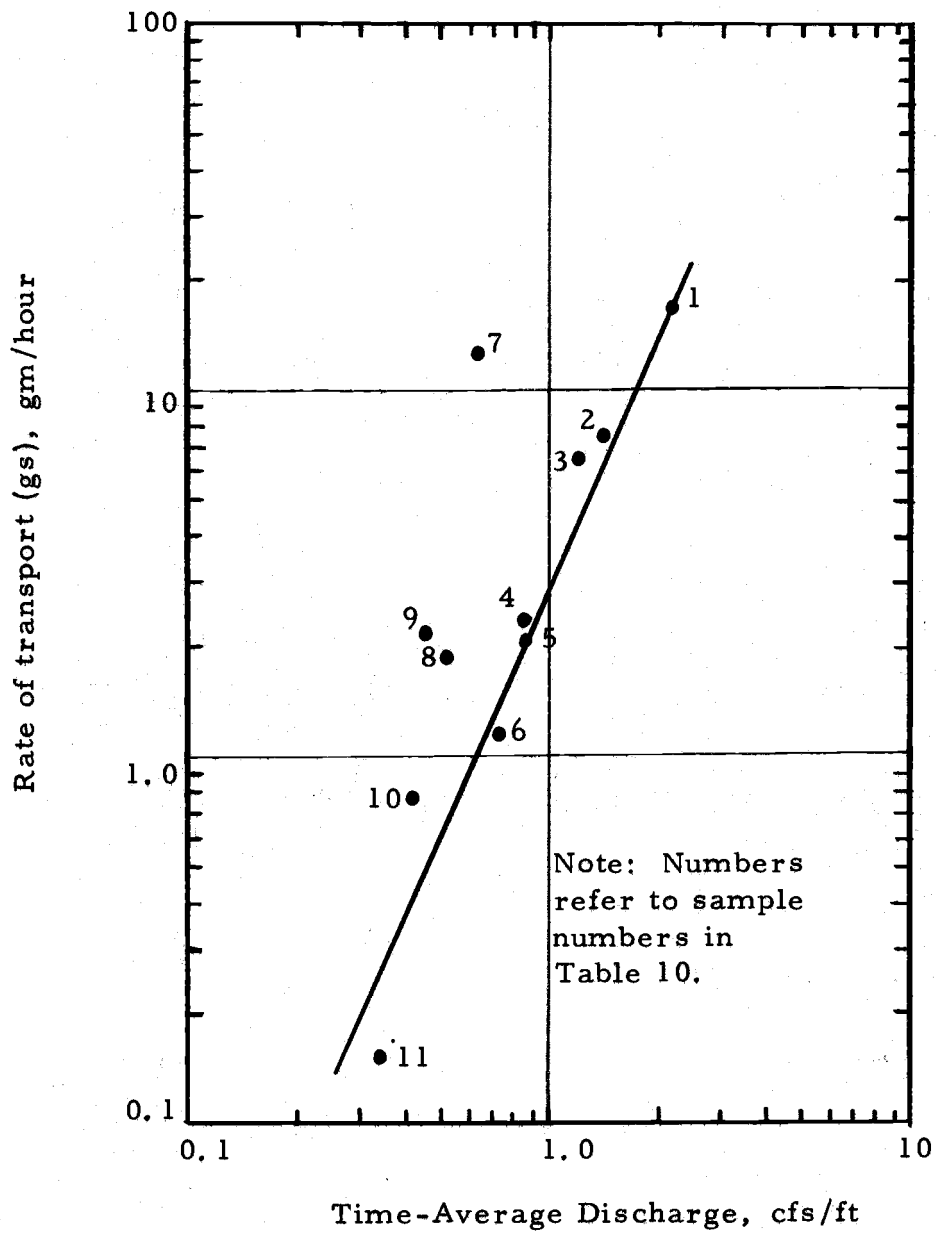


Figure 31. Gravel transport rate as function of mean stream flow rate during period (from Helland-Hansen, 1971).

unattended in an area occasionally visited by people and animals. Hence, there was no guarantee that the gravel bed and downstream pool were undisturbed at all times. By manipulating the gates on the flume surging could occur and these could be opened and closed by anyone who happened by. A surge at the channel was reflected in stage changes at the gaging station at the bed load sampling station. These records indicate that the gates were operated during the collection of sample 7. Hence, the data for sample 7 are not useable in studying bed load transport at low shear stresses.

The use of a single time-average discharge for each sample on Figure 31 implies that constant transport conditions prevailed between samplings, a condition that clearly was not satisfied. The actual discharge varied and the total transport in the period was composed of a relatively small number of discrete particles moved. Nevertheless, use of an average discharge is considered adequate for the purposes of the analysis.

Visual observations of the gravel bed during the experimental period always gave the impression that the bed was stable. Although no movement or instability could be detected during short-term observations, particles were carried out of the gravel bed, given sufficient time and a fool-proof observation method.

The data points plotted in Figure 31 represent gravel transport at low rates undetectable by normal visual means. For example,

sample 1 represents transport of particles 3/4" to 1" diameter at the rate of one particle per hour, sample 5 corresponds to one 3/8" diameter particle transported per two hours, and sample 11 corresponds to one 3/8" diameter particle transported per day. It is interesting to note that even these extremely low transport rates seem to be functionally related to the strength of flow (here described by discharge). This behavior strengthens the probability based concept of particle motion by random turbulence, since the degree of turbulence is recognized to be related to the flow strength. It furthermore points out the weakness of the concept of a threshold of movement.

As can be seen from Figure 31, samples 7, 8, and 9 fall above a curve that is fitted to the remaining samples. Samples 8 and 9 were collected subsequent to mechanical disturbance of surface particle arrangement in two isolated areas of the stream bed. Sample 7 is not representative of low shear transport because of flow surging of unknown origin, as stated above.

Figure 32 shows grain size distribution curves for the gravel bed material and for the collected transported material. Collection of the trapped transported material was carried out such that only the gravel fraction coarser than 5 mm could be reliably recovered. Consequently, sand was discarded from the trapped samples and only material retained on a #4 standard sieve has been included in the

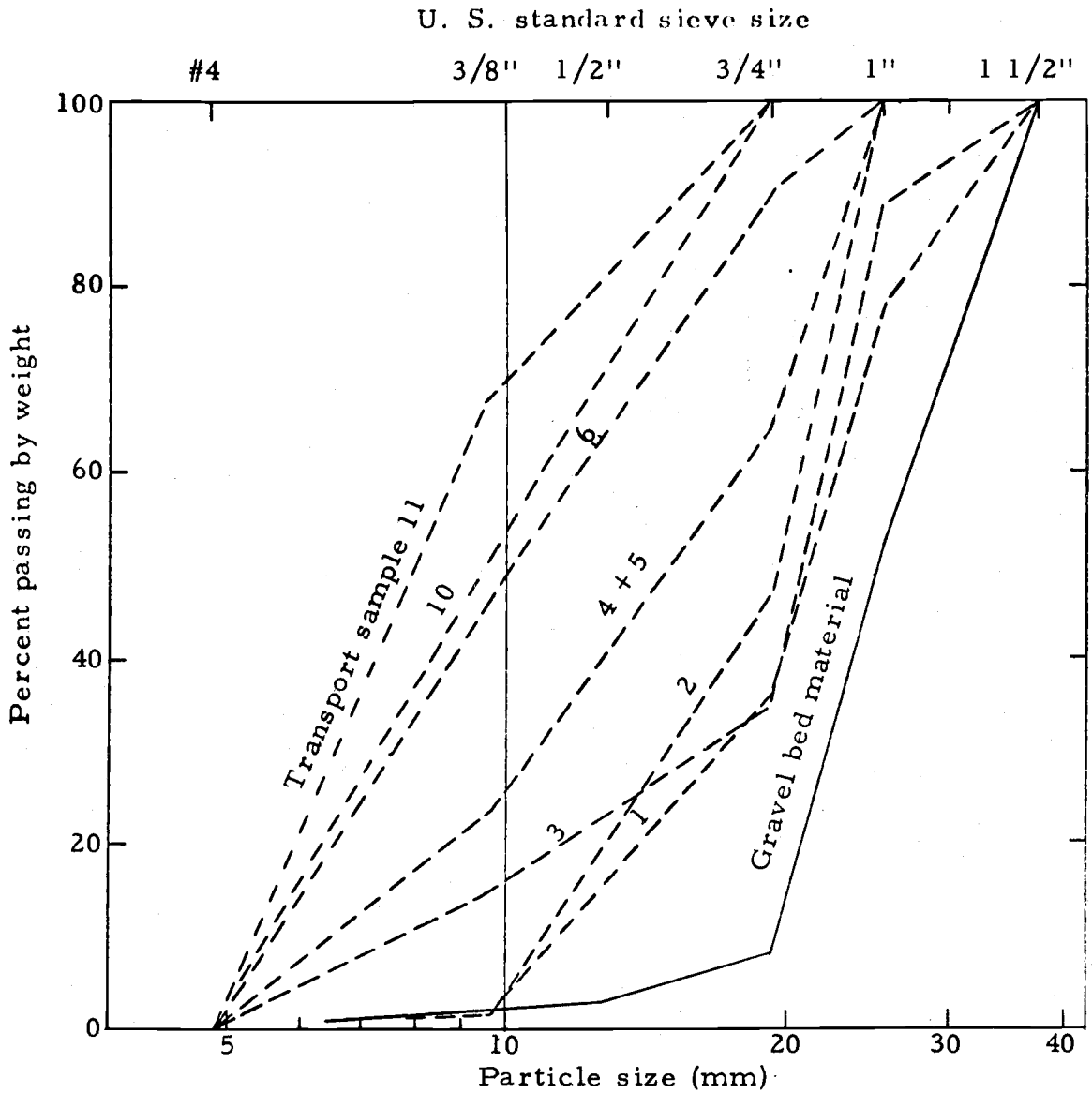


Figure 32. Grain size distribution curves for gravel bed and transported material (from Helland-Hansen, 1971).

analysis.

The grain size distribution curves in Figure 33 shows the selectiveness of the flow in dislodging particles under gradually decreasing discharge. It is of interest here that the flow does not only transport the medium-sized particles as described by Neill (1968), but transports the larger ones also, as long as the flow is sufficiently turbulent. The curves are basically similar in shape to the curve for the bed material but shift progressively farther from this curve toward finer sizes as the discharge decreases. This sequence of events conforms to what one might expect from a statistical viewpoint. Unfortunately, an accurate check of the degree of turbulence cannot be made. But rough checks of  $Re^*$  indicate its value to be above 1000 for all samples.

The relative roughness (roughness height  $D$  over depth of flow  $d$ ) values (1/8 to 1/3) do not satisfy Shields limit of 1/40 and are, for some of the lower discharges, also in conflict with Einstein's upper limit of about 1/5 for relative roughness. However, they do fall within Neill's (1968) specified limits (see Table 11).

The shear stress for Helland-Hansen's experiments could not be calculated directly, but can be calculated indirectly. If we assume a uniform velocity distribution, we have

$$\tau_o = \rho \left( \frac{U}{\ln (12.27 R/K_s)} \right)^2 \quad (50)$$

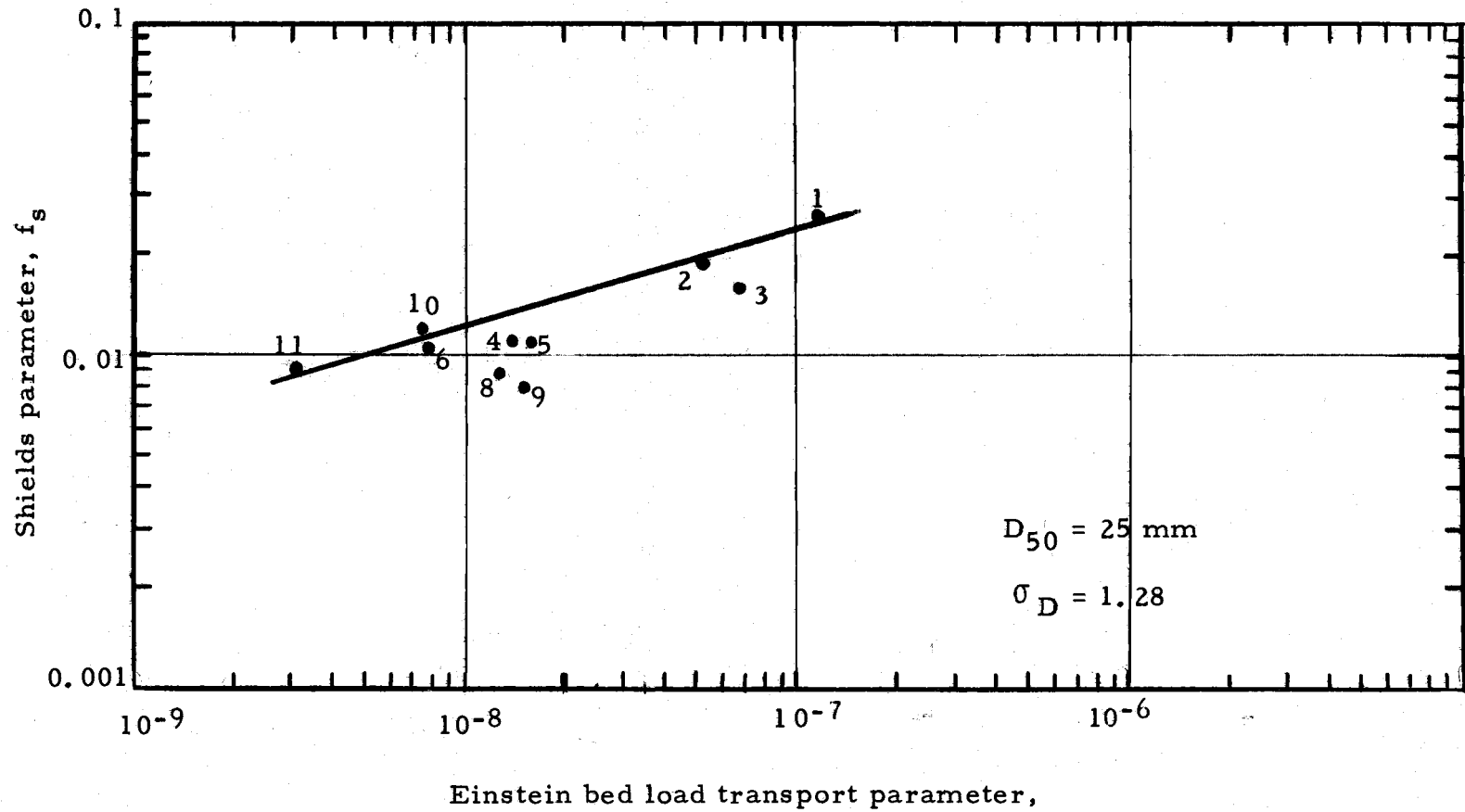


Figure 33. Shields parameter versus Einstein bed load transport parameter for the Helland-Hansen data.

Table 11. Einstein and Shields parameters for the Helland-Hansen data.

Sample Number	Discharge, cfs	D/d	Mean Velocity, fps	$f_s$	$\Phi \times 10^7$
1	6.6	0.13	3.55	0.027	1.8
2	4.35	0.16	2.84	0.019	0.52
3	3.6	0.18	2.61	0.016	0.68
4	2.55	0.21	2.12	0.011	0.14
5	2.55	0.21	2.12	0.011	0.16
6	2.16	0.23	2.00	0.010	0.079
7	1.86	0.25	1.88	0.0098	0.86
8	1.56	0.28	1.73	0.0087	0.13
9	1.38	0.31	1.70	0.0080	0.15
10	1.26	0.33	1.68	0.012	0.075
11	1.02	0.38	1.63	0.0090	0.031

where  $U$  is the mean velocity and  $K_s$  is a representative roughness taken to be the  $D_{65}$  size of the bed material. The  $D_{65}$  size is 2.8 cm for the 11 sets of data described above. Using this equation, the shear stress was calculated using the data in Figure 31. The Shields parameter was then calculated. The Shields parameter and the Einstein bed load transport parameter are given in Table 11 for each of the measurements given in Table 10. The relationship between the Shields parameter,  $f_s$ , and the Einstein bed load transport parameter,  $\Phi$ , is shown on Figure 33. The Einstein bed load transport parameter,  $\Phi$ , for a uniform bed material is given as

$$\Phi = \frac{q_s}{G_s D^{3/2} \sqrt{G_s - 1}} \quad (51)$$

where  $q_s$  is the bed load transport per unit width of channel;  $G_s$  is the specific gravity of the particles.

The line on Figure 33 is an approximate upper bound line based on the concept that as the time a bed is subjected to a given flow increases the bed will increase in stability. In terms of the probability function, we can say that the function is not stationary but changes with time. The concept given above is that when the bed is disturbed some of the particles lose their imbrication protection. Hence, the probability of particles of a given size being moved decreases with time. This is known to have occurred in the case of



samples 8 and 9. In the case of sample 3 there may have been a slight amount of disturbance caused by an increase in stream flow in the stream supplying water to the flume. This would result in the estimated Shields parameter being too low and in some disturbance to the bed. Disturbance of the bed imbrication can result from mechanical disturbance and from the disturbance caused by an increase in sediment transport, especially if the shear stress is above the critical shear stress.

#### Comparison of Concepts with Paintal Data

The data of Paintal (1969) can be used to obtain some idea of the validity of the ideas presented above. Paintal made measurements of the sediment transport rate at low shear stresses using a three-foot wide channel, 50 feet long. For bed material he used granular materials with three mean sizes: 22.5 mm, 7.95 mm, and 22.2 mm. Three different materials were used with a mean size of 22.2 mm. The materials varied in their ranges of sizes such that the standard deviations were 1.07 (uniform gradation), 1.57, and 2.73. The experiments were made by flooding the gravel slowly and then increasing the discharge to a desired value in a relatively short time. The flume was dewatered between runs. Paintal makes the following statement:

During the first several runs of each series the gravel bed remained plane as if it was molded at the commencement of the series. After the first few runs, however, the number depending upon the type of gravel, slope of the bed, etc., the bed became irregular at isolated points and small waves seem to have appeared. The general practice in this series was to remold the bed and repeat the run. (Paintal, 1969)

Each series consisted of a set of runs for a given material. The last part of the quotation above indicates that the bed was mechanically disturbed during a series of tests. Based on the experience at the Oak Creek flume and information in the literature, it is likely that the smaller sizes were mechanically disturbed more often than the 22.2 mm size. If the experiments were made with no mechanical disturbance, we would expect each series of measurements to define a minimum transport line and the initial runs to have higher Einstein bed load transport parameters than would be expected from the minimum transport line. Also, we would expect that when a run with a high shear stress was followed by a run with a significantly lower shear stress, then the point for low shear stress should have a higher Einstein parameter than would be expected from the minimum transport line.

The data for Paintal's three series at a mean size of 22.2 mm are given in Figures 34 and 35. Figure 34 presents the data for series A. Apparently, this experiment was a series made with each successive run at a higher shear stress. The data agree with the

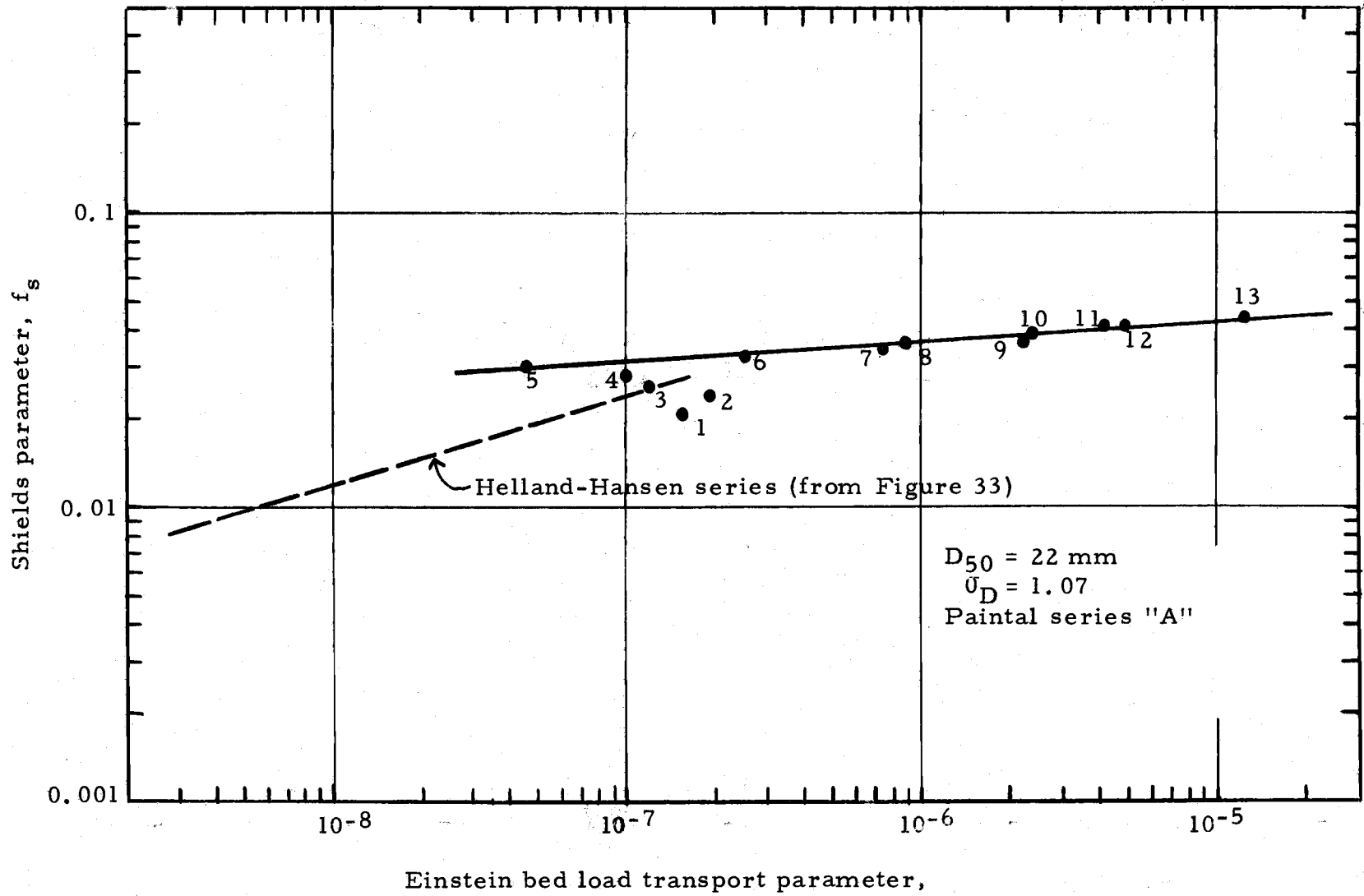


Figure 34. Shields parameter versus Einstein bed load transport parameter for the Paintal series "A".

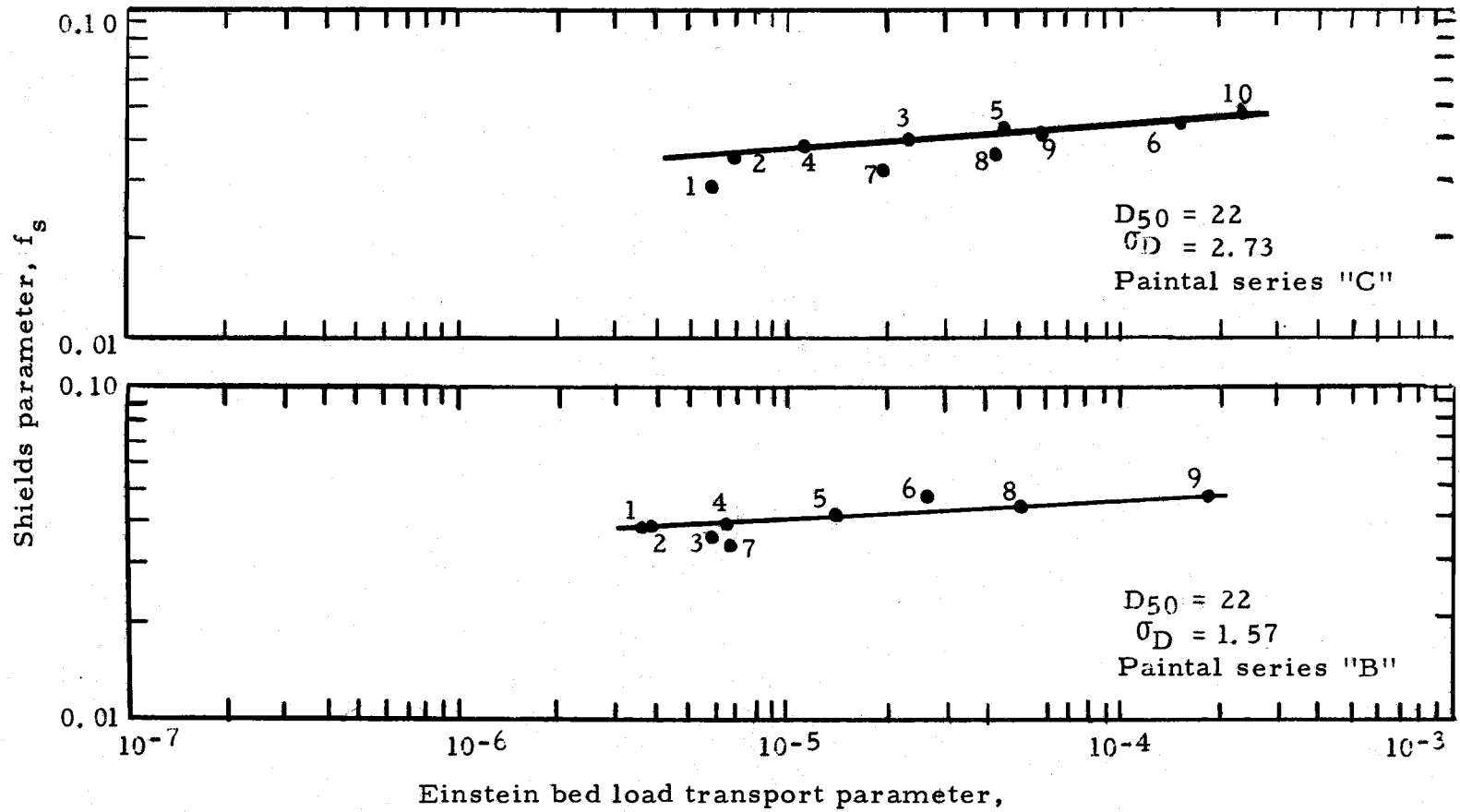


Figure 35. Shields parameter versus Einstein transport parameter for Paintal series "B" and "C".

concept given above: the first five points indicating a decrease in sediment transport with an increase in shear stress. This observation indicates that the bed became increasingly stable with time.

In series "B" (Figure 35), the results do not support the concept as well as for series "A" because the points for runs 3 and 6 do not agree with the concept. Run 7 was at a lower shear stress than run 6 and had a higher stress than would be expected from the minimum line.

The runs for series "C" do agree with the concept, with run 1 being in line with the initial mechanical disturbance concept, and runs 7 and 8 being in line with the disturbance due to high shear stress concept.

Only two points of the total of 32 shown in Figures 34 and 35 do not agree with the results expected on the basis of the concepts given above. Run B-3 could have followed mechanical disturbance. This leaves run B-6 as the only "wild" point. Consequently, the writer believes that the Paintal data support the concept described above.

Also given on Figure 34 is the lower bound from the Helland-Hansen data. The Helland-Hansen data indicate that the movement of isolated particles is still possible at quite low Shields parameters. The lower bound on previous information presented here was 0.012. In contrast, the lower bound on the Helland-Hansen data is 0.008.

The implications of the result above is that the armour particles are likely to move at almost all flows. Consequently, the fines protected by the armour will always be available for transport by the stream. Of course, the transport rate will be quite low for the lower flows.

## V. THE MOVEMENT OF SEDIMENT IN A GRAVEL BOTTOMED STREAM

The purpose of this chapter is to present the results of the study of general sediment transport system in Oak Creek. The concepts presented were developed as a result of subjective field observations, field measurements, and laboratory analysis of field samples.

A major portion of the research work has been devoted to measuring the suspended load, bed load, hydraulic properties, and bed material of Oak Creek. An object of the research was to determine the influence of bed load movement on the total sediment yield process and on the suspended load of the stream. Another object was to investigate the bed load process itself for a gravel-bottomed stream. The bed load was sampled using the sampler described previously. The first section of this chapter presents the results and analysis of the bed load measurements; the second section examines the applicability of simplified Einstein bed load and stability functions for analysis of the armour layer; the third section gives a conceptual model for the movement of bed material, the fourth section discusses the division of sediment load into bed load, and the fifth section presents and examines the measurements obtained for suspended sediment transport and the final section gives a conceptual model of the interaction of bed and suspended load.

## Bed Load Transport

### Transport Rate

A total of 145 samples of the bed load were obtained during the study period. These are from three periods, as shown in Table 12. The first set of samples was obtained during the winter of 1969-70. At the start of the bed load sampling program, procedures had to be developed on the basis of the observed characteristics of the sampler. The samples in set 1 were obtained during this developmental phase. Consequently, the quality of the samples is low relative to the samples in sets 2 and 3. Nevertheless, set 1 does contain useful information about the bed load transport system.

Table 12. Bed load sampling periods during Oak Creek study.

Data Set	Number of Samples	Range in Flows, cfs	Number of samples in various flow ranges		
			< 10 cfs	10-30 cfs	> 30 cfs
1 December 1969-February 1970	26	8-54	4	11	11
2 January 1971-March 1971	66	5-120	18	25	23
3 October 1971-November 1971	53	0.67-22	51	2	0
TOTAL	145	0.67-120	73	38	34

The second set of samples was obtained during the winter of 1971 and covers flows typical for the winter and early spring. The samples are generally of good quality and are the best available for the purpose of analyzing the movement of sediment in a gravel bottomed stream with an armour layer.



The third set of bed load samples was obtained in the fall of 1971. The samples were obtained in order to obtain information on the nature of bed load at the beginning of the winter's runoff as the catchment area becomes quite wet.

The complete data are given in Appendix I. The data for the winter of 1969-70 (data set 1) are shown in Figure 36. These data have a fair amount of variance due to experimental error in the sampling program during development of the operating procedure for the vortex sampler. The data for the winter of 1971 (data set 2) are shown in Figure 37. These data, the best data available, were obtained using operating procedures which were developed as a result of the 1969-70 sampling program. The data obtained in the fall of 1971 are shown in Figure 38. These data represent very low transport rates and hence represent small total sample sizes subject to considerable experimental (sampling) error. Sampling problems introduce a large possible error into the measurements when the bed load discharge is below 10 gm/hour. Nevertheless, the samples do contain information on the sediment transport system.

The stream expends energy in transporting sediment. The rate of energy use is called the power of the stream. The resulting sediment transport is dependent upon this stream power and upon the effective weight of the sediment. The immersed weight of the bed material being transport is "effective" weight.

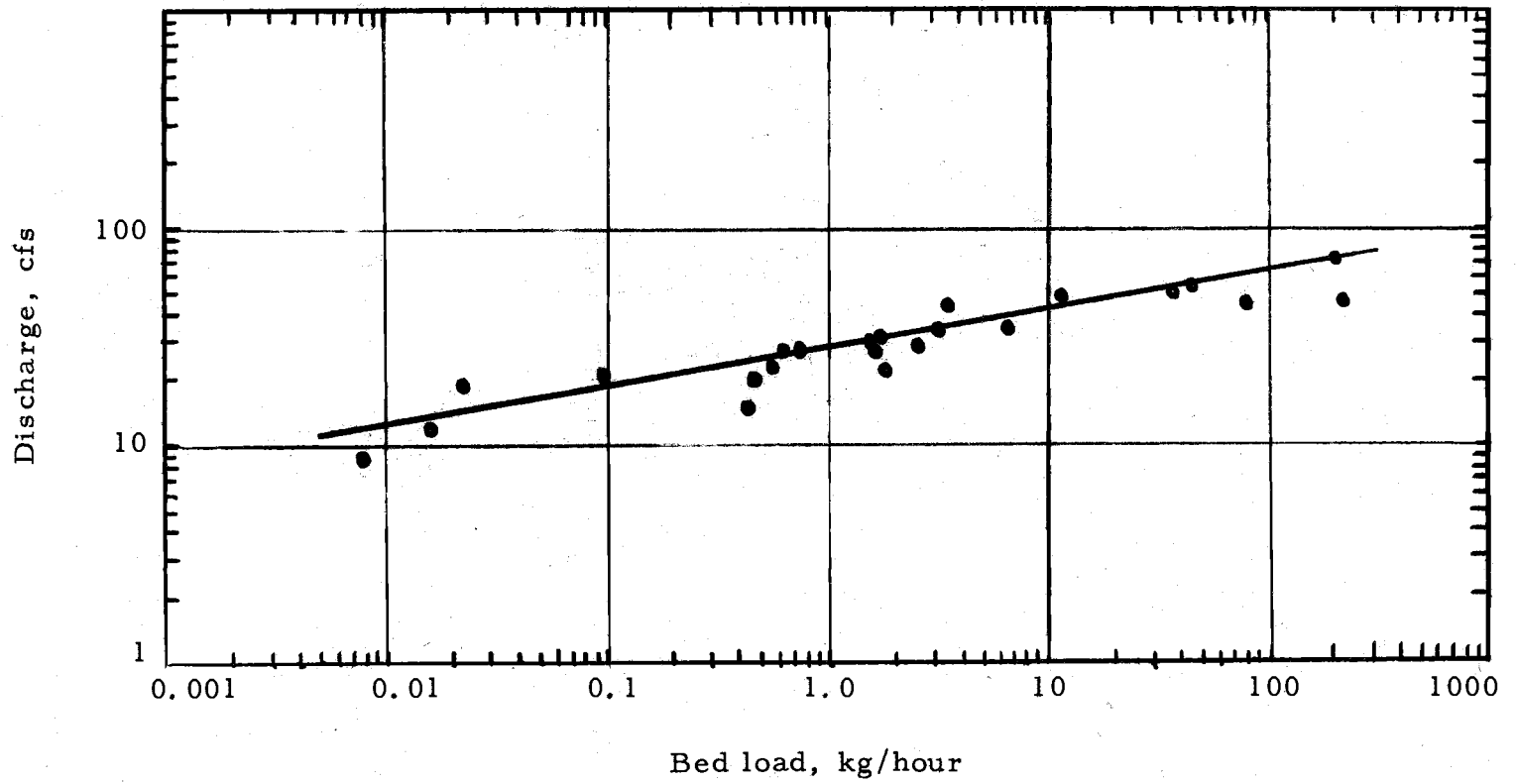


Figure 36. Bed load in Oak Creek as a function of water discharge, winter 1969-70.

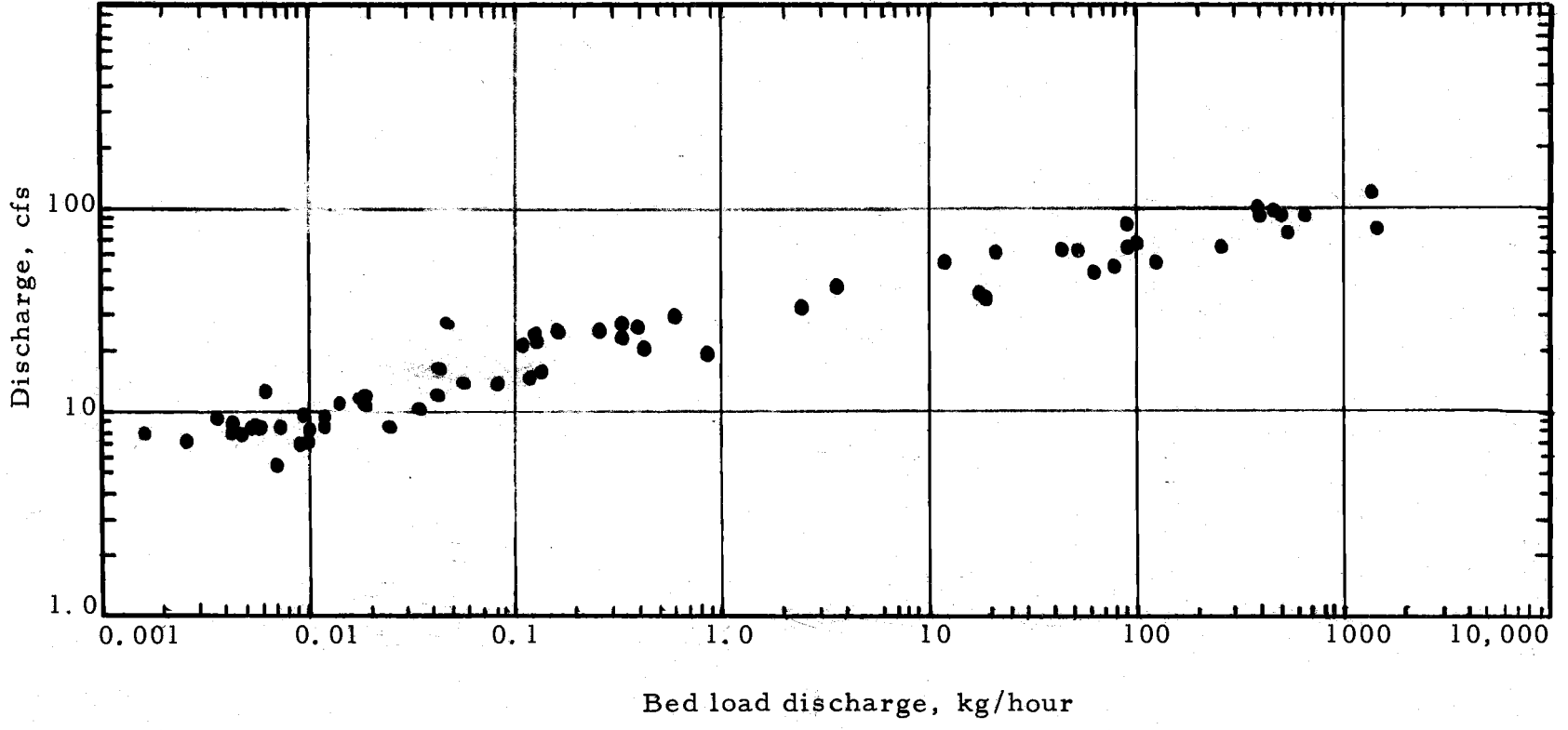


Figure 37. Bed load in Oak Creek as a function of water discharge, winter 1971.

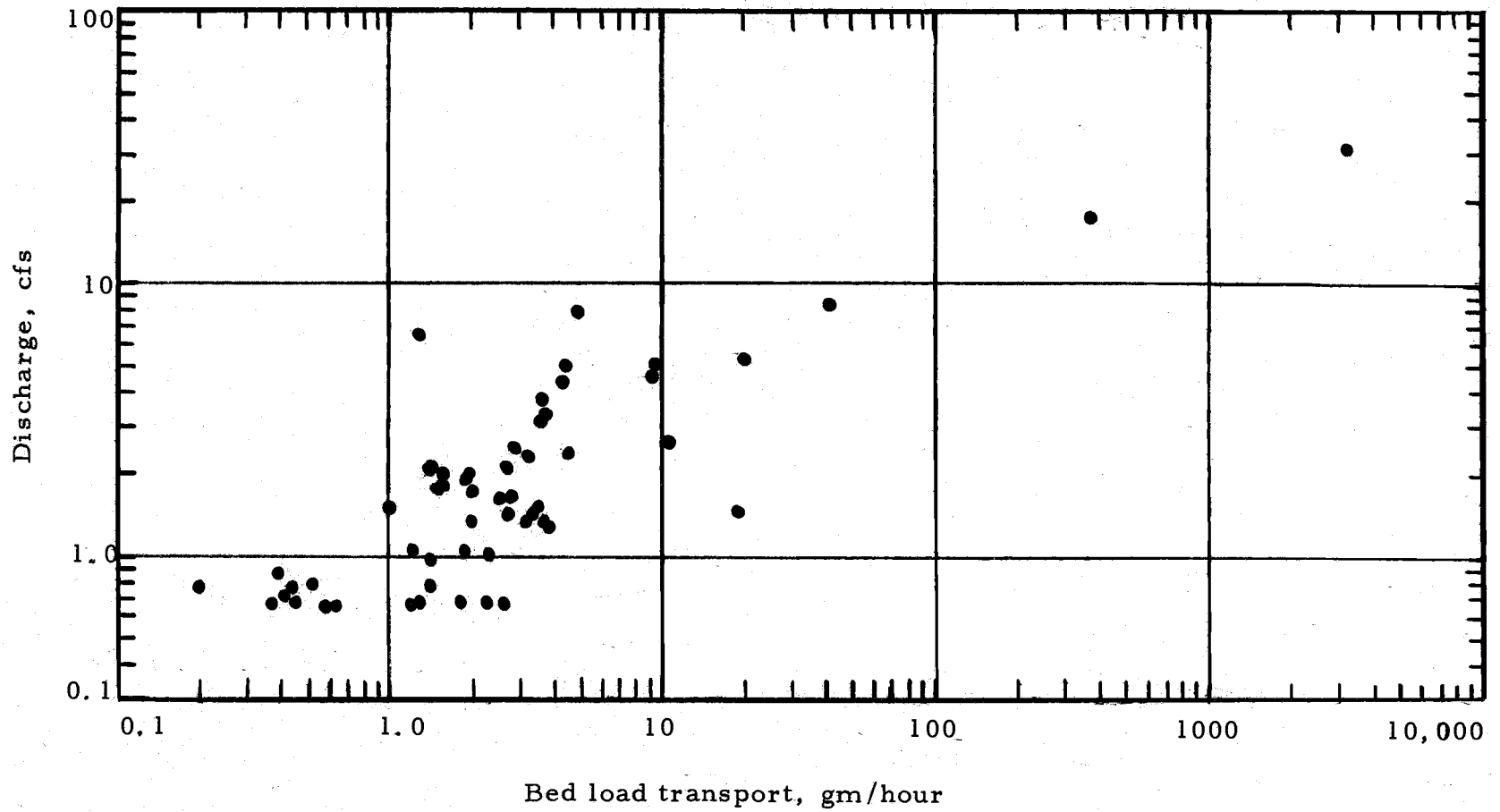


Figure 38. Bed load in Oak Creek as a function of water discharge, fall 1971.

The equations used to calculate the stream power and immersed weight are:

$$P = \gamma S Q \quad (52)$$

$$Q'_{BL} = \frac{G_s - 1.0}{G_s} Q_{BL} \quad (53)$$

where:  $P$  is the power per unit length of channel

$G_s$  is the specific gravity of solids

$Q_{BL}$  is the bed load discharge in dry weight per unit time

$Q'_{BL}$  is the bed load discharge in immersed weight per unit time.

The plot of stream power versus bed load discharge in terms of immersed weight is given in Figure 39. The power of a stream represents the energy per unit time available to move the immersed weight of the bed material. The equation for the upper line in Figure 39 is

$$Q'_{BL} = (3.3 \times 10^{-6}) P^{5.3} \quad (54a)$$

The equation for the lower line in Figure 39 is

$$Q'_{BL} = (6.7 \times 10^{-6}) P^{5.3} \quad (54b)$$

Combining and rearranging equations (52), (53), and (54a) gives

$$Q_{BL} = \left[ \frac{G_s}{G_s - 1.0} 3.3 \times 10^{-6} (\gamma S)^{5.3} \right] Q^{5.3} \quad (55)$$

If  $S$  is constant for all discharges the term in brackets is constant.

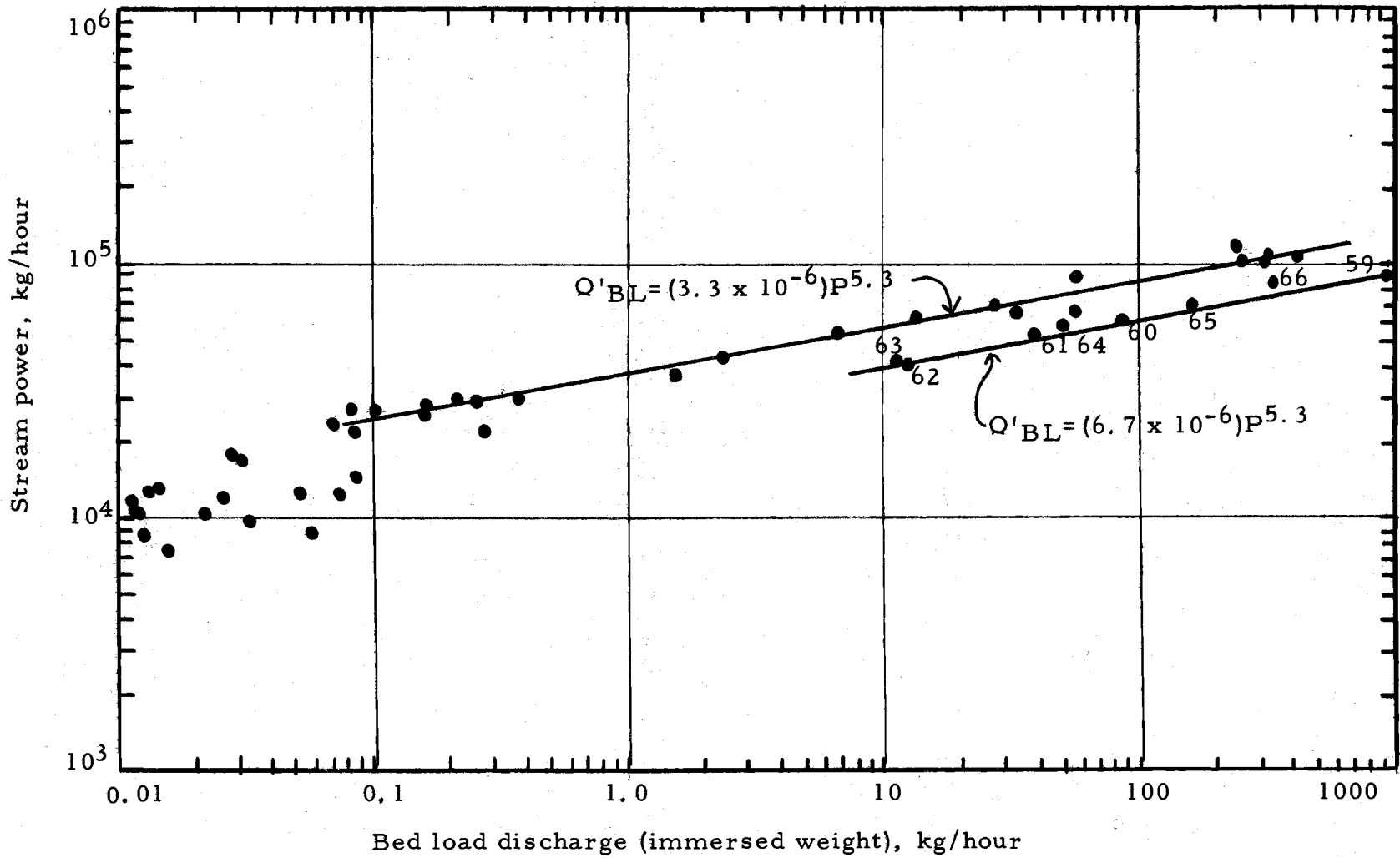


Figure 39. Bed load discharge versus stream power, winter 1971 samples from Oak Creek.

Consequently, in this case

$$Q_{BL} = K Q^{5.3} \quad (56)$$

In Oak Creek the energy slope is nearly constant. Hence, the use of stream power and immersed weight is not a significant improvement over stream discharge and dry weight, because the energy slope is nearly constant and the other multipliers only shift the data a constant amount relative to the axes.

As is shown on Figure 39, there is considerable scatter for stream powers less than  $2.5 \times 10^4$  kg/hour. Furthermore, the data for stream powers greater than  $2.5 \times 10^4$  kg/hour can be divided into two groups. The lower group on the graph consists of samples 59 through 66 while the upper group includes high-flow samples obtained prior to sample 59. Samples 59 through 66 all follow a period of high flow on 115 cfs on March 10, 1971. The other samples for power greater than  $2.5 \times 10^4$  kg/hour were obtained prior to this high flow period.

The ratio of  $Q'_{BL}/P^{5.3}$  is  $3.3 \times 10^{-6}$  for most of the data on Figure 39 for stream power greater than  $2.5 \times 10^4$  kg/hour except for samples 59 through 66 where the constant is  $6.7 \times 10^{-6}$ . This change in constant was investigated in the chapter on incipient movement of the armour layer. In that chapter it was postulated that the change resulted from a change in the critical discharge for the armour layer.

### Grain Size of Bed Load Material

Most of the bed load material transported during low flows is sand and fine gravel, with a few particles having diameters as large as 2 to 3 cm. As the flow increases, the size of transported particles also tends to increase. Data on the median particle size for the winter, 1969-70 samples are given on Figure 40 (the median size is the  $D_{50}$  size). The data for the winter, 1971 samples are given in Figure 41. The 1969-70 data are not of high quality as already discussed. The 1971 data are of adequate quality for study of the variation of median size with discharge.

There is considerable variation in the relationship between the median size and stream discharge. Figures 40 and 41 show that for a discharge greater than 20 cfs, the median size tends to increase with an increase in discharge.

The data in Figure 41 also indicate the median size increases with a decrease in discharge for stream discharges below 20 cfs. This unexpected result can be explained. The data median sizes presented in Figures 40 and 41 were determined from gradation curves developed using standard analysis techniques except for an adjustment of certain samples in order to reflect the probabilistic nature of movement of armour particles. Every once in a while a sample obtained when the flow was between 5 and 15 cfs would contain a single large



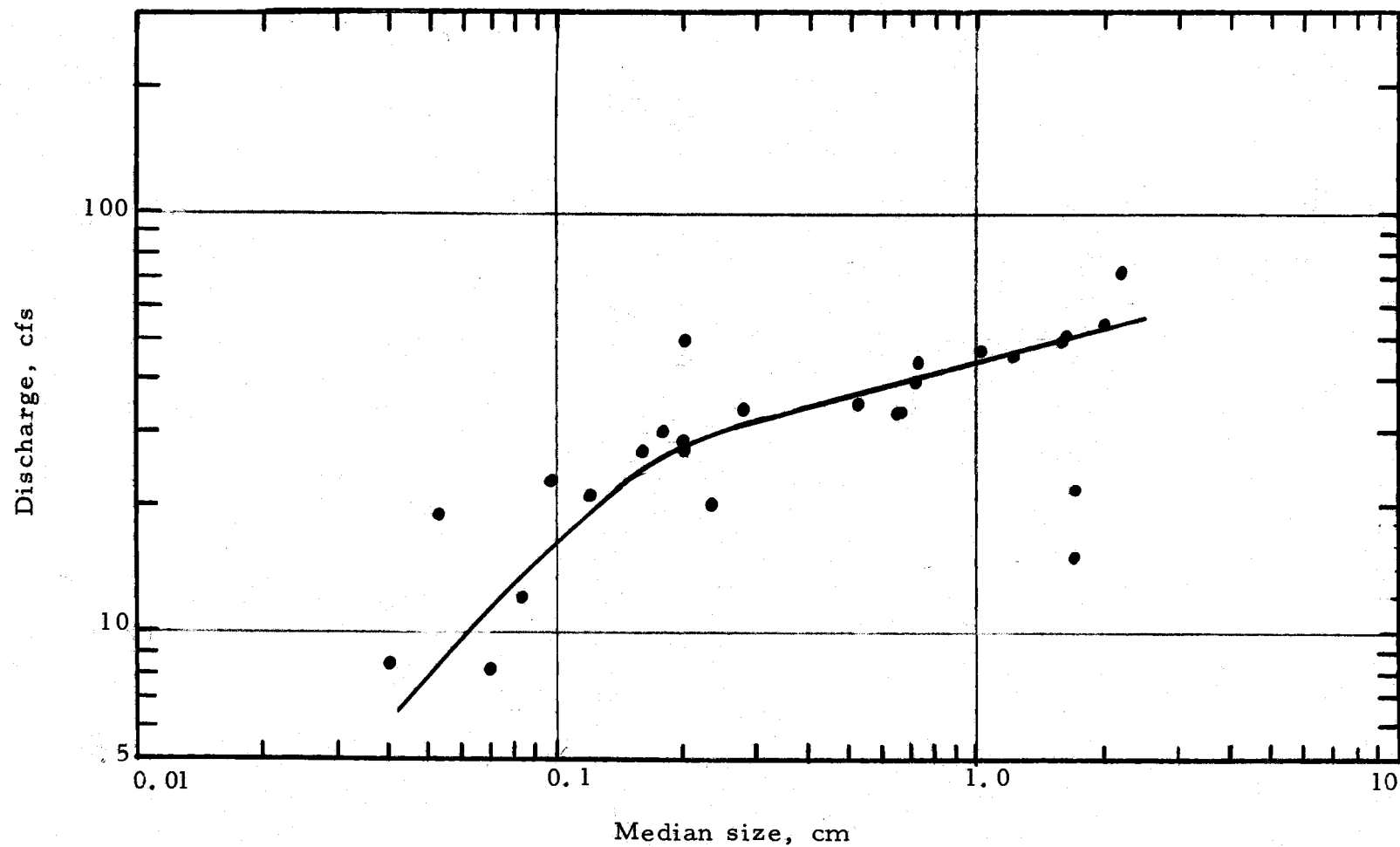


Figure 40. Median size of bed load material versus stream discharge, winter 1969-70.

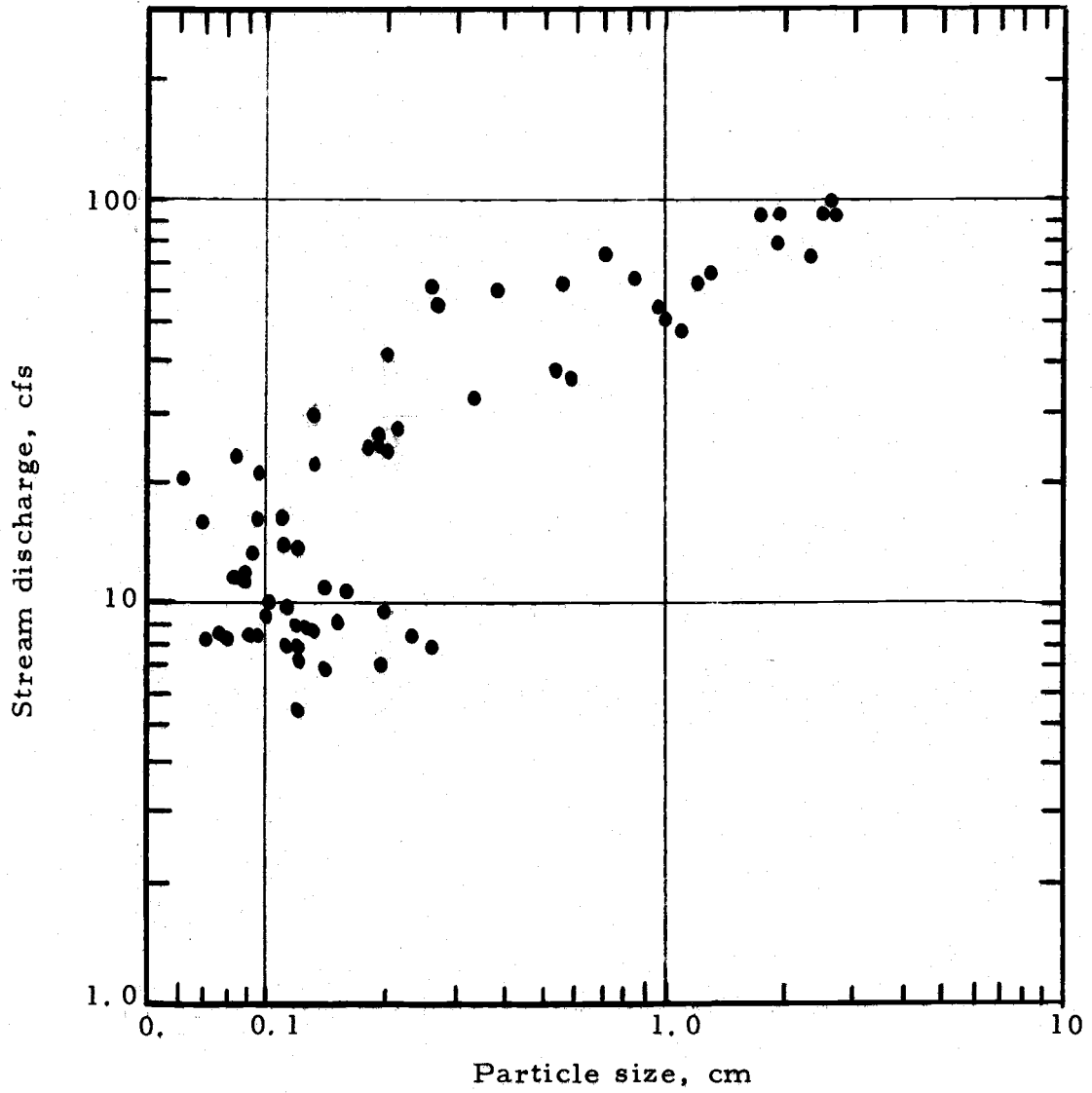


Figure 41. Median size of bed load material versus stream discharge, winter 1971.

particle between one and two inches in diameter. This single particle was much larger than any of the other particles in the sample. Often the next one or two sizes used in the gradation analysis would be missing. The analysis given in the previous chapter indicates that every particle in the armour layer has some probability of being dislodged and moved downstream for almost any discharge in the stream.

During a time of low flow the probability will be quite low but still greater than zero. In other words, each sample obtained during a low flow period had some probability of having an exotic particle because there was some probability that a particle would be found in the sample (about 0.14 for a one inch particle, using the analysis in the previous chapter, or about 0.28, as calculated based on the total number of samples with flows between 5 and 14 cfs and the number of samples with the large particle). Consequently, the unlikely particle is not representative of a given sample because the sampling period is short relative to the probability of the larger particle being moved at the stream discharge prevailing during the period. The particle is representative of the flow. Hence, a sample collected over a relatively long period would contain a number of the larger particles. Because the larger particles are not representative of the short sampling period for the bed load, an adjustment was made to nine samples with flows between 5.4 and 13.5 cfs. Of the nine samples, six had one-inch particles, two had 1-1/2 inch particles, and one had

a 1/2-inch particle. The minimum critical shear stress for the armour occurred for two-inch particles (see Figure 25). In the case of the nine samples, the unlikely particle was not included in the gradation analysis nor in the transport rate analysis.

Although the median size was used in Figures 40 and 41, the mean size is considered to contain more information about the sample than does the median size. The mean size was calculated using information obtained from the grain size distribution curve for each sample. The method is that developed by Folk and Ward as described in King (1967). The equation is:

$$\log_2 D (\text{mean}) = \frac{\log_2 D_{84} + \log_2 D_{50} + \log_2 D_{16}}{3} \quad (57)$$

where  $D_x$  is the size at which x percent of the material is finer.

The data for the winter 1971 are subdivided chronologically and given in Figures 42 through 47. in terms of mean particle size.

Figure 42 are the data for the first nine samples obtained in 1971.

From this diagram it is clear that there is not a simple relationship between discharge and median size for low flows.

In Figure 43 the data for samples 10 through 32 are shown. The samples 10 through 22 show a good relationship between discharge and median size. Samples 23 through 32 indicate a decrease in mean size with a decrease in discharge but it appears that there was more sand available for transport in the case of samples 23 through 27 than for

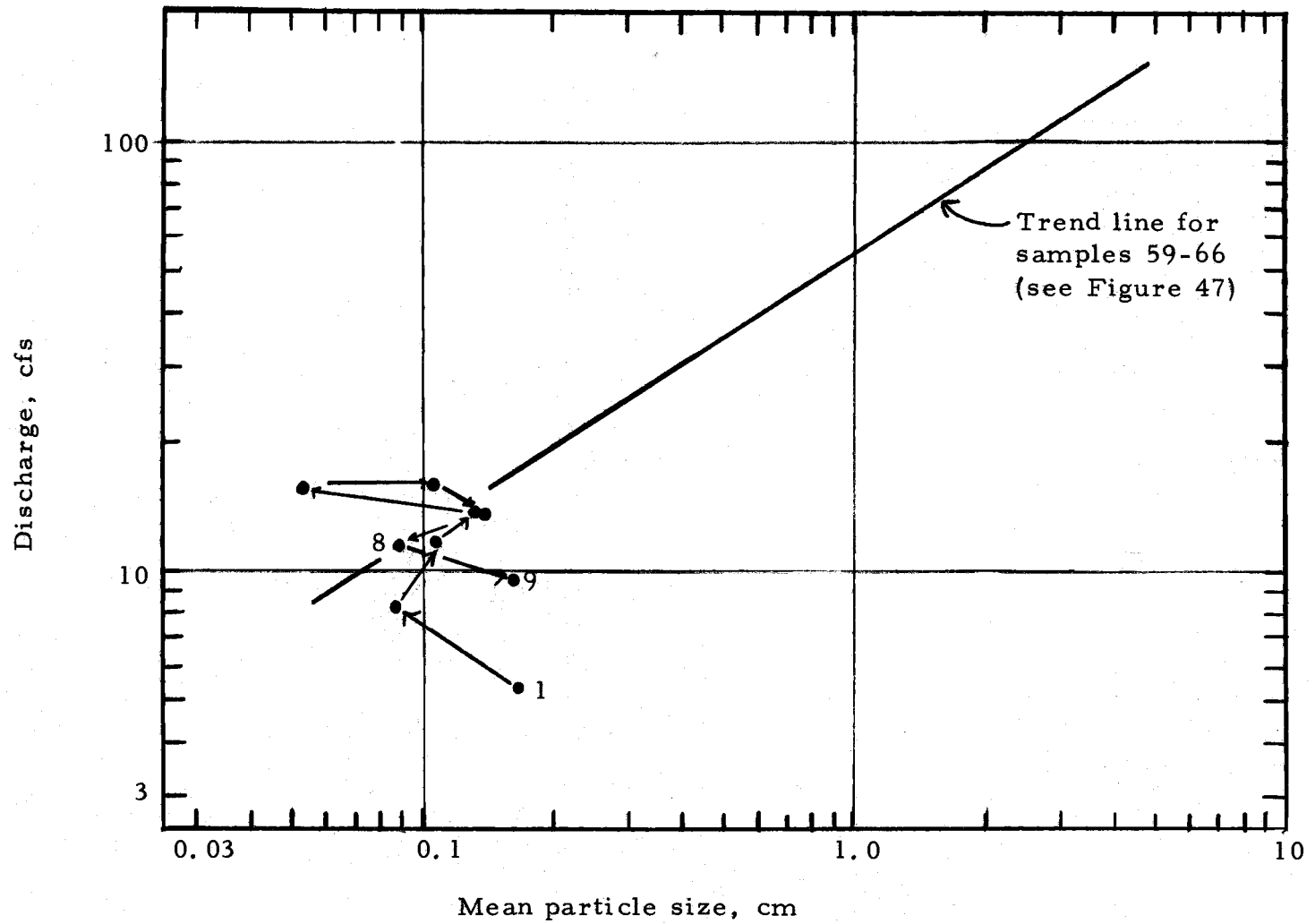


Figure 42. Variation of mean size of bed load samples with discharge, 1971 samples 1-9.

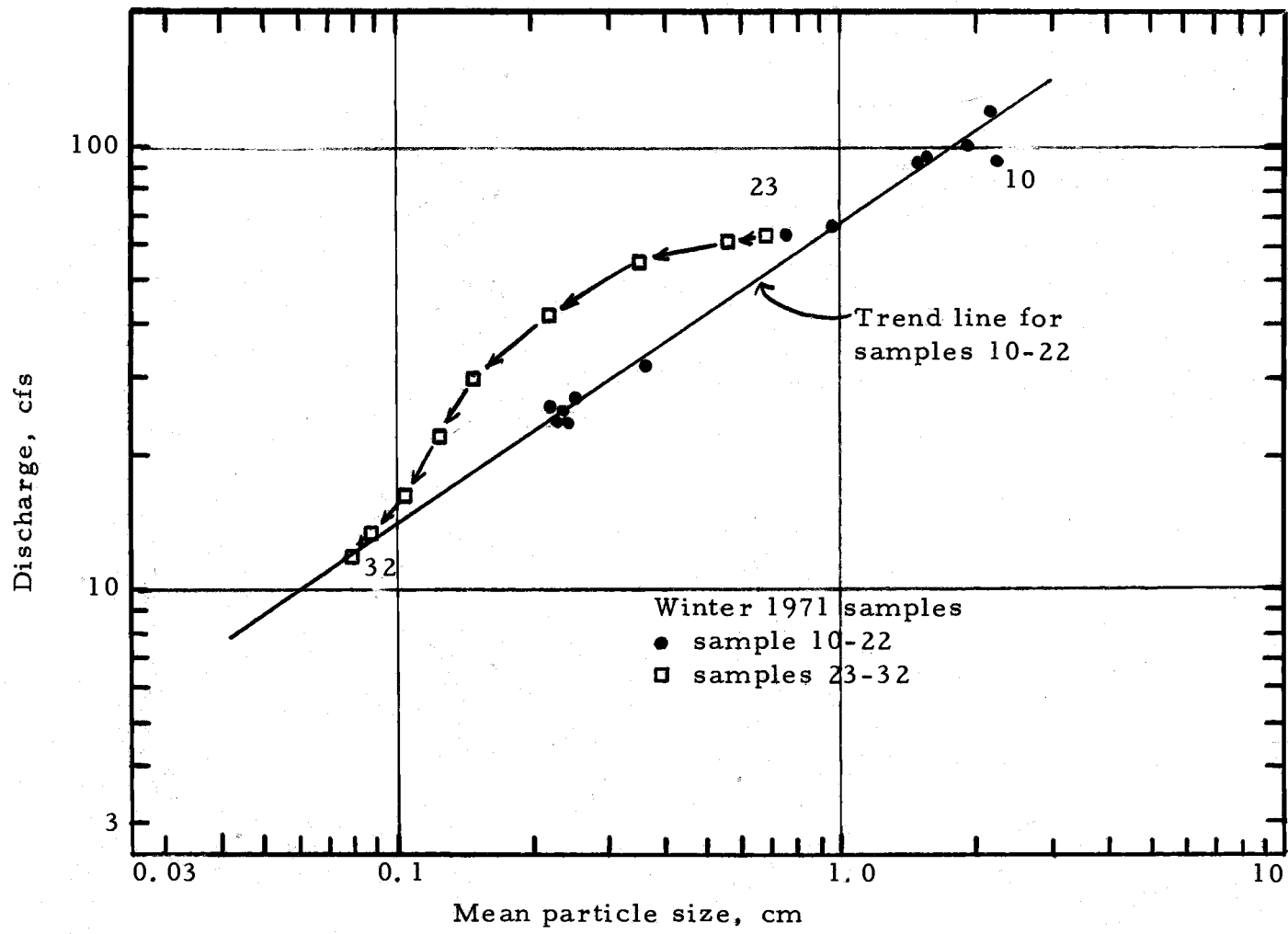


Figure 43. Variation of mean size of bed load sample with discharge, 1971 samples 10-32.

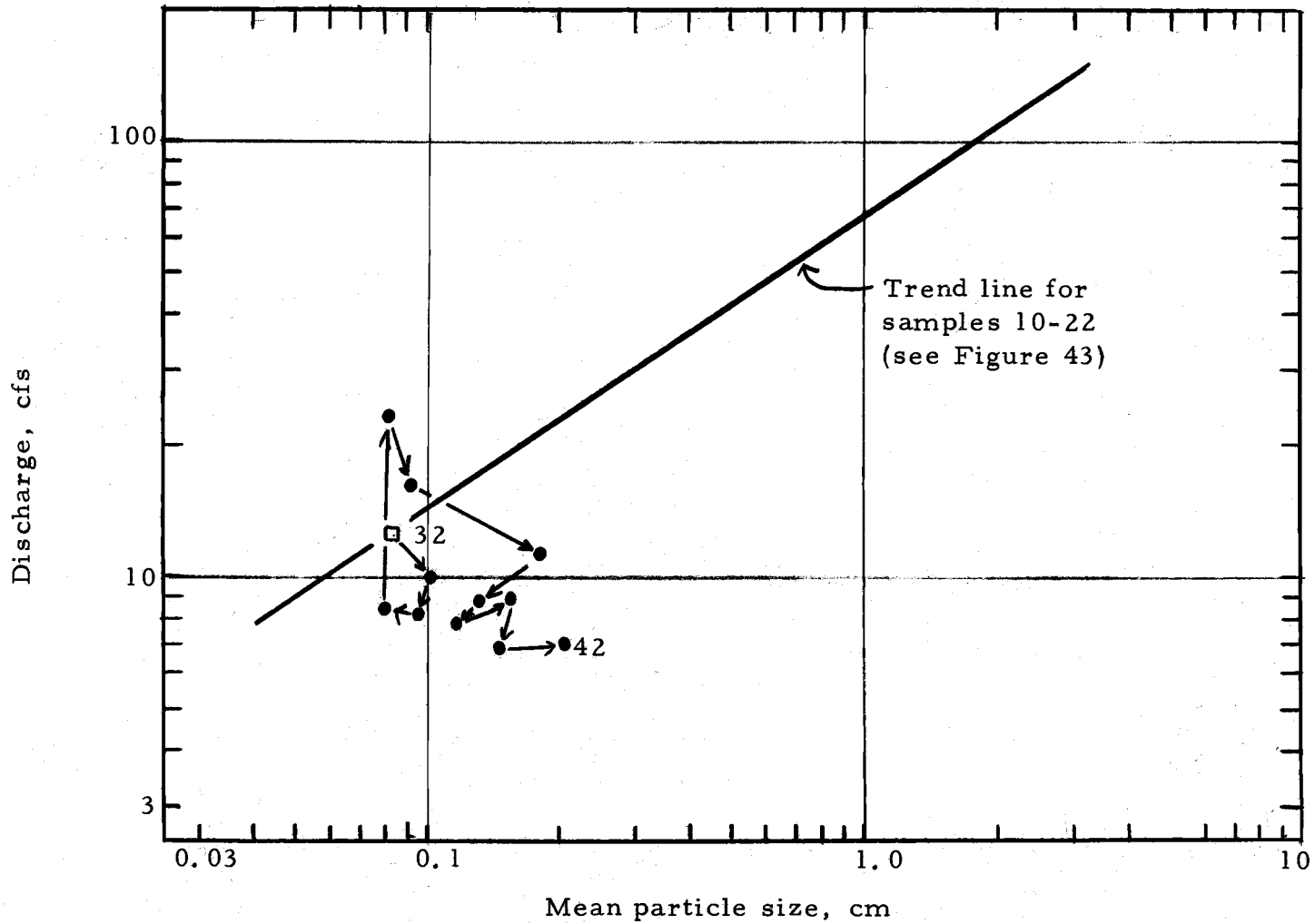


Figure 44. Variation of mean size of bed load samples with discharge, 1971 samples 32-42.

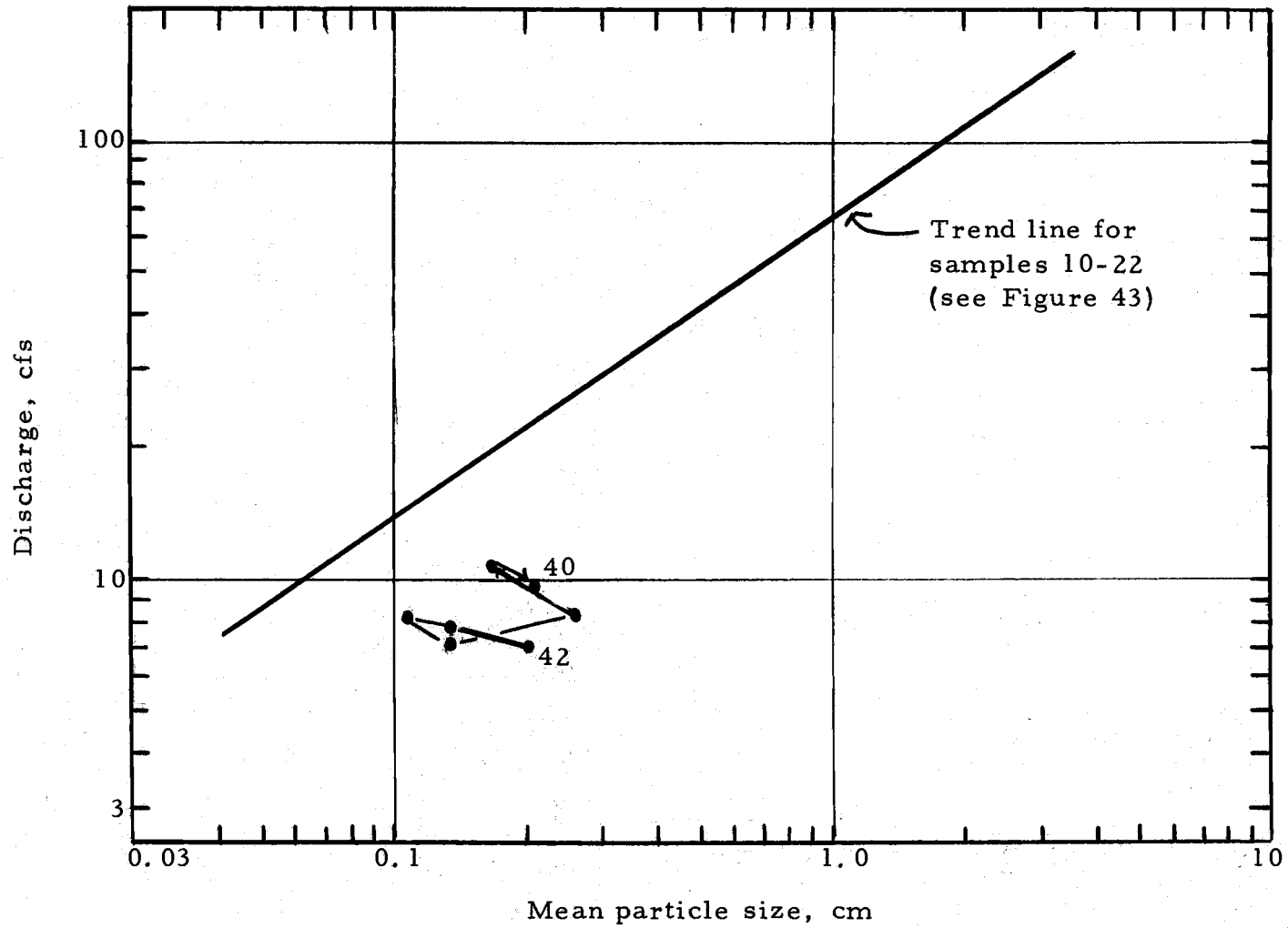


Figure 45. Variation of mean size of bed load samples, with discharge, 1971 samples 42-48.



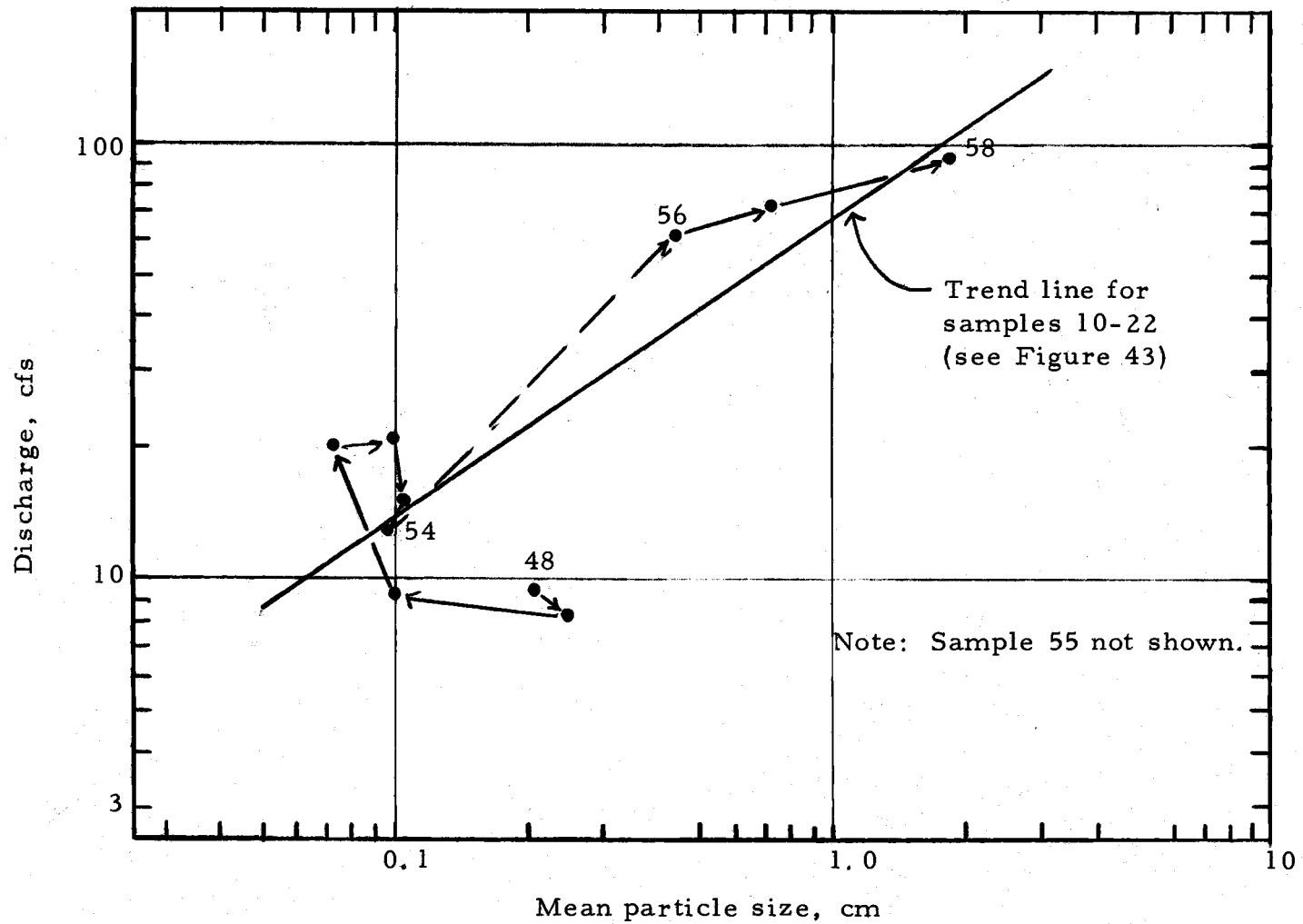


Figure 46. Variation of mean size of bed load samples with discharge, 1971 samples 48-58.

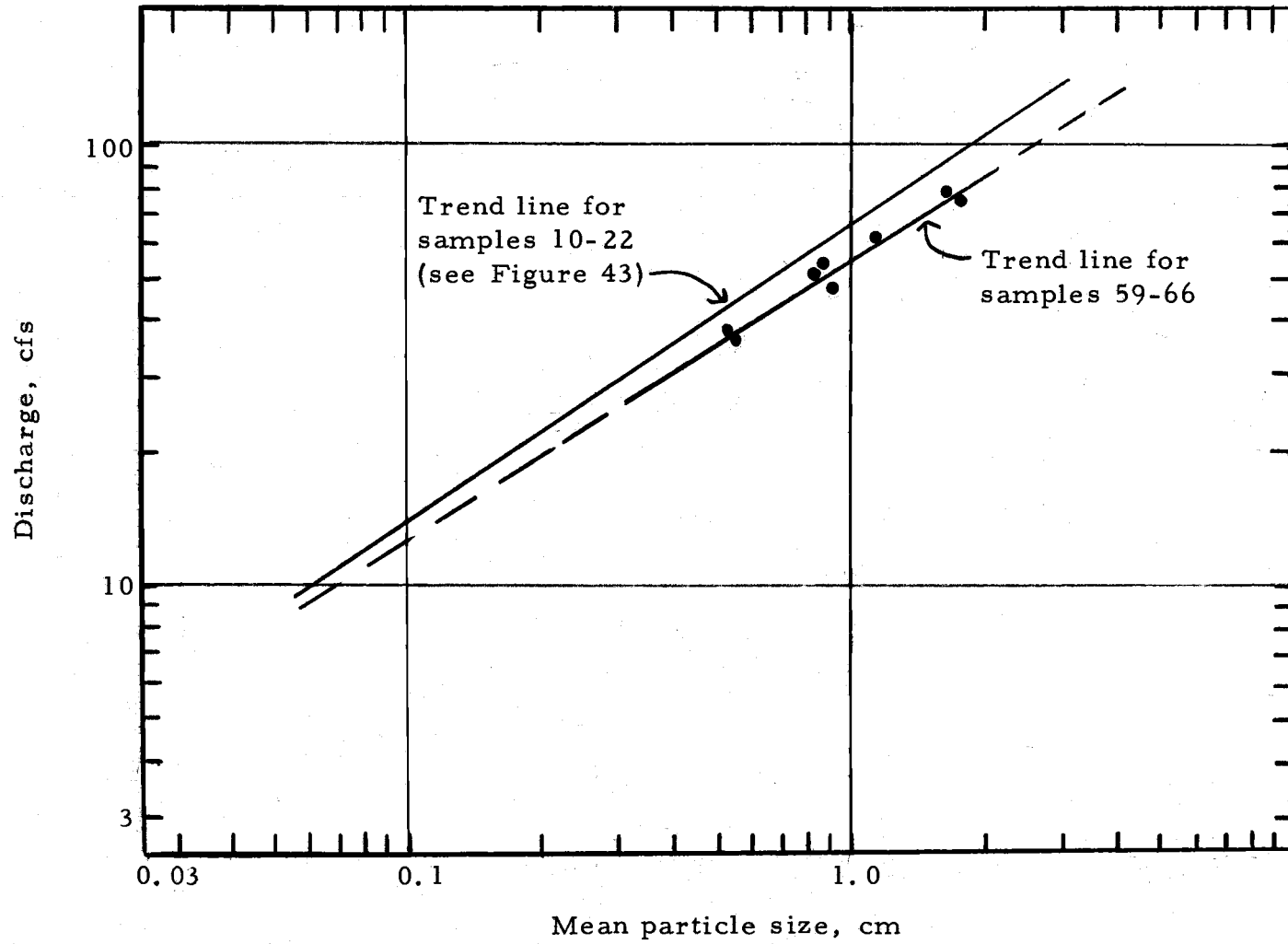


Figure 47. Variation of mean size of bed load samples with discharge, 1971 samples 59-66.

samples 10 through 22. Samples 23 through 32 are on the falling limb of a runoff event with a peak discharge of 78 cfs (critical particle diameter of 8.3 cm). Using the information on the probability of movement given previously, the probability of movement of the  $D_{35}$  size of the armour layer is 0.44 compared to a probability of 0.28 at the critical discharge and 0.83 for the peak discharge associated with samples 10 through 22. These observations suggest that a peak discharge of 78 cfs was sufficient to disturb the armour layer but not remove the sand and fine gravel thus freed from among the armour particles. Hence, the sand and small gravel were available for transport on the falling limb of the hydrograph because such material was in greater than usual abundance among the armouring particles. In contrast, the higher discharges associated with samples 10 through 22 probably removed more of the sand and small gravel as the material was released from below the armour particles.

The data on mean size for samples 32 through 42 are given on Figure 44. These data suggest the possibility that the change in mean size is inversely related to the change in discharge at relatively small discharges.

Data on mean size for samples 42 through 48 are given on Figure 45. These data suggest that the mean size may increase with time at a constant discharge.

Data for samples 48 through 58 are given on Figure 46. These data indicate a return to the trend line for samples 10 through 22 with a very definite tendency for the initial increase in stream discharge to cause a decrease in the mean size. Sample 55 is not considered useable for analysis because of a wide range in discharge during the sampling period.

It appears that the rising limb transports more sand than was transported after a period of intense bed load movement (as defined by samples 10 through 22).

The data for samples 59 through 66 are given on Figure 47. These data plot parallel to the line for samples 10 through 22 and represent data for bed load discharge after an intense period of bed material movement. The shift in the mean size toward a larger size probably results from a decrease in the  $D_{35}$  size of the bed material which increased the ability of the stream to transport more of the armouring particles.

The main observation which can be made at this point from the foregoing discussion is that the mean size of the transport bed material is a function of the discharge and the past history of discharge, especially for discharges below the critical discharge.

The data for the fall 1971 samples are given in Figure 48. These samples, for low discharge, have relatively large mean grain sizes.

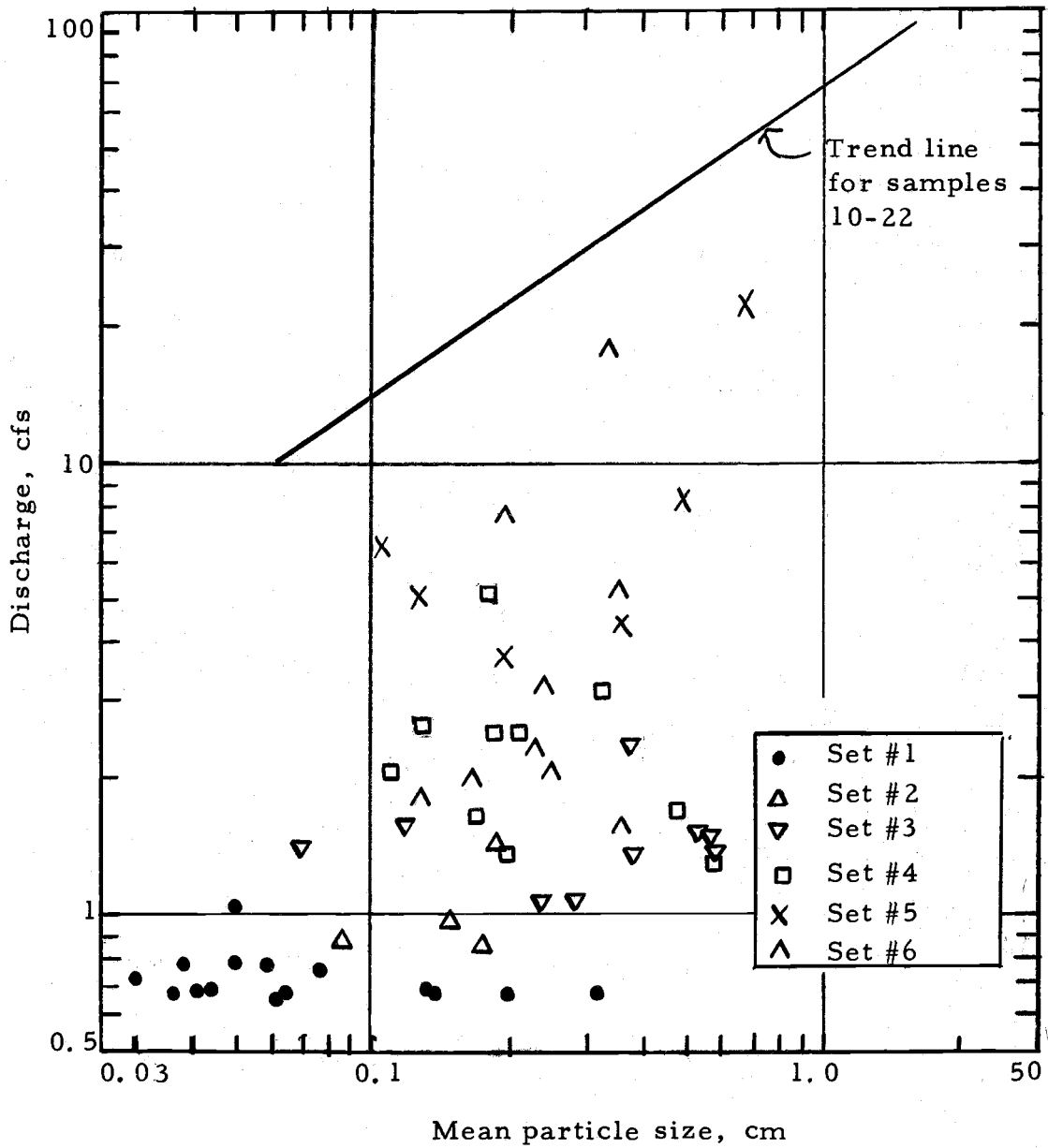


Figure 48. Variation of mean size of bed load samples with discharge, fall 1971 samples.

All of the 1971 data from winter and fall are given on Figure 49. The data form a reasonably well defined region on the diagram, except for points for three autumn samples (109, 110, 111). These three samples are much coarser than would be expected from the other 116 points. These data were collected on the 13th and 14th of November during a storm that reached a peak discharge of 31 cfs.

An explanation of the coarse composition of samples 109, 110, and 111 may be offered. On November 10th, it was observed and noted that leaf build-up around particles increased the drag on particles. The particles that caught leaves were the larger particles protruding above the general level of the stream bed. Leaf drop from the alders bordering the stream may have started about the 1st of November, but no note was made of the date at which the samples started containing a fair amount of leaves and other vegetative material.

On November 13th, when there was a low-intensity storm which caused a runoff event with a peak flow of 31 cfs, two samples (109 and 110) were obtained on the rising limb of the hydrograph. Sample 110 covered flows rising from 12 to 31 cfs (mean flow of 22 cfs) and it was noted that this sample contained a large amount of leaves, bark, and twigs. The next sample (111) was on the falling limb and contained almost no leaves, bark, or twigs according to field notes. The suspended load samples taken at the end of the bed load sampling period

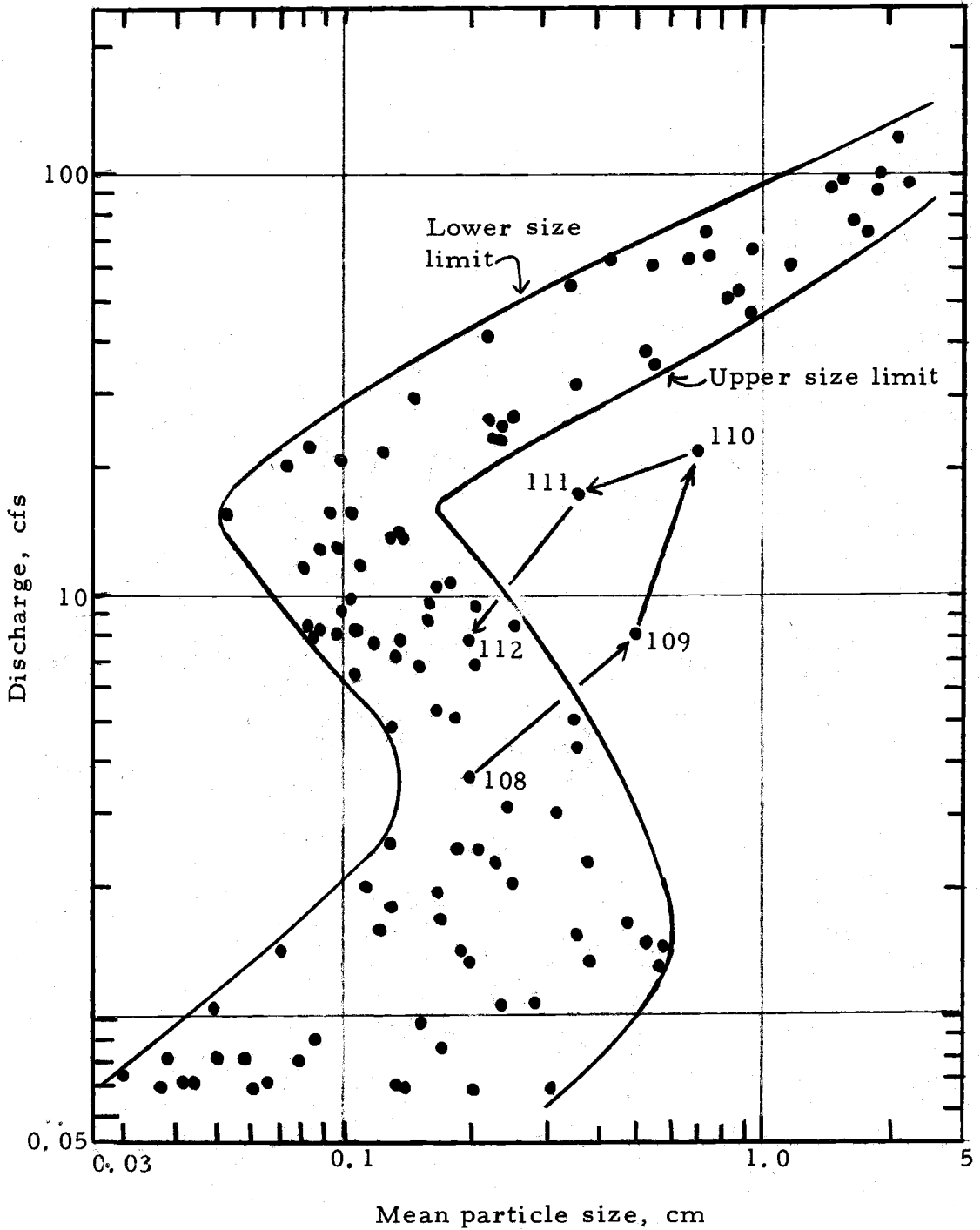


Figure 49. Variation of mean size of bed load samples with discharge, all 1971 samples.

for samples 110 and 111 appeared to have a high sediment concentration and contained a surprising amount of fine material in the same range. Unfortunately notes were not taken on the other samples from the same period.

Laboratory analysis showed that sample 110 had 12% of the sample in the size ranges greater than  $D_{35}$  of the armour (5.2 cm). The bed load transport rate for sample 110 was 3.2 kg/hour. Sample 111 had a single particle greater than 5.2 cm and a bed load transport of 0.37 kg/hour. The hydrograph for the November 13th-14th runoff event is given in Figure 50, the bed load data are shown in Table 13 and suspended load data are given in Table 14.

Table 13. Bed load data for the November 13-14, 1971 runoff event.

Bed Load Sample Number	Discharge, cfs	Bed Load Discharge, kg/hour	Suspended Load Discharge, kg/hour	Dissolved Load, kg/hour	Total Solid Load, kg/hour	Bed Load, Suspended Load	Mean Size of Bed Load, cm
108	3.8	0.0036	4.26	53.0	57.3	0.0008	0.20
109	8.5	0.0410	52.0	95.5	147.5	0.0009	0.48
110	22	3.200	258.0	195.0	456.2	0.012	0.67
111	18	0.37	138.0	169.0	297.4	0.027	0.37
112	7.9	0.0049	16.9	89.2	86.1	0.0003	0.19



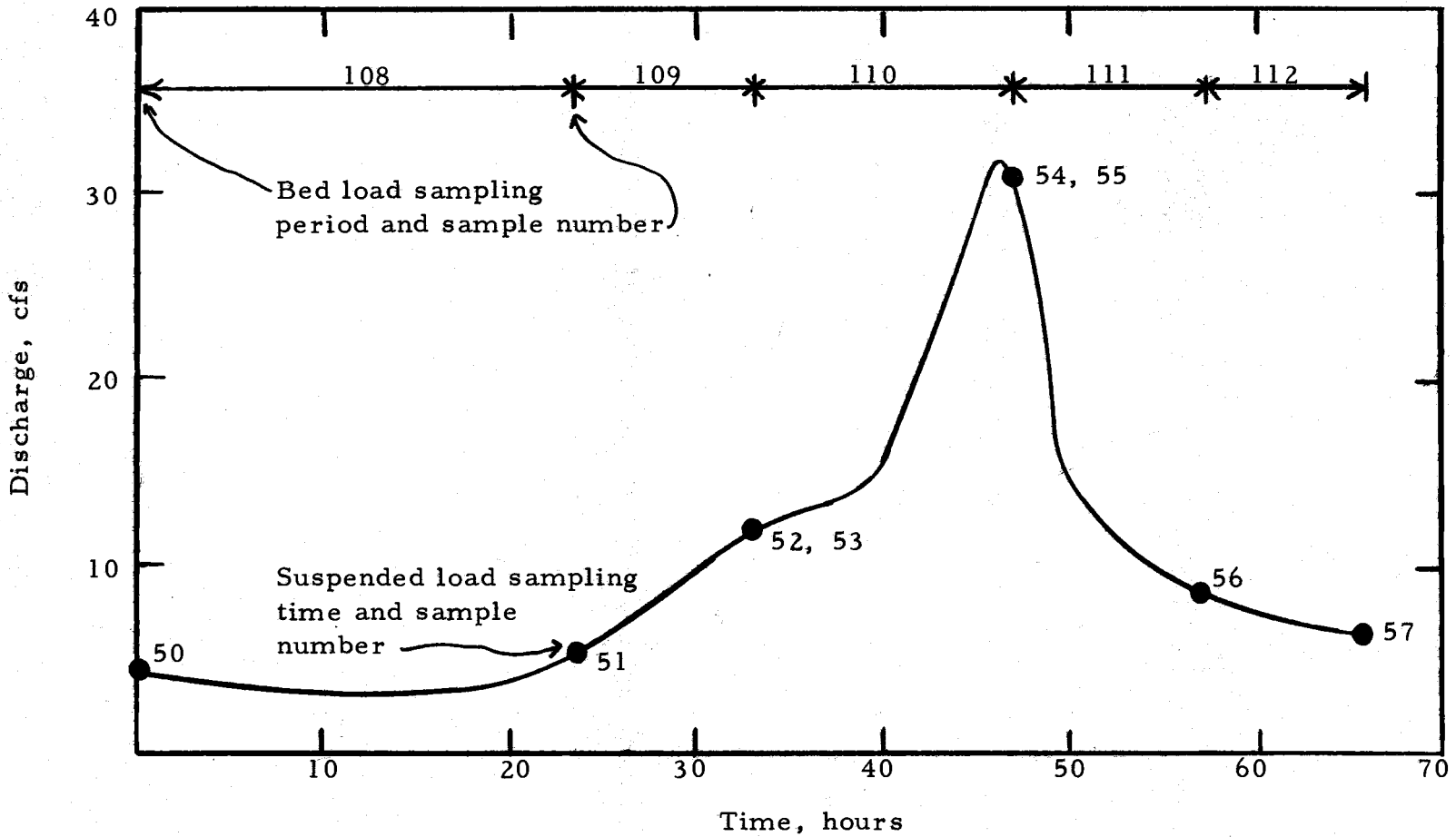


Figure 50. Hydrograph of the November 13-14, 1971 runoff event, showing bed load and suspended load sampling schedule.

Table 14. Suspended load data for the November 13-14, 1971 runoff event.

Suspended Load Sample Number	Discharge, cfs	Suspended Sediment concentration, mg/liter	Rank in order of decreasing sand concentration	Notes
C-50	4.1	12.68	6	Very little sand.
C-51	5.2	15.75	3	Some sand
C-52	12	131.00	1	Very large amount of sand.
C-53	12	161.67		
C-54	31	149.01	2	Very large amount of sand.
C-55	30	140.57		
C-56	9.4	22.80	4	Little sand
C-57	6.4	18.33	5	Little sand

The flows associated with sample 110 were about the same as for sample 111 but the bed load was about ten times as large for sample 110. The suspended load samples obtained at both ends of the sampling period for sample 110 contained a very large amount of sand. The cause of the relatively large amount of sediment transport associated with sample 110 is related to the leaves, bark, and twigs found in the sample. The November 13th-14th runoff event was the first storm of any size after the beginning of leaf drop. The rainfall itself would tend to increase the effective weight of the leaves so that more of the leaves would drop from the trees into the stream. As a result,

the stream had a large amount of twigs and leaves in the water during the rising limb of the runoff event. The observations on the 10th of November indicate that the leaves will catch on the larger particles. This results in a very considerable increase in the drag applied to a particle without increasing the ability of the particle to resist the drag. Hence, the particle will move at lower-than-usual discharges.

In the following sections of this chapter the concept is developed that the armour layer controls the release of sand and small gravel into the transport system. In other words, when an armour particle moves, smaller particles also move. If this is the case the gradation curves for samples 110 and 111 should be similar but sizes for sample 111 should be smaller. In the latter case, not as many of the armour particles will be disturbed because the leaves and other vegetative debris have been carried away by the flow. The gradation curves are shown on Figure 51. The curves are similar but the curve for sample 111 shows smaller sizes, as expected. The reason that sample 111 is still coarser than the other samples on Figure 49 is that the bed was disturbed considerably by the leaves, with the result that more coarse sand material was available for transport than would normally be available.

The odd shape of Figure 49 may be related to the relative ability of the various sizes of particles to "hide" in the armour layer. The mean size tends to increase with an increase in discharge when the

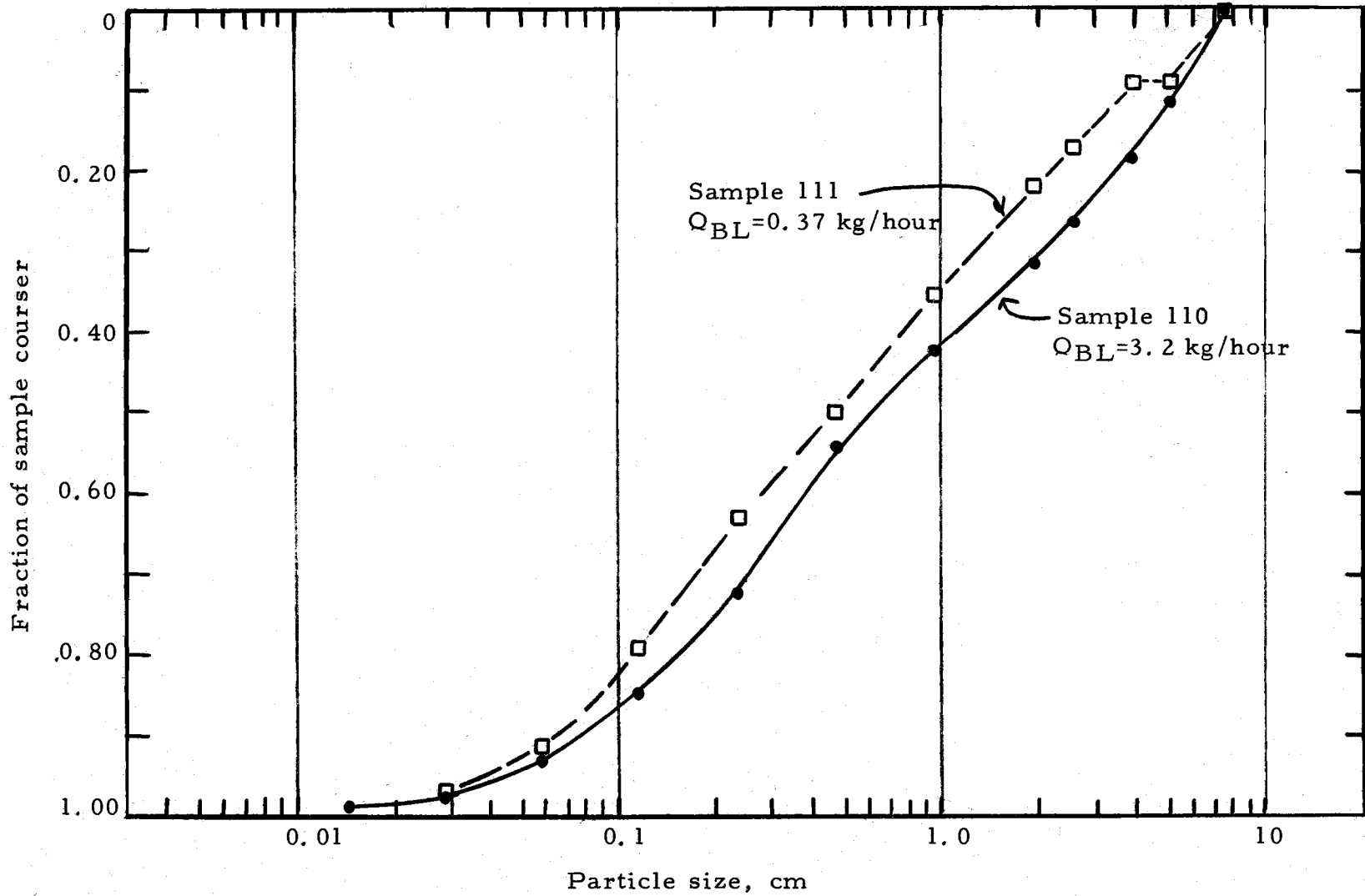


Figure 51. Gradation curves for bed load samples 110 and 111, fall 1971.

flow is over 20 cfs because more of the armour material is disturbed by the flow. As the discharge falls below 20 cfs, the ability of the stream to move the armouring particles is still relatively high but the fine sands will be removed from general transport by falling into places in the armour layer where they are "hidden" from the hydraulic forces. This filtering action of the armour layer is discussed in a following section. The coarser particles are harder to hide and are transported with relative ease. As a result the mean size of the sample increases with a decrease in discharge. At about 3 cfs the ability of the stream to move any of the armouring particles is very nearly zero with the result that sand and some gravel are all that is transported.

#### Bed Load Transport and Stability Functions

If we assume that the bed load transport and the stability of the bed material can be represented by one characteristic particle size, we can compare the results of the measurements from Oak Creek to the simplified Einstein bed load function. This simplified function was used in order to obtain an idea of how the observations compare to the function and to obtain some idea of the importance of the armour layer. The armour layer is fairly uniform in size, which fits the assumption of the simplified function that the material can be characterized by a single size. The bed load and stability functions were calculated using

the following equations:

$$\bar{\Phi} = \frac{q_s}{G_s (D_r)^{3/2} \sqrt{G_s - 1}} \quad (58)$$

$$\psi = \frac{(G_s - 1) D_r}{R S} \quad (59)$$

where:  $\bar{\Phi}$  is the bed load transport function

$\psi$  is the bed stability function

$D_r$  is the representative grain size

$G_s$  is the specific gravity of solids

$R$  is the hydraulic radius

$q_s$  is the bed load transport per unit width of channel

$S$  is the energy slope.

The work on bed stability presented previously indicated that a particle size corresponding approximately to the  $D_{30}$  or  $D_{35}$  size ( $0.69 D_{65}$  for the armour layer) represents the size with minimum stability in a bed. The  $D_{35}$  is typically considered to be representative of the bed material movement properties of a bed. Hence, the  $D_{35}$  size of the armour layer has been used to calculate the transport and stability functions for each bed load sample (identified as assumption 1). The results of the calculations are given in Figure 52 for the winter 1971 data. The data are below the Einstein function and diverge from the function when the stability is high.

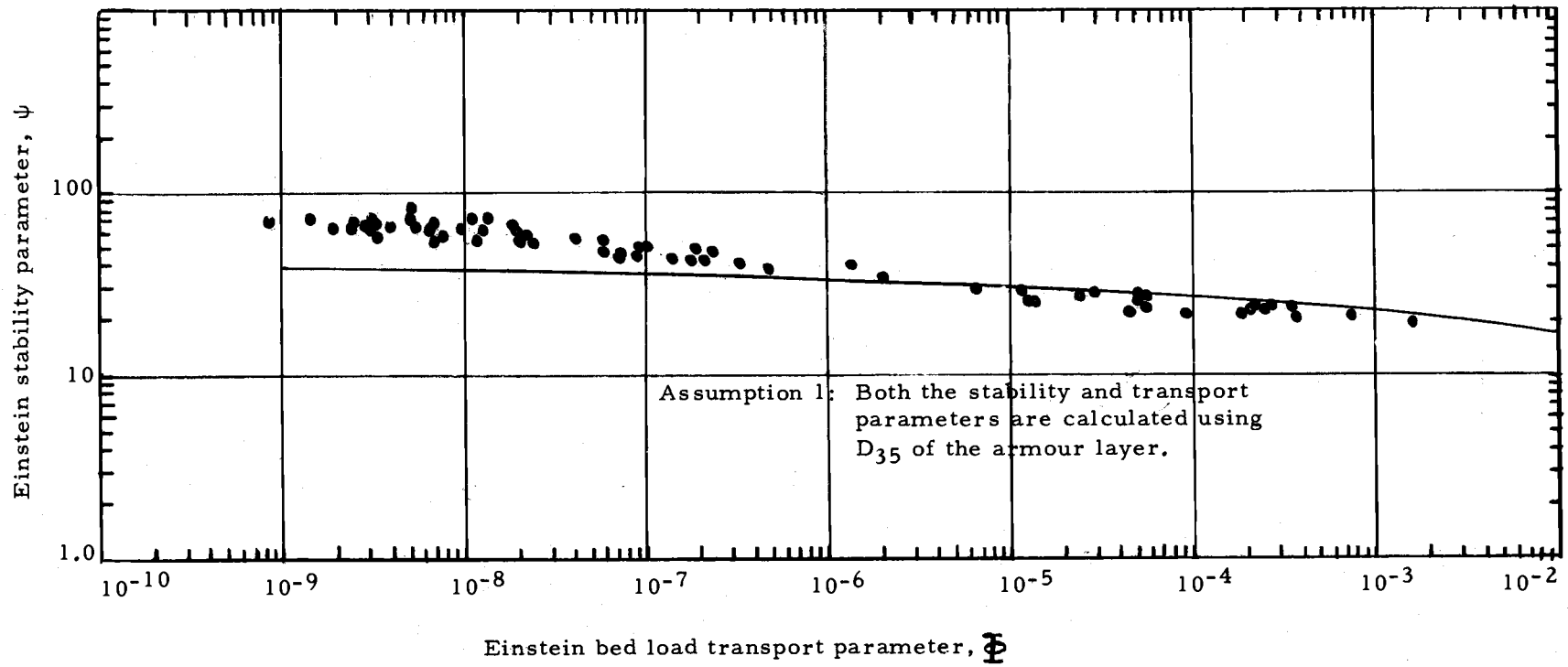


Figure 52. Comparison of winter 1971 Oak Creek data to Einstein bed load function for Assumption 1.

Another way of looking at an armoured stream bed would be to consider the stability of the bed material to be due to the size of the armouring material, and the bed material transport to be a function of the bed material size below the armour layer. Consequently, the  $D_{35}$  of the armour layer could be used to calculate the stability parameter and the  $D_{35}$  of the bed material below the armour layer to calculate the transport parameter (identified as assumption 27). The winter 1971 data are plotted on Figure 53. In this case, almost all of the points occur above the Einstein function on the graph.

Neill (1969) has used the  $D_{50}$  size as representative of the bed material movement. Therefore, the  $D_{50}$  size of the Oak Creek bed material was used to calculate the transport parameter whereas  $D_{35}$  of the armour was used to calculate the stability parameter (assumption 3). The results of these calculations are given in Figure 55. In this case, the data for the higher transport rate are scattered around Einstein function but diverge from the function when the stability parameter is above about 30. The discharge corresponding to a stability parameter of 30 is in the order of 45 cfs, i. e., near the "critical" discharge.

The data given in Figure 54 suggest that the concept given above (that the stability is a function of the armouring material while the bed material transport is a function of the material below the armour layer) is a realistic way of approaching the problem of bed material



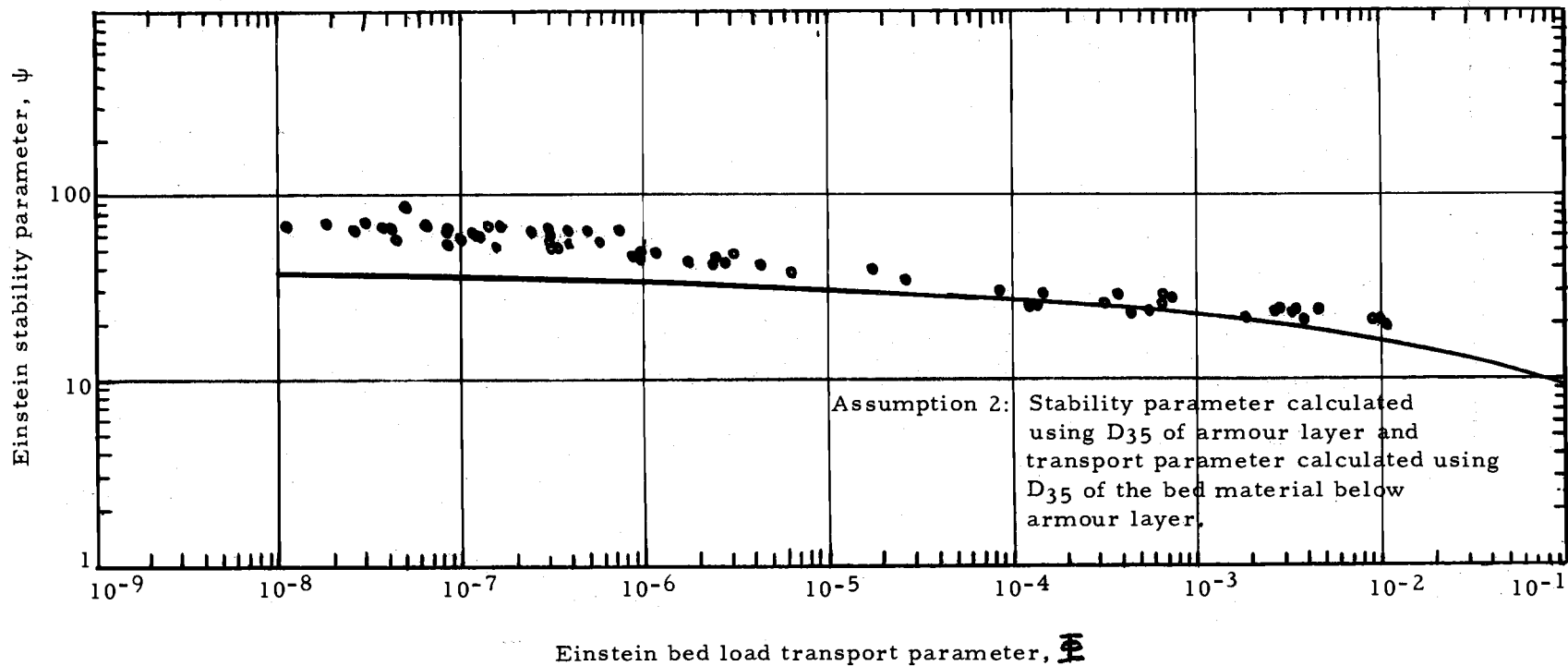


Figure 53. Comparison of winter 1971 Oak Creek data to Einstein bed load function for Assumption 2.

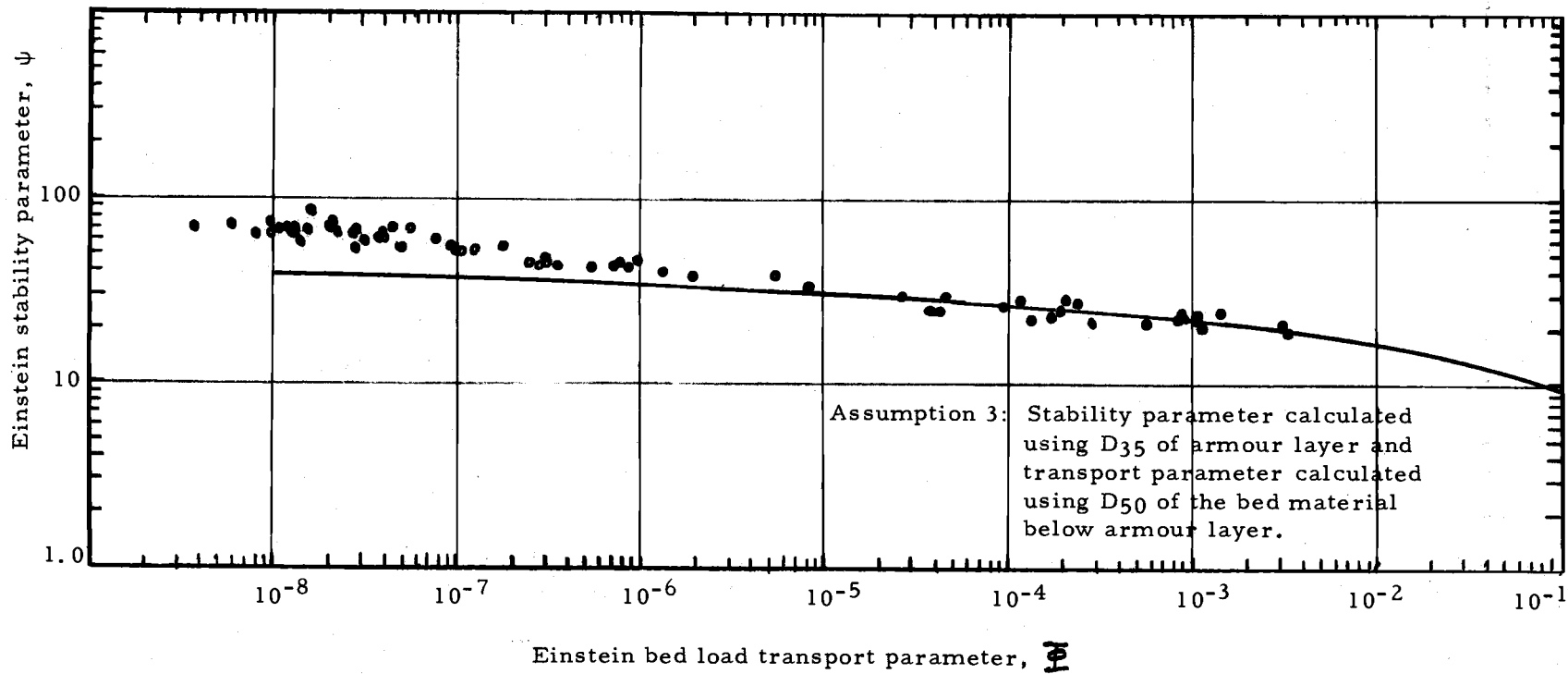


Figure 54. Comparison of winter 1971 Oak Creek data to Einstein bed load function for Assumption 3.

transport in a heterogeneous bed with an armour layer. The fact that the  $D_{50}$  of the bed material gives good results is probably related to the nature of the bed material "release" to the moving interface (see a following section). When an armouring particle is disturbed, the material covered by the particle is then subject to hydraulic forces greater than those required to move the particles with the result that the particles are plucked from the opening in the armour layer until the hole is filled by other particles or the particles not removed are of such a size that they are stable. Consequently, the  $D_{50}$  size is more representative of the material moving as bed load when the discharge is greater than the critical discharge.

When the armour layer is "stable", the material actually being transported is related to the availability of material within the armour layer. The stability of these particles is not as much related to the general stability of the armouring material as to the ability of the smaller material to "hide" among the larger armouring particles. Also, the points plotted above the function curve are for discharges where the entire bed would not be in motion but where only scattered movement would be taking place. The fact that the points are above the Einstein function is probably related to the movement of isolated members of the armour layer. Such movement releases sand to the flowing water for transport among the armour particles.

The data for the winter of 1969-70 are given in Figure 55.

Assumption 3 was used in making the necessary calculations. These data are near but generally below the Einstein function shown on the graph.

All of the data for winter 1969-70 and winter 1971 are given in Figure 56, based on assumption 3. A line fitted to the winter 1971 data above the critical shear stress and tangent to the Einstein function is shown on the diagram. The data with stabilities below 31 are scattered around the Einstein function but they fit the function as well as most data. The assumptions made, as described previously, are (1) the stability of the system is related to the  $D_{35}$  size of the armour layer, and (2) the transport is related to the  $D_{50}$  size of the bed material below the armour layer.

### Bed Load Transport Model for Oak Creek

#### Proposed Model

The following model is proposed to describe the sediment transport system in Oak Creek. During low flow periods the bed load transport is limited by the availability of material. The armour layer protects most of the fine material that the stream has a capability of transporting so that only sand scattered among the armouring particles is transported. As the flow increases to the point where the smaller

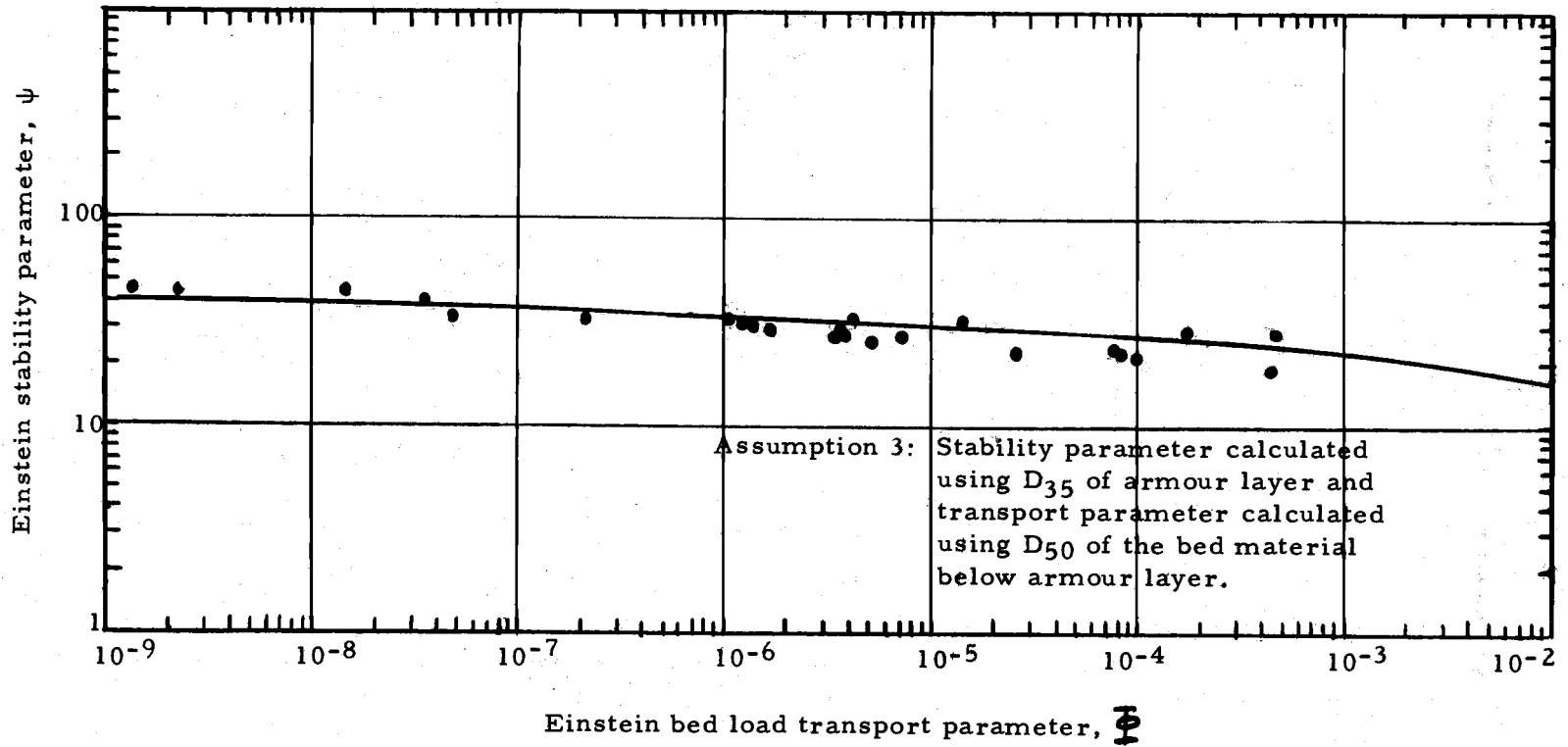


Figure 55. Comparison of winter 1969-70 Oak Creek data to Einstein bed load function using Assumption 3.

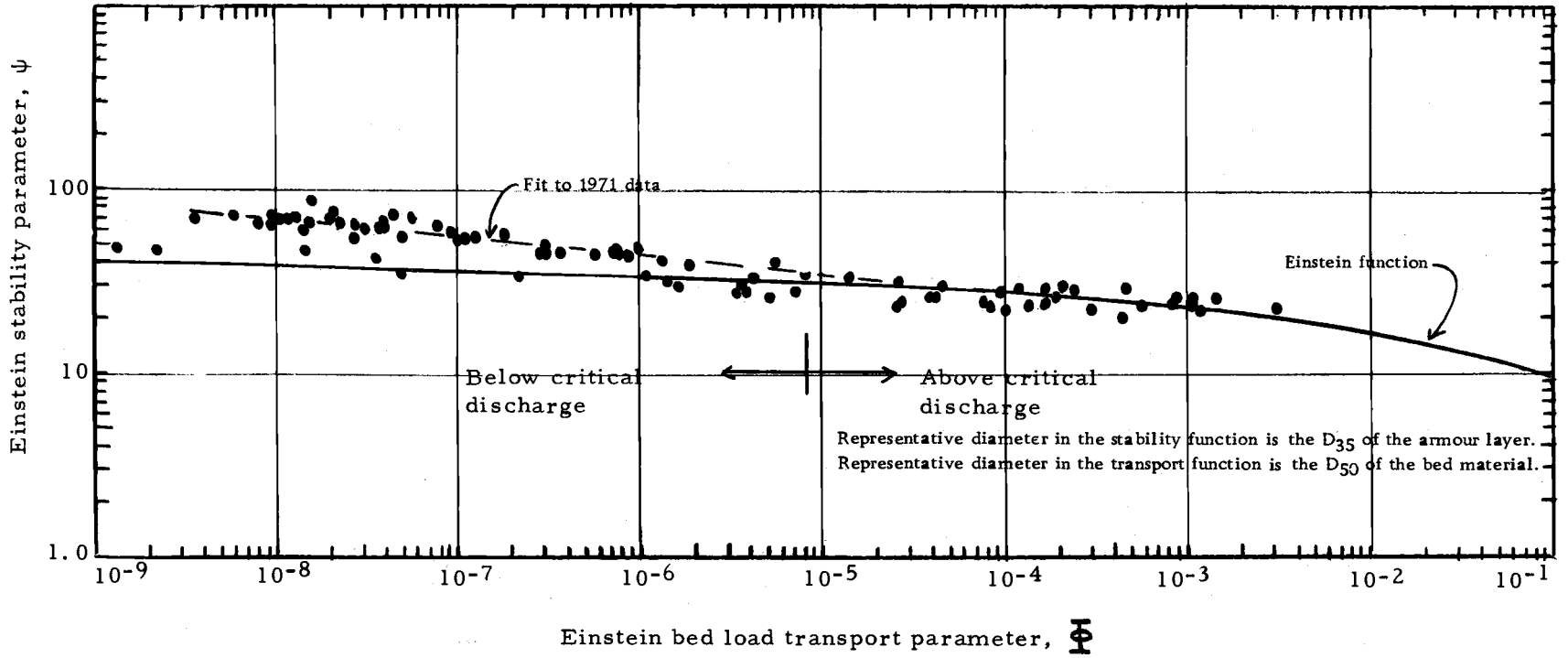


Figure 56. Comparison of all winter Oak Creek bed load data to Einstein bed load function using Assumption 3.

armour particles of the armour layer can be dislodged, the finer-sized material protected by such particles is released to the bed-water interface. This fine material is then transported over and around other armour particles as bed load, with some of the sand and small gravel being "filtered" out by the armour layer as individual small particles fall into areas protected by armour particles. Whenever such protective particles move, the process is repeated. When the flow is between 10 and 20 cfs, few of the armour particles move and the bed load transport is low. As the stream discharge increases, more particles of the armour are placed in motion and the bed load transport is higher. When the "critical" discharge is exceeded, a significant portion (about one third) of the armour layer is in motion. As the bed material below the armour layer is exposed to lift and drag forces resulting from removal of the protective surface material, small gravel, sand, and finer particles are placed in the surface layer. The sand and smaller sediment placed into the armour layer in this manner move downstream until they reach a "hiding" place at which they are not exposed to the hydraulic forces of the stream. As the discharge increases to a point where a large fraction of the armouring particles are in motion, the moving armour particles are mixed with the bed material. During high flows not all of the particles in the armour layer are moved. After the stream flow falls from above critical to below critical discharge, armour particles become stable

against movement but the sand and fine gravel originally moving with the armour layer continue to be removed from around the stable armour particles.

### Information Supporting the Model

The information given below supports the concepts given in the proposed model. Each item supports a portion of the model but no data are available which directly supports the complete model. In other words, the various data collected during the study have been interpreted to give the model described above.

Field observations suggest that for a given discharge near or just above the critical discharge, the bed load transport rate is larger on the falling limb than on the rising limb of the discharge hydrograph (when leaves and other debris are not involved). Unfortunately, no good data were obtained at flows in the critical flow region for a rising hydrograph. However, data for four samples were obtained which can be used to compare transport on the falling limb to transport on the rising limb. The four samples make up two sets of samples with similar discharges just above the critical discharge. Each set has one sample from the rising limb and one sample from the falling limb.

The data are presented in Figure 57 in terms of accumulative weight of material transported versus the particle size. The transport data for individual size ranges are given in Table 15. Sample 15



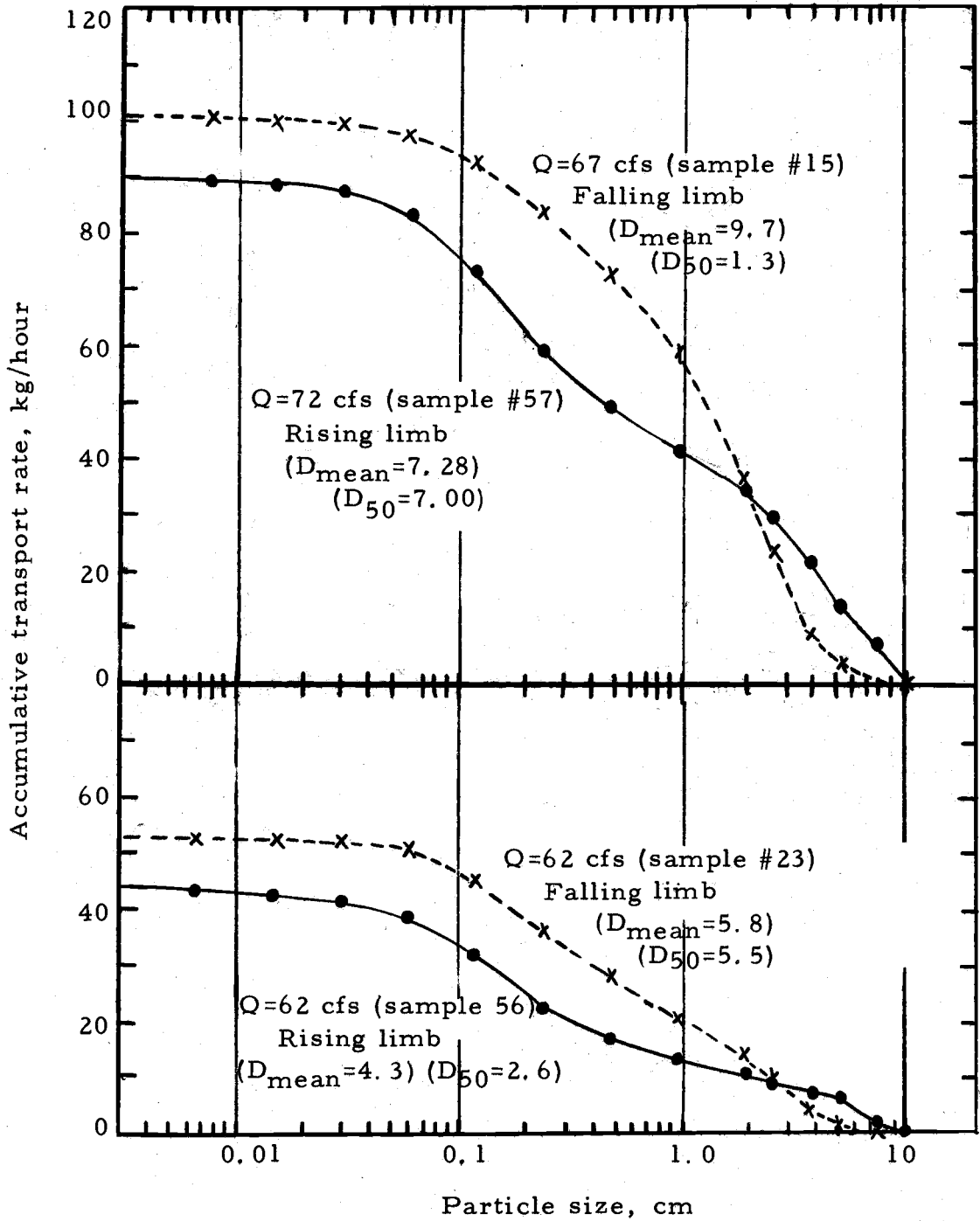


Figure 57. Comparison of bed load transport on rising and falling limbs of hydrographs.

Table 15. Incremental weights of transported material for two sets of data used to compare falling limb to rising limb bed load transport.

Size Range, cm	Transport Rate, kg/hour			
	Set 1		Set 2	
	Falling Limb 15	Rising Limb 57	Falling Limb 23	Rising Limb 56
7.62 - 10.2	0.61	7.12	0	1.91
5.08 - 7.62	3.13	6.48	1.79	4.16
3.81 - 5.08	5.15	8.10	2.32	1.09
2.54 - 3.81	14.54	8.18	5.37	1.95
1.90 - 2.54	14.04	4.81	4.57	1.52
0.952 - 1.90	21.61	6.84	6.75	2.48
0.476 - 0.952	14.54	7.74	7.21	3.96
0.238 - 0.476	10.30	10.18	8.11	5.82
0.119 - 0.238	8.68	14.12	9.17	9.13
0.0595- 0.119	4.96	10.18	5.15	6.95
0.0297- 0.0595	1.83	3.96	1.42	2.74
0.0149- 0.0297	0.71	1.26	0.37	1.00
0.0074- 0.0149	0.50	0.54	0.21	0.52
0.074	0.40	0.45	0.16	0.30
TOTAL	101.0	89.96	52.6	43.5
Stream discharge, cfs	67	72	62	62

was from the falling limb of a major storm with a maximum discharge in excess of 250 cfs, sample 23 is from the falling limb of a storm hydrograph with a peak discharge of about 80 cfs and a relatively short duration, and samples 56 and 57 are from the rising limb of a storm hydrograph following a five week period of low flows after the storm associated with sample 23.

The interesting result is that the transport of the larger particles and of sand is greatest for the rising limb and transport of the small gravel is greatest for the falling limb. The total for all particle sizes is largest for the falling limb samples. Both of these observations are consistent with the model described previously. On the rising limb, all of the armour layer is exposed to the hydraulic forces. As individual armour particles are moved, the sand and fine gravel is released but the fine gravel is filtered out over a short distance while the sand is transported farther as bed load. Consequently, the transport of the larger particles is relatively great and of the finer gravel relatively small. In contrast, as the flow level recedes the armour layer is reformed but not as much of the armour is exposed to hydraulic forces because some of the smaller gravel will be mixed in with the armour size particles at the surface of the bed. As this fine gravel is removed, the armour becomes re-exposed to the hydraulic forces. On the falling limb, the sand is believed to be protected by the smaller gravel.

Support for the idea that not all of the armour particles are moved during a high flow is shown by experiments made during the field studies where painted rock of the same size as the armour particles was placed among the armour particles. A total of 69 rocks were placed. After a storm where the maximum discharge was 115 cfs it was found that 11 (16%) of the particles were not moved.

After a bed has again become stable and the discharge is below the critical discharge, the newly stable armour layer would have some of the particles relatively exposed to the hydraulic forces. These particles would tend to be removed from the armour layer. After movement, the tendency would be for the disturbed particles to come to rest in a more stable position. After a period of time, the transport rate of the larger particles should decrease as compared to the case of that part of the falling limb transport just after the flow has receded through the critical discharge.

When the armour layer first becomes stable it is believed that there is a large amount of sand and fine gravel among the armour particles. Over time these smaller particles will be removed and the hiding place cleaned of sand and finer material because the hydraulic forces are comparatively strong. Later, as the flow recedes further, the hiding places are effective in removing sand and finer material from active transport. As the "hiding" places are filled, the transport of sand and fines would be expected to increase.

Two comparable samples in the discharge region of from 22 to 23 cfs are shown on Figure 58. Sample 28 was obtained on the falling limb of a storm with a peak discharge of 80 cfs, while sample 35 was obtained after a long period of armour stability. The data indicate that the falling limb sample is coarser than the sample obtained after a long period of stability and that the total sediment transport is larger after a period of armour layer stability. Most of the increase in transport rate is in the medium sand size range, although all sizes (except for the largest in the falling limb sample) show an increase in transport rate.

The observation that the bed load transport rate is highest during the stable period because less material is finding a place to hide. The observation that the transport of the maximum size particles in the samples is highest for the falling limb sample supports the idea that the armour is less stable on the falling limb.

To complete the discussion on the bed load transport model, the data for one set of bed load samples are given in Figure 59. These data are for the case where the critical discharge is 49 cfs and the bed load discharge is above 0.1 kg/hr. A line showing the lower bound of bed load transport associated with any discharge has been drawn. Samples 15, 16, 17, 18, and 23 are all below the line and are falling limb samples. Some of the other samples (19, 20, 24, 25, 26, 27, and 28) are also falling limb samples but the armour layer probably

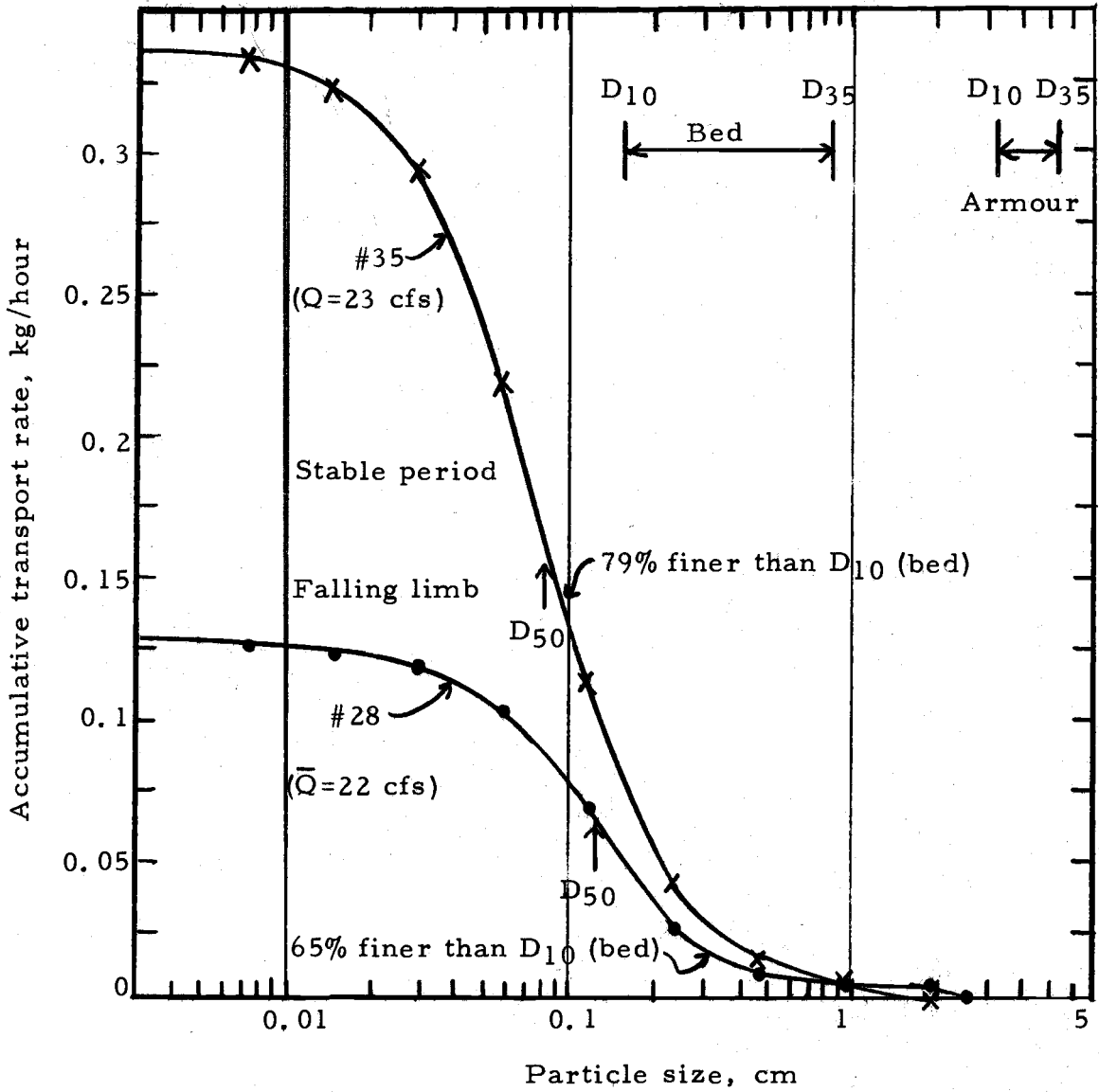


Figure 58. Comparison of bed load transport on a falling limb and after a period of steady low flow.

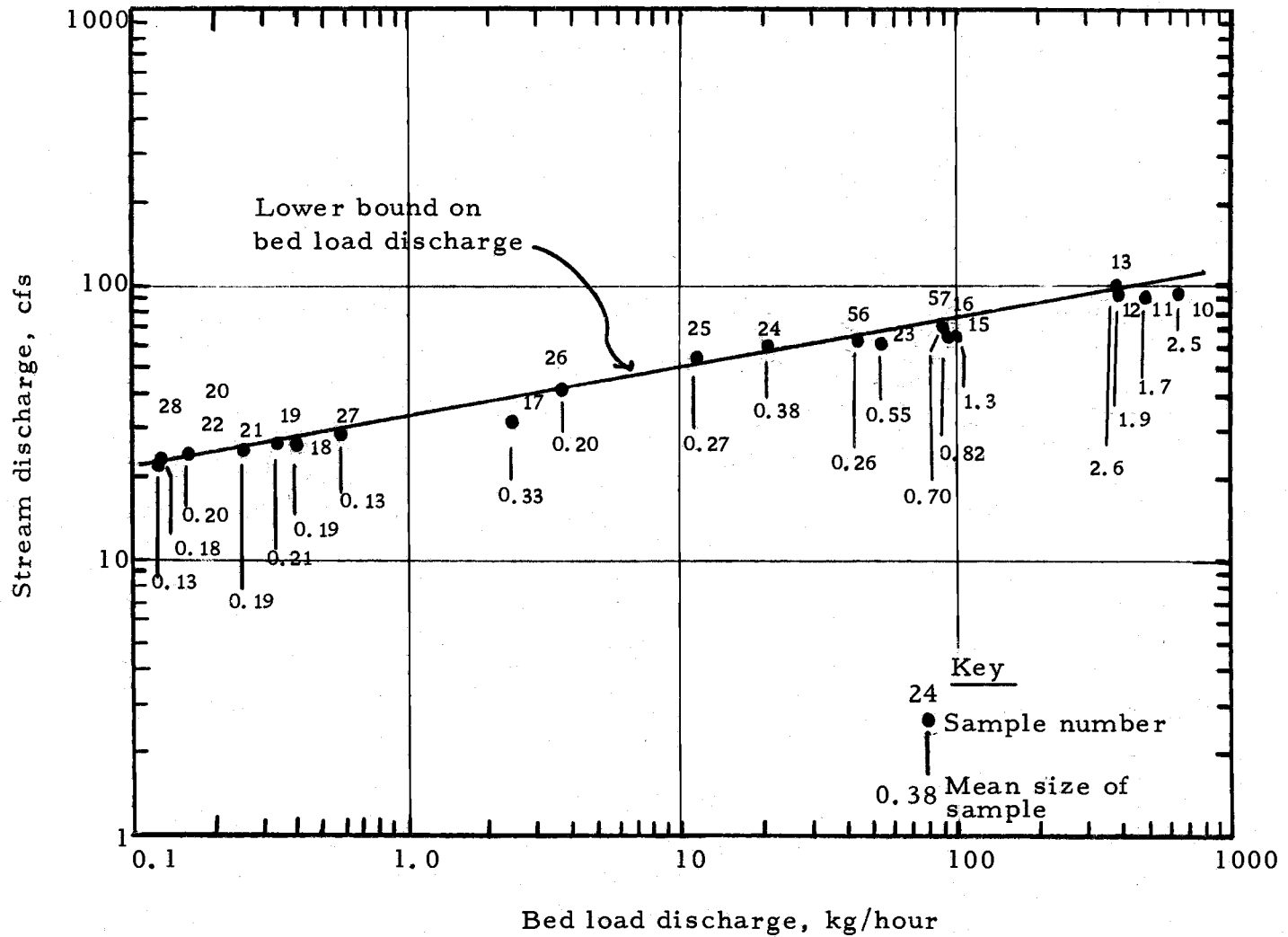


Figure 59. Specific information for early 1971 bed load data (to March 10, 1971).

controlled the sediment transport in these cases.

Samples 10, 11, 12, and 13 are of interest because the transport efficiency was decreasing with time (transport efficiency is the ratio of immersed bed load transport rate to stream power). The efficiencies are given in Table 16. The samples were obtained in sequence with a total elapsed time of 2.35 hours. One problem with the samples is that when the sampling trough has been filled and the trough is then cleared, the bed load measured is large compared to other samples under similar conditions. This is due to an accumulation of material on the stream bed near the sampler (when the vortex trough is closed) which is subject to an increase in forces tending to move it after cleaning and reopening the sampling trough. Samples 10, 15, and 17 are "start up" samples. Also, samples 11 and 16 could easily be influenced by the transient conditions just upstream of the sampler caused by a change cleaning of the trough.

Table 16. Variation of bed load transport efficiency.

Sample Number	Stream Discharge, cfs	Bed-load Transport, kg/hour	Efficiency
10	92	641	0.0040
11	92	484	0.0030
12	93	392	0.0024
13	100	385	0.0022



The mean sizes of the bed load material are also included in Figure 59 to show the range of mean particle size and the variability of mean size associated with each discharge range.

On Figure 60 are data for the samples obtained in March, 1971, when the critical discharge was 29 cfs. Sample 59 was a "start up" sample.

The general conclusions of this section are that: (1) the bed load transport is related to stream power but the relationship is a function of the critical discharge associated with the armour layer; (2) the data on critical shear stress associated with individual particles agrees well with other published data; and (3) in general, the mean size of the bed load material increases with discharge.

The model described above is a conceptual model which can help in interpreting suspended sediment measurements in a gravel-bottomed stream. A following section presents information on the interaction of the suspended load and the bed load for a stream having an armoured bed.

The working model presented indicates the armour layer is the most important single factor in limiting the availability of sediment and in controlling the relationship between stream flow and bed load discharge.

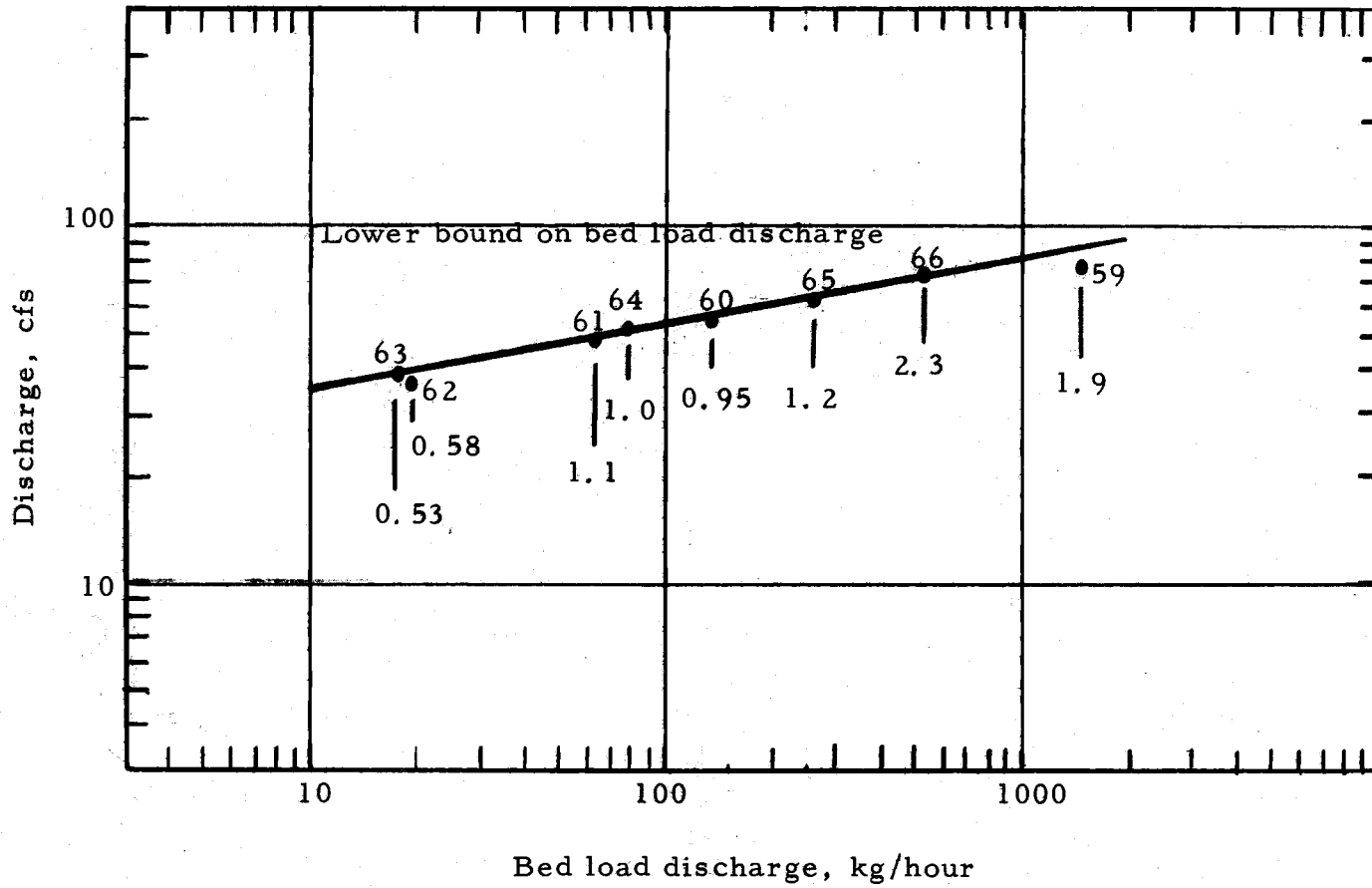


Figure 60. Specific information for bed load data for March 10-11, 1971.

### Division Between Bed Material and Suspended Load

The total sediment load of a stream is typically divided into suspended load and bed material load. The bed material load is then divided into the bed load and the bed material being transported in suspension. The bed load is the material moving in the immediate vicinity of the bed while the suspended bed material is bed material suspended in the flow above the bed.

For any given particle size found in the stream bed, the amount of the bed material load of particles of that size will depend upon the turbulence in the flow and, hence, upon the discharge.

The division of sediment load into bed material load and suspended load (or wash load) has often been based upon use of a limiting grain size finer than most of the bed material. Using this concept and the  $D_{55}$  size of the bed as the division size, the wash load would be made up of particles of less than about 0.5 to 1.0 mm (see, for example, Table 3 or Figure 7).

Another way of distinguishing the wash load from the bed material load is to consider the wash load to be that material with a fall velocity less than the fall of the water in the stream. In equation form this is:

$$V_f = S V \quad (60)$$

where  $V_f$  is the fall velocity,  $S$  is the stream slope, and  $V$  is the mean

velocity of flow. If the fall velocity of particles of a given size is greater than that of the vertical velocity as the parcel moves downstream along the hydraulic guideline, then we would expect the particle size to be found in the stream bed. In contrast, if the downward vertical velocity of the parcel of water is less than the particle fall velocity, we would not expect the particle size to be part of the bed material. Of course, turbulence transfers some of the particles of any size to the bed material so that all sizes are found in the bed material. The particle diameter with a fall velocity equal to the product of mean velocity times the slope is an alternative arbitrary division between wash load and bed material load. The division defined in this manner is a function of the discharge,

The data from Oak Creek have been used to develop the diameter equivalent to the product of velocity times hydraulic slope. This equivalent diameter was calculated using a drag coefficient ( $C_d$ ) of

$$C_d = \frac{24}{R_e^*} (1.0 + 0.15 R_e^{*0.687}) \quad (61)$$

which was developed by Schiller (Graf, 1971). The equation used to calculate the particle diameter is

$$D = \frac{3}{4} C_d \frac{y}{v_s} \frac{(V S)^2}{g} \quad (62)$$

where terms as defined previously. The results are given in Figure 61.

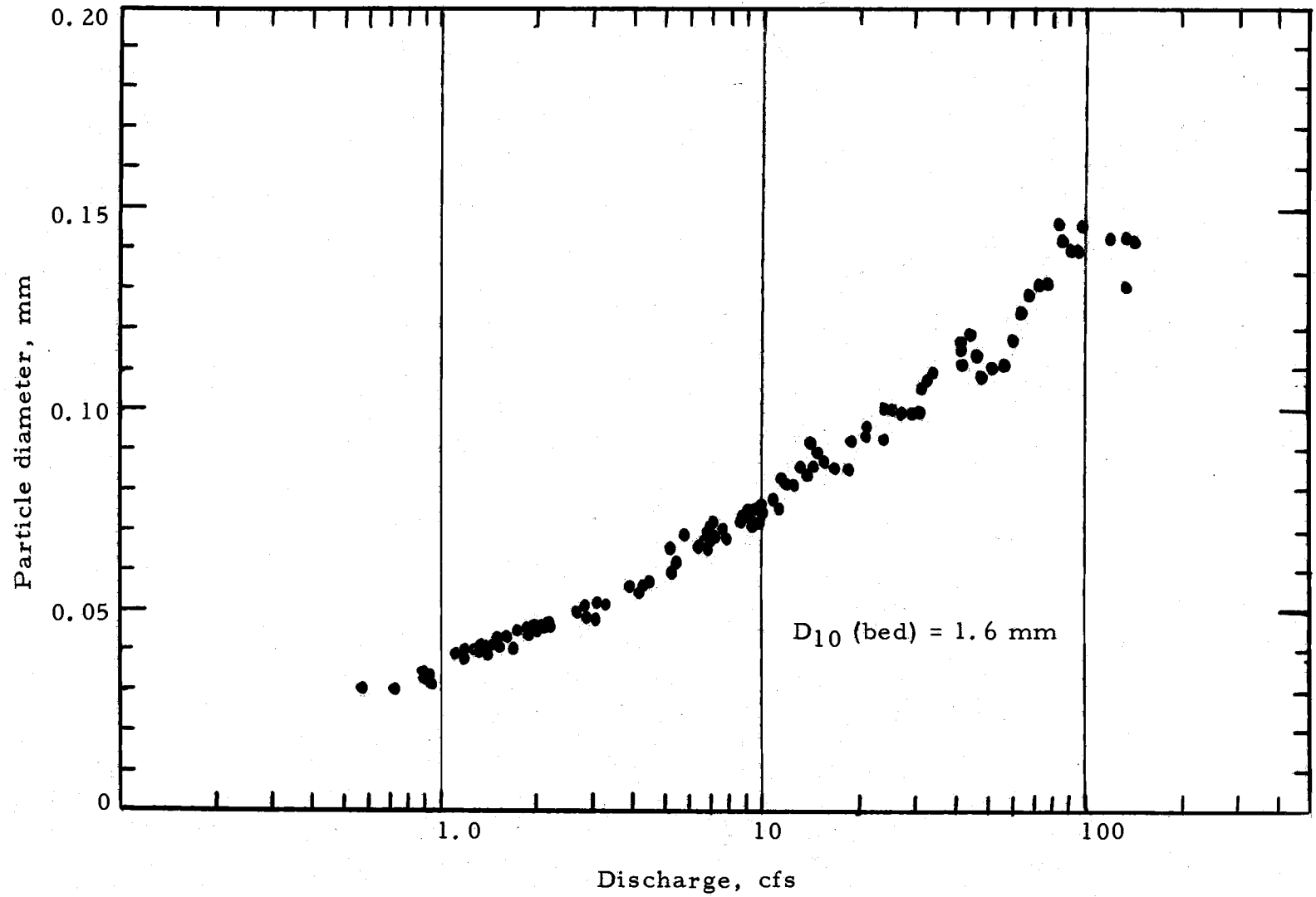


Figure 61. Particle diameter forming the division between bed material load and suspended load.

At the critical discharge for initiating bed load transport in Oak Creek, Figure 61 shows that the particle size dividing wash load from bed material load at the critical discharge is about 0.11 to 0.12 mm. Particles of less than 0.11 millimeter probably would not be found in the bed material because the armour layer would return to a stable state before the finer particles would have had a substantial probability of settling in to the bed.

Typically, a low winter flow is on the order of 10 cfs. The division between wash load and bed material load is then on the order of 0.08 mm (Figure 41). Particles coarser than 0.08 millimeters would likely be rapidly "filtered" from the water. Finer materials would take longer but would also be filtered because of turbulent transfer to the bed. During the summer, flows are on the order of 1 cfs and the division is on the order of 0.03 mm. This small size may help explain why considerable quantities of fine material can be held in the armour layer during the summer with the result that the water is quite clear. In other words, fine material reaching the stream is readily filtered from the water.

The parent earth material in the Oak Creek watershed is basalt. Chemical weathering processes tend to produce clays while physical processes in the watershed tend to form sand and gravel. This may be part of the reason material in the particle sizes in regions of 0.5 to 0.1 are not common in the bed material.

### Suspended Sediment Load

The variation of suspended load with river discharge is given in Figure 62, for the data collected in winter 1971. There is considerable scatter of the points, as is typical of suspended loads which are dependent upon the availability of particles for transport. Thus, some of the variation is related to the time of sampling in comparison with the position on the discharge hydrograph. It was noted during data analysis that the first high flow after a period of lower flows transported more suspended sediment than did later flows of the same magnitude or did even higher flows.

One of the objectives in obtaining the suspended sediment information was to determine the relative importance of bed load transport in the total sediment yield from a forested watershed. Suspended sediment concentrations were obtained at the start and finish of each bed load sampling period for the lower discharges and during the middle of the bed load sampling period for the higher discharges. These were then used to determine a concentration corresponding to the representative stream flow for the bed load sample.

Using the suspended load and bed load information, a ratio of the bed load to the suspended load was calculated for each bed load sample. The results are given in Figure 63.

The data in Figure 63 indicate that the importance of bed load increases as the discharge increases. The maximum bed load to

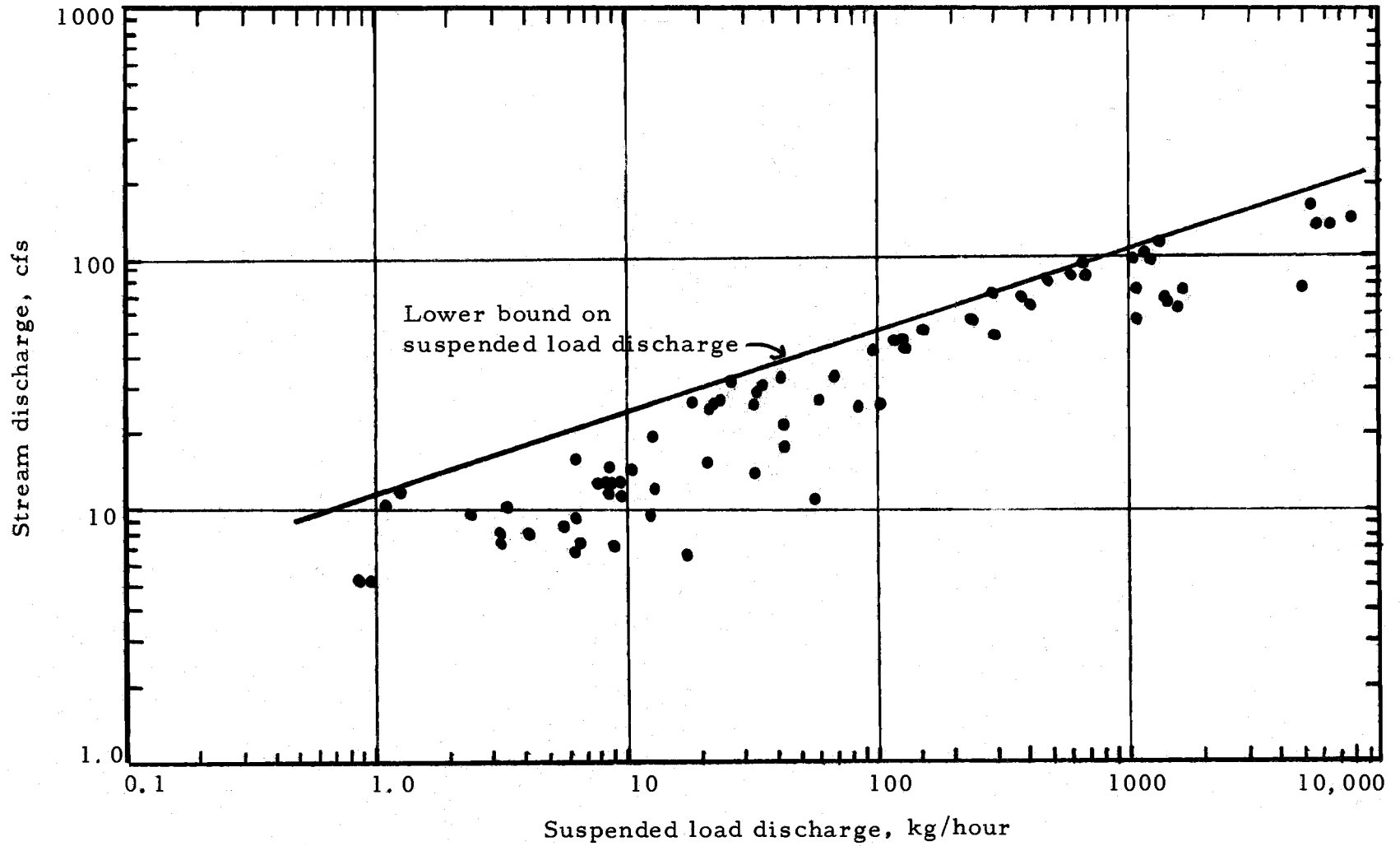


Figure 62. Suspended load discharge in Oak Creek (winter 1971).



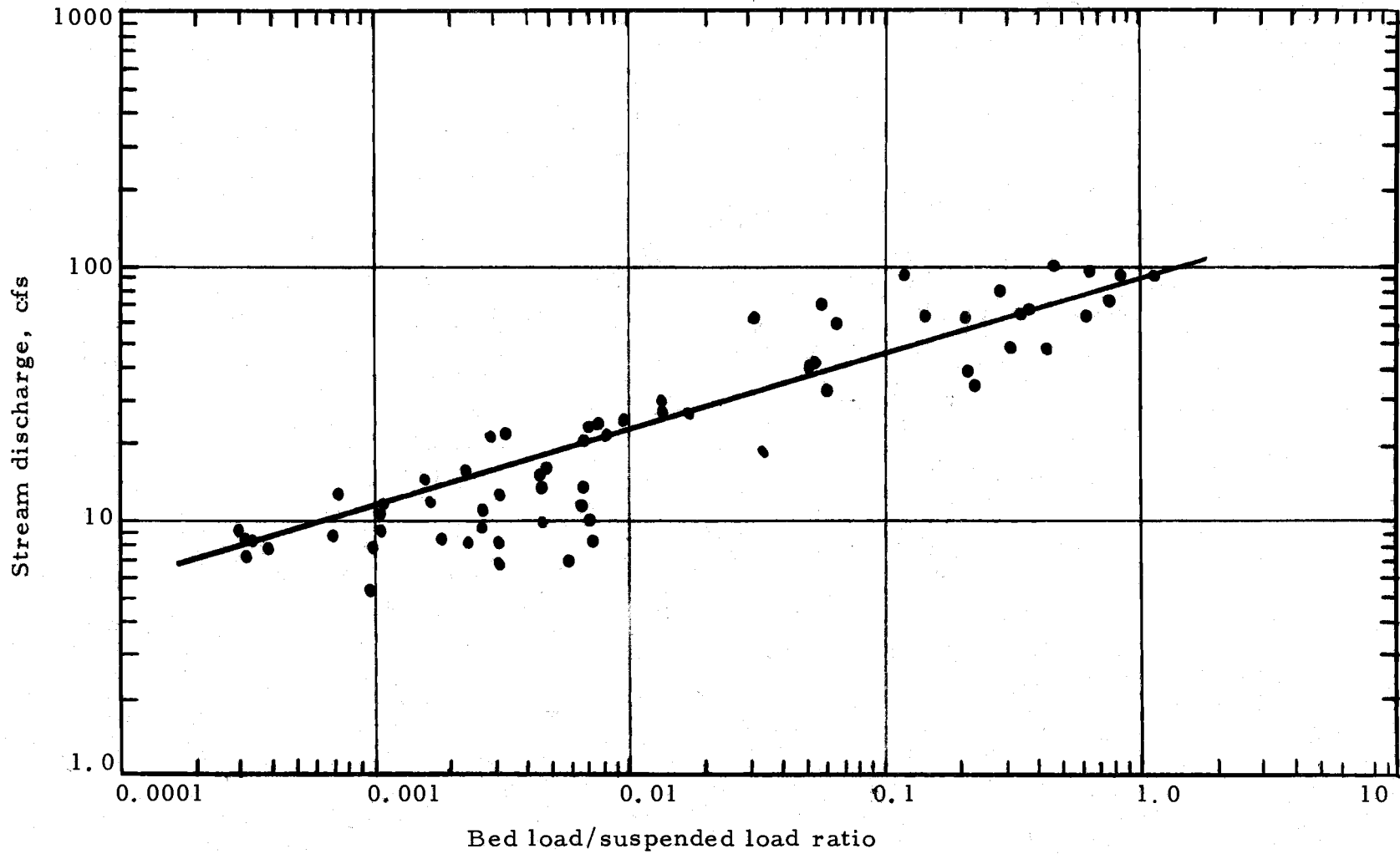


Figure 63. Variation of bed load to suspended load ratio with stream discharge (winter 1971 data).

suspended load ratio was 0.112 for a stream discharge of 92 cfs.

The bed load and suspended load hydrographs for an isolated storm following a low-flow period are out of phase. The peak bed load transport occurs nearly concurrently with the peak storm flow but the peak suspended load precedes the peak stream flow. For several runoff events in close succession the suspended load and bed load hydrographs become more nearly in phase with each other and with the storm hydrograph as the storm system progresses. These phase relationships account for much of the scatter shown on Figure 63.

### Interaction Between Bed Load and Suspended Load

#### Conceptual Framework

In this section a possible explanation of the interaction between bed load and suspended load is described. Other explanations may be advanced to explain part of the variance found in the relationship between discharge and sediment load. The concept given here does explain variations in the observed relationship of discharge versus sediment load, but data from other armoured streams must be collected before the usefulness of the concepts is adequately demonstrated.

The model presented here is purely descriptive and cannot be used to predict the amount of sediment transported by a stream. The

object of the model is to assist in the interpretation of sediment load measurements made on gravel-bottomed streams.

As described in the section of Chapter II, the physical characteristics of a gravel-bottomed stream in the Oregon Coast Range are that the bed material of the stream is gravel with an armoured surface and has relatively stable banks. The armour is a nearly uniform layer of relatively large particles at the surface of the bed material. It protects the finer, better graded, material below. In the Oak Creek Study area the best estimate of the mean size of the armour layer is 6.3 cm, compared to 2.0 cm for the material below the armour layer.

In describing the conceptual model, we first have to select a starting point on the stream flow hydrograph. To do this, let us assume that a storm has moved a large amount of bed material, including the armouring material. We might select as a starting point a place on the recession limb of the hydrograph just after the end of direct storm runoff while the base flow is still relatively high. Also, let us assume that the armour layer is stable at this flow.

Just after a high flow, when the armour layer has been moving, the finer material which had been moving with the moving armour layer will be washed from among the armouring particles as they come to rest. This occurs at the flow which is just slightly below that required to move most of the armouring particles. Although some of the armour particles will be moved, the system is generally stable at this

moment. As the flow recedes, sand is completely removed from around the armour. Thereafter, the only small gravel and sand available for transport are those particles which are released by any armour particles that are moved periodically. The armour layer will increase in stability with time as a result of rearrangement of the armouring particles, as has already been described. As the flow recedes further, locations within the armour layer will act as a trap for sand particles and both the armour material and the bed material below will begin acting as a filter in removing sand and fines from the water. With time, this "reservoir" is filled and additional fines and sand cannot be removed into void spaces but can only settle on the armour. If there would be an increase in flow after this reservoir is filled, some of the traps within the armour layer would cease to protect stored material, and the traps would become a source of fines and sand to be transported as both bed load and suspended load. If the reservoir is not full, the armour layer would not be as good a source as in the case where the reservoir is full.

The amount of material that can be contained in the armour layer's silt-and-sand reservoir is inversely related to the discharge of the stream. Typically in the Northwest, the rainy season base flow for a stream will be higher than during the dryer season, with a corresponding increase in the size of the silt-and-sand reservoir as the flow recedes to the summer base flow level.

The consequence of having a full or nearly full silt trap in the armour layer is that the suspended sediment load of the stream will become more erratic. This is for two reasons: (1) the silt reservoir in the armour layer will yield sediment when the flow increases for the first time after the reservoir is filled but not for the second unless the supply to the reservoir has been replenished; and (2) the armour layer silt trap will not act as a buffer on the sediment yield from the watershed. The sediment yield from a watershed is quite variable, whereas the rate of removal of suspended particles from the water, when the silt reservoir is not full, will depend on the concentrations in the flow. Thus, an increase in the rate of removal of fines will result from an increase in the sediment yield from the watershed. This will tend to stabilize the sediment load versus discharge relationship. When the reservoir is full, however, this stabilizing effect cannot occur.

When the stream flow increases from a low level and the silt reservoir is full, the silt reservoir will yield some of its fines and sand. With further increases in flow, part of the armour layer will move, yielding silt and sand from both the bed material below the armour and from the armour layer silt reservoir, until all of the silt from the reservoir is suspended in the flow.

If the discharge is constant at a magnitude that causes the armour material to move, the silt load will fall from the peak associated with the initial movement of the armour material until a

constant level is reached which is associated with the dynamics of the total sediment load process and the yield from the watershed. The initial peak will be greater than the yield from the watershed.

As the discharge decreases, the particles in the armour layer will cease to move and the sand associated with the armour layer will continue to move until sufficient armour particle movement allows the sand to become part of the bed again. Sometime during or after this process of cleaning the armour of sand, the armour layer will again act as a silt trap. Then the transported suspended sediment will be less than the yield of such material from the watershed until the silt reservoir is again filled, at which time the transported suspended sediment will once more be in balance with the yield.

A diagram applying the above ideas and illustrating the type of relationship between sediment load and time to expect from a step increase in discharge followed by a step decrease is given on Figure 64.

As stated previously, the size of the silt reservoir will depend on the flow in the stream. This change in silt storage capacity results from a change in particle uplift force exerted by the stream flow. This force decreases as the flow decreases.

If the discharge increases prior to filling of the silt reservoir, the suspended load of the stream will not have as large a peak amount as would be expected from a similar flow increase with a silt full

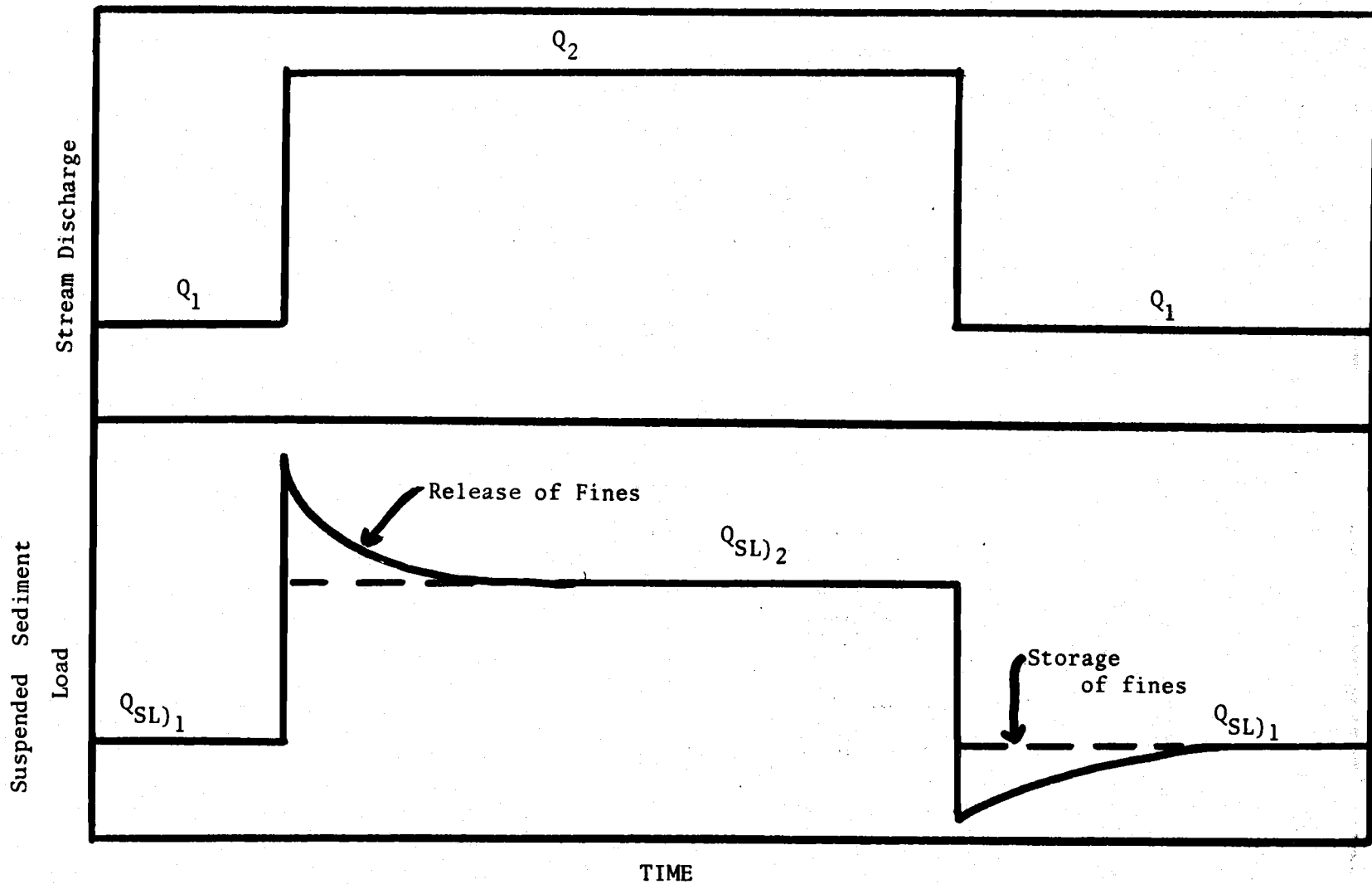


Figure 64. Conceptual variation of suspended load with a step increase and decrease in stream discharge.

reservoir.

The armour layer also protects the bed material beneath it from being transported. On a rising limb, the bed load transport will be lower than for the same discharge on the falling limb because the sand moving with the armour layer on the falling limb will be removed from transport as the armour layer stabilizes.

On a falling limb, the sand will first be removed, as just stated, but as the discharge declines further, the system will pass through a discharge range where sand is neither added nor removed from the armour layer. A few armour particles, however, will be moved as a result of turbulence in the flow. As these particles move, the finer material they protect will be released to the flow and transported as both bed load and suspended load. After the flow has decreased to the point where a very few armour particles are moved, the net effect will be the removal of sand from bed load transport.

After the silt reservoir is filled, the bed load transport should be higher than prior to filling for an equivalent stream flow.

### Supporting Data

The concept of silt removal by a gravel bed has been described by Einstein (1968), along with supporting experimental data. The concept presented is applicable to the case of a point source with the suspended sediment concentration decreasing downstream. The



equation relating the time required to filter out half the suspended sediment is:

$$T = \frac{0.692d}{V_s} \quad (64)$$

where T = half life of any particle size in suspension

d = depth of water

$V_s$  = settling velocity of a particular grain size.

This natural filtering action has been observed in the field by Miner (1968), with the rate of change in sediment concentration found to be much as would be expected from Einstein's work.

For a line source, such as the case of storm runoff from a watershed entering a stream along the length of its channel, the suspended load during the storm would not decrease in the direction of flow but would be lower than the input load. This is because of the filtering action, assuming that the silt reservoir was not full and that the flow was such that a reservoir existed.

The idea that the silt reservoir can be filled is supported by data obtained from Oak Creek. Data obtained between two major storms have been sub-divided into two groups: a low yield period just after the first storm (group A) and a high yield period later, after the silt reservoir was filled (group B). The data are presented in Figure 65, along with other data from a period just after the second storm (group C). Lines have been drawn for the three groups of data which

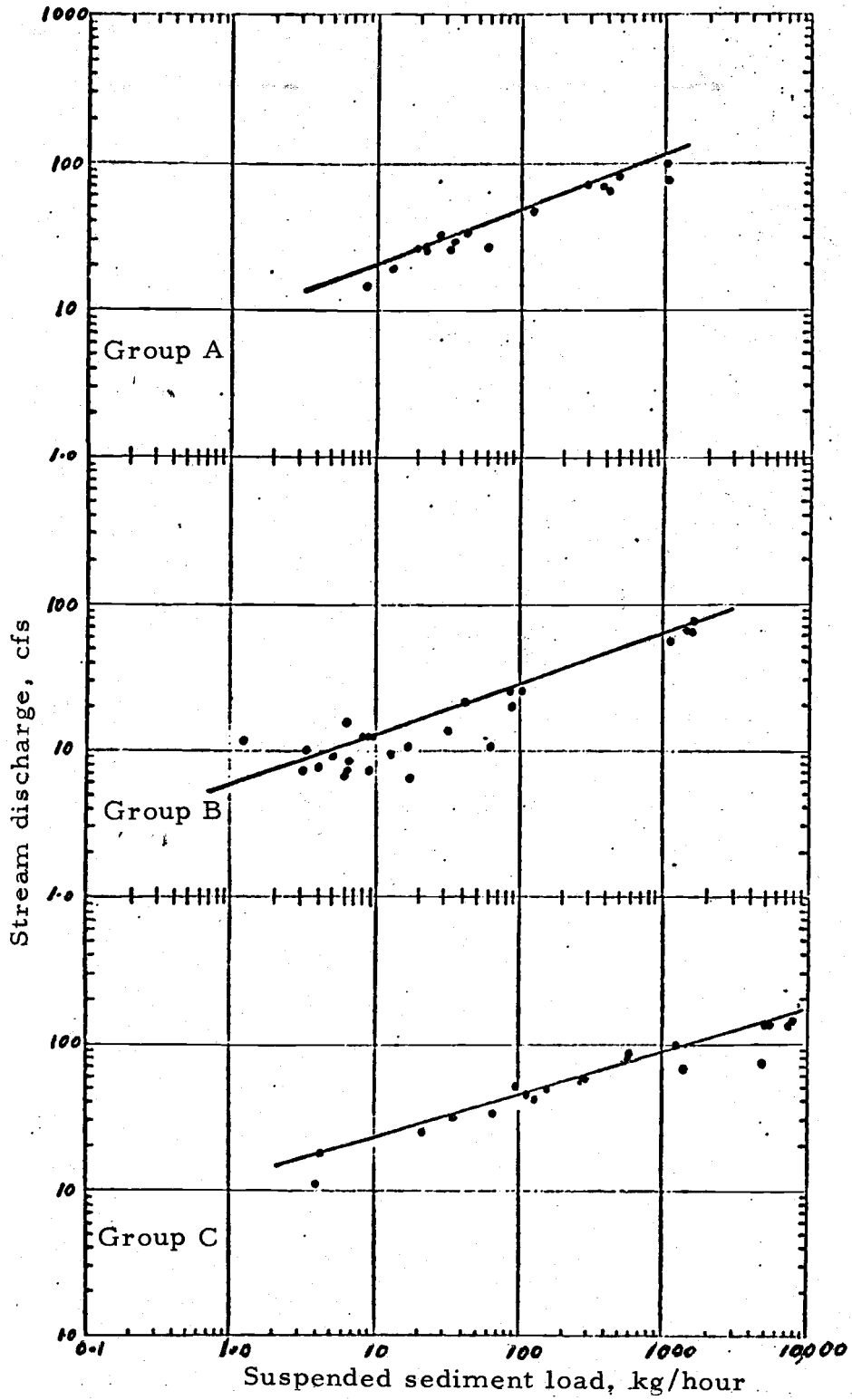


Figure 65. Suspended sediment data in groups by period of sampling.

indicate a lower bound to the suspended sediment load for a given discharge. The lines are shown together in Figure 66. As is shown, the line for group B indicates a greater suspended sediment load at a given flow than do the other two lines. Line B corresponds to the full silt reservoir case.

The scatter of points on Figure 65 for data in group B below about 25 cfs is a result of sand and fines which had been stored in the system and which were removed from the reservoir as the flow increased. Subsequently, the discharge declined and the reservoir was again replenished. The points in the 50-to-80 cfs range on Figure 65 for group B data are from the rising limb of the following storm when the silt reservoir was full. The points at high flow on Figure 65 for data from group C are for the case where the silt reservoir is comparatively empty.

Combination of the data from Figure 65 for groups A and C probably gives a good idea of the suspended sediment load in the stream with an empty silt reservoir. These combined data are given in Figure 67. The line drawn on the figure represents the expected suspended load when the silt reservoir is empty. It is extrapolated somewhat arbitrarily to lower flows than those sampled.

In fall 1971, after an extended period of low flows, a series of suspended sediment and bed load measurements were made. These measurements were made during a time when the silt and sand

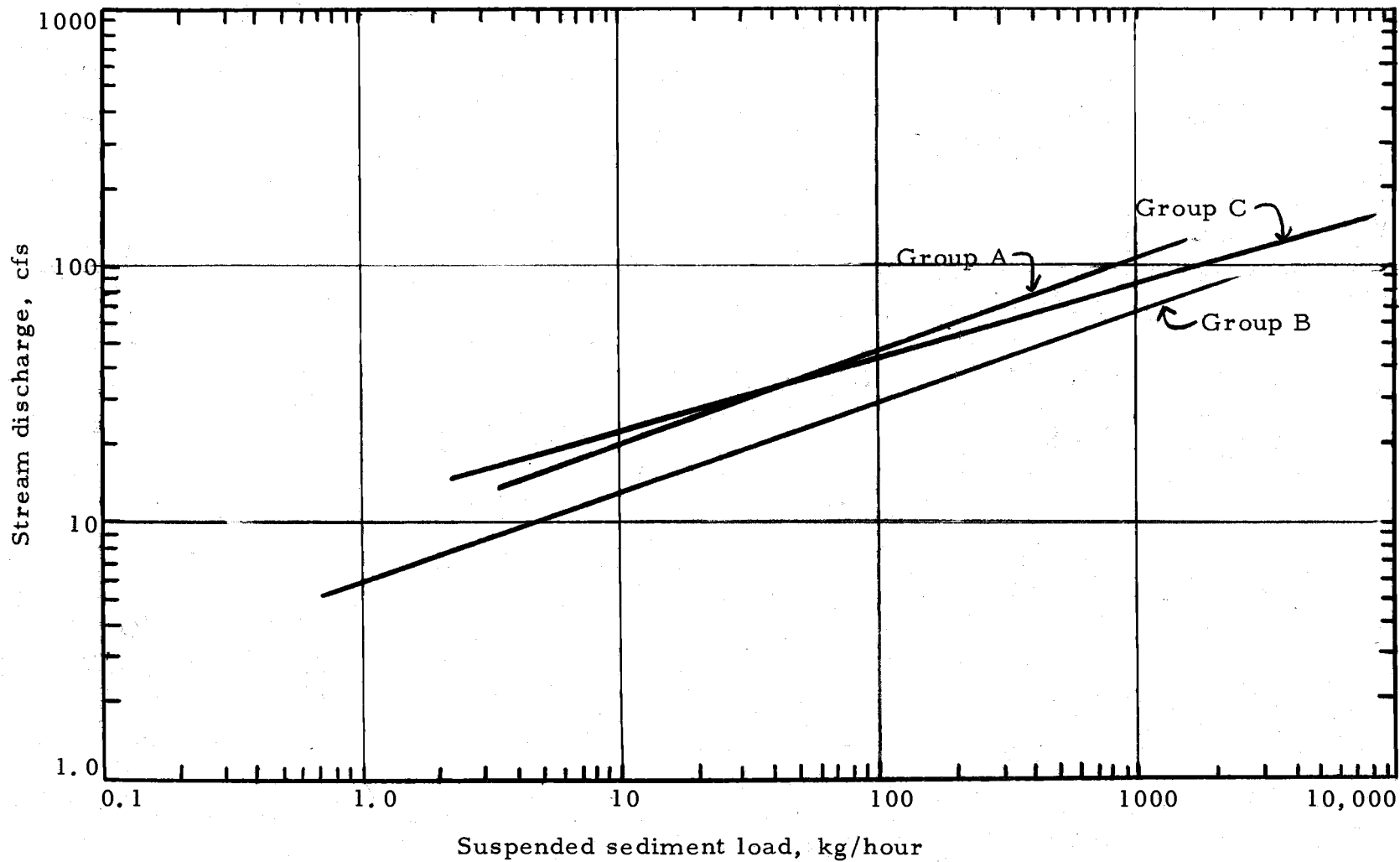


Figure 66. Suspended sediment load curves superimposed from Figure 65.

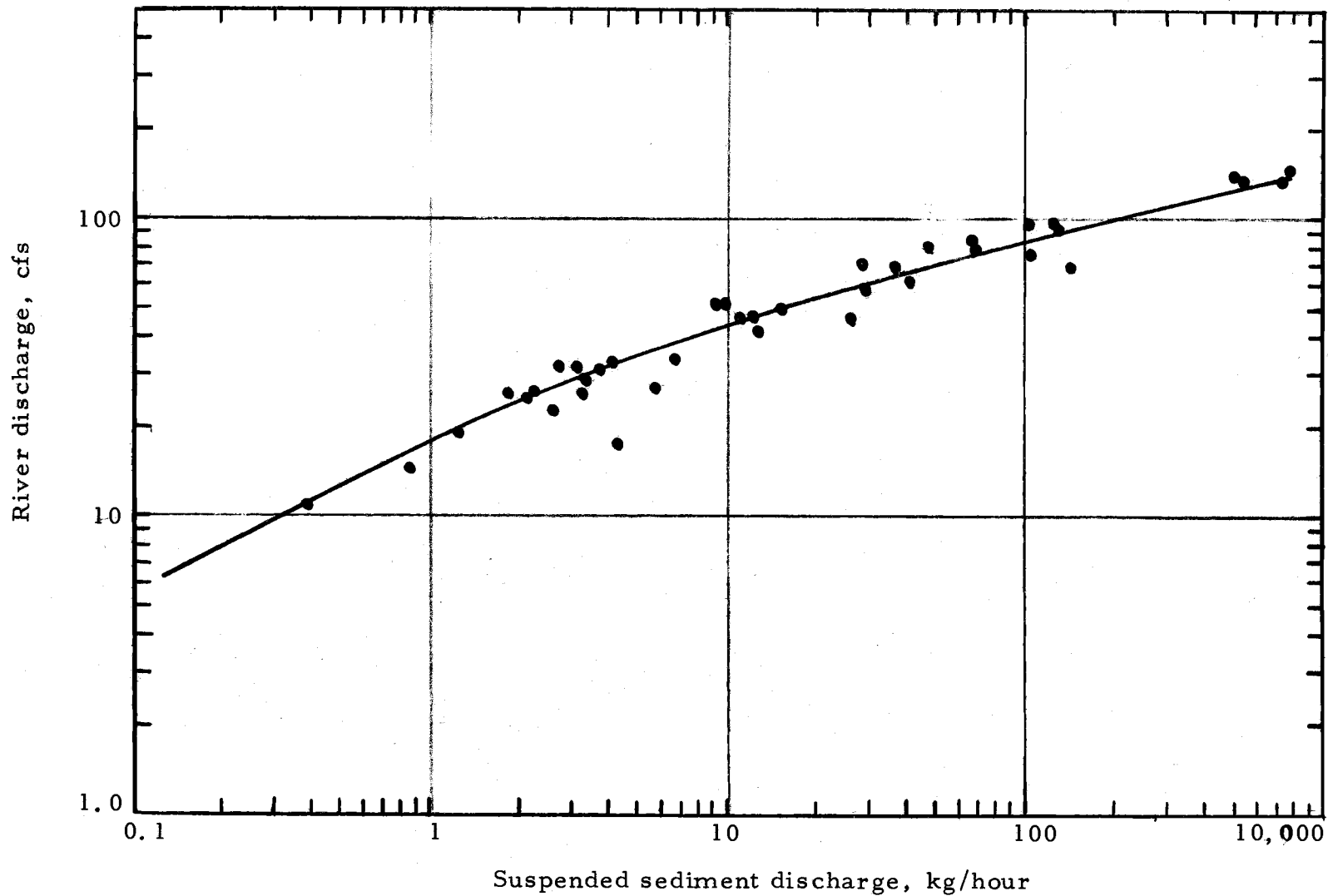


Figure 67. Suspended sediment load for the "empty reservoir" case.

reservoir in the armour layer was filled and the input of sediment to the stream channel was essentially equal to the output. The suspended load data are given in Figure 68. The data have been subdivided into seven sets, as designated in Figure 68. Each set presents the suspended sediment measurements made up to the peak of a direct runoff from a stream. The samples on the recession limb and up to the next storm event with a peak greater than (or about the same as) the previous event constitute the next set. The end of the sampling program was actually the end of set 6 but suspended load samples were taken at random during the remainder of 1971. These make up set 7.

The curve representing the expected value of suspended sediment load as a function of discharge from Figure 67 has been plotted on Figure 68. The data suggests that the suspended load is quite variable with time and is strongly influenced by the events preceding the time of sampling. The information on Figure 68 suggests the discharge versus suspended sediment load relationship moves in the direction of the empty reservoir case as the sand and silt is removed from the armour layer during the fall. There are other sources of sediment in the watershed which will be transported as the watershed wettens in the fall. Nevertheless, the "full reservoir" can be important.

The effect of a full reservoir on the bed load is illustrated by the data taken between the peaks of two of the major storms and shown in Figure 69. Two lines are drawn through the lower discharge data--

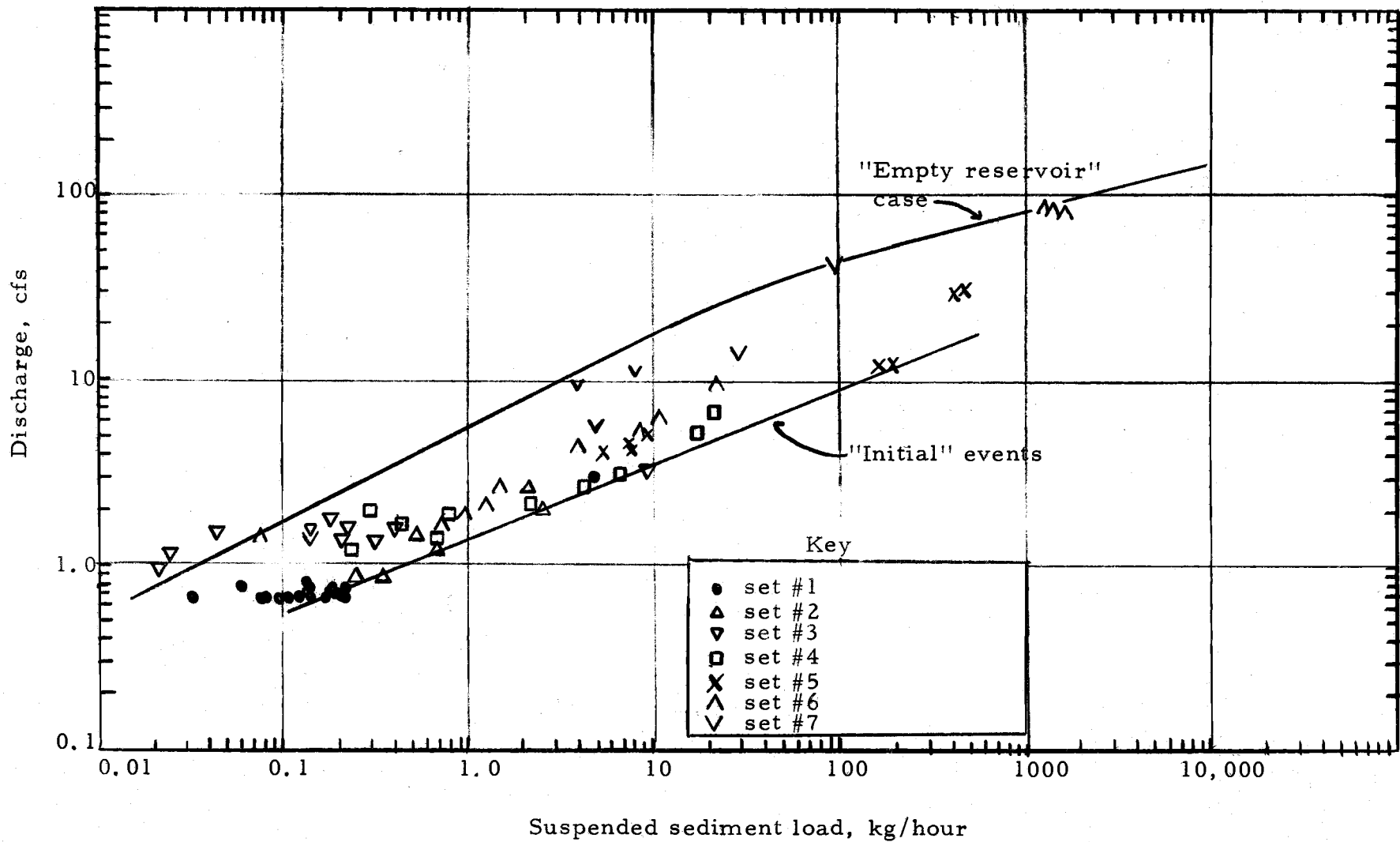


Figure 68. Suspended sediment load in fall of 1971.

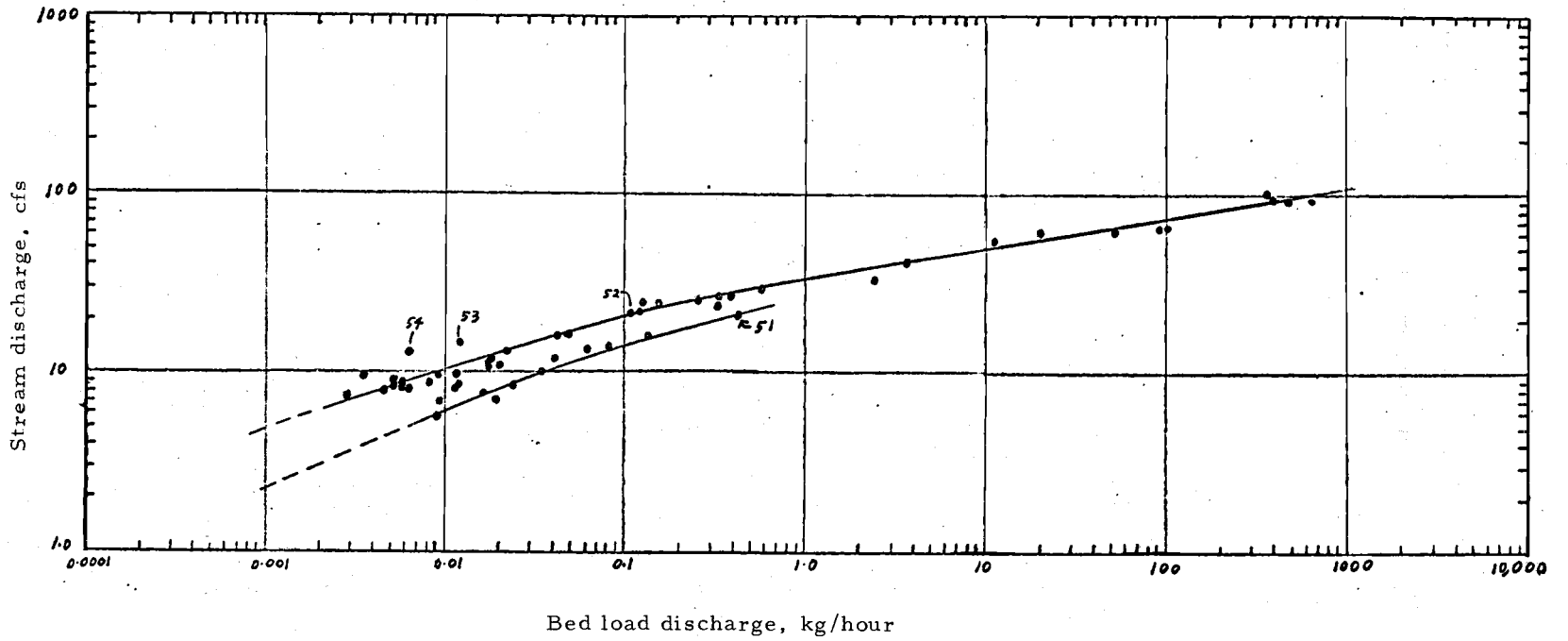


Figure 69. Bed load discharge versus stream discharge, winter 1971 (prior to 10 March).



one through an upper set and the other through a lower set. Examination of the stream hydrograph indicates that the upper set is for the case where the silt reservoir is only partly full while the lower set is for the case where the reservoir is likely to be full. Sample numbers have been shown for samples 51, 52, 53 and 54. Sample 51 probably included fine material removed from storage in the armour layer reservoir while sample 52 probably does not have material from the silt reservoir. Consequently, there is a wide range in bed load for nearly the same stream flow. As the stream discharge declined, the silt reservoir absorbed more sand than is typical for a given flow because of the cleansing effect of the flow associated with sample 51. Because of this, the bed load transport was much lower for samples 53 and 54 than for the other samples in the 12 to 15 cfs region.

The bed load data obtained in fall 1971 are presented in Figure 70. These data have been divided into six sets on the same basis as was the suspended sediment data (there are no bed load data corresponding to set 7). Also shown is the relationship between river discharge and bed load discharge from Figure 69.

Data sets 4, 5, and 6 shown in Figure 70 were obtained after the leaf drop mentioned previously. Consequently, both the bed load and the suspended sediment load would be higher for these sets than for similar stream flows in the winter and spring because more of the armouring particles were moved. The samples of set 6 in the

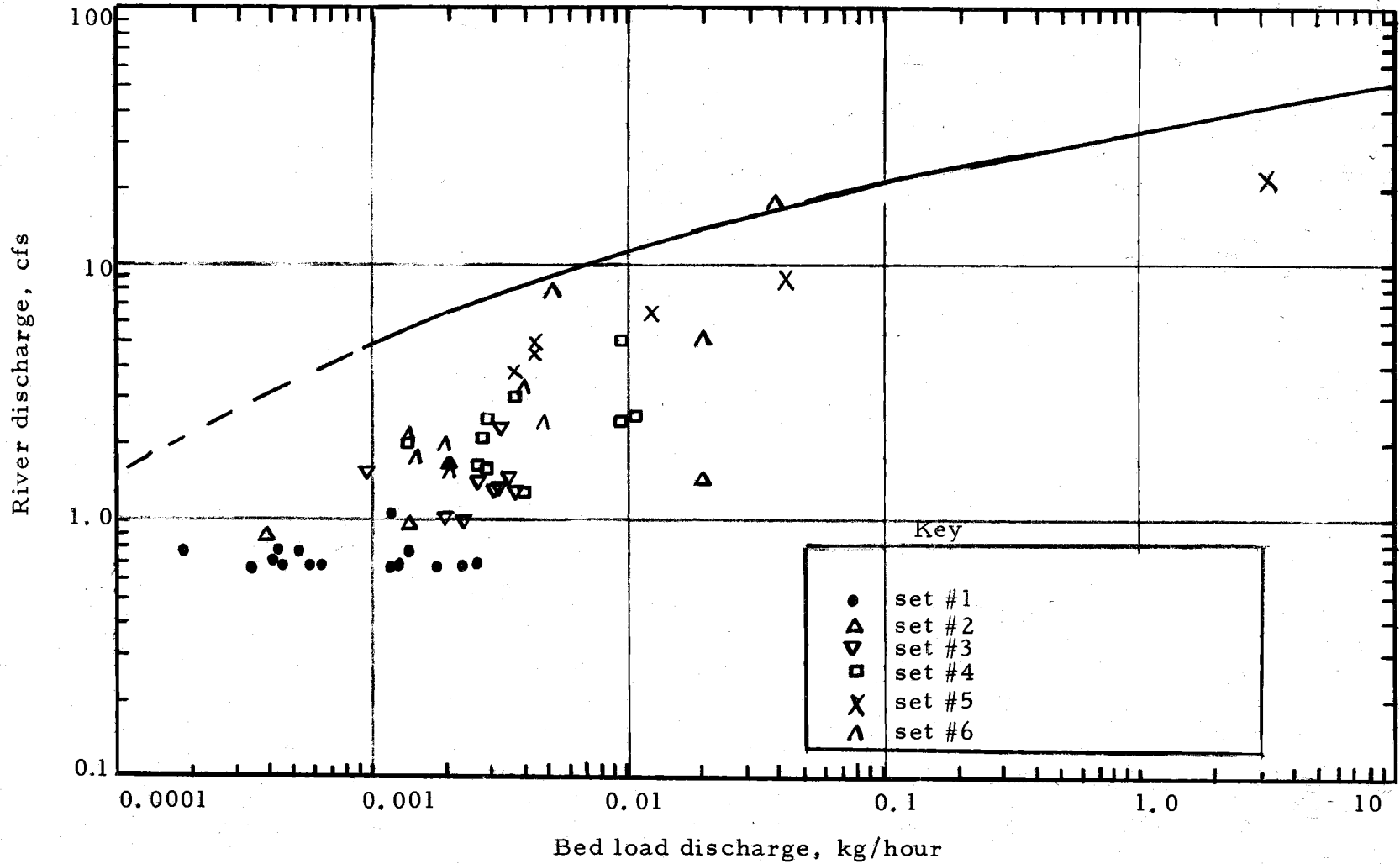


Figure 70. Bed load discharge versus stream discharge, fall 1971.

80 cfs region were obtained during the first autumn storm with a discharge above the critical discharge for the armour layer.

The interaction of suspended load and bed load can be further investigated by studying two groups of samples from fall, 1971.

One of these groups consist of samples collected before, during and after the first runoff event (the event dividing set 1 from set 2) in the fall. The hydrograph of this event is given in Figure 71. The times of the suspended sediment concentration measurements and the intervals over which bed load samples were obtained are also shown on Figure 71. Data on the suspended load measurements are given in Table 17 and data on the bed load measurements are shown in Table 18. Estimates of the mean suspended sediment load and dissolved solids load corresponding to the bed load sampling are also given on Table 18. The peak discharge was 3 cfs, which has a 1% chance of locally exceeding the critical discharge for the armour. Consequently, we would not expect a large degree of stored fines to be removed from the silt reservoir. The data indicate that the bed load and suspended load were in the same order of magnitude before and after the event. The data for suspended load sample C-20 and for bed load sample 82 indicate that there was an ample supply of fines available. The data in Table 18 also indicate that the bed and suspended sediment loads were minor in comparison to the dissolved solids load.

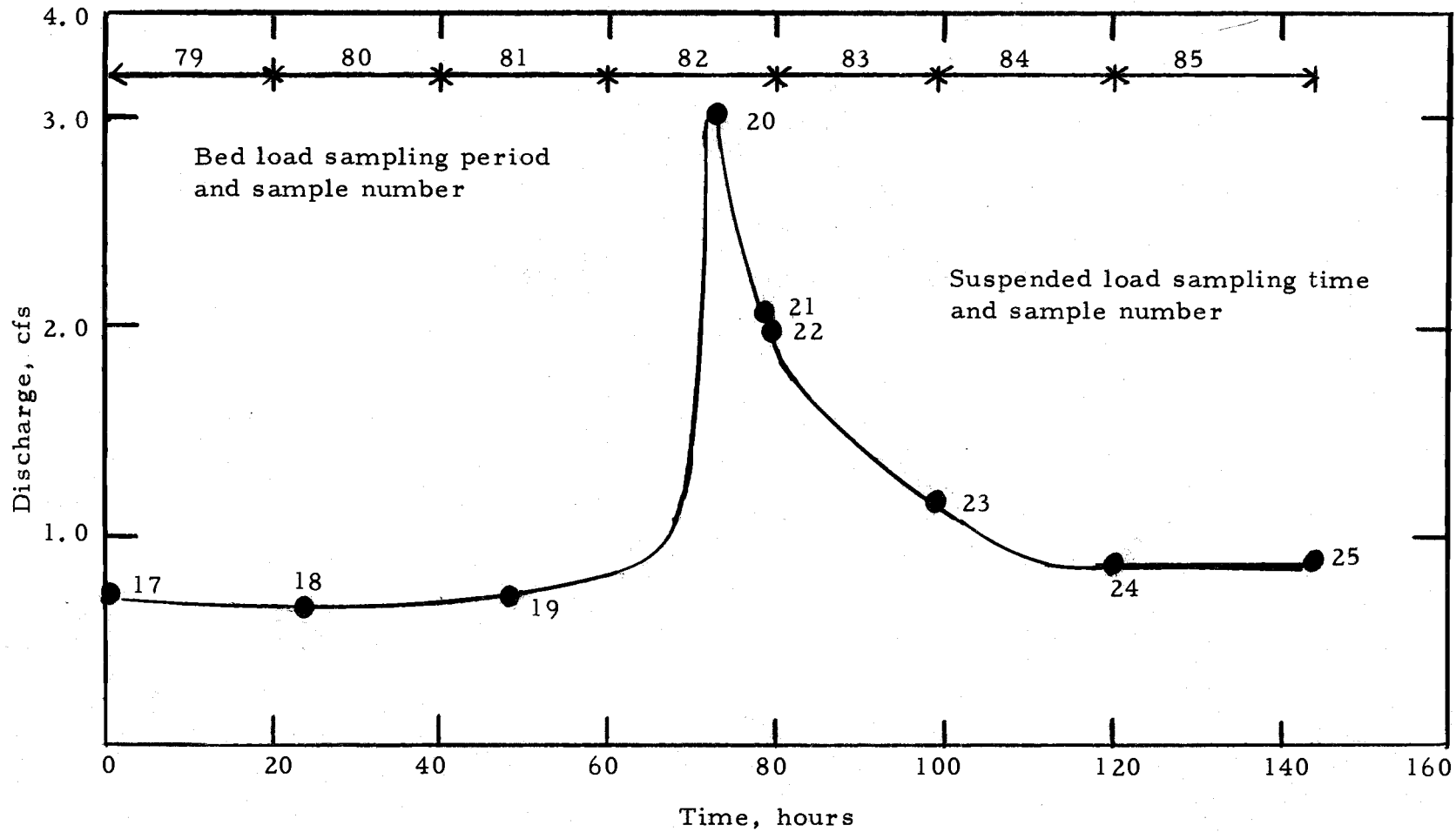


Figure 71. Hydrograph for October 16-22, 1971, showing bed load and suspended load sampling schedule.

Table 17. Suspended load data for the October 16-22 1971 period.

Suspended Sediment Sample Number	Discharge, cfs	Suspended Sediment Concentration, mg/liter
C-17	0.76	2.227
C-18	0.82	2.649
C-19	0.76	2.750
C-20	3.00	15.165
C-21	2.10	12.624
C-22	2.00	12.136
C-23	1.20	5.579
C-24	0.89	3.761
C-25	0.89	2.667

Table 18. Bed load data for the October 16-22 1971 period.

Bed Load Sample Number	Discharge, cfs	Bed Load Discharge, kg/hour	Suspended Load Discharge, kg/hour	Dissolved Load, kg/hour	Total Solid Load, kg/hour	Bed Load Suspended Load	Mean Size of Bed Load, cm
79	0.79	0.00043	0.19	16.5	16.7	0.002	0.038
80	0.79	0.00018	0.21	16.5	16.7	0.0009	0.050
81	1.05	0.00120	0.54	20.4	20.9	0.002	0.049
82	1.41	0.01920	1.22	25.2	26.4	0.016	0.18
83	0.98	0.00140	0.44	19.2	19.6	0.003	0.12
84	0.89	0.00039	0.29	18.0	18.3	0.001	0.085

Data for another group of samples were given on Figure 50 and in Tables 13 and 14. These data are for a runoff event on November 13-14 with a peak discharge of 32 cfs. This was the first storm runoff event in fall 1971 which had sufficient discharge to dislodge the fines in the armour layer. This event separated set 0 from set 0 in Figure 70. The peak discharge had about a 15% chance of locally exceeding the critical shear stress, but more armour particles moved because of leaf drag.

Between the two events given above there were three events with peak discharges in the 3 to 6.6 cfs range.

The fact that the particles within the armour layer were disturbed during the runoff event accounts for some of the relatively high transport during the event and for the relatively high transport of both suspended load and bed load following the runoff events.

The suspended sediment data indicate a wide range in the suspended load when the discharge is below 2 cfs. The data for sets 1 through 4 tend to be near the "initial" events line, given that the discharge is greater than 2 cfs; but the 6.6 cfs event separating sets 4 and 5 changed the relationship somewhat and the following events tended to have lower suspended sediment discharges for a given stream discharge. The path of the suspended sediment concentration versus discharge relationship for the two events is shown on Figure 72. Data for samples C-43 through C-59 are shown on Figure 73. The diagram

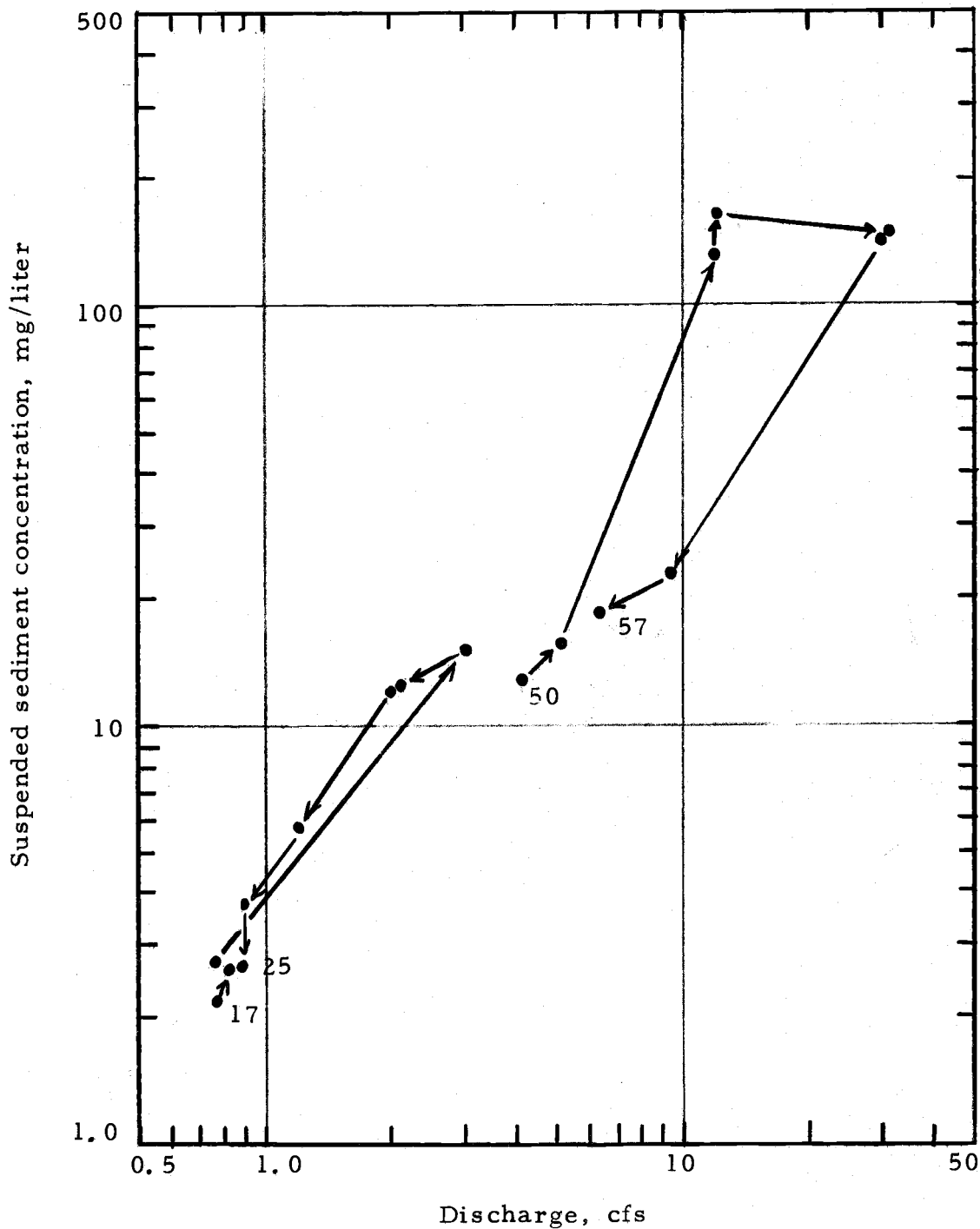


Figure 72. Path of the suspended load versus discharge relationship during two runoff events, fall 1971.

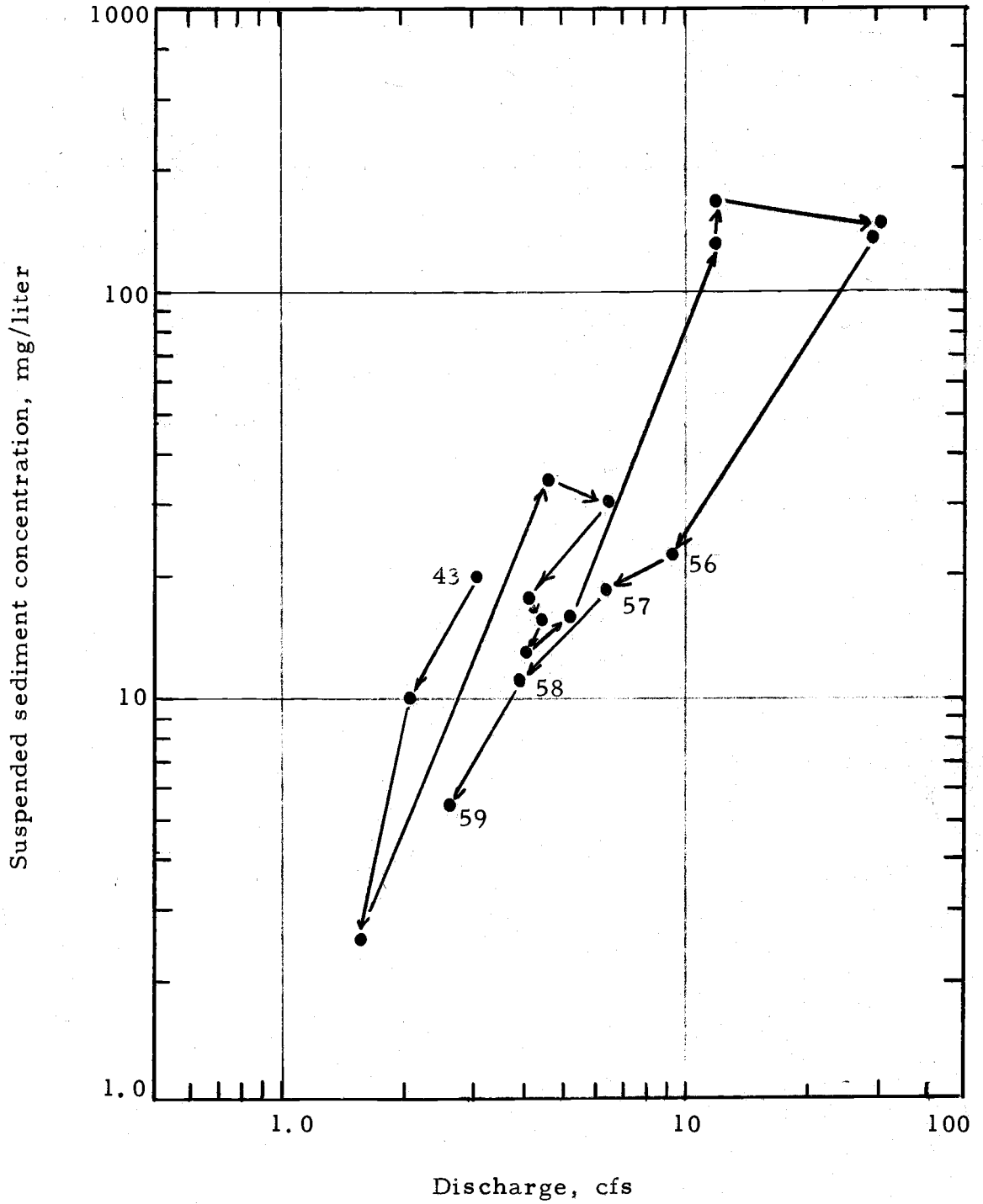


Figure 73. Suspended sediment versus discharge, November 7-16, 1971.



illustrates the decrease in the sediment load for a given discharge as the peak discharge for a sequence of storm events increases.

At the start of the fall sampling period, the sampler control gate was kept closed during the sampling period. Consequently, the bed load material would fall into the sampler trough and not be carried into the sampling pit. The trough was swept clean each morning, with the bed load material being swept into the sampling pit. During the initial sampling periods, it was observed that a cloud of fines was stirred up by the sweeping. This occurred each day until after the runoff event given in Figure 71. Thereafter, the cloud was not observed. This indicates that the first storm moved the fine material out of the stream system.

During mid-October, white sand was placed in the stream just downstream of the deep pool downstream of the sediment weir/trap. The sand was placed in a high-velocity area and immediately began moving downstream. The sand mounded over all of the bed material and did not disperse rapidly. The moving sand wave moved downstream until the particles fell into a protected area around the armour particles protruding above the general level of the bed. By the next morning, the sand was dispersed over an area extending about 15 to 20 feet downstream of the point of placement and was about a foot wide. The sand surrounded the protruding armour particles and appeared to be stable. The sand seemed to remain where initially deposited the

first day after placement until the November 13-14 runoff event given in Figure 50. After the recession of this storm flow, it was observed that the sand had been removed except for a little sand downstream of a particle that well-protected the area.

The relative sand concentrations in the suspended load samples taken during the October runoff event shown on Figure 50 are given on Table 14. These were determined by visual observation. The amount of sand in the samples and the general visual turbidity for C-52 through C-55, taken at flows of 12 and 30 cfs, was very similar to conditions for samples obtained in January 1971 for discharges in excess of 100 cfs. The high concentrations are partially related to excessive movement of armouring particles caused by the large amount of leaves in the stream. But part of the reason for the high concentrations is related to a higher-than-usual availability of sand in the armour layer.

The observations above support the idea that armour-layered systems "store" smaller sediment (fines and sand) which is then released as to the stream flow as the discharge increases. Some of the increase could be due to an increase in effective tributary area as the autumn rains wet the watershed. But this increase does not explain the change in the suspended load versus discharge relationship shown on Figure 73.

In general, the available data are in agreement with the concepts given in the beginning of this section. The basic idea is that the

presence of an armoured stream bed has an impact on the suspended sediment by being a source of sediment under certain conditions and a sediment sink under other conditions.

## VI. SUMMARY AND CONCLUSIONS

The primary objective of the research was to develop a better understanding of the sediment transport system for a stream with an armour layer. This objective has been accomplished -- at least in a qualitative way.

The main conclusion of the research is that the armour layer acts as a "valve" and a "reservoir" in the sediment transport system of a gravel-bottomed stream. The armour layer removes material from the system at small flows which is again released at larger flows. The armour layer also prevents bed material beneath it from getting entrained in the flow on a rising hydrograph, but does supply fines to the flow from the reservoir. On the falling limb of a hydrograph, when the armour is again stable, sand can be entrained in the flow.

The armour layer is the most important single factor in limiting the availability of stream bed sediment and in controlling the relationship between stream flow and bed load discharge. The armour layer controls bed load transport at flows large enough to move the armour layer and can cause a considerable shift in the bed load versus stream-power relationship. For instance, the data indicate the following relationships were valid at different times:

$$(1) Q'_{BL} = 3.3 \times 10^{-6} p^{5.3} \quad (55a)$$

$$(2) Q'_{BL} = 6.7 \times 10^{-6} p^{5.3} \quad (55b)$$

where  $Q'_{BL}$  = the immersed bed load discharge in kilograms per hour and  $P$  is the stream power per linear foot of stream in kilograms per hour.

The critical shear stress can be determined using the  $D_{65}$  size of the armour layer and the equation:

$$\tau_c = 0.047 (\gamma_s - \gamma) D_{65} \quad (29)$$

The critical discharge can then be determined using the hydraulic properties of the stream.

As a result of the study on incipient motion for an armoured stream bed, the following conclusions are made:

1. The critical shear stress of an armour bed corresponds to that for the  $0.69 D_{65}$  size of the armour layer. This size is approximately the  $D_{30}$  size of the armour layer,
2. The armour layer "breaks up" when the probability of particles remaining in bed is in the order of 80% (20% probability of particle being moved).
3. The movement of armour layer particles is possible during much of the time in Oak Creek, even when the flows are small.
4. The bed load discharge is related to  $\tau_o/\tau_c$  (or  $\tau_c/\bar{\tau}$ ) as postulated by Kalinske and Einstein.
5. Following bed disturbance, the probability of a given particle size moving decreases with time because the bed becomes progressively more stable with time.

The "critical" discharge represents a division between those larger flows for which the bed load discharge can be estimated using an analytical function and those smaller flows for which an analytical function does not exist at this time.

The bed load is directly related to the stream discharge when the stream discharge is greater than the critical discharge for the armouring material. The rate of bed load transport is related to the critical discharge because both are related to the size of particles in the armour layer. The bed load discharge can be calculated using Einstein's simplified bed load functions if the representative size used is the  $D_{35}$  size of the armour layer for the stability function and the  $D_{50}$  size of the material below the armour for the transport function.

In calculating the bed material load for another stream, an estimate of the relationship between bed load and stream discharge can be developed using the hydraulic properties of the stream, the particle size gradation data for the bed and armour material, Einstein's functions, and the assumptions given above. The relationship is valid for a stability function having a value below 31. The concepts used to estimate the bed load will need additional verification using data from other streams.

The bed load for discharges below the critical discharge is related to the past history of flows and cannot be calculated using any of the existing analytical procedures or concepts. The concepts

developed in Chapter IV, that the armour layer acts as source and sink of both bed load and suspended load when the discharge is below the critical discharge, does help explain some of the variation in suspended load samples. The concepts indicate that in comparing suspended sediment data from different streams, low flow samples from similar points on the hydrograph should be used.

The observations made concerning the role of vegetation on the movement of both bed load and suspended load suggest that the initial peak in sediment concentrations observed for the first autumn runoff event, at least in the Pacific Northwest, may be due to debris in the stream channel as well as to sediment available in the armour layer and in the watershed.

Typically, office and laboratory studies of sediment transport in rivers and streams assume a steady two-dimensional process as a starting point. In a real stream transporting sediment, three-dimensional factors are very important. Also, the stream system is not in a steady state, so that changes over long periods influence that sediment transport which occurs over short periods of time in response to a given runoff event.

The research in this dissertation brings out the fact that a stream is a very dynamic system and varies considerably in both time and space. Consequently, an understanding of the natural sediment system requires the development of considerable basic concepts in the field based on analytical and laboratory studies.

## BIBLIOGRAPHY

- Barnes, Jr., Harry H., "Roughness Characteristics of Natural Channels," U.S. Geological Survey Water-Supply Paper 1849, 1967.
- Benedict, Barry H., and Bent A. Christensen, discussion of "Self-Stabilizing Tendencies of Alluvial Channels," Journal of the Waterways Harbors and Coastal Engineering Division, vol. 97 no. WW1, pg. 213-216, Feb 1971.
- Cary, Allen S., "Origin and Significance of Openwork Gravel," Transactions, American Society of Civil Engineers, Vol. 116, pg. 1296-1318, 1951.
- Chien, N., The Present Status of Research on Sediment Transport, Proc. Am. Soc. Civil Engineers, vol. 80, 1954.
- Colby, B. R., and C. H. Hembree, "Computations of Total Sediment Discharge Niobrara River Near Cody, Nebraska," Geological Survey Water-Supply Paper 1357, U.S. Government Printing Office, 1955.
- Einstein, Hans Albert, The Bed-Load Function for Sediment Transportation in Open Channel Flows, Technical Bulletin No. 1026 U.S.D.A., Washington D.C., Sept. 1950.
- \_\_\_\_\_ "River Sedimentation," in Handbook of Applied Hydrology, ed. by Ven te Chow, McGraw-Hill, New York, 1964.
- Einstein, H. A., "Deposition of Suspended Particles in a Gravel Bed," Journal of the Hydraulics Division, ASCE, Vol. 94, No. HY5, pg. 1197-1205, Sept. 1968.
- Fahnestock, Robert K., "Morphology and Hydrology of a Glacial Stream-White River, Mount Rainier Washington," U.S. Geological Survey Professional Paper 422-A, 1963.
- Gessler, Johannes, "Self-Stabilizing Tendencies of Alluvial Channels," Journal of the Waterways and Harbors Division, vol. 96, No. WW2, May 1970.
- \_\_\_\_\_ closure to "Self-Stabilizing Tendencies of Alluvial Channels," Journal of the Waterways Harbors and Coastal Engineering Division, Vol. 97, No. WW4, p. 757-8, Nov. 1971.



- Graf, Walter H., Hydraulics of Sediment Transport, McGraw-Hill Book Co., New York, 1971.
- Helland-Hansen, Erik, Time as a Parameter in the Study of Incipient Motion of Gravel, paper presented at the Annual Meeting of the Northwest Regional Section, American Geophysical Union, Corvallis, Oregon, 1971.
- Helland-Hansen, Erik Andreas, Stability of Gravel at Artificially Created Spawning Beds in Uncontrolled Streams, M.S. Thesis, Oregon State University, Corvallis, 1972.
- King, Kuchlaine A. M., Techniques in Geomorphology, Edward Arnold publishers Ltd., London, 1967.
- Klingeman, Peter C. and R. T. Milhous, Evaluation of Bed Load and Total Load Yield Processes on Small Mountain Streams, Engineering Experiment Station, Oregon State University, Corvallis, Oregon, August 1970.
- Leopold, L. B., M. G. Wolman, and J. P. Miller, Fluvial Processes in Geomorphology, W. H. Freeman and Co., San Francisco 1964.
- McNeil, William J., and Warren H. Ahnell, "Success of Pink Salmon-Spawning Relative to Size of Spawning Bed Materials," United States Fish and Wildlife Service Special Scientific Report-- Fisheries No. 469, Washington D. C., Jan. 1964.
- Matthes, Gerard H., "Macroturbulence in Natural Stream Flow," Transactions, American Geophysical Union, Vol. 28, No. 2, pg. 255-264, April 1947.
- Meyer-Peter, E., and Müller, R., "Formulas for Bed-Load Transport International Association for Hydraulic Structures Research," Second meeting Sept. 7-9 VI, 1948, Stockholm, 1948.
- Miner, Norman H., "Natural Filtering of Suspended by a Stream at Low Flow," U.S. Forest Service Research Note PNW-88, Sept. 1968.
- Neill, C. R., A Re-examination of the Beginning of Movement for Coarse Granular Bed Materials, Hydraulics Research Station, Int 68, Wallingford, June 1968.

- Paintal, A. S., The Probabilistic Characteristics of Bed Load Transport in Alluvial Channels, Ph. D. Thesis, University of Minnesota, 1969.
- Porch, Michael, Abraham Sagive, and Ido Seginer, "Sediment Sampling Efficiency of Slots," Journal of the Hydraulics Division, ASCE, Vol. 96, No. HY10, pg. 2065-2078, October 1970.
- Robinson, A. R., "Vortex Tube Sand Trap," Transactions of the American Society of Civil Engineers, Vol. 127, Part III, paper no. 3371, pg. 391-423, 1962.
- Snavely, J. R., Parke, D., Norman S. Macleod, and Holly C. Wagner, "Tholeiitic and Alkalic Basalts of the Eocene Siletz River Volcanics, Oregon Coast Range," American Journal of Science, vol. 266, pg. 454-481, June 1968.
- Shields, A., "Anwendung der Aehnlichkeits-mekhanik und der Turbulenzforschung auf die Geschiebebevegund," Mitteilungen der Preussischen Versuchsanstalt fur Wasserbau und Schiffbau, Berlin, Germany, 1936, Translated to English by W. P. Ott and J. C. Vanllchelen, Calif. Inst. of Tech., Pasadena, California,
- U.S. Waterways Experiment Station, War Department, Corps of Engineers U.S. Army, Studies of River Bed Materials and their Movement, with Special Reference to the Lower Mississippi River, paper 17, Vicksburg, Mississippi, 1935.
- Vaux, Walter G., "Intragravel Flow and Interchange of Water in a Streambed," Vol. 66, pg. 479-489, 1968.
- Yalin, M.S., An Expression for Bed-Load Transportation, Proc. Am. Sec. Civil Engrs., vol. 89, no. HY3, May 1963.

## APPENDICES

## APPENDIX I

## BED LOAD DATA

The bed load data are given in this appendix. There are three data sets. These are:

1. Data obtained in the winter of 1969-70
2. Data obtained in the winter of 1971
3. Data obtained in the fall of 1971.

The reader is referred to the main body of the dissertation for information on the purpose for which each data set was obtained and for information on the limitations in the data.

The 1969-70 measurements were the first group of measurements made using the vortex sampler and were not made using a consistent procedure. As a result of operating the sampler during 1969-70 and as a result of the data analysis, a procedure was developed which was followed, with some variation, during the subsequent sampling periods.

In Table I-1 are the data for the winter of 1969-70. The discharge is the average discharge during the sampling interval, the slope is the energy slope in the reach just upstream of the sampler, and the hydraulic radius is a composite hydraulic radius for the study reach. The reach used to estimate the slope and hydraulic radius is 153 feet long. The composite hydraulic radius was estimated using procedures given in Einstein (1950). The sorting coefficient is a

semi-graphical estimate of the sample variance. The equation used to calculate the sorting coefficient is:

$$\sigma = \frac{\log_2 (D_{84}) - \log_2 (D_{16})}{4} + \frac{\log_2 (D_{95}) - \log_2 (D_5)}{6.6}$$

where  $\sigma$  is the sorting coefficient and  $D_x$  is the particle size, in millimeters, at which x percent of the particles are finer (by weight).

The gradation of the bed load samples was obtained by dry sieving. These data are given in Table I-2 for the winter of 1969-70 samples.

Every once in a while during a low flow period a single particle much larger than any others would be found in a bed load sample. There is some chance that a stone could have been tossed into the trough or pit by a passerby, but the most probable explanation is that the particle was moved by turbulence with a low probability of moving the stone. The fact that the particle was found in a sample is representative of the flow strength but not of the time period associated with the sample. Hence, the bed load rate and mean size calculated from the sample and its associated sampling time would not be representative of the conditions associated with the discharge. Consequently, these single large particles were not used in calculating the bed load rate or the median size of the sample.

The data on bed load collected during the winter of 1971 were obtained during January through March 1971. The bed load data are

given in Table I-3 and the sample gradation data in Table I-4. With the exception of one of the 66 samples, the data are the best data available. This poor sample is sample 55, which was collected during an interval having a very large range in discharge and therefore should not be used in most analyses of bed load.

A problem with some of the samples is that they are "start-up" samples. In other words, the vortex trough had been previously filled and sampling was only started after first removing this material from the trough. This change at the trough increased the fluid shear exerted on the stream bed just upstream of the sampler, with the result that the bed load may not be representative of the discharge. Start-up samples are samples 1, 10, 15, 17, 23, 59, and 60. These seven samples probably have measured bed load rates somewhat in excess of the rate representative of the hydraulic conditions at the time.

The measured bed load data for the fall of 1971 are given in Table I-5. The gradation data are given in Table I-6. The fall 1971 data were obtained in October and November 1971.

Many of the samples are very small and the sampler was not designed to sample very small samples. Consequently, there is an error in some of the measured samples for which only the sample caught in the box is included. During most of the sampling program, the sample obtained in the box was combined with the material

deposited in the pit around the box. Because of the small size of the fall 1971 samples, this was not done, although an overall estimate of efficiency was made. This was then used to better estimate the bed load transport rates. The efficiency factor and improved estimates of bed load for the fall 1971 samples are given in Table I-7.

Table I-1. Bed load data for samples obtained during the winter of 1969-70.

Sample Number	Discharge, cfs	Bed Load Discharges, kg/hour	Energy Slope, Ft/100 ft	Hydraulic Radius, ft	Water Temperature, °F	D50 cm	Sorting Coefficient	Sampling Period, hours	Weight of Largest particle in sample gm
1	27	1.67	1.23	0.70	--	0.16	1.66	25.0	--
2	12	0.016	1.22	0.52	--	0.084	1.28	19.8	--
3	8.7	0.0067	1.20	0.47	--	0.055	1.54	23.0	--
4	8.6	0.0010	1.20	0.47	--	0.018	1.06	22.8	--
5	8.5	0.0010	1.20	0.47	--	0.05	1.13	23.8	--
6	8.1	0.00062	1.20	0.46	--	0.07	1.96	25.8	--
7	30	1.58	1.26	0.73	--	0.18	1.67	21.2	--
8	21	0.096	1.24	0.63	--	0.12	1.34	21.2	386
9	19	0.022	1.24	0.61	--	0.052	1.72	6.2	--
10	49	11.8	1.25	0.90	--	0.20	2.03	4.8	--
11	71	200	1.26	1.08	--	2.2	1.75	2.8	695
12	15	0.43	1.21	0.56	42	1.7	2.39	2.2	240
13	23	0.56	1.23	0.66	42	0.096	1.85	2.1	--
14	34	3.18	1.24	0.77	42	0.28	2.91	1.7	563
15	33	1.77	1.23	0.76	42	0.65	2.60	5.5	--
16	20	0.46	1.22	0.62	--	0.24	2.96	13.2	--
17	22	1.87	1.22	0.64	--	1.8	2.20	64.9	--
18	54	45.5	1.25	0.95	--	2.0	1.86	3.2	690
19	50	37.6	1.25	0.91	--	1.6	1.90	2.8	626
20	39	2.58	1.24	0.81	--	0.72	2.12	3.6	346
21	28	0.76	1.26	0.71	--	0.20	1.84	11.9	--
22	27	0.63	1.22	0.69	--	0.20	2.06	28.3	--
23	44	35.0	1.24	0.86	--	0.72	2.07	1.5	286
24	46	212.	1.02	0.88	--	1.25	2.13	1.0	1340
25	45	78.5	1.01	0.87	--	1.04	1.97	1.3	--
26	45	6.4	1.01	0.77	--	0.52	1.99	5.5	--



Table I-2. Gradation data for bed load samples obtained in the winter of 1969-70.

Sample Number	Particle size, cm, and accumulation distribution, fraction courses by weight											
	76.2	50.8	38.1	19.05	9.52	4.76	2.38	1.19	0.595	0.297	0.149	<0.149
1	0	0.006	0.008	0.045	0.098	0.179	0.319	0.614	0.857	0.946	0.982	1.000
2				0	0.004	0.008	0.086	0.325	0.638	0.866	0.955	1.000
3					0	0.026	0.065	0.222	0.461	0.738	0.873	1.000
4							0	0.030	0.105	0.233	0.633	1.000
5						0	0.024	0.126	0.367	0.754	0.936	1.000
5					0	0.135	0.215	0.369	0.534	0.788	0.918	1.000
7		0	0.003	0.049	0.116	0.210	0.375	0.674	0.891	0.962	0.984	1.000
8			0	0.018	0.036	0.074	0.185	0.513	0.805	0.931	0.977	1.000
9				0	0.054	0.070	0.116	0.238	0.454	0.762	0.919	1.000
10	0	0.006	0.028	0.117	0.194	0.285	0.419	0.677	0.887	0.965	0.966	1.000
11	0.001	0.074	0.195	0.555	0.739	0.818	0.870	0.930	0.976	0.992	0.996	1.000
12			*	0.451	0.595	0.691	0.743	0.798	0.878	0.939	0.976	1.000
13			0	0.034	0.060	0.093	0.176	0.432	0.682	0.832	0.923	1.000
14	0	0.121	0.141	0.252	0.358	0.428	0.520	0.660	0.810	0.897	0.951	1.000
15	0	0.025	0.081	0.301	0.468	0.509	0.563	0.707	0.845	0.914	0.963	1.000
16		0	0.097	0.272	0.358	0.414	0.500	0.666	0.820	0.919	0.927	1.000
17	0.016	0.055	0.130	0.434	0.653	0.739	0.787	0.859	0.931	0.962	0.978	1.000
18	0	0.080	0.194	0.512	0.697	0.792	0.860	0.933	0.978	0.992	0.996	1.000
19	0	0.046	0.136	0.442	0.646	0.762	0.837	0.922	0.976	0.993	0.997	1.000
20	0	0.065	0.101	0.230	0.421	0.584	0.699	0.850	0.947	0.981	0.992	1.000
21			0	0.076	0.156	0.273	0.417	0.688	0.888	0.960	0.985	1.000
22		0	0.018	0.129	0.236	0.331	0.461	0.724	0.905	0.966	0.986	1.000
23	0	0.022	0.056	0.239	0.432	0.535	0.641	0.821	0.944	0.982	0.992	1.000
24	0	0.023	0.072	0.333	0.560	0.672	0.748	0.849	0.931	0.965	0.983	1.000
25	0	0.007	0.036	0.279	0.516	0.647	0.740	0.867	0.964	0.991	0.996	1.000
26		0	0.006	0.010	0.285	0.532	0.652	0.773	0.871	0.921	0.955	1.000

\* Largest particle not included in sample, particle is in size range shown.

Table I-3. Bed load data for samples obtained during the winter of 1971.

Sample Number	Discharge, cfs	Bed Load Discharges, kg/hour	Energy Slope, ft/100 ft	Hydraulic Radius, ft	Water Temperature, °F	D50 cm	Sorting Coefficient	Sampling Period, hours	Weight of Largest particle in sample gm
1	5.4	0.0071	0.83	0.36	--	0.12	1.95	27.4	58.5
2	8.4	0.025	0.84	0.44	--	0.076	1.86	21.2	3.4
3	11.9	0.018	0.86	0.48	--	0.089	1.84	22.8	6.7
4	13.8	0.082	0.83	0.55	--	0.11	1.31	4.8	5.3
5	15.8	0.14	0.87	0.59	41	0.068	3.21	16.0	62.1
6	13.5	0.056	0.86	0.54	41	0.12	1.69	7.2	56.7
7	11.4	0.018	0.86	0.49	39	0.081	1.86	20.3	8.0
8	9.7	0.0092	0.85	0.44	38	0.11	2.36	21.7	21.6
9	8.0	0.0043	0.84	0.42	38	0.070	1.77	29.8	62.5
10	92.	641.	0.97	1.31	41	2.5	1.36	0.51	944.
11	92.	484.	0.97	1.31	41	1.7	1.54	0.54	1259.
12	93.	392.	0.97	1.31	41	1.9	1.74	0.38	1732.
13	100.	385.	0.98	1.37	41	2.6	1.71	0.92	1455.
14	120.	1362.	0.99	1.46	41	2.4	1.25	0.47	1185.
15	67.	101.	1.00	1.12	44	1.3	1.84	1.45	944.
16	64.	91.	1.00	1.08	44	0.82	1.77	0.97	424.
17	32.	2.41	0.98	0.80	43	0.33	1.92	6.8	107.
18	26.	0.39	0.97	0.74	41	0.19	1.7	12.7	66.
19	27.	0.33	0.97	0.75	43	0.21	1.89	6.9	53.
20	24.	0.13	0.97	0.72	43	0.18	1.77	21.0	45.
21	25.	0.25	0.97	0.73	44	0.19	1.90	19.7	127.
22	24.	0.16	0.97	0.72	44	0.20	1.71	29.0	75.
23	62.	53.	1.00	1.07	44	0.55	2.04	1.21	434.
24	60.	21.	1.00	1.05	45	0.38	1.96	1.00	223.
25	54.	12.	1.00	1.03	45	0.27	1.98	2.92	324.
26	41.	3.7	0.99	0.90	45	0.20	1.82	12.5	630.
27	29.	0.59	0.98	0.77	45	0.13	1.45	8.6	643.
28	22.	0.13	0.97	0.70	45	0.13	1.31	20.4	24.3
29	16.	0.048	0.96	0.61	44	0.11	1.25	27.6	7.5
30	13.	0.022	0.96	0.59	43	0.093	1.31	22.7	2.1

Table I-3. Bed load data for samples obtained during the winter of 1971 (Continued)

Sample Number	Discharge, cfs	Bed Load Discharges, kg/hour	Energy Slope, ft/100 ft	Hydraulic Radius, ft	Water Temperature, °F	D50 cm	Sorting Coefficient	Sampling Period, hours	Weight of Largest particle of sample gm
31	11.7	0.042	0.96	0.56	42	0.078	1.19	20.6	1.9
32	10.0	0.035	0.95	0.53	42	0.10	1.46	26.6	12.2
33	8.2	0.010	0.95	0.50	42	0.095	1.43	50.6	62.8
34	8.5	0.0070	0.95	0.50	41	0.079	1.44	38.6	0.8
35	23.	0.34	0.97	0.71	42	0.084	1.37	5.6	5.2
36	16.	0.044	0.96	0.61	42	0.095	1.32	21.3	4.1
37	11.	0.014	0.96	0.54	42	0.14	2.10	22.1	143.
38	8.9	0.0043	0.95	0.51	43	0.12	1.71	55.5	49.2
39	7.8	0.0046	0.94	0.49	44	0.11	1.73	29.9	8.7
40	8.9	0.0056	0.95	0.51	45	0.12	2.17	86.4	36.7
41	6.8	0.0093	0.94	0.46	45	0.14	1.44	50.8	4.6
42	7.0	0.020	0.94	0.47	46	0.19	1.73	21.5	6.7
43	7.7	0.0016	0.94	0.48	44	0.12	1.98	71.5	120.
44	8.3	0.0053	0.94	0.49	44	0.092	1.89	49.5	8.1
45	7.2	0.0026	0.94	0.47	45	0.12	1.49	51.0	3.1
46	8.4	0.0058	0.94	0.50	42	0.26	2.26	64.2	27.
47	10.6	0.018	0.96	0.53	40	0.16	1.64	27.5	11.6
48	9.5	0.012	0.95	0.52	39	0.19	1.81	24.5	61.7

Table I-3. Bed load data for samples obtained during the winter of 1971 (Continued)

Sample Number	Discharge, cfs	Bed Load Discharges, kg/hour	Energy Slope, ft/100 ft	Hydraulic Radius, ft	Water Temperature, °F	D <sub>50</sub> cm	Sorting Coefficient	Sampling Period, hours	Weight of Largest particle of sample gm
49	8.2	0.012	0.94	0.50	40	0.23	2.06	25.0	29.3
50	9.3	0.0036	0.95	0.51	40	0.10	1.65	43.5	1.5
51	20.0	0.43	0.97	0.67	40	0.062	2.13	7.5	56.
52	21.2	0.11	0.97	0.69	40	0.096	1.39	19.2	6.8
53	14.8	0.012	0.96	0.60	41	0.087	1.87	26.3	6.2
54	12.8	0.0062	0.96	0.57	41	0.085	1.90	24.2	7.3
55	19.0	0.86	0.97	0.83	41	0.18	2.52	94.0	1789.
56	62.	43.	1.00	1.17	42	0.26	2.63	1.0	1033.
57	72.	90.	1.01	1.21	42	0.70	2.50	1.0	1307.
58	92.	480.	1.02	1.27	42	2.7	1.92	2.2	2393.
59	78.	1460.	1.08	1.22	42	1.9	1.57	0.41	1046.
60	54.	130.	1.05	1.12	42	0.95	1.79	1.17	715.
61	47.	63.	1.04	1.07	42	1.1	1.86	2.0	497.
62	36.	19.	1.02	1.01	42	0.58	1.83	5.9	310.
63	38.	18.	1.02	1.00	42	0.53	1.89	2.8	462.
64	51.	78.	1.00	1.10	42	1.0	1.90	2.42	601.
65	62.	260.	1.00	1.17	42	1.2	1.88	1.17	1222.
66	74.	523.	1.00	1.22	42	2.3	1.71	0.75	1447.

Table I-4. Gradation data for bed load samples obtained in the winter of 1971.

Sample Number	Particle size, cm, and accumulative distribution, fraction courses by weight															
	101.6	76.2	50.8	38.1	25.4	19.05	9.52	4.76	2.38	1.19	0.595	0.297	0.149	0.074	0.074	
1						0	0.134	0.223	0.349	0.490	0.692	0.918	0.980	0.992	1.000	
2						0	0.016	0.115	0.237	0.373	0.569	0.807	0.937	0.981	1.000	
3						0	0.057	0.143	0.236	0.394	0.658	0.872	0.959	0.984	1.000	
4						0	0.072	0.188	0.306	0.470	0.707	0.877	0.958	0.986	1.000	
5				0	0.028	0.070	0.113	0.143	0.205	0.345	0.541	0.685	0.766	0.816	1.000	
6					*	0	0.065	0.165	0.307	0.507	0.768	0.924	0.975	0.990	1.000	
7						0	0.056	0.107	0.209	0.375	0.611	0.827	0.939	0.979	1.000	
8					0	0.108	0.170	0.216	0.337	0.485	0.686	0.873	0.951	0.978	1.000	
9					*	0	0.031	0.102	0.186	0.332	0.588	0.834	0.937	0.973	1.000	
10	0	0.017	0.137	0.260	0.486	0.660	0.843	0.910	0.942	0.970	0.988	0.995	0.998	0.999	1.000	
11	0	0.015	0.097	0.172	0.318	0.452	0.673	0.842	0.919	0.968	0.989	0.995	0.997	0.998	1.000	
12	0	0.012	0.112	0.215	0.374	0.505	0.691	0.818	0.987	0.956	0.987	0.996	0.998	0.999	1.000	
13	0	0.036	0.176	0.301	0.518	0.642	0.762	0.844	0.912	0.960	0.985	0.995	0.997	0.998	1.000	
14	0	0.092	0.1304	0.257	0.476	0.646	0.838	0.927	0.962	0.983	0.994	0.997	0.998	0.999	1.000	
15	0	0.006	0.037	0.088	0.232	0.370	0.582	0.724	0.826	0.912	0.961	0.979	0.987	0.993	1.000	
16		0	0.028	0.063	0.167	0.265	0.456	0.651	0.804	0.919	0.974	0.991	0.996	0.998	1.000	
17					0	0.059	0.127	0.247	0.403	0.587	0.795	0.932	0.980	0.994	1.000	
18					0	0.013	0.048	0.132	0.256	0.417	0.670	0.874	0.961	0.987	0.995	1.000
19					0	0.043	0.081	0.169	0.304	0.455	0.687	0.871	0.951	0.982	0.995	1.000
20					0	0.061	0.128	0.233	0.388	0.642	0.848	0.944	0.978	0.992	1.000	
21			0	0.025	0.043	0.075	0.146	0.256	0.415	0.669	0.869	0.949	0.977	0.988	1.000	
22					0	0.023	0.037	0.136	0.257	0.424	0.672	0.876	0.956	0.984	0.994	1.000
23	0	0.034	0.078	0.180	0.265	0.393	0.531	0.686	0.861	0.959	0.986	0.993	0.997	1.000	1.000	
24	0	0.018	0.041	0.127	0.191	0.298	0.444	0.628	0.835	0.952	0.985	0.993	0.997	1.000	1.000	
25	0	0.010	0.043	0.087	0.131	0.226	0.356	0.541	0.797	0.938	0.979	0.991	0.997	1.000	1.000	
26	0	0.035	0.042	0.060	0.082	0.141	0.240	0.433	0.731	0.921	0.974	0.988	0.993	1.000	1.000	
27					0.013	0.028	0.056	0.118	0.304	0.528	0.853	0.956	0.986	0.997	1.000	
28					0	0.018	0.034	0.078	0.204	0.536	0.820	0.936	0.978	0.992	1.000	
29					0	0.006	0.012	0.046	0.159	0.454	0.764	0.925	0.976	0.994	1.000	
30						0	0.007	0.036	0.124	0.380	0.685	0.886	0.966	0.987	1.000	
31						0	0.002	0.016	0.081	0.288	0.644	0.890	0.969	0.990	1.000	
32					0	0.013	0.031	0.082	0.191	0.429	0.720	0.911	0.969	0.989	1.000	
33					*	0	0.011	0.054	0.177	0.409	0.694	0.899	0.963	0.988	1.000	
34						0	0.025	0.140	0.352	0.604	0.840	0.947	0.992	1.000	1.000	
35						0	0.018	0.045	0.125	0.339	0.654	0.874	0.959	0.989	1.000	
36						0	0.017	0.049	0.141	0.391	0.697	0.901	0.966	0.990	1.000	
37				*	0	0.056	0.166	0.227	0.343	0.536	0.751	0.924	0.974	0.988	1.000	
38				*	0	0.054	0.163	0.288	0.502	0.745	0.926	0.973	0.987	1.000	1.000	
39						0	0.103	0.124	0.224	0.459	0.729	0.927	0.973	0.986	1.000	
40					0	0.108	0.145	0.213	0.323	0.497	0.726	0.907	0.964	0.986	1.000	
41						0	0.016	0.127	0.323	0.578	0.804	0.956	0.989	0.996	1.000	
42			*	0	0	0	0.105	0.266	0.432	0.654	0.842	0.956	0.984	0.994	1.000	
43			*	0	0	0	0.104	0.191	0.291	0.498	0.729	0.894	0.956	0.979	1.000	
44						0	0.078	0.146	0.231	0.409	0.663	0.863	0.947	0.979	1.000	
45						0	0.036	0.136	0.259	0.518	0.796	0.956	0.988	0.993	1.000	
46					0	0.134	0.193	0.353	0.514	0.691	0.835	0.929	0.965	0.985	1.000	
47						0	0.056	0.191	0.371	0.597	0.807	0.942	0.979	0.991	1.000	
48				*	0	0.102	0.224	0.345	0.454	0.602	0.777	0.918	0.968	0.988	1.000	
49					0	0.098	0.190	0.325	0.470	0.654	0.824	0.945	0.981	0.992	1.000	
50						0	0.016	0.076	0.216	0.445	0.679	0.855	0.938	0.983	1.000	
51				0	0.043	0.056	0.077	0.115	0.197	0.334	0.518	0.736	0.913	0.991	1.000	
52						0	0.026	0.072	0.154	0.397	0.754	0.921	0.977	0.994	1.000	
53						0	0.090	0.139	0.226	0.394	0.648	0.866	0.954	0.988	1.000	
54						0	0.075	0.132	0.215	0.395	0.636	0.842	0.933	0.975	1.000	
55	0	0.045	0.087	0.120	0.156	0.182	0.227	0.282	0.395	0.643	0.869	0.953	0.980	0.992	1.000	
56	0	0.044	0.140	0.165	0.210	0.245	0.302	0.393	0.527	0.737	0.897	0.960	0.983	0.995	1.000	
57	0	0.079	0.151	0.241	0.332	0.386	0.462	0.548	0.661	0.817	0.930	0.974	0.988	0.994	1.000	
58	0	0.193	0.305	0.504	0.605	0.726	0.815	0.887	0.946	0.978	0.990	0.994	0.996	1.000	1.000	
59	0	0.009	0.101	0.200	0.378	0.509	0.709	0.851	0.930	0.975	0.991	0.996	0.998	1.000	1.000	
60	0	0.005	0.040	0.104	0.225	0.323	0.500	0.671	0.819	0.928	0.980	0.994	0.998	1.000	1.000	
61	0	0.040	0.104	0.220	0.339	0.549	0.710	0.822	0.915	0.970	0.987	0.992	0.995	1.000	1.000	
62	0	0.016	0.040	0.099	0.173	0.351	0.551	0.725	0.879	0.962	0.985	0.992	0.996	1.000	1.000	
63	0	0.010	0.051	0.106	0.186	0.350	0.522	0.694	0.860	0.960	0.989	0.996	0.999	1.000	1.000	
64	0	0.040	0.096	0.211	0.325	0.517	0.676	0.798	0.907	0.970	0.988	0.992	0.995	1.000	1.000	
65	0	0.014	0.117	0.218	0.353	0.452	0.604	0.747	0.865	0.945	0.983	0.994	0.997	0.999	1.000	
66	0	0.025	0.150	0.271	0.447	0.563	0.718	0.830	0.908	0.961	0.986	0.994	0.996	0.997	1.000	

\* Largest particle not included in sample, particle is in size range shown.

Table I-5. Bed load data for samples obtained during the fall of 1971.

Sample Number	Discharge, cfs	Bed Load Discharges, kg/hour	Energy Slope, ft/100 ft	Hydraulic Radius, ft	Water Temperature, °F	D50 cm	Sorting Coefficient	Sampling Period, hours	Weight of Largest particle of sample gm
67	0.68	0.00080	0.94	0.21	51	0.070	1.72	24.0	0.4
68	0.67	0.00072	0.94	0.21	52	0.053	1.86	23.2	1.2
69	0.68	0.0016	0.94	0.21	54	0.22	2.30	24.5	24.2
70	0.68	0.0011	0.94	0.21	53	0.13	2.05	23.5	1.4
71	0.67	0.0014	0.94	0.21	52	0.44	2.09	24.3	6.5
72	0.67	0.0021	0.94	0.21	56	0.039	1.70	24.0	0.15
73	0.68	0.00037	0.94	0.21	56	0.080	2.65	24.5	2.3
74	0.68	0.00034	0.94	0.21	54	0.042	1.46	23.5	0.10
75	0.69	0.00025	0.94	0.21	52	0.049	2.07	24.0	0.40
76	0.72	0.00023	0.94	0.21	51	0.037	1.59	25.0	0.02
77	0.76	0.00086	0.94	0.22	50	0.070	2.12	21.5	0.55
78	0.78	0.00029	0.94	0.22	48	0.049	2.34	25.5	0.70
79	0.79	0.00024	0.94	0.22	46	0.047	1.87	24.0	0.12
80	0.79	0.000096	0.94	0.22	46	0.049	1.26	24.0	0.01
81	1.05	0.00070	0.94	0.24	48	0.048	1.08	24.0	4.1
82	1.41	0.019	0.94	0.26	50	0.16	1.95	24.0	19.8
83	0.98	0.00084	0.94	0.23	50	0.075	2.61	24.2	2.5
84	0.89	0.00022	0.94	0.23	48	0.067	2.01	23.4	0.6
85	1.75	0.0012	0.94	0.28	47	0.045	2.08	24.7	1.0
86	1.34	0.0020	0.94	0.26	46	0.050	1.95	24.4	31.2
87	1.03	0.0012	0.94	0.24	44	0.34	2.34	23.2	2.1
88	1.01	0.0014	0.94	0.23	46	0.48	2.41	24.0	6.0
89	1.46	0.0017	0.94	0.26	46	0.92	1.80	24.0	3.2
90	1.52	0.00058	0.94	0.27	43	0.060	2.50	23.9	2.5
91	1.30	0.0023	0.94	0.26	40	0.10	2.27	24.5	16.4
92	1.38	0.0020	0.94	0.26	41	0.056	2.01	24.5	36.7
93	1.50	0.0022	0.94	0.27	44	1.00	2.26	23.8	13.2
94	2.3	0.0020	0.94	0.31	45	0.046	2.11	24.0	3.7
95	2.5	0.0018	0.94	0.32	46	0.20	2.28	23.8	5.6

Table I-5. Bed load data for samples obtained during the fall of 1971. (Cont.)

Sample Number	Discharge, cfs	Bed Load Discharges, kg/hour	Energy Slope, ft/100 ft	Hydraulic Radius, ft	Water Temperature, °F	D50 cm	Sorting Coefficient	Sampling Period, hours	Weight of Largest particle of sample gm
96	1.62	0.0017	0.94	0.27	44	0.17	2.02	23.8	3.6
97	1.36	0.0012	0.94	0.26	45	0.17	2.12	24.2	4.2
98	1.66	0.0016	0.94	0.28	44	0.95	2.09	24.2	9.5
99	1.30	0.0024	0.94	0.26	41	1.10	2.16	24.1	17.8
100	3.1	0.0023	0.94	0.27	42	0.43	2.02	24.2	6.9
101	2.6	0.0071	0.94	0.32	44	0.10	1.84	24.0	139.0
102	2.1	0.0017	0.94	0.28	44	0.10	1.60	23.8	39.1
103	2.5	0.0062	0.94	0.39	46	0.16	2.32	9.3	6.4
104	5.1	0.0062	0.94	0.41	48	0.24	2.45	14.5	6.2
105	6.5	0.0086	0.94	0.41	48	0.14	1.64	8.0	3.2
106	5.0	0.0028	0.94	0.40	48	0.13	1.90	16.2	1.6
107	4.4	0.0027	0.94	0.39	48	0.50	2.03	24.1	4.9
108	3.8	0.0023	0.94	0.36	47	0.24	2.02	23.9	4.6
109	8.5	0.032	0.94	0.49	47	0.55	2.09	8.6	35.4
110	22.	3.2	0.94	0.68	47	0.86	2.37	5.5	883.0
111	18.	0.34	0.94	0.64	47	0.36	2.06	10.0	351.0
112	7.9	0.0049	0.94	0.48	47	0.18	1.68	7.2	2.8
113	5.2	0.020	0.94	0.41	46	0.34	2.23	17.0	25.8
114	3.3	0.0037	0.94	0.34	46	0.23	2.09	24.0	5.2
115	2.4	0.0046	0.94	0.31	46	0.20	1.95	23.9	4.9
116	2.0	0.0020	0.94	0.29	44	0.12	2.00	23.8	1.7
117	1.80	0.0015	0.94	0.28	45	0.12	1.79	24.2	1.5
118	1.57	0.0020	0.94	0.27	46	0.41	1.98	54.5	8.9
119	2.1	0.0014	0.94	0.29	46	0.24	2.09	89.8	9.7

Table I-6. Gradation data for bed load samples obtained in the fall of 1971.

Sample Number	Particle size, cm, and accumulation distribution, fraction courses by weight															
	101.6	76.2	50.8	38.1	25.4	19.05	9.52	4.76	2.38	1.19	0.595	0.297	0.149	0.074	0.074	
67							0	0.041	0.128	0.296	0.561	0.775	0.887	0.944	1.000	
68							0	0.126	0.151	0.232	0.446	0.750	0.895	0.950	1.000	
69						*	0.180	0.378	0.486	0.614	0.745	0.873	0.933	0.965	1.000	
70							0	0.292	0.399	0.525	0.705	0.861	0.930	0.962	1.000	
71							0	0.264	0.482	0.575	0.695	0.830	0.935	0.970	1.000	
72								0	0.042	0.125	0.322	0.605	0.792	0.896	1.000	
73						0	0.268	0.326	0.361	0.431	0.582	0.803	0.895	0.965	1.000	
74								0	0.029	0.117	0.306	0.680	0.840	0.906	1.000	
75							0	0.071	0.086	0.190	0.414	0.706	0.794	0.880	1.000	
76								0	0.017	0.086	0.258	0.620	0.723	0.880	1.000	
77							0	0.109	0.240	0.366	0.559	0.765	0.870	0.925	1.000	
78							0	0.103	0.145	0.261	0.435	0.682	0.812	0.865	1.000	
79								0	0.069	0.149	0.392	0.674	0.800	0.873	1.000	
80									0	0.146	0.410	0.775	0.910	0.956	1.000	
81						*	0	0.002	0.118	0.398	0.783	0.940	0.981	1.000	1.000	
82					0	0.043	0.132	0.276	0.417	0.565	0.765	0.950	0.985	0.995	1.000	
83							0	0.226	0.316	0.372	0.426	0.544	0.760	0.905	0.960	1.000
84								0	0.118	0.265	0.367	0.530	0.795	0.898	0.960	1.000
85								0	0.102	0.182	0.266	0.409	0.706	0.855	0.932	1.000
86						*	0	0.109	0.188	0.286	0.440	0.750	0.898	0.960	1.000	
87							0	0.256	0.464	0.534	0.604	0.709	0.884	0.956	0.985	1.000
88							0	0.314	0.502	0.610	0.681	0.780	0.856	0.947	0.976	1.000
89							0	0.490	0.750	0.798	0.844	0.895	0.955	0.984	0.997	1.000
90							0	0.185	0.289	0.348	0.407	0.533	0.795	0.920	0.970	1.000
91					0	0.288	0.561	0.745	0.787	0.806	0.852	0.933	0.976	0.992	1.000	
92					*	0	0.312	0.541	0.667	0.764	0.856	0.940	0.972	0.990	1.000	
93					0	0.249	0.510	0.604	0.702	0.770	0.850	0.945	0.985	1.000	1.000	
94							0	0.322	0.481	0.605	0.743	0.840	0.920	0.860	0.984	1.000
95							0	0.204	0.350	0.465	0.616	0.758	0.885	0.935	0.973	1.000
96							0	0.086	0.272	0.419	0.584	0.765	0.900	0.955	0.976	1.000
97							0	0.188	0.344	0.437	0.605	0.779	0.914	0.966	0.992	1.000
98							0	0.507	0.558	0.662	0.756	0.859	0.945	0.982	0.996	1.000
99					0	0.298	0.548	0.621	0.676	0.780	0.880	0.952	0.975	0.991	1.000	
100							0	0.241	0.441	0.608	0.731	0.846	0.935	0.973	0.991	1.000
101				*			0	0.064	0.178	0.295	0.440	0.659	0.895	0.970	0.991	1.000
102					*		0	0.029	0.102	0.231	0.450	0.710	0.895	0.961	0.988	1.000
103							0	0.201	0.301	0.411	0.571	0.730	0.879	0.945	0.966	1.000
104							0	0.117	0.343	0.502	0.628	0.719	0.835	0.892	0.930	1.000
105							0	0.102	0.252	0.384	0.530	0.700	0.856	0.935	0.970	1.000
106								0	0.186	0.352	0.533	0.686	0.855	0.944	0.980	1.000
107							0	0.268	0.523	0.666	0.764	0.853	0.930	0.970	0.994	1.000
108							0	0.084	0.342	0.516	0.670	0.776	0.896	0.952	0.981	1.000
109					0	0.214	0.372	0.521	0.665	0.800	0.900	0.963	0.986	0.996	1.000	
110	0		0.118	0.182	0.261	0.316	0.421	0.543	0.726	0.848	0.936	0.977	0.989	0.995	1.000	
111			*	0	0.085	0.133	0.284	0.448	0.584	0.769	0.911	0.977	0.993	0.998	1.000	
112							0	0.094	0.227	0.415	0.621	0.839	0.960	0.991	0.998	1.000
113					0	0.185	0.342	0.417	0.561	0.682	0.846	0.962	0.986	0.995	1.000	
114							0	0.210	0.332	0.499	0.659	0.800	0.930	0.973	0.990	1.000
115							0	0.175	0.326	0.456	0.628	0.805	0.943	0.980	0.990	1.000
116							0	0.128	0.242	0.335	0.505	0.711	0.908	0.964	0.984	1.000
117							0	0.041	0.151	0.272	0.495	0.723	0.891	0.950	0.975	1.000
118							0	0.321	0.455	0.632	0.758	0.874	0.955	0.985	0.994	1.000
119							0	0.222	0.320	0.485	0.652	0.819	0.925	0.964	0.985	1.000

\* Largest particle not included in sample; particle is in size range shown.



Table I-7. Corrected bed load discharge for the fall 1971 samples.

Sample Number	Gate Position	Was Pit Material		Correction Factor	Measured Bed Load, gm/hour	Adjusted Bed Load, gm/hour	Discharge cfs
		Included in sample?					
67	C *	No		0.60	0.80	1.3	0.68
68	C	No		0.60	0.72	1.2	0.67
69	C	No		0.62	1.6	2.6	0.68
70	C	No		0.61	1.1	1.8	0.68
71	C	No		0.62	1.4	2.3	0.67
72	I	No		0.56	0.21	0.37	0.67
73	I	No		0.58	0.37	0.64	0.68
74	I	No		0.57	0.33	0.58	0.68
75	I	No		0.56	0.25	0.45	0.69
76	I	No		0.56	0.23	0.41	0.72
77	I	No		0.60	0.86	1.4	0.76
78	I	No		0.57	0.29	0.51	0.78
79	I	No		0.56	0.24	0.43	0.79
80	I	No		0.54	0.096	0.18	0.79
81	I	No		0.60	0.70	1.2	1.05
82	O, I	Yes		1.0	19.2	19.2	1.41
83	I	No		0.60	0.84	1.4	0.98
84	C	No		0.56	0.22	0.39	0.89
85	I	No		0.62	1.22	2.0	1.75
86	I	No		0.63	2.0	3.2	1.34
87	I	No		0.62	1.2	1.9	1.03
88	I	No		0.62	1.4	2.3	1.01
89	I	No		0.62	1.7	2.7	1.46
90	I	No		0.60	0.58	0.97	1.52
91	C	No		0.63	2.3	3.7	1.30
92	C	No		0.63	2.0	3.2	1.38
93	I	No		0.63	2.2	3.5	1.50
94	I	No		0.63	2.0	3.2	2.3

Table I-7. Corrected bed load discharge for the fall 1971 samples. (Continued)

Sample Number	Gate Position	Was Pit Material Included in sample?	Correction Factor	Measured Bed Load, gm/hour	Adjusted Bed Load, gm/hour	Discharge cfs
95	I	No	0.62	1.79	2.9	2.5
96	I	No	0.62	1.72	2.8	1.62
97	I	No	0.61	1.20	2.0	1.36
98	I	No	0.62	1.63	2.6	1.66
99	I	No	0.64	2.4	3.8	1.30
100	I	No	0.64	2.3	3.6	3.1
101	II	No	0.67	7.1	10.6	2.6
102	II	No	0.62	1.7	2.7	2.1
103	II	No	0.66	6.2	9.4	2.5
104	II	No	0.66	6.2	9.4	5.1
105	II	No	0.67	8.6	12.8	6.5
106	II	No	0.64	2.8	4.4	5.0
107	II	No	0.63	2.7	4.3	4.4
108	II	No	0.64	2.3	3.6	3.8
109	II	No	0.78	32	41	8.5
110	II	Yes	1.0	3200	3200	22
111	O	Yes	1.0	3700	3700	18
112	O	Yes	1.0	4.9	4.9	7.9
113	II	Yes	1.0	20	20	5.2
114	II	Yes	1.0	3.7	3.7	3.3
115	II	Yes	1.0	4.6	4.6	2.4
116	I	Yes	1.0	1.96	1.96	2.0
117	II	Yes	1.0	1.5	1.5	1.8
118	II	Yes	1.0	2.0	2.0	1.57
119	II	Yes	1.0	1.4	1.4	2.1

\* C: sampler gate was closed during sampling period.

O: sampler gate was completely open during sampling period.

I, II: sampler gate was partially open during sampling period, II was open more than I, hence more water went through sampler.

## APPENDIX II

## SUSPENDED LOAD DATA

In this appendix are presented the suspended sediment data collected during the study of sediment transport in Oak Creek.

All of the samples were obtained using a DH-48 sampler and almost all were taken at the upstream end of the bed load sampler.

The samples were analyzed in the Forest Sciences Laboratory, School of Forestry, Oregon State University, by John Fekete. The technique used was a filtration method.

The data collected during the winter of 1969-70 are given in Table II-1. The 1969-70 samples were obtained infrequently during the bed load sampling period.

During the winter of 1971 samples were obtained relatively frequently during the bed load sampling period. The data are presented in Table II-2.

During the fall of 1971, samples were obtained in order to study sediment transport after an extended period of low flows and prior to a period of relatively high water. These data are given in Table II.

Table II-1. Oak Creek suspended sediment concentrations, winter 1969-70.

Date	Time	Discharge, cfs	Suspended Sediment Concentration, mg/liter
9 January	13:43	35	204
9 January	14:50	35	166
9 January	20:18	28	49
10 January	9:30	13	9
14 January	15:42	60	147
14 January	17:00	50	111
14 January	23:15	34	28
15 January	11:15	21	7
16 January	15:25	45	25
16 January	16:45	40	96
17 January	1:00	138	417
17 January	9:15	52	75
17 January	11:00	46	52
17 January	12:55	44	195 (?)
16 February	17:00	80	86
17 February	12:10	35	23
19 Feb- 16 Mar <sup>(1)</sup>		8	5
16 Mar- 8 Apr <sup>(1)</sup>		3	< 2

(1) Obtained with composite automatic sampler; all other samples obtained with DH 48 hand sampler.

Table II-2, Oak Creek suspended sediment data for the winter and spring of 1971.

Sample Number	Date	Time	Discharge, cfs	Suspended Sediment Concentration, mg/liter	Temperature °F
1	7 January	14:55	5.3	1.53	--
2	8	16:20	5.3	1.78	--
3	9	13:00	11.8	7.22	--
4	10	11:50	12.0	10.62	--
5	10	16:30	15.0	13.79	--
6	11	8:25	14.4	7.22	41
7	11	15:55	12.5	5.45	41
8	12	12:00	10.2	1.06	39
9	13	9:45	9.2	2.62	38
10	14	15:30	6.8	4.51	38
11	15	10:10	136	391.88	38
12	15	15:15	115	114.90	--
13	16	10:30	95	67.37	--
14	16	12:10	105	110.36	--
15	16	13:25	140	364.76	41
16	17	12:55	98	101.52	42
17	18	8:45	76	134.04	42
18	18	15:03	70	39.57	43
19	18	15:53	68	39.01	44
20	20	14:30	33	12.61	43
21	20	20:10	29	11.48	41
22	21	09:10	27	21.04	41
23	21	16:00	26	8.62	43
24	22	13:40	25.5	12.44	43
25	23	08:45	26	8.43	44
26	24	14:15	23	--	44
27	25	08:45	80	58.72	--
28	25	15:33	62	63.47	45
29	25	21:00	47	25.42	45
30	26	08:07	32	8.47	45
31	26	15:15	26	7.02	45
32	27	13:35	19.0	6.58	45
33	28 January	17:00	14.5	5.94	44
34	4 February	08:10	20.0	43.19	41
35	4	13:00	21.5	19.02	43
36	5	08:30	12.5	8.14	42
37	9	22:50	10.4	16.01	44
38	14	15:35	7.2	4.47	46
39	15	13:05	8.3	6.74	46
40	17	9:50	6.4	26.84	--
41	18 February	12:40	7.8	5.25	44

Table II-2. Oak Creek suspended sediment data for the winter and spring of 1971 (Cont.)

Sample Number	Date	Time	Discharge, cfs	Suspended Sediment Concentration, mg/liter	Temperature, °F
42	22 February	16:30	7.0	12.58	45
43	25	08:45	10.7	51.42	40
44	25	16:30	11.6	1.06	41
45	26	13:30	10.0	3.33	39
46	27 February	13:30	9.0	5.59	39
47	1 March	13:45	6.7	9.19	41
48	2	13:50	7.1	8.90	40
49	2	22:15	9.3	13.29	40
50	3	09:15	13.5	23.54	40
51	3	16:45	26.0	38.17	40
52	3	17:10	25.5	31.28	40
53	4	12:45	15.5	3.91	40
54	5	13:45	12.6	6.98	42
55	6	14:40	12.4	6.5	41
56	10	12:30	56	191.42	--
57	10	13:15	63	246.78	42
58	10	13:45	67	205.65	--
59	10	14:15	74	216.81	--
60	10	18:45	75	649.2	--
61	10	21:45	56	46.88	--
62	10	22:55	50	30.11	42
63	11	01:40	42	30.37	--
64	11	07:55	34	19.1	42
65	11	11:00	46	23.55	42
66	11	12:45	58	49.89	42
67	11	14:20	69	199.77	--
68	11	15:00	81	71.86	--
69	11	15:10	83	68.83	--
70	11	17:05	131	552.9	--
71	11	17:38	142	548.72	--
72	11	17:49	135	395.79	--
73	11	17:51	138	358.33	42
74	11	20:00	96	131.58	--
75	11	20:00	96	126.22	--
76	12	13:30	52	17.62	--
77	12	14:00	52	18.18	43
78	13	12:20	32	9.58	44
79	13	14:20	31	11.92	45
80	14	15:30	25	8.44	45
81	15	16:15	17.5	2.41	44
82	17 March	14:25	11.0	3.52	45

Table II-3. Oak Creek suspended sediment data for the fall of 1971.

Sample Number	Date	Time	Discharge, cfs	Suspended Sediment Concentration, mg/liter	Temperature, °F
1	30 September	16:30	0.77	1.743	50
2	1 October	08:30	0.77	0.75	49
3	2	08:45	0.72	1.778	47
4	3	09:15	0.68	1.985	49
5	4	09:00	0.68	1.094	50
6	5	09:30	0.68	3.111	52
7	6	08:45	0.67	1.570	53
8	7	09:15	0.68	0.457	54
9	8	08:45	0.68	1.732	52
10	9	09:00	0.67	1.111	53
11	10	09:00	0.67	1.351	58
12	11	09:30	0.69	2.857	54
13	12	09:00	0.68	2.423	53
14	13	09:00	0.71	2.450	52
15	14	10:00	0.72	2.391	50
16	15	07:30	0.80	1.628	49
17	16	09:00	0.76	2.227	47
18	17	09:00	0.82	2.649	45
19	18	09:00	0.76	2.750	47
20	19	09:00	3.00	15.165	49
21	19	16:00	2.10	12.624	50
22	19	16:45	2.00	12.136	--
23	20	08:50	1.20	5.579	47
24	21	09:15	0.89	3.761	47
25	22	08:25	0.89	2.667	48
26	22	16:30	1.47	3.351	48
27	23	09:15	1.55	1.370	48
28	24	09:30	1.12	.213	45
29	25	09:00	0.94	.215	44
30	26	08:50	1.50	.280	48
31	27	08:50	1.75	1.005	45
32	28	08:45	1.30	2.353	41
33	29	09:10	1.30	1.505	39
34	30	09:25	1.55	2.603	43
35	31 October	08:40	1.45	0.909	44
36	1 November	08:20	3.2	28.250	46
37	1	16:15	2.65	15.471	47

Table II-3. Oak Creek suspended sediment data for the fall of 1971. (Cont.)

Sample Number	Date	Time	Discharge, cfs	Suspended Sediment Concentration, mg/liter	Temperature, °F
38	2 November	08:10	1.86	4.060	45
39	3	07:45	1.38	.472	43
40	4	08:10	1.93	1.463	47
41	5	08:10	1.40	.959	42
42	6	08:15	1.20	1.887	40
43	7	08:30	3.1	19.737	44
44	8	08:15	2.1	10.000	43
45	9	08:10	1.6	2.535	45
46	9	17:25	4.60	35.498	47
47	10	08:40	6.6	30.493	48
48	10	16:00	4.1	17.866	49
49	11	08:10	4.4	15.846	48
50	12	08:15	4.1	12.679	47
51	13	08:10	5.2	15.752	47
52	13	16:35	12	131.002	47
53	13	17:05	12	161.670	--
54	13	22:20	31	149.007	--
55	13	22:45	30	140.570	47
56	14	08:50	9.4	22.796	47
57	14	15:45	6.4	18.326	47
58	15	08:55	3.9	11.398	46
59	16	09:00	2.64	5.405	47
60	17	08:50	2.16	5.570	44
61	18	08:50	1.90	4.859	44
62	19	09:10	1.70	4.218	46
63	21	15:30	1.45	0.510	47
69	25	09:00	5.3	15.873	45
65	26	10:40	86	140.393	48
66	26	10:55	82	158.658	48
67	26	10:55	82	195.484	48
68	27 November	13:30	14.6	18.824	47
69	4 December	11:30	5.8	7.90	44
70	12	13:30	42	21.10	43
71	19	16:00	9.6	3.86	44
72	27 December	15:00	11.2	6.67	42
73	2 January	12:30	6.2	6.45	43
74	10 January	12:30	15.0	11.19	43